Hepatitis B Virus X protein-mediated transcription of covalently closed circular DNA and its inhibition by blocking neddylation

Dissertation

submitted to the

Combined Faculty of Natural Sciences and Mathematics

of the Ruperto Carola University Heidelberg, Germany

for the degree of

Dr. rer. nat. of Natural Sciences

Bingqian Qu

2019

Dissertation
submitted to the
Combined Faculty of Natural Sciences and Mathematics
of the Ruperto Carola University Heidelberg, Germany
for the degree of
Dr. rer. nat. of Natural Sciences

Presented by
M.Sc. Bingqian Qu
Born in: Shenyang, China
Oral examination: 27.11.2019

Hepatitis B Virus X protein-mediated transcription of covalently closed circular DNA and its inhibition by blocking neddylation

Referees:

First supervisor**:** Prof. Dr. Stephan Urban

Second supervisor: Prof. Dr. Martin Löchelt

The applicant, Bingqian Qu, declares that he is the sole author of the submitted dissertation and no other sources or help from those specifically referred to have been used. Additionally, the applicant declares that he has not applied for permission to enter examination procedure at another institution and this dissertation has not been presented to other faculty and not used in its current or in any other form in another examination.

…… ……

Date Signature

I. ACKNOWLEDGEMENTS

First of all, I would like to express my sincerest and deepest gratitude to my mentor, Prof. Dr. Stephan Urban, who gave me the opportunity to work in his laboratory. In the past years under his supervision, I started from a freshman who knew nothing about hepatitis viruses, learned more and more knowledge in this field, conducted my projects, supervised master students and the most importantly, I am about to finish my doctorate adventure.

Stephan not only preaches me his comprehensive understandings in biology and philosophy but also advises me how to carry on my own projects and build up a “researcher” career and kindly addresses most of my questions during this long journey. As a mentor, he always gives me the maximal flexibility to try every option in the HBV field (including immature ideas) and patiently tolerates my mistakes, especially during the early trials of my doctorate study. This rigorous and relaxed research environment in his laboratory (like heating and cooling cycles in a PCR swim) allows me to maintain scientific motivation and eventually shapes me a junior researcher and an honorable Ph.D.-to-be made in Germany.

I would like to thank my second supervisor, thesis examiners and TAC committee members: Prof. Dr. Martin Löchelt, Prof. Dr. Ralf Bartenschlager, Prof. Dr. Ursula Klingmüller, Prof. Dr. Michael Nassal (Freiburg), Prof. Dr. Volker Lohmann and Dr. Steeve Boulant, who gave me a great amount of suggestions during not only two advisory meetings but the whole study.

I would like to thank our coordinator, Ms. Martina Weiss, who helped me millions of times in non-scientific issues, for instance, contracts and visa issues. She always provides immediate assistance when I encounter a language barrier while working in Germany. I herein extend thanks to the SFB/TRR179 transregional program that offers my funding in recent three years and its administrative staffs, Dr. Sandra Bühler, Steffi Schimang and Dr. Eva Schnober (Freiburg) for their help within the program.

I further extend my gratitude to all group leaders in our department, Prof. Dr. Ralf Bartenschlager, Prof. Dr. Volker Lohmann, Dr. Marco Binder and Dr. Alessia Ruggieri, who have given me fruitful advice and suggestions on routine department seminar and shared valuable protocols and materials during my study. Special thanks also are given to external collaborators, Prof. Dr. Renate König (Langen), Prof. Dr. Florian W.R. Vondran (Hannover), Prof. Dr. Maura Dandri (Hamburg) and Prof. Dr. Bernd Wollscheid (Zürich) for bringing extra resources.

Next, I would like to thank adorable previous and current colleagues in our team. A special thank goes to senior scientist Yi, who spent much of his working time to help me when I was a

first-year student. I learned techniques but also his stringent scientific attitude. I have many thanks to Florian, Pascal, Benno, Thomas, Zhenfeng, Mila, Jessica, Katrin, Shirin, Christina, Wenshi, Volkan, Franziska, Anja, Lisa and Christa for helping me with benchwork and creating a friendly atmosphere in the laboratory.

I would like to thank all my external workmates and fellows, who have co-worked with me in the past years: Yong-Xiang Wang, Lise Rivière, Andreas F. Sommer, Lena Allweiss, Emanuela S. Milani, Gianna A. Palumbo and Lester Suárez-Amarán. They helped me deepening my understandings in this field. Due to space limitation, I could not list all the names of the people who ever gave a piece of help over time.

From the bottom of my heart, I express my thanks to my dearest wife, Xue, who gave me constant courage, strength and love over the years and gave birth to our daughter Fiona. It is certain that I can not finish my doctorate study without her continuous and innumerable supports. Finally, I thank my parents, Ying Qu and Chunmin Liu living in China. Their willpower and loves always support me in walking forward.

August 8th 2019 in Heidelberg

II. ABSTRACT

Hepatitis B Virus (HBV) leads to chronic infection of the liver and is a risk factor for the development of cirrhosis and hepatocellular carcinoma. Virus persistence requires the establishment and maintenance of covalently closed circular (ccc)DNA, serving as the episomal template for transcription of viral genes in the nucleus of infected hepatocytes. Viral cccDNA-dependent gene expression requires HBV X protein (HBx) and HBx-mediated degradation of the host restriction factors structural maintenance of chromosome 5/6 (SMC5/6). A prerequisite for SMC5/6 ubiquitination and degradation is that HBx binds DNA damage-binding protein 1 (DDB1) and further recruits Cullin 4A ring ligase complex, which requires neddylation for its activation.

After the establishment of a reliable quantitative PCR, the kinetics of cccDNA formation in four *in vitro* infection systems and the effect of drugs (interferon-α, nucleos(t)ide analogues, entry inhibitors, and capsid inhibitors) on cccDNA were analyzed. Compared to replicative relaxed circular (rc)DNA, copy numbers of cccDNA in infected hepatocytes are unexpectedly low (1~6 copies per infected cell). Entry inhibitor, Myrcludex B, efficiently blocked cccDNA formation. Interferon-α reduced cccDNA level at high dose, whereas nucleos(t)ide analogues did not reduce it. Treatment with capsid inhibitors during the infection phase but not afterward led to a decline of cccDNA levels.

Using HBx-minus virion for infection, we verified HBx as a key controller of cccDNA transcription. HBx expressed by its authentic promoter showed nuclear localization. Using lentiviral-based transcomplementation assay to restore the transcription of HBx-minus virus to the wild-type level, key fragments and residues of HBx were identified. The whole C-terminus of HBx (51~154 amino acids) was sufficient and indispensable to enhance transcription of HBx-minus virus, whereas N-terminal HBx (1~50 amino acids) displayed no transactivation. In addition, two shorter truncations (51~142 and 58~142 amino acids) showed residual function. Remarkably, the HBx(R96E) mutant with impaired binding activity to DDB1 totally abolished its transactivation activity, supporting that foundation of the HBx-DDB1 complex is required for maximal transcription from cccDNA.

We further investigated whether blockage of neddylation hampers transcription. MLN4924, a specific NEDD8-activating enzyme 1 inhibitor, was identified to notably possess antiviral potential. MLN4924 potently reduced HBV transcription and viral antigen expression at nanomolar doses. After the establishment of cccDNA, the drug profoundly suppressed transcription from cccDNA without affecting cccDNA levels. Withdrawal of MLN4924 did not lead to restoration of cccDNA transcription in HepaRG^{hNTCP} cells, however fast HBV rebound

was observed in infected HepG2^{hNTCP} cells. Peculiarly, transcription from cccDNA of HBx-minus virus was not significantly affected, suggesting that MLN4924 effect on wild-type virus replication is HBx dependent. MLN4924 selectively reduced transcription from all HBV promoters on cccDNA but not integrants. MLN4924 prevented SMC6 from degradation and the restoration of SMC6, in turn, silenced transcription from cccDNA.

Taken together, nuclear HBx binds DDB1, induces SMC6 degradation and thereby promotes transcription from cccDNA. Targeting neddylation blocks transcription from cccDNA and restores SMC6 restriction on cccDNA. Therefore, MLN4924 treatment traps cccDNA in “transcriptional silence”. Small molecules that target the HBx-DDB1-Cullin complex might be foresight as the next possible therapeutic option combating HBV.

III. ZUSAMMENFASSUNG

Das Hepatitis B Virus (HBV) kann zu chronischer Leberinfektion führen und ist ein Risikofaktor für die Entstehung von Leberzirrhose und dem hepato-zellulären Karzinom. Für die Persistenz des Virus ist die Bildung und die Aufrechterhaltung der kovalent geschlossenen zirkulären DNS („covalently closed circular“ (ccc)DNS) zwingend notwendig, da sie als episomale Matrize für die Transkription im Kern der infizierten Hepatozyten dient. Die an cccDNS gebundene virale Transkription hängt vom HBV X Protein (HBx) sowie den durch HBx initiierten Abbau des wirtsspezifischen Restriktionsfaktors „structural maintenance of chromosome 5/6“ (SMC5/6) ab. Eine Grundvoraussetzung für die Ubiquitinierung und den Abbau von SMC 5/6 ist, dass HBx das Protein “DNA damage-binding protein1“ (DDB1) bindet und somit den Cullin 4A Ringligasekomplex rekrutiert, welcher für seine Aktivierung neddyliert werden muss.

Nachdem eine verlässliche quantitative PCR etabliert wurde konnte die Kinetik der cccDNS Bildung in vier verschiedenen *in vitro* Infektionsmodellen sowie der Einfluss von Medikamenten (Interferon-α, Nukleos(t)id-Analoga, Inhibitoren des viralen Zelleintritts („entry Inhibitor“) und Kapsid-Inhibitoren) auf die cccDNS untersucht werden. Im Vergleich zum Replikationsintermediat der gelockerten zirkulären („relaxed circular“; (rc)DNS) sind die Kopienzahlen der cccDNS in infizierten Hepatozyten niedrig (1-6 Kopien/infizierter Zelle). Der „entry Inhibitor“ Myrcludex B unterband effizient die (ccc)DNS Bildung. Hohe Interferon-α Dosen verringerten die cccDNS Menge während Nukleos(t)id-Analoga diese nicht vermindern konnten. Die Gabe von Kapsid Inhibitoren während der Infektionsphase, aber nicht zu einem späteren Zeitpunkt, führte zu einer Verringerung der cccDNS Menge.

Indem wir HBx negative Virionen für die Infektion verwendet haben, konnten wir die Schlüsselrolle von HBx in der Kontrolle der cccDNS Transkription verifizieren. Wird HBx transient von einem authentischen Promotor exprimiert befindet es sich im Zellkern. Mit Hilfe eines lentiviral basierten Transkomplementationsansatzes, in dem die Transkription von HBx defizienten Virionen auf das Level von Wildtypviren gehoben wurde, konnten Schlüsselfragmente und -bereiche des HBx bestimmt werden. Der gesamte C-Terminus von HBx (Aminosäuren 51-154) war sowohl ausreichend als auch unentbehrlich um die Replikation HBx-defizienter Viren wieder herzustellen während der N-Terminus (Aminosäuren 1-50) keine transaktivierende Funktion aufzeigte. Zusätzlich waren zwei kürzere Fragmente (Aminosäure 51-142 und 58-142) teilweise funktional. Bemerkenswerterweise wies die HBx Mutante (R96E), welche nur noch eine geringe Bindeaktivität zu DDB1 aufweist, überhaupt keine Transaktivierungsaktivität mehr auf, was darauf hindeutet, dass die Bildung des HBx-DDB1 Komplexes für die maximal mögliche Transkription der cccDNS nötig ist.

Des Weiteren untersuchten wir ob eine Hemmung der Neddylierung die Transkription erschwert. MLN4924, ein spezifischer Inhibitor des NEDD8-aktivierenden Enzyms 1 zeigte ein bemerkenswertes antivirales Potenzial. MLN4924 verringerte die HBV Transkription und virale Antigenexpression wirksam in nanomolarer Dosierung. Nach der Bildung der cccDNS unterdrückte das Medikament hochgradig die Transkription selbiger ohne dabei die cccDNS Menge zu beeinflussen. Die Unterbrechung der MLN4924 Gabe führte in HepaRG^{NTCP} Zellen nicht zu einer Reaktivierung der cccDNS Transkription, wohingegen in HepG2^{NTCP} Zellen eine schnelle Erholung von HBV beobachtet wurde. Bemerkenswerter Weise wurde die Transkription der cccDNS HBx-defizienter Viren nicht signifikant beeinfluss, was darauf schließen lässt, dass der MLN4924 Effekt auf das Wildtypvirus HBx-abhängig ist. MLN4924 verringert dabei selektiv die Transkription aller HBV Promotoren im Kontext der cccDNS, jedoch nicht bei integrierter viraler DNA. MLN4924 verhinderte der Abbau von SMC6, förderte dessen Wiederherstellung und unterband somit die Transkription der cccDNS.

Zusammenfassen lässt sich sagen, dass nukleäres HBx DDB1 bindet, den Abbau von SMC6 induziert und so die Transkription der cccDNS fördert. Ein Angriff auf die Neddylierung unterbindet die Transkription der cccDNS und stellt die SMC6-abhängige Restriktion der cccDNS wieder her. Somit friert eine MLN4924 Behandlung die cccDNS in einem Zustand der „transkriptionellen Stille“ ein. Kleine Moleküle, die auf den HBx-DDB1-Cullin Komplex zielen könnten somit eine Vorausschau auf die nächstmögliche Therapie für HBV sein.

IV. CONTENTS

V. LIST OF ABBREVIATIONS

aa	Amino acids
Ad	Adenovirus
APS	Ammonium persulfate
ATP	Adenosine triphosphate
bp	Base pairs
BSA	Bovine serum albumin
℃	degree Celsius
Ca^{2+}	Calcium ion
CC_{50}	50% cytotoxic concentration
cccDNA	HBV Covalently closed circular DNA
cDNA	Complementary DNA
CMV	Cytomegalovirus
CIP	Calf intestine phosphatase
C-terminus	Carboxy terminus
CTP	Cytidine triphosphate
CTL	Cytotoxic T lymphocyte
d	Day(s)
ddH2O	Double distilled water
DDB1	DNA damage-binding protein 1
DHBV	Duck Hepatitis B Virus
DMEM	Dulbecco's Modified Eagle Medium
DMSO	Dimethylsulfoxide
dNTP	Deoxyribonucleotide triphosphate
DR	Direct repeat
dslDNA	Double-stranded linear DNA
DTT	Dithiothreitol
EC_{50}	50% effective inhibitory concentration
ECL	Enhanced chemiluminescence
E. coli	Escherichia coli
EDTA	Ethylenediaminetetraacetic acid
ELISA	Enzyme-linked immunosorbent assay
ER	Endoplasmic reticulum

FACS	Fluorescence-activated cell sorting
FCS	Fetal calf serum
g	Gram
GAG	Glycosaminoglycan
GE	Genomic equivalents
GFP	Green Fluorescent Protein
h	Hour(s)
HAP	Heteroaryldihydropyrimidine
HBcAg	Hepatitis B core antigen
HBeAg	Hepatitis B e antigen
HBsAg	Hepatitis B surface antigen
HBV	Hepatitis B virus
HBx	Hepatitis B X protein
HCC	Hepatocellular carcinoma
HCV	Hepatitis C virus
HDAC	Histone deacetylase
HDV	Hepatitis Delta virus
HDAg	Hepatitis Delta antigen
HIV	Human immunodeficiency virus
(h)NTCP	Human sodium taurocholate cotransporting polypeptide
HSPG	Heparan sulfate proteoglycan
IF	Immunofluorescence
IFN-α	Interferon alpha
ISG	Interferon-stimulated gene
IRES	Internal Ribosomal Entry Site
IU/mL	International unit/milliliter
k	Kilo, a thousand
kD	kilo Dalton
LB	lysogeny broth
L-HDAg	Large Hepatitis Delta antigen
LTR	Long terminal repeat
M	Mol/Liter
MCS	Multiple cloning site

MGE	Multiplicity of genome equivalents
min	Minutes
mRNA	Messenger RNA
MVB	Multivesicular body
MW	Molecular Weight
MyrB	Myrcludex B (Brand name: Bulevirtide)
N-terminus	Amino terminus
nt	Nucleotide(s)
NTCP	Sodium taurocholate cotransporting polypeptide
NUC	Nucleos(t)ide analogue
OD	Optical Density
ORF	Open reading frame
PAGE	Polyacrylamide gel electrophoresis
PBS	Phosphate buffered saline
PCR	Polymerase chain reaction
PEG	Polyethylene glycol
PEG-IFN-α	Pegylated interferon alpha
PEI	Polyethylenimine
PFA	Paraformaldehyde
pgRNA	Pregenomic RNA
pH	Pondus hydrogenii
PHH	Primary human hepatocytes
p.i.	Post infection
Pol.	Viral polymerase
PTH	Primary Tupaia hepatocytes
qPCR	Quantitative polymerase chain reaction
rcDNA	Relaxed circular DNA
RNAi	RNA interference
RNP	Ribonucleoprotein
Rpm	Revolution per minute
RT	Room temperature/Reverse transcription
rtTA	Tetracycline/Doxycycline-controlled transactivator
SCID	Severe combined immunodeficiency

SDS	Sodium dodecyl sulfate
sec	seconds
S-HDAg	Small Hepatitis Delta Antigen
SMC5	Structural maintenance of chromosome 5
SMC6	Structural maintenance of chromosome 6
SN	Supernatant
SSC	Standard saline citrate
ssDNA	Single-stranded DNA
SV40	Simian virus 40
SVP	Subviral particle
TAE	Tris-acetate-EDTA
TAT	Transactivator of transcription
TBS	Tris buffered saline
TBST	Tris buffered saline with tween 20
TEMED	N, N, N', N'-tetramethylethylenediamine
Tet	Tetracycline/Doxycycline
TGF-α	Transforming growth factor alpha
TK	Thymidine kinase
TP	Terminal protein
Tris	Tris(hydroxymethyl)-aminomethane
U	unit
uPA	Urokinase plasminogen activator
V	Volt
VSV	Vesicular stomatitis virus
WHO	World Health Organization
WHV	Woodchuck Hepatitis Virus
WHx	Woodchuck Hepatitis Virus X protein
WST-1	Water-soluble tetrazolium salts 1
WT	Wild type
X	Hepatitis B Virus X protein
Xd.	HBx deficient/HBx minus

VI. LIST OF FIGURES AND TABLES

Figures:

Tables:

1. INTRODUCTION

1.1. Hepatitis viruses

According to WHO's statistics, annually killing more people than HIV, tuberculosis and malaria, viral hepatitis has become the seventh leading cause of death and disability worldwide (Stanaway et al., 2016). Viral hepatitis is acute or chronic liver inflammation induced by viral infection. Most of common causes of viral hepatitis are one of the five hepatotropic viruses as shown in Table 1.1.: hepatitis A virus (HAV), hepatitis B virus (HBV), hepatitis C virus (HCV), hepatitis D virus (HDV), and hepatitis E virus (HEV) (Zuckerman, 1996). It can not be neglected that a number of new-class hepatitis viruses discovered later (HGV, TT, SEN) may also lead to viral hepatitis (Reshetnyak et al., 2008). In addition, other viruses including herpes simplex virus, Epstein-Barr virus, and cytomegalovirus also cause local liver inflammation. Although all the five hepatitis viruses induce liver damage, they are genetically unrelated to each other and classified in distinct genera. A myriad of basic and clinical features of these viruses are summarized as shown.

Table 1.1. Hepatitis viruses.

	HAV	HBV	HCV	HDV	HEV
Classification	Picornavirus	Hepadnavirus	Hepacivirus	Deltavirus	Hepevirus
Genome	+ssRNA	dsRNA-RT	+ssRNA	-ssRNA	+ssRNA
Incubation (d)	20~40	45~160	15~150	30~60	15~60
Transmission route	Fecal-oral	Parenteral Perinatal Sexual	Parenteral Perinatal Sexual	Parenteral Sexual	Fecal-oral
Chronicity	Acute	5-10% chronic[1] 80% neonates	70% chronic	Chronic with HBV	Acute[2, #]
Carcinogenesis	–	+	+	–	–
Prophylaxis	vaccine	vaccine	NA	HBV vaccine	vaccine[3]
Therapy	NA	IFN, NUCs	DAAs	IFN	RBV

[1]5~10% in immunocompetent adults; [2]mild in normal adults and severe in pregnant women; [3]licensed in China. #: chronic in immunocompromised patients. ss: single stranded, ds: double stranded, RT: reverse transcriptase, IFN: interferon-α, NUC: nucleos(t)ide analogue, DAA: direct-acting antiviral, RBV: ribavirin; NA: therapy not required.

Leading to acute hepatitis in most cases, HAV and HEV are usually fecal-oral transmitted through either person-to-person communication or ingestion of contaminated foods. Decades ago, both viruses caused outbreaks in the Third World countries (central Africa, southern Asia and southern America) where hygiene conditions were bad. Until 2012, HAV prevalence was only high in India, south-Sahara Africa and moderate in the Middle East, North Africa and

Latin America. For pre-exposure prevention, the application of HAV vaccines worldwide is highly effective in protecting healthy people for ten years. However, HEV is highly endemic in the whole Asia, northern and eastern Africa, Mexico and also present in the whole Europe, USA and South America, threatening more people in larger geographic regions. The first HEV vaccine was approved in China in 2011, yet it is not available in other countries (Tahaei et al., 2012).

One the other hand, HBV, HCV and HDV cause chronic infection and lead to a more serious global burden of public health. In 2013, HBV and HCV accounted for more than 95% of viral hepatitis-related mortality. By the year 2018, it was estimated that chronically infected people worldwide are 240 million (caused by HBV mono-infection), approximate 15~20 million (by HBV/HDV co-infection) and 75 million (by HCV infection) (WHO's statistics 2018). Recent estimates have ranked viral hepatitis and associated clinical manifestations that account for more than 1 million death cases every year (Stanaway et al., 2016).

HCV is a blood-borne hepatitis virus and prevalent all over the world. In 70% of HCV-infected patients, HCV develops persistent infection and gradually leads to cirrhosis and hepatocellular carcinoma over the years. Because of its high mutation rate during replication, HCV vaccine is still not available. Combinational therapy of interferon and ribavirin was not efficient enough to control the virus. However, 25 years after its characterization, interferon-free direct-acting antivirals have been developed. Antiviral medication using inhibitors targeting two or three HCV viral enzymes at the same time was approved and this therapy resulted in sustained virological response (SVR) rate to above 90% in patients. Reduced therapy duration and side effects of direct-acting antivirals allow a cure of HCV within 8 or 12 weeks (Asselah et al., 2016).

In contrast to HCV, HBV and HDV chronic infections are not curable by the approved drugs. HBV is commonly transmitted from mother to neonate during birth delivery, as well as in adults through contact with blood or other body fluids. In immunocompetent adults, acute HBV infection is self-cleared and resolved in 90~95% of infected individuals, 80% of the neonates, however, can not naturally eliminate the virus. 5% of infected adults and 80 % of infected newborns develop chronic infection and are, similar to HCV chronic infection, at a very high risk of developing liver cirrhosis and hepatocellular carcinoma over decades. Therefore, among hepatitis viruses, HBV is the major health problem. HDV, a satellite virus of HBV, requires HBV envelope proteins for entry, assembly and spread. Patients with HBV and HDV coinfection show the most severe live injury and are with the highest risk to develop liver diseases.

1.2. Hepatitis B virus

Hepadnaviridae is a collection of viruses with natural hosts, humans, apes and birds. Belonging to the *Hepadnaviridae*, all the viruses are divided into two genera: *Avihepadnavirus* that infects avian hepatocytes, and *Orthohepadnavirus*, with the best-known member the hepatitis B virus (HBV), which merely infects humans and chimpanzees (International Committee on Taxonomy of Viruses, 2018). HBV is a hepatotropic, small DNA virus in size and genome length, which is categorized into four serotypes (adw, ayw, adr, ayr) and into at least eight genotypes (A through H). Diseases and complications associated with chronic HBV infection contain hepatitis, liver cirrhosis and hepatocellular carcinomas.

Three centuries ago, there were epidemic outbreaks of jaundice and of serum hepatitis after receiving vaccination in civilians, although people did not know what caused hepatitis. Later on, it was postulated that this infectious jaundice was caused by an unknown virus. In 1946, MacCallum classified “infectious hepatitis” termed hepatitis A and “serum hepatitis” as hepatitis B (Mac, 1946). Using molecular biology that was further developed, Blumberg et al discovered the “Australia antigen” (HBsAg) among Australian aborigines and characterized a new pathogen, HBV. A few years later Dane et al observed the “dane” particle (complete HBV particle) isolated in the serum of infected patients (Blumberg et al., 1965, Dane et al., 1970).

After HBV characterization, researchers started to seek preventive and therapeutic options. In the early 70s, Blumberg and his colleagues developed the first HBV vaccine that was a heat inactivation of the virus. In 1981, a plasma-derived HBV vaccine produced by inactivating pooled blood of HBsAg-positive donors by formaldehyde and pasteurization was approved. Merck further developed this inactivated type of vaccine as “Hepavax”. Nowadays safer, more effective and genetically engineered recombinant HBV vaccines have completely replaced the old ones (Hepatitis B Foundation, 2019). On the other hand, Interferon-α-2b (Intron A) as the first drug was approved by the FDA in 1981. In recent 25 years, Lamivudine (1998), Adefovir dipivoxil (2002), peginterferon (2002), Entecavir (2005), Telbivudine (2006), Tenofovir (2008) were one-by-one approved for treating chronic HBV infection as shown in Figure 1.1 (Thomas et al., 2015). The prodrug of tenofovir, Tenofovir alafenamide, was approved in 2016.

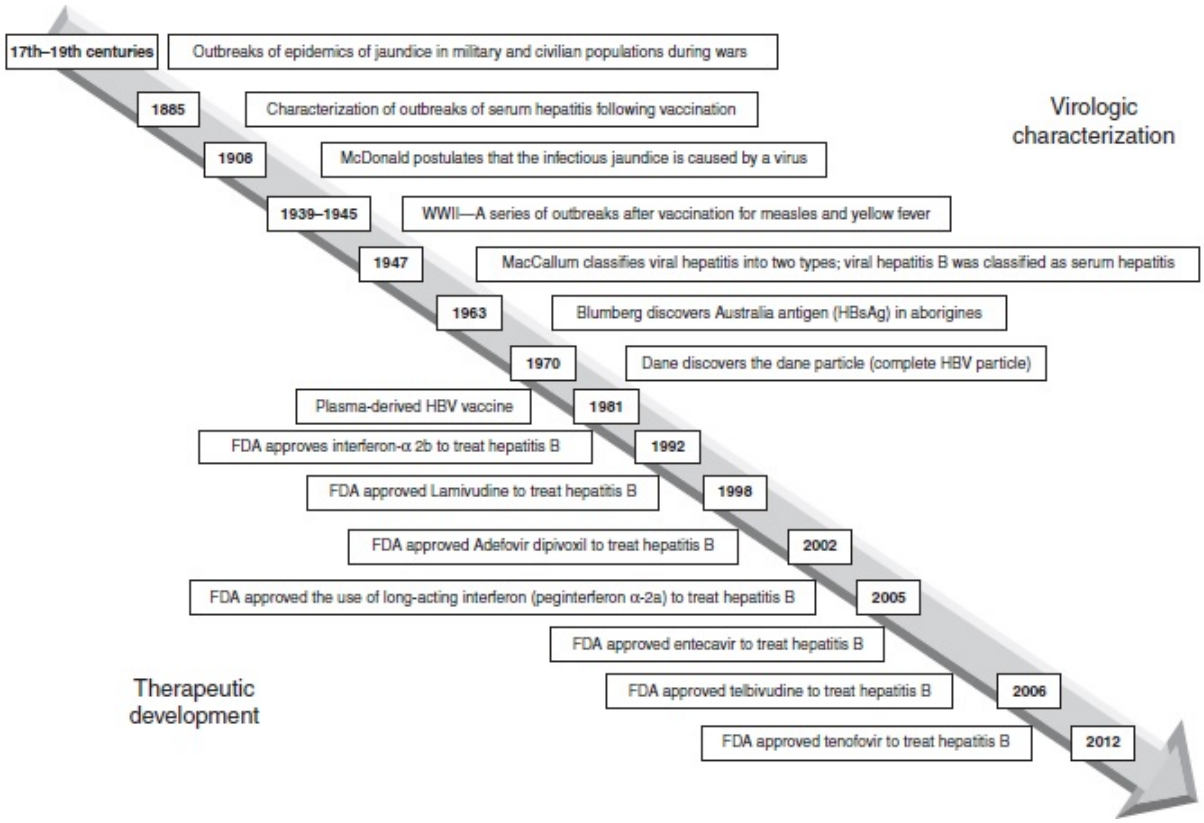

Figure 1.1. Timeline of HBV virologic characterization and therapeutic development. Events in discovery history and early HBV science (right upper, 1885~1970) and treatment options (1981~2012). (Emmanuel Thomas, 2015) with permission.

1.2.1. Epidemiology

In the global regions, WHO estimates that there are 240 million people with chronic HBV infection, which is defined as HBsAg positive. HBsAg prevalence is highest in Southeast Asia and Middle Africa (> 6%) and China (> 5%) in all-aged individuals. Prevalence is moderate in East Europe and South-East Asia (China excluded)(2.6~5%). HBsAg positive rate is pretty low in Australia, Western Europe (< 1%) and the whole America (0.7%) (Polaris Observatory, 2018) (Figure 1.2.).

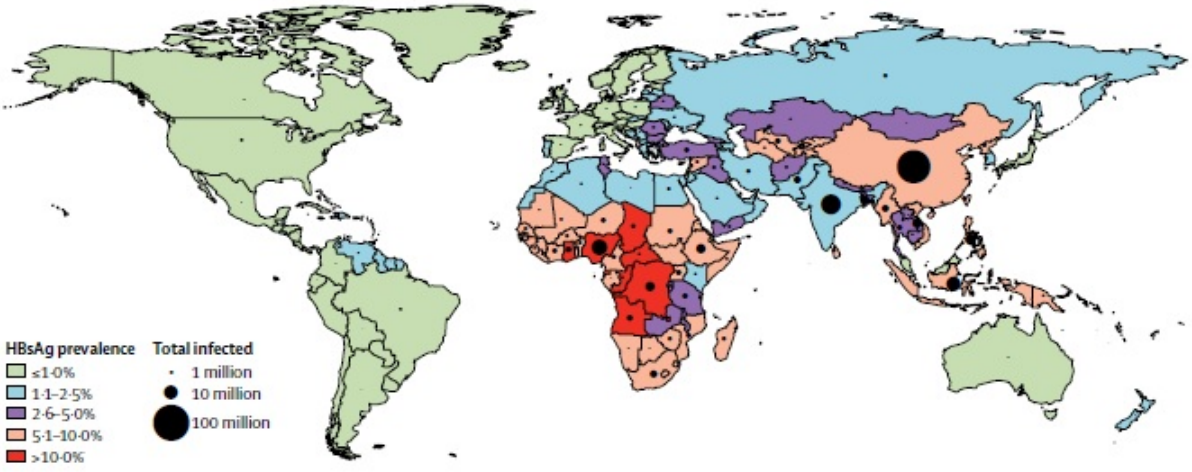

Figure 1.2. HBsAg prevalence estimates in all-aged individuals in 2016. Estimated for countries with data and data extrapolated from countries in the same global burden of diseases with available data (all ages). Rates of HBsAg prevalence are shown in colors as indicated. Circles show absolute infection numbers (millions) (The Polaris Observatory Collaborators, Lancet, 2018) with permission.

The epidemiological study also showed HBsAg prevalence in children at 5 years old. This value reveals preventive efforts in the regions by vaccination since mother-to-child transmission is one of the major routes accounting for HBV prevalence. Initiated a national vaccination program for 30 years, nowadays China has controlled HBsAg prevalence rate down to < 0.5% in children aged at 5 years, compared to 10~50 fold higher prevalence in all-age people (> 5%) (Polaris Observatory, 2018) (Figure 1.3.), however, China still has more than 100 million chronic HBV carriers in the elders, waiting for a curative therapy (Figure 1.2). In contrast, rates of HBsAg prevalence in children aged at 5 year in India and Indonesia are ascending compared to the rates in all-aged individuals, which may be due to unstable vaccination programs towards newborns under high birth rate.

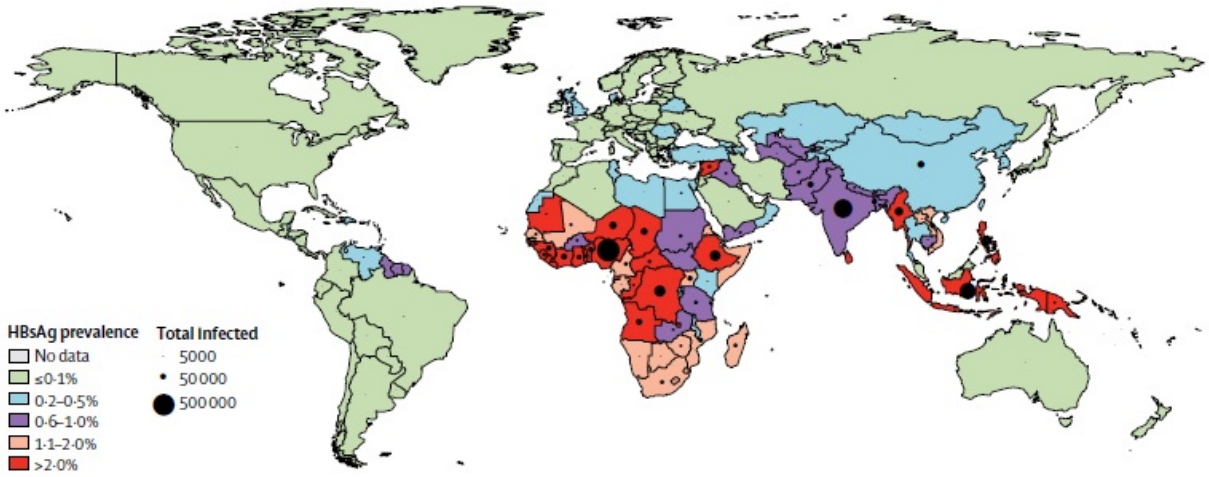

Figure 1.3. HBsAg prevalence estimates in children aged at 5 years in 2016. Estimated for countries with data and data extrapolated from countries in the same global burden of diseases (children only aged at 5 years). Colors: HBsAg prevalence. Circles: total infected numbers. (The Polaris Observatory Collaborators, Lancet, 2018) with permission.

1.2.2. Genomic organization

Inside equipped capsid, HBV has a small but compact genome, which is a single copy of relaxed circular (rc)DNA with the length of 3182~3248 bp among genotypes (3182 bp, genotype D as shown in Figure 1.4.). Every rcDNA is covalently bound to one viral polymerase (P). Double-stranded rcDNA consists of an entire minus strand and one partial plus strand. The minus-strand DNA is not covalently closed but covers the entire genome, while the plus strand starts from direct repeat 2 (DR2) and has variable 3' ends at 50~80% of the whole genome (Lutwick and Robinson, 1977). 5' plus strand terminates with a short RNA oligo that is derived from the 5'

end of pregenomic RNA (pgRNA), the template for reverse transcription of the minus strand. Minus strand is covalently bound to polymerase via phosphotyrosine and has a short nucleotide terminus, which is essential for the formation of rcDNA, when sequences of DR1 and DR2 are identical (Seeger et al., 1986). In addition to rcDNA, approximate 10% of HBV genomes contain double-stranded linear DNA (dslDNA) generated from *in situ* priming of plus strand synthesis when DR1 and DR2 share mismatches (Staprans et al., 1991). After infection, dslDNA is the major component for HBV integration by homologous recombination (Tu et al., 2017).

The circular HBV genome contains four authentic promoters (core/preS1/preS2/X) and two enhancers (Enh1/Enh2). All transcripts have the same polyadenylation signal at their 3' ends. Accordingly, open reading frames (precore-core/P/preS1-preS2-S/X) are under the four promoters. RcDNA and dslDNA are genomes in virus, however in cell rcDNA is converted into another type of genome, covalently closed circular (ccc)DNA by host DNA repair machinery including α/κ/λ polymerases, ligases and topoisomerases (Nassal, 2008, Qi et al., 2016, Long et al., 2017, Sheraz et al., 2019, Tang et al., 2019). CccDNA serves as the major template of viral transcription and all transcripts can be expressed by the minus strand on the same cccDNA genome, then capped at their 5' ends and polyadenylated at 3' ends. At RNA level, HBV expresses preC/C (3.5 kb), preS1 (2.4 kb), S (2.1 kb), X transcripts (0.6~0.8 kb) and spliced RNA. They mostly share the same 3' ends by the polyadenylation signal (Cattaneo et al., 1983b, Cattaneo et al., 1984). Furthermore, pgRNA (the shorter 3.5 kb) is -as a replicative pre-genome- encapsidated in infected cells as the template for rcDNA synthesis via reverse transcription but also is translated to core protein (HBcAg) and polymerase, whereas non-genomic precore mRNA (the longer 3.5 kb) is translated and processed to HBeAg (Figure 1.4.).

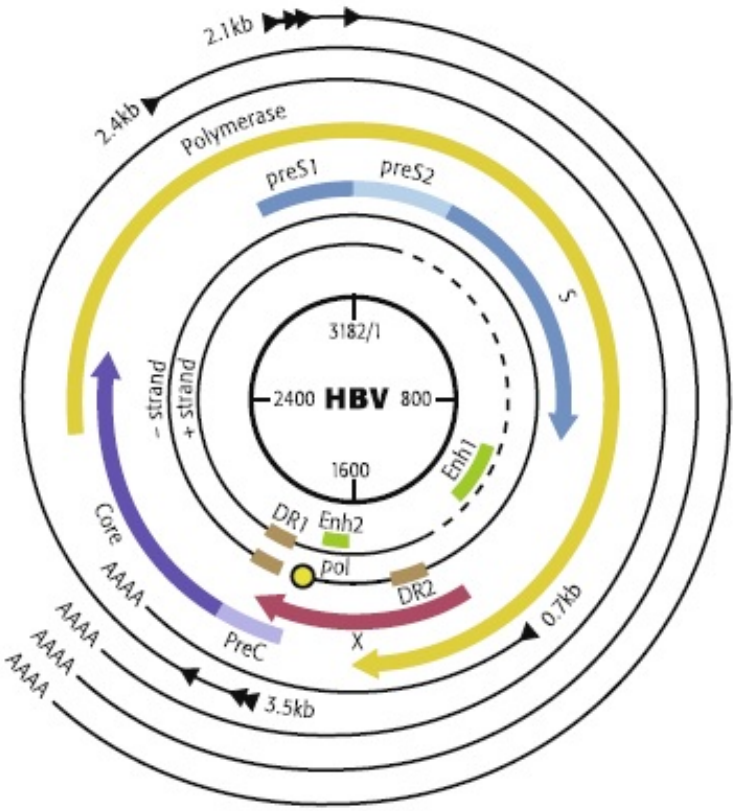

Figure 1.4. HBV genomic structure. In the center, it shows the genomic scale (3182/1: EcoRI cutting site). The HBV genome is composed of a circular and double-stranded rcDNA. rcDNA is repaired to form cccDNA with both strands entired and closed that serves as the template for viral transcription to generate viral RNAs with 3.5 kb (two, different starting points), 2.4 kb, 2.1 kb and 0.6~0.8 kb (uncertain) in size. Among these transcripts, the longer 3.5 kb PreC mRNA is translated to a pre-core protein and cleaved to HBeAg, whereas the shorter 3.5 kb pgRNA is translated to HBcAg and polymerase. The 2.4 kb mRNA is translated to the large surface antigen (L) and the 2.1 kb mRNA is responsible for the middle (M) and small (S) envelope proteins. The smallest mRNA encodes HBx protein. PreC: precore; pol: polymerase; DR1: direct repeat 1; DR2: direct repeat 2; Enh: enhancer; AAAA: polyadenylation ends. (Robert Gish, Antiviral Res, 2015) with permission.

1.2.3. Structure and viral proteins

Infectious virions (Dane particles) are made of 120 dimers of core proteins (T=3 or T=4 symmetry) with an inner size of 22 nm (Dryden et al., 2006). The capsids are surrounded by a lipid membrane containing three viral envelopes, large (L), middle (M) and small proteins (S). Outer size of the enveloped particle is 47 nm. Molecular ratio of the L, M, and S proteins are 1:1:4 (Heermann et al., 1984). Every nucleocapsid contains one copy of rcDNA genome that covalently links to one viral polymerase at 5' end of its minus-strand. The virion has a density of 1.24~1.26 g/mL in CsCl gradients. Besides, non-infectious subviral particles, spheres and filaments, are also generated during HBV replication. Spheres with a size of 22 nm contain M and S proteins at a ratio of 1:2 and very little amount of L protein (Heermann et al., 1987). However, filaments are organized as a rod-like structure with variable length and contain L, M,

and S proteins at the same ratio of 1:1:4, similar to virion (Short et al., 2009). These subviral particles do not contain any viral rcDNA genomes and stay at a density of 1.18 g/mL in CsCl gradients (Figure 1.5.).

HBV encodes seven viral proteins, five of which are structural (polymerase, core, L, M and S proteins) and two are non-structural (HBeAg and HBx protein) (Gish et al., 2015).

Core protein has 183 amino acids with a molecular weight of approximate 21 kD. Within it, 45 amino acids in the center form a spike (Bringas, 1997). Carboxyl amino acids are arginine-rich and this domain is required for pgRNA encapsidation and productive rcDNA synthesis (Nassal, 1992). It was further demonstrated that arginines in the SPRRR motif help pgRNA packaging and DNA replication (Lewellyn and Loeb, 2011). The C-terminus of core protein also contains three serine sites (Ser 155/162/170) that are phosphorylated and overlapped with the arginine-rich SPRRR motif. Phosphorylation of core protein is responsible for its nuclear localization (Eckhardt et al., 1991, Kann et al., 1999, Lan et al., 1999, Li et al., 2010a, Liao and Ou, 1995, Yeh et al., 1990).

The HBeAg precursor is translated from precore mRNA with an upstream start codon in the frame of the core ORF. After translation, HBeAg precursor undergoes a cleavage of its C-terminal 34 amino acids and anchors to the ER membranes via its signal peptide, before it is secreted as a 15 kD mature HBeAg from infected cells (Bruss and Gerlich, 1988, Garcia et al., 1988, Ou et al., 1986, Ou et al., 1989, Standring et al., 1988, Zhou and Standring, 1991). Secreted HBeAg suppresses host immune response and increases the frequency of chronic infections. However, HBV mutations that lead to devoid of HBeAg expression have been frequently identified in long-term chronic infection in HBeAg negative patients (Brunetto et al., 1999).

L (preS1-preS2-S) and M proteins (preS2-S) are N-terminally longer than S protein. All three proteins share the same C-terminus. They also share topogenic signal I and II and hydrophobic C-terminus that direct these proteins to the ER membranes. L protein is N-terminally myristoylated (glycine 2) and M protein is acetylated (Persing et al., 1987, Schmitt et al., 1999). N-terminus of L protein is crucial to capsid binding and is exposed on the surface of the virion and initiates effective infection of hepatocytes (Prange and Streeck, 1995). Another region located at transmembrane domain II and hydrophobic C-terminus of S contains a second infectivity determinant (Le Duff et al., 2009, Salisse and Sureau, 2009). M protein is dispensable for infectivity but acts as a spacer for virus assembly (Ni et al., 2010). M and S proteins containing export signals can be assembled and independently secreted as subviral particles as described in Figure 1.5..

HBV polymerase with a size of 90 kD consists of three domains: terminal protein (TP) for the priming of minus-strand synthesis, reverse transcriptase (RT) for DNA synthesis and RNase H region for pgRNA degradation. Spacer with unclear function is a flexible region between the TP and RT domains (Bartenschlager and Schaller, 1988, Chang et al., 1990). The viral polymerase is specific to pgRNA template, utilizes itself to bind the ε packaging signal at the 5' end of pgRNA and results in the priming of reverse transcription in the TP domain (tyrosine 65) (Lanford et al., 1997, Wang and Seeger, 1992, Weber et al., 1994). Once encapsidated, one single polymerase catalyzes a complete round of DNA synthesis. Polymerase and pgRNA template co-exist at similar amounts but the molar ratio of polymerase molecules per virion DNA is approximate 0.7 in each virion (Bartenschlager et al., 1992, Bartenschlager and Schaller, 1992, Zhang and Tavis, 2006). Owing to its enzymatic activity, reverse transcriptase becomes an antiviral target of approved nucleos(t)ide inhibitors. RNase H is also a target of potential inhibitors in development. Moreover, the polymerase may regulate host responses. Uncoupled from its function in DNA synthesis, polymerase anchors to the mitochondria via mitochondrial targeting signal in its TP domain (Unchwaniwala et al., 2016). Via its RT domain, polymerase interacts with the stimulator of interferon genes (STING), blocks its polyubiquitination and thereby suppresses interferon production (Liu et al., 2015)

The other non-structural protein encoded by HBV is HBx, which has 154 amino acids (16.5 kD). HBx was identified to bind many cellular proteins and involved in multiple host processes. In terms of its high importance in this thesis, the biological functions of HBx were separately introduced in session 1.3.2..

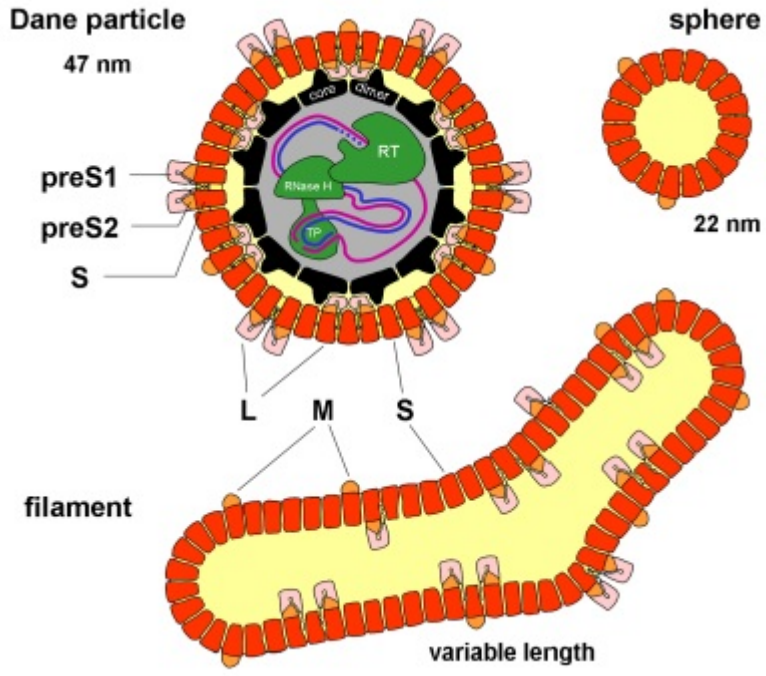

Figure 1.5. Structure of virions and subviral particles. Infectious virions (Dane particles) are composed of envelopes (L (preS1-preS2-S): M (preS2-S): S = 1:1:4) embedded with nucleocapsids (black). Polymerase (TP-RT-RNase H) and its associated rcDNA (dslDNA is not shown in this scheme) are located inside the nucleocapsid. Non-infectious subviral particles, spheres with mostly M and S proteins, filaments with L, M and S proteins (1:1:4), are made up by envelope proteins but do not contain any DNA genomes. TP: terminal protein; RT: reverse transcriptase. Adapted from an internal scheme in Urban's laboratory.

1.2.4. Overview of the HBV life cycle

HBV infection initiates with an L envelope-dependent binding to heparan sulfate proteoglycans (HSPG) on the cellular membrane (Schulze et al., 2007). After attachment, myristoylated N-terminal preS1 domain via the NPLGFFP motif binds the bona fide receptor, sodium taurocholate cotransporting polypeptide (NTCP) (Yan et al., 2012). Reconstitution of human NTCP but not rodent NTCP renders human hepatoma cells susceptible to HBV infection (Ni et al., 2014). After membrane fusion and uncoating, nucleocapsids are transported into the nuclear periphery, where capsids move into the nucleus in an importin α/β-dependent manner (Rabe et al., 2006, Schmitz et al., 2010). In the nucleus, rcDNA genome is released (Rabe et al., 2003, Rabe et al., 2009). How rcDNA is converted to cccDNA is not fully understood, it is likely that tyrosyl-DNA-phosphodiesterase 2 (TDP2) specifically cleaves the viral polymerase out of rcDNA (Koniger et al., 2014), and DNA polymerase κ/λ and ligases 1 and 3 are involved in rcDNA-to-cccDNA conversion (Qi et al., 2016, Long et al., 2017).

Once cccDNA is formed, it serves as a template for viral transcripts, including pregenomic RNA (pgRNA), subgenomic RNAs, preCore mRNA and HBx mRNA. pgRNA acts as the template for translation of core and polymerase proteins and for the generation of new rcDNA. When translated, viral polymerase binds the epsilon signal ε of pgRNA, this ribonucleoprotein complex further recruits HBcAg and is packaged into nucleocapsids (Bartenschlager and Schaller, 1992, Hirsch et al., 1990, Huang and Summers, 1991). Within capsids, minus-strand DNA is firstly synthesized by reverse transcription complementary to pgRNA and the polymerase remains covalently bound to the minus-strand (Gerlich and Robinson, 1980, Molnar-Kimber et al., 1983, Molnar-Kimber et al., 1984). Then pgRNA template is degraded by the RNase H activity of viral polymerase (Chen and Marion, 1996, Radziwill et al., 1990, Summers and Mason, 1982). Plus-strand DNA synthesis always starts after complete synthesis of minus-strand DNA and is primed via the remaining RNA oligomer of pgRNA. To prime it, the RNA oligomer anneals with DR2 that is identical to DR1 (Lien et al., 1986, Seeger et al., 1986, Will et al., 1987, Staprans et al., 1991). If DR1 and DR2 are not exactly the same, their mismatches block rcDNA formation but promote an *in situ* DNA priming leading to the

formation of dslDNA that can be integrated into host genomes (Figure 1.6.) (Staprans et al., 1991, Condreay et al., 1992, Yang and Summers, 1998).

Nucleocapsids gain the opportunity to interact with envelopes (Huovila et al., 1992, Lenhoff and Summers, 1994, Patzer et al., 1984). Through the ER-Golgi apparatus, it is plausible that ubiquitin ligase Nedd4, γ2-adaptin and thioredoxin-related transmembrane protein 2 (Rost et al., 2006, Hartmann-Stuhler and Prange, 2001, Toh et al., 2005) help virions locating at the ESCRT vesicles (endocytic sorting complexes required for transport) in which supports virus budding. Virions are secreted by multivesicular bodies. Alternatively, non-enveloped nucleocapsids can be secreted as naked capsids.

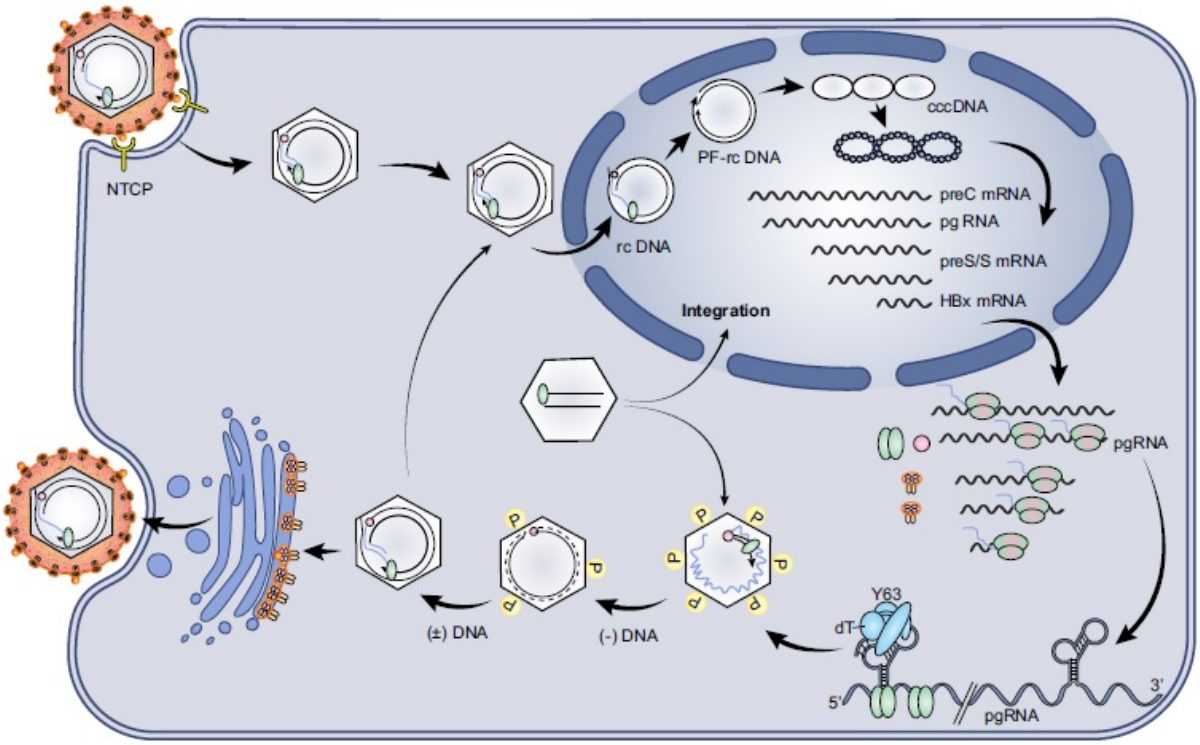

Figure 1.6. Overview of the HBV life cycle. HBV entry begins with a reversible attachment to HSPG (not drawn in the scheme) and a preS1 protein-mediated specific interaction with hepatocyte-specific bile acid cotransporter NTCP. After membrane fusion and uncoating, the nucleocapsid is either assembled out or transported into the nucleus to release viral rcDNA genome. rcDNA afterward is repaired by cellular proteins to convert to cccDNA, which is coupled with histones and core proteins and forms a mini-chromosome. RNA polymerase II-driven transcription of cccDNA produces five capped and polyadenylated transcripts (PreC mRNA, pgRNA, preS, S and X mRNA) that are exported into cytoplasm where they are translated to seven viral proteins. One of these proteins, viral polymerase, binds the ε signal region of the pgRNA. This ribonucleoprotein complex is encapsidated with phosphorylated core proteins. In most nucleocapsids, reverse transcription of pgRNA generates a complete minus-strand DNA and further pgRNA is degraded and partial plus-strand DNA is synthesized. In a minority of nucleocapsids, dslDNA is formed and responsible for HBV integration. rcDNA-containing nucleocapsids are either recycled into the nucleus, directly secreted as naked capsids (not shown), or enveloped in the ER membrane and secreted as virions. Virions are secreted by multivesicular bodies. Spheres and filaments (see 1.1.4.) are secreted via the classical secretory pathway. (Tong et al. 2016) with permission.

1.3. cccDNA, HBx and HBx-mediated transcription of cccDNA

1.3.1. cccDNA and mini-chromosome

CccDNA plays a central role in HBV replication. Nucleocapsids in the cytoplasm either enter the nucleus to release rcDNA genome or being assembled with envelopes and secreted as virions. In the first option, released rcDNA is converted to cccDNA (Tuttleman et al., 1986). As a non-integrated circular genome, the cccDNA is not replicative as genomic DNA by host DNA synthesis system, however it produces all viral transcripts essential for protein production (Mason et al., 1982). In a non-dividing hepatocyte, cccDNA formation occurs early when viral envelope expression is low in DHBV infection (Summers et al., 1990). Once formed, the cccDNA pool is relatively stable and cccDNA copy number per cell is 1~50 (Jilbert et al., 1987, Kajino et al., 1994, Miller and Robinson, 1984, Zhang et al., 2003). The pool has a long half-life comparable to its host in non-dividing cells (Levrero et al., 2009) but during mitosis loss of cccDNA was observed in *in vivo* experiments (Lutgehetmann et al., 2010, Allweiss et al., 2018). Due to its stability, cccDNA is also the key factor responsible for chronic HBV infection.

For transcription, nuclear episomal cccDNA is bound to histones and transcriptional regulators. They organize into a chromatin-like structure termed “mini-chromosome”, which recruits also liver-specific nuclear proteins and viral HBcAg (Bock et al., 1994, Bock et al., 2001, Newbold et al., 1995). The organization of viral DNA and nucleosomal proteins is usual for human papillomavirus and adenovirus (Favre et al., 1977, Tate and Philipson, 1979). Unlike latent DNA viruses, HBV replication requires a minichromosome composed of transcriptionally active chromatin. It is believed that RNA polymerase II binds cccDNA, bypasses the polyadenylation signal located in the core region and continues transcription for another 3.2 kb to generate 3.5 kb pre-C/C transcripts (Russnak, 1991). In addition to RNA polymerase and histones, under physiological situation, many liver-specific (HNF1, HNF3, HNF4α) and non-specific host factors (RARα/β, RXRα, PPARα, C/EBP, etc.) may be involved in transcription of cccDNA (Quasdorff and Protzer, 2010, Courtois et al., 1988, Guo et al., 1993, Lopez-Cabrera et al., 1990, Raney et al., 1995, Chen et al., 1994, Ori and Shaul, 1995). Besides, two enhancers EnhI and EnhII, regulate the transcription from all four promoters and enhance the expression amounts of pgRNA, PreC, preS/S and HBx mRNA (Trujillo et al., 1991).

1.3.2. Multi-functional HBx

HBx is a multifunctional protein of all orthohepadnaviruses and essential to initiate infection and maintain replication *in vivo* and *in vitro* (Zoulim et al., 1994, Lucifora et al., 2011). Early

conceptions were established by overexpression analysis of HBx in various hepatoma and HEK293T cells, using these systems HBx was identified to interact with more than fifty host factors, including transcriptional factors and co-activators, key proteins in DNA damage, ubiquitin-proteasome pathway, mitochondrial components and effectors in signaling cascades (Bouchard and Schneider, 2004, Murakami, 2001). Transfection studies without HBV infection suggested that HBx is involved in various cellular processes (transcription, cell cycle, cell adhesion, DNA repair, apoptosis, protein stability). However, most functions were not further characterized in authentic infection systems.

HBx is encoded by all orthohepadnaviruses. Although DHBV genome has a hidden open reading frame (ORF) as X-like encoding region and the putative protein expressed by a construct activated mitogen activated protein kinase (MAPK) pathway and was localized in the cytoplasm (Chang et al., 2001), a follow-up study showed that DHBV with a stop codon in the X-like ORF showed similar infectivity and replication level *in vivo* compared to the WT DHBV, questioning whether DHBV HBx-like protein really exists (Meier et al., 2003). Functional X proteins have been identified in infected mammals (humans, chimpanzees, woodchucks [WHx], ground squirrels [GSHx], horseshoe and tent-making bats [bat X] and so on). HBx protein has 154 amino acids. WHx, GSHx and bat X have between 139~142 amino acids and a shorter C-terminus compared to the HBx (Figure 1.7.). The additional C-terminal HBx (143~154 amino acids) is essential for its stability, transcriptional activation and replication stimulation (Lizzano et al., 2011, Luo et al., 2012, Li et al., 2016b).

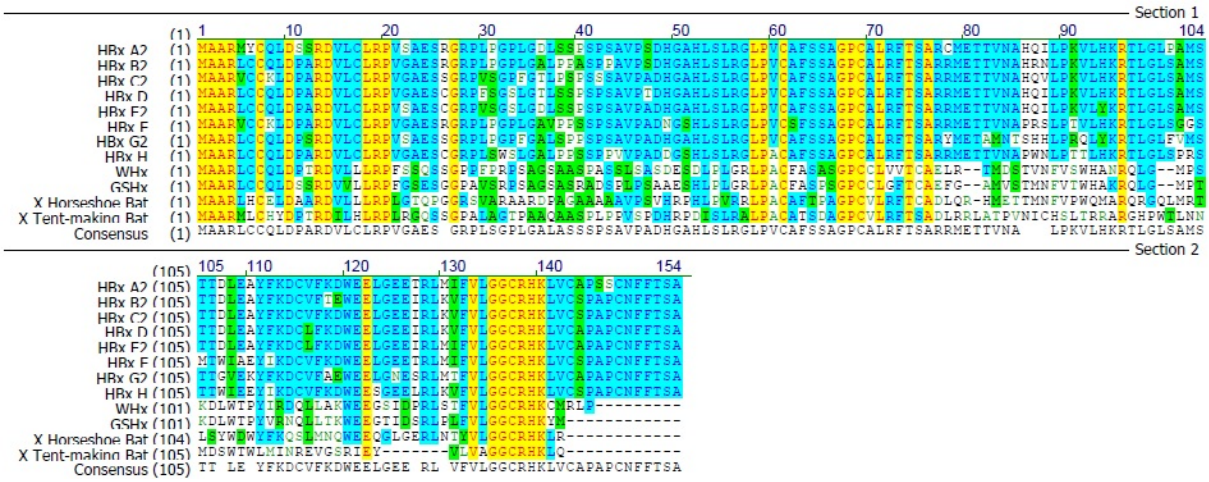

Figure 1.7. Alignment of HBx, WHx, GSHx and two bat X. Representative HBx proteins from all genotypes (A2, B2, C2, D, E2, F, G2, H) and WHx, GSHx, X from horseshoe and tent-making bat were aligned using VectorNTI software. Homology was shown in different colors (yellow: the same residues; green: high conserved; blue: moderate conserved; white: not conserved).

Full-length HBx protein has been divided into five regions based on their sequence homologies among eight genotypes. Three of the five regions (1~20, 58~84 and 120~154 amino

acids) are conserved and contain eight conserved cysteines (C7, C17, C61, C69, C115, C137, C143, C148) and two histidines (H52, H139), the other two (21~57 and 85~119 amino acids) however are less conserved (Kumar et al., 1996). This similarity suggests that HBx among all eight genotypes have common biochemical features. Purified recombinant HBx protein (genotype D) contained metal ions in particular zinc and iron (Jiang et al., 2016). Further characterization showed that zinc binding activity through conserved CCCH motif (C61, C69, C137 and H139) is required for its function (Ramakrishnan et al., 2019) (Figure 1.8.)

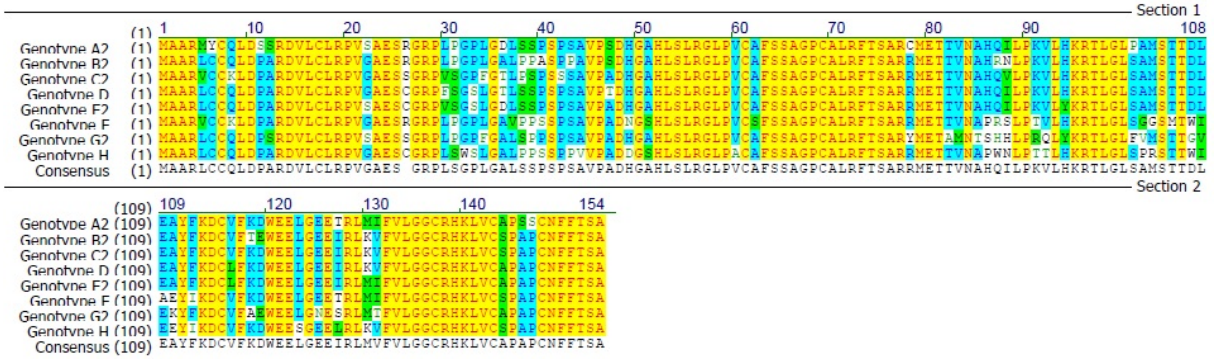

Figure 1.8. Alignment of HBx from eight genotypes. HBx proteins among eight genotypes (A2, B2, C2, D, E2, F, G2, H) were aligned using VectorNTI software. Conserved domains: 1~20 aa, 58~84 aa and 120~154 aa. Conserved C61, C69, C137 and H139 residues are shown in yellow. Variable domains: 21~57 aa and 85~119 aa. Yellow: the same residues; green: high conserved; blue: moderate conserved; white: not conserved.

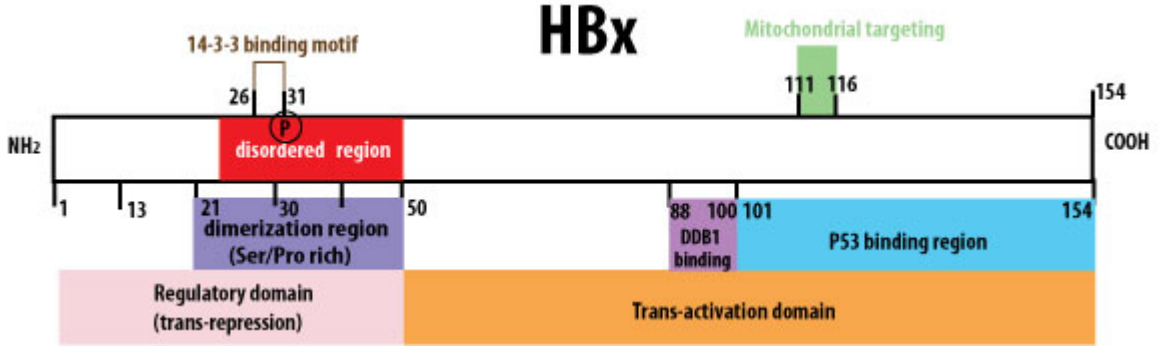

Figure 1.9. Scheme of the HBx protein. HBx has 154 amino acids and 17 kD in size. This scheme presents identified HBx domains. For transcriptional regulation, a negative regulatory domain (light purple) is located at the N-terminus (1~50 aa) and C-terminal HBx (51~154 aa) is the trans-activation region (brown). Highly variable disordered region (red) is overlapping with the dimerization region (Serine and proline rich). Other regions are responsible for binding of 14-3-3 protein (white) (26~31 aa), DDB1 (dark purple) (88~100 aa), p53 binding (light blue) (101~154 aa) and mitochondrial targeting (light green) (111~116 aa). The scheme is adapted from the ExPASy database.

As shown in Figure 1.9., modulating transcription is one of the major functions of HBx. The N-terminal domain (1~50 amino acids) was firstly identified as a transcriptional repressor *in trans* (Murakami et al., 1994) and this repression was further mapped to the conserved 1~20 amino acids (Misra et al., 2004). The N-terminal one third (1~50 amino acids) is not required but the whole C-terminal two-thirds (51~154 amino acids) is the trans-activation domain, which was confirmed using alanine scanning mutagenesis assay (Tang et al., 2005). Specifically, two

regions (52~65 and 88~154 amino acids) are crucial for the augmentation function of HBx. This finding showed similar findings as the earliest report presenting that HBx C-terminus (58~140 amino acids) retained trans-activation and was indispensable. In the nucleus, HBx promotes transcription from cccDNA, presumably associated with DNA-damage binding protein 1 (DDB1) by binding the motif (88~101 amino acids) (Li et al., 2010c). Although the association of HBx and DDB1 is not sufficient for maximal HBV replication (Hodgson et al., 2012), this complex recruits host ubiquitin machinery and promotes degradation of SMC5/6 restrictive on cccDNA to enhance HBV replication (Decorsiere et al., 2016) (Murphy et al., 2016, Livingston et al., 2017). These findings provided concrete evidence that HBx in an authentic infection system enhances transcription of cccDNA. C-terminal HBx also binds p53 and inhibits p53-mediated transcriptional trans-activation, apoptosis and DNA-specific binding (Elmore et al., 1997).

HBx is primarily located in the nucleus and also accumulates in the cytoplasm (Cha et al., 2009). Since HBx has a nuclear export signal (key residues L98 and L100) that is overlapping with DDB1 binding domain, the interaction of HBx and nuclear export receptor Crm1 allow cytoplasmic trans-localization of HBx (Forgues et al., 2001). When HBx is located in the cytoplasm, it forms a complex with MEKK1, SEK1, SAPK/JNK and 14-3-3 proteins (Diao et al., 2001). These interactions result in prolonged cell survival and maintain a cellular environment favorable to HBV replication.

Besides nuclear localization, a proportion of HBx is transported to the mitochondria via its six amino acids at the C-terminus (111~116 amino acids). When cysteine 115 was mutated to alanine, mitochondria targeting of HBx was lost (Li et al., 2008). Mitochondrial HBx disrupts innate immunity by binding and down-regulating mitochondrial antiviral signaling protein (MAVS) and inhibits the activation of interferon regulatory factor 3 (IRF3) and β-interferon *in vitro* and *in vivo* (Wei et al., 2010, Wang et al., 2010, Kumar et al., 2011). On the mitochondria, HBx also binds the anti-apoptotic Bcl-2 protein to increase intracellular calcium level for virus replication and induces cell death (Bouchard et al., 2001, Chami et al., 2003, McClain et al., 2007, Gearhart and Bouchard, 2010, Yang and Bouchard, 2012, Casciano and Bouchard, 2018). Similarly, HBx interacts directly with the Bcl-2 homolog CED-9 through Bcl-2 homology 3 (BH3)-like motif, and as a result, trigger cytosolic calcium increase and cell death (Geng et al., 2012a, Geng et al., 2012b). Later on, a structural study confirmed the binding of a synthesized BH3-like HBx peptide (110~135 amino acids) with recombinant Bcl-2 protein. Remarkably, the binding of HBx peptide and Bcl-2 required iron and zinc for its stability (Jiang et al., 2016). HBx also interacts with Bcl-xL with a similar structure as Bcl-2 via the same motif (Zhang et al., 2019). Nevertheless, most findings were based on the overexpression of HBx using

transfection. Due to its low expression level during HBV replication, it is unclear whether HBx displays the same functions in infection models.

1.3.3. HBx-mediated transcription of cccDNA

Efficient transcription from cccDNA requires a collection of transcriptional factors and co-factors, including ubiquitous factors and liver-specific factors (Quasdorff and Protzer, 2010). Chromatin immunoprecipitation method (ChIP) allows the identification of the DNA binding sites of these factors. Using this technique, H3 and H4 Histones were identified to bind cccDNA and transcription from cccDNA was enhanced when the histones are acetylated (Pollicino et al., 2006). ChIP-seq analysis further identified that high levels of methylated and acetylated histones associate with active transcription occurring at specific regions on the cccDNA, whereas low levels of modified histones correlate with transcriptional repression (Tropberger et al., 2015). HBcAg and HBx are also associated with the minichromosome by direct or indirect binding (Belloni et al., 2009).

HBx protein associates with the ubiquitin-proteasome system (Minor and Slagle, 2014, Slagle and Bouchard, 2016, Slagle and Bouchard, 2018). Twenty years ago, HBx was firstly reported to interfere with cellular DNA repair (Becker et al., 1998). DDB2 directly binds damaged DNA and the whole DDB1-DDB2 complex is required for repair. HBx associates with DDB1 but not DDB2 and induces cell death, but this function is antagonized by DDB2 (Bontron et al., 2002). In turn, DDB2 induces nuclear accumulation of HBx that is independent of its DDB1 binding, and HBx protein is stabilized by the DDB1-DDB2 complex (Nag et al., 2001, Bergametti et al., 2002). However, HBx protein stimulates HBV replication via a DDB1-dependent manner distinct from that leading to cell death, when DDB2 is also required (Leupin et al., 2003, Leupin et al., 2005). Binding of HBx and DDB1 affects the cell cycle and causes chromosome segregation defects (Martin-Lluesma et al., 2008).

There are two predicted roles of the HBx-DDB1 complex in cccDNA transcription. The first model suggested that HBx does not directly bind cccDNA but associates with cccDNA via DDB1 binding, and the C-terminal HBx recruits transcriptional factors. However, so far no evidence using ChIP method supports the DDB1-cccDNA binding. The second model predicted HBx to recruit the whole DDB1 and ubiquitin ligases to “degrade a host restriction factor” or “prevent degradation of a dependency factor in transcription from cccDNA” (Hodgson et al., 2012). Later, such restriction factors were identified. HBx binds DDB1 and hijacks the Cullin 4A, an E3 ubiquitin ligase (Li et al., 2010c, Guo et al., 2014). HBx therefore bridges Cullin 4A

and ubiquitin-proteasome complex and promotes degradation of SMC5/6 and Talin-1 proteins that are all host restriction factors suppressing transcription from cccDNA (Decorsiere et al., 2016, Murphy et al., 2016, van de Klundert et al., 2016a).

1.4. Neddylation

Post-translation modification of proteins enlarge biological utilization efficacy of each protein and enable degradation of proteins when they are redundant. Proteins can be modified in different ways, such as ubiquitination, sumoylation and neddylation involving conjugation of small messenger proteins.

Ubiquitin is a well-characterized modifier required in many cellular processes that link to the ubiquitin-proteasome machinery (Ravid and Hochstrasser, 2008). Ubiquitination requires either one ubiquitin connected to the target protein (monoubiquitination) or -in most cases- a chain of multiple ubiquitins (polyubiquitination). Secondary ubiquitins are linked to one of the lysine residues or the first methionine of the primary ubiquitin that couples to the target protein and that number referring to the residues is defined for instance as “K48”, “M1”. Most K29 and K48 ubiquitination recruits the proteasome and initiates degradation of the target protein, whereas monoubiquitination and M1 and K63 polyubiquitination may regulate the protein but not mediate its degradation (Miranda and Sorkin, 2007). Of another ubiquitin-like messenger, SUMO (small ubiquitin-like modifier) labeling regulates protein aggregation, DNA repair and transcription (Gareau and Lima, 2010), Coupling of ATG8 and ATG12 regulates autophagy (Schreiber and Peter, 2014).

NEDD8 (neural precursor cell expressed developmentally downregulated protein 8) has been characterized as a modifier of its major target, the E3 ubiquitin ligase family of Cullin-ring ligases (CRL) (Enchev et al., 2015). NEDD8 is a conserved nuclear protein (Kamitani et al., 1997) and usually overexpressed with other neddylation enzymes in human cancers (Hori et al., 1999). Despite sharing 59 % similarity, NEDD8 and ubiquitin have no interchangeable functions because of their structural differences (Whitby et al., 1998). Mature NEDD8 protein is transferred by specific E1 and E2 enzymes and finally conjugated by E3 enzymes to a specific lysine in a targeted substrate protein.

1.4.1. NAE1 mediated NEDD8 transfer cascade

As shown in Figure 1.10.., the NEDD8 transfer cascade begins with one of the E1 activating enzymes (NAE1 in this thesis as an example), which is a heterodimer composed of amyloid-β precursor protein binding protein 1 (APPBP1) and ubiquitin activating enzyme 3 (UBA3) subunits. Binding NEDD8, ATP and magnesium at the adenylation site of UBA3 subunit is followed by AMP binding to the NEDD8 and leads to a pyrophosphate release. Therefore, NEDD8 is activated and attacked by the catalytic domain of the NAE1. At this step, the ATP binding of NEDD8 and NAE1 can be chemically blocked by a small molecule, termed MLN4924, which is an ATP competitor (Zhao et al., 2014). NAE1 restructures itself to be a closed confirmation that allows thiolation of the NEDD8 to the NAE1 active site and AMP release. NAE1 afterward recovers to its open confirmation and adenylates a second NEDD8 leading to conformational rearrangement again. Dual NEDD8-loaded NAE1 binds specific E2 enzymes, like UBE2M and UBE2F (not shown in the scheme). They catalyze a thiolation reaction and the transfer of NEDD8 from the active site of NAE1 onto the active site of the E2 enzyme (Huang et al., 2005). In addition, UBE2M directly binds the NEDD8 conjugated with the NAE1 (Huang et al., 2007). In both cases, NEDD8 is transferred from NAE1 to UBE2M or UBE2F in close proximity. Furthermore, E3 ligases catalyze the transfer of NEDD8 from the E2 enzymes onto the substrate protein. The well-characterized E3 ligases are the ring domain subunit ring-box protein 1 (RBX1), one of the components of CRL1~4, and their close homologue CRL5 complex (Walden et al., 2003, Huang et al., 2007, Huang et al., 2009, Olsen et al., 2010). Fully validated neddylation substrates are the cullin members that nucleate the largest class of ring ligases, CRLs. CRL neddylation leads to the activation of ubiquitin transfer activity by alternative conformations of RBX1 and the CRLs (Duda et al., 2008, Saha and Deshaies, 2008, Yamoah et al., 2008).

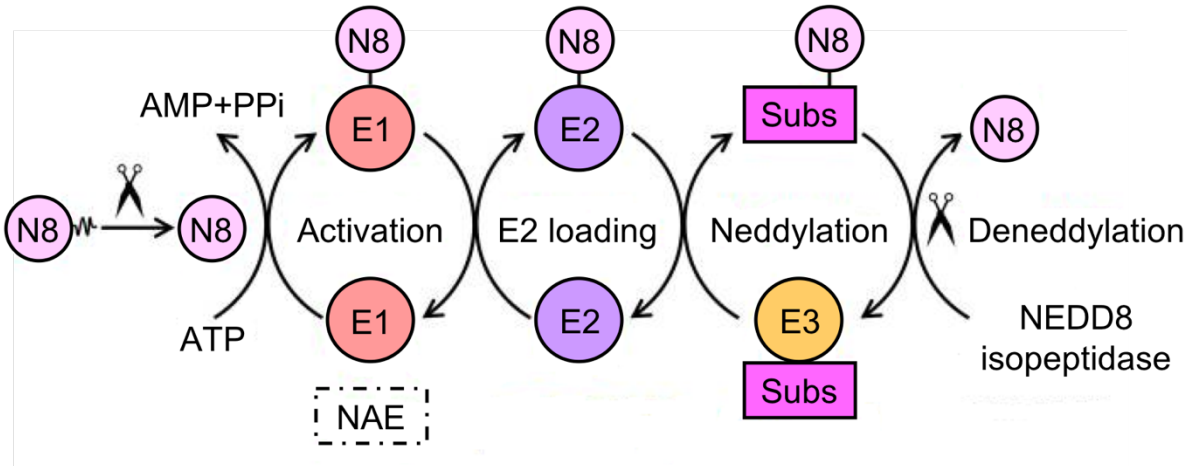

Figure 1.10. Scheme of the NEDD8 transfer cascade. The C-terminus of progenitor NEDD8 protein is cleaved to generate mature NEDD8 messenger. One of eight host enzymes, NAE1, couples NEDD8 protein to the E1 enzyme in an ATP-dependent manner. NEDD8 protein is further loaded on the E2 enzyme, the E3 enzyme and finally substrates (mostly Cullin-ring

ligases). Neddylation of the substrates is reversible by cleaving NEDD8 out of the targets by the NEDD8 isopeptidase. Adapted from (Zhao et al., 2014) with permission.

1.4.2. NAE1 inhibitor MLN4924 and its antiviral potential

HBx enhances HBV replication *in vivo* and *in vitro* (Balsano et al., 1993, Lucifora et al., 2011). HBx induces degradation of host restriction factor(s) (Minor and Slagle, 2014) that were identified as SMC5/6 proteins, which are ubiquitin labelled and degraded in an HBx-dependent manner (Decorsiere et al., 2016, Murphy et al., 2016), raising up the opportunity that this function of HBx may become a drug target. A prerequisite of SMC5/6 degradation is the HBx binding of DDB1 and recruitment of host E3 ubiquitin ligase CRL4A. As depicted above, to be fully activated, CRL4A neddylation is mandatory, and thereby neddylation inhibitor MLN4924 may result in the unavailability of the HBx-DDB1-CRL4A complex.

Pharmacologic inhibition of CRL4A neddylation is thus practical. MLN4924 is a first-in-class NAE1 inhibitor being tested in phase III clinical trial towards patients with melanoma and lymphoma, since it selectively and potently inhibits catalytic activity of NAE1 at EC_{50} value of nanomolar concentration (EC_{50} = 4 nM in biochemical analysis) (Soucy et al., 2009, Brownell et al., 2010). MLN4924 resembles AMP and binds the adenylation site of NAE that competes for loading of NEDD8. MLN4924 also forms a sulphamate adduct and inhibits CRL4A neddylation and activity (Embade et al., 2012). From the virological point of view, it has been reported that MLN4924 blocks simian immunodeficiency virus and lentiviral infections by disrupting Vpx-mediated neddylation-dependent SAMHD1 degradation, suggesting that host neddylation signaling is hijacked by retrovirus and the inhibition of neddylation restricts lentivirus replication (Hofmann et al., 2013, Wei et al., 2014). Furthermore, a recent study extends MLN4924 application to broader and more potent antiviral activities against human and mouse cytomegalovirus, and herpes simplex virus (Le-Trilling et al., 2016). Taking that HBx also hijacks host CRLs in the context of transactivation into account, it is reasonable to speculate that MLN4924 may have an antiviral effect on HBV replication.

1.5. Antivirals for HBV

Vaccines and antivirals are two major ways of preventing or controlling viral infection. Although HBV vaccines are safe and effective, they have no effect against established chronic HBV infection. Potential therapeutic vaccines that may stimulate the host immune system for HBV clearance are far from being approved. Moreover, some people who do not generate protective anti-HBsAg antibodies after complete vaccinations are deemed “non-responders”. It is estimated that 5% of people who are at elder age or have cigarette smoking, alcohol drinking,

obesity, chronic illness and other factors might not respond to vaccines. HBV vaccine non-responsiveness also varies among each subject population (Saco et al., 2018). In addition, a small proportion of people are responders but have a rapid decline of anti-HBsAg titer over 2~3 years after successful vaccination (Propst et al., 1998). Therefore, antivirals with curative potential are required.

1.5.1. Overview of anti-HBV agents

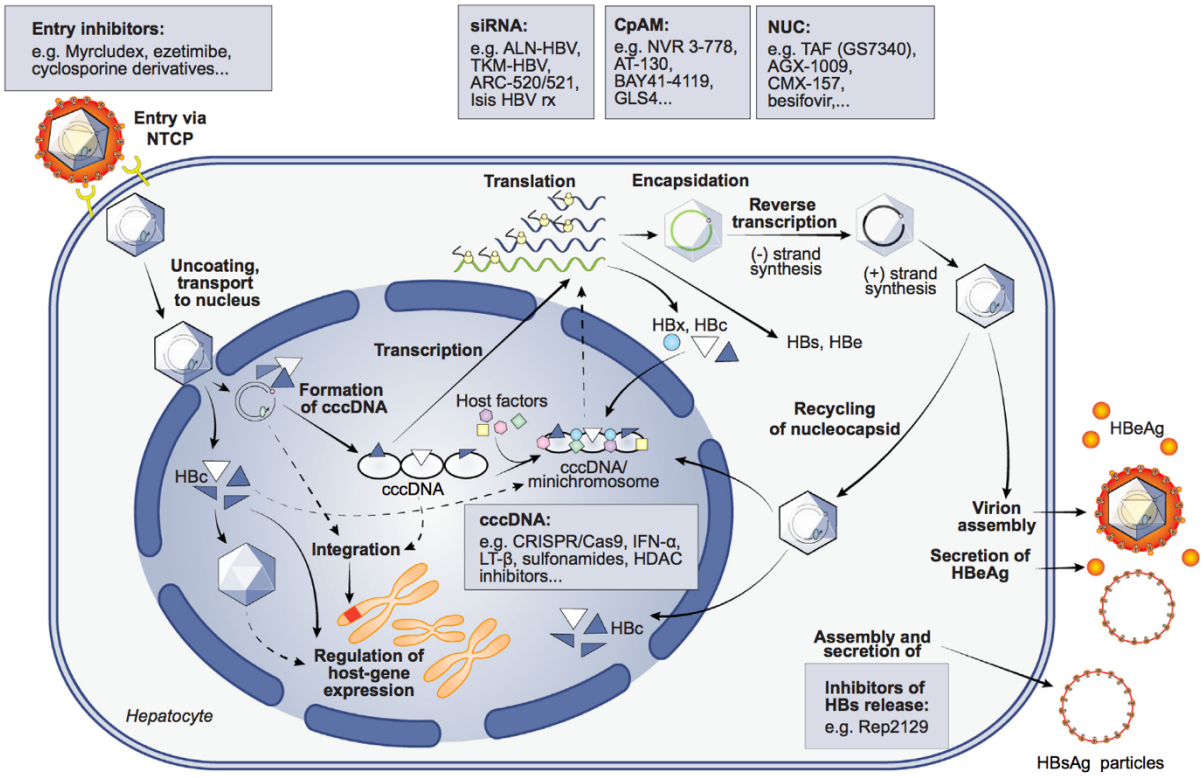

Figure 1.11. Antiviral targets on HBV replicative steps in development. Listed entry inhibitors interfere with HBV entry via NTCP. rcDNA-to-cccDNA conversion can be affected by sulfonamides. cccDNA can be degraded by specific CRISPR or transcriptionally silenced by histone deacetylase inhibitors. Transcription of cccDNA is hampered by specific siRNA. Reverse transcription is blocked by nucleos(t)ide analogues (NUC). Capsid assembly is targeted by capsid modulator (CpAM). Assembly ad secretion of HBsAg is blocked by nucleic acid polymers. Adapted from (Durantel and Zoulim, 2016) with permission.

As shown in Figure 1.11., except HBx, most of the viral proteins and replicative steps have been targeted with approved drugs or investigational inhibitors. Targeting viral entry, entry inhibitors Myrcludex B and cyclosporine derivatives interfere with preS1-mediated NTCP binding. How virus trafficking after its entry is largely unknown, but the rcDNA-to-cccDNA conversion has been tested as an *in vitro* drug target. Two disubstituted sulfonamides, termed CCC-0346 and CCC-0975 and selected from a small molecule library with 85,000 compounds, affect rcDNA conversion to cccDNA without inhibiting viral polymerase and rcDNA

replication (Cai et al., 2012). Decomposition of established cccDNA can be induced not only by cytokines (IFN-α, IFN-γ, and TNF-α) (Xia et al., 2016) but theoretically also by exogenous engineered nucleases (ZFNs, TALENs, and CRISPR/Cas9) (Bloom et al., 2013, Weber et al., 2014, Seeger and Sohn, 2014, Seeger and Sohn, 2016). In the next step, cccDNA transcription may be silenced by epigenetic modifiers targeting cccDNA methylation, histone methylation and acetylation (e.g. HDAC inhibitors). Host nuclear receptors (e.g. retinoid X receptor α) seems to positively regulate cccDNA transcription. RXRα-specific agonist Bexarotene was found to inhibit HBV replication and silencing of RXRα led to evaluated cccDNA formation and antigen production (Song et al., 2018).

Whether HBx will be a pharmacologic target? It may be an ideal target of blocking transcription of cccDNA that requires HBx. Although one of the FDA-approved drugs, terbinafine, specifically and potently inhibits HBx-mediated HBV RNA transcription in HepG2.2.15 and transfected HepG2 cells, it is unclear whether it inhibits transcription from authentic cccDNA in *de novo* infection (van de Klundert et al., 2016b).

Many silencing RNAs (siRNA) induce degradation of viral transcripts without specificity. Among them (ARB-1467, ARB-1740, ARC-520, RG6004, ARO-HBV, ALN-HBV, etc.), ARC-520 consists of two siRNAs conjugated to cholesterol and shows favorable tolerability in phase I clinical trial (Schluep et al., 2017). In the phase II trial, HBsAg is strongly suppressed in treatment-naïve HBeAg positive patients but less significantly reduced in patients who are either HBeAg negative or received long-term NUC treatment (Wooddell et al., 2017).

For the next step, NUCs are approved as first-line drugs. As HBV polymerase is a reverse transcriptase with ribonuclease H activity, the latter is also a target of specific RNase H inhibitors (Tavis et al., 2013, Hu et al., 2013, Cai et al., 2014, Lu et al., 2015, Tavis and Lomonosova, 2015, Lomonosova et al., 2017, Tavis et al., 2018).

Disturbing nucleocapsid formation and assembly, at least three classes of capsid inhibitors are in development. However, neither NUCs nor capsid modulators induces HBsAg reduction. Nucleic acid polymers (NAPs) are first-in-class HBsAg secretion inhibitors, which interfere with the formation of subviral particles and prevent the release of them from infected hepatocytes. Two of the NAPs, REP 2139 and REP 2165, are well tolerated and have substantial antiviral activity in patients in phase I/II trials. REP 2139 administration leads to rapid elimination of HBsAg and reduction of viral load in patient sera (Roehl et al., 2017, Bazinet et al., 2017). Recently, a small molecule, RG7834, belonging to the dihydroquinolizinones, was discovered by screening a small molecule library with one million compounds. RG7834

profoundly reduced HBsAg as well as viral load in infected PHH and humanized mice. Moreover, Entecavir and pegylated IFN-α-2a when treated in combination with RG7834 resulted in more potent reductions of HBsAg and DNA levels in humanized mice (Mueller et al., 2018).

Taken together, small molecule inhibitors in development have targeted most of the intracellular steps in HBV replication. However, elimination of cccDNA or silence of HBx-mediated transcription from cccDNA (one way of functional cure) is still not possible. In the following table, all compounds approved and in development for chronic hepatitis B are summarized (Table 1.4.).

Table 1.2. Compounds approved and in development for therapeutic use (updated July 2019).

Name	Brand Name	Nature	Mechanism	Company	Status
IFN-α-2b	Intron A	cytokine	immunomodulator	Merck	Approved
Pegylated IFN	Pegasys	cytokine	immunomodulator	Genentech	Approved
Lamivudine	Epivir	NUC	inhibits polymerase	GlaxoSmithKline	Approved
Adefovir dipivoxil	Hepsera	NUC	inhibits polymerase	Gilead	Approved
Entecavir	Baraclude	NUC	inhibits polymerase	Bristol-Myers Squibb	Approved
Telbivudine	Tyzeka	NUC	inhibits polymerase	Novartis	Approved
Tenofovir	Viread	NUC	inhibits polymerase	Gilead	Approved
Tenofovir alafenamide	Vemlidy	NUC	inhibits polymerase	Gilead	Approved
ANA 380	Besivo	NUC	inhibits polymerase	Ildong Pharma	Approved§
Myrcludex B	Bulevirtide	peptide	NTCP	MYR GmbH	Phase III
Cyclosporin A	Sandimmune	peptide	NTCP	Norvatis	Approved#
HBIG	HepaGam B	antibody	L/M/S	Aptevo Bio	Approved
BAY 41-4109		HAP	capsid assembly	Bayer GmbH	Preclinical
GLS4 (morphothiadin)		HAP	capsid assembly	HEC Pharma	Phase II
NVR 3-778		SBA	capsid assembly	Janssen	Phase II
JNJ 56136379		CpAM	capsid assembly	Janssen	Phase II
ABI-H0731		CpAM	capsid assembly	Assembly Bio.	Phase II
AB-506		SBA	capsid assembly	Arbutus Bio.	Phase I
RG7907		CpAM	capsid assembly	Roche	Phase I
VIR-2218		siRNA	RNAi silencer	Vir Biotech	Phase II

RG6004	siRNA	RNAi silencer	Roche	Phase II
ARO-HBV	siRNA	RNAi silencer	Janssen	Phase II
AB-729	siRNA	RNAi silencer	Arbutus Bio.	Phase I
DCR-HBVS	siRNA	RNAi silencer	Arbutus Bio.	Phase II
EBT106	sgRNA	CRISPR/Cas	Excision Bio.	Preclinical
RNase H inhibitor		inhibits polymerase	Arbutus Bio.	Preclinical
ccc_R08		cccDNA decay	Roche	Preclinical
RG7834	carboxylic acid	HBsAg inhibitor	Roche	Phase I
REP 2139	NAP	HBsAg inhibitor	Replicor	Phase II
REP 2165	NAP	HBsAg inhibitor	Replicor	Phase II
EYP001	unknown	FXR agonist	Enyo Pharma	Phase I

NUC: nucleos(t)ide analogue, NTCP: sodium taurocholate cotransporting polypeptide, HAP: heteroaryldihydropyrimidines, SBA: sulfamoyl benzamides, CpAM: core protein allosteric modifiers. NAP: nucleic acid polymer.

§: approved outside USA, #: approved for other diseases. Adapted from the Hepatitis B Foundation.

1.5.2. Interferon-α and pegylated interferon-α

Interferon-α (IFN-α) is the first drug, which was approved by the FDA in 1991. As a natural first-line defense against viruses, IFN-α with interferon-stimulated genes (ISG) has a broad antiviral activity. Later on, polyethylene glycol was conjugated to IFN-α and this modification allows interferon lasting longer *in vivo.* Pegylated IFN-α was licensed in 1995. Both pegylated IFN-α and IFN-β are medically used, yet only pegylated IFN-α-2a (PegaSys) and IFN-α-2b (IntronA/PegIntron) given by subcutaneous injection are currently used for chronic HBV treatment. However, the response rate of pegylated interferons remains low (5~20%) and side effects are common including influenza-like symptom, headache and fatigue (Janssen et al., 2005, Xia and Protzer, 2017).

IFN-α and ISG play pleiotropic roles in counteracting HBV replication. Firstly, IFN-α-treated HBV-infected HepaRG cells release soluble factors that compete with the virus for HSPG binding and restrict HBV spread to neighbor cells. The interferon-induced secreted factors inhibited HBV binding to heparin. Size exclusion purification showed that they are larger than 100 kD, although the nature of these factors was never characterized (Xia et al., 2017b). Secondly, high doses of IFN-α mediate non-cytolytic clearance of cccDNA in infected PHH and HepaRG cells. To be specific, IFN-α specifically induces nuclear deaminase APOBEC3A, which is also an ISG and binds nuclear HBcAg to tether on cccDNA (Lucifora et

al., 2014). Deaminated cccDNA by APOBEC3A becomes prone to be degraded by hydrolysis of another nuclease ISG20 (personal communications with Daniela Stadler). IFN-α upregulates APOBEC3A level *in vitro* and in the livers of treated patients and chimpanzees, the response to IFN-α treated patients correlates with IFN-mediated base excision repair that leads to cccDNA decay (Li et al., 2017). Thirdly, IFN-α inhibits transcription of viral RNA from cccDNA minichromosome by regulating its epigenetic modification *in vitro* and in humanized mice. IFN-α leads to histone hypo-acetylation (via reducing the H3K9 and H3K27 acetylation) and recruitment of transcriptional repressors such as histone deacetylase 1 (HDAC1) on cccDNA (Belloni et al., 2012, Liu et al., 2013). The reduction of histone activity by IFN-α in HBV-infected PHH can be recapitulated by an epigenetic modulator, C646, which inhibits histone acetyltransferases (Tropberger et al., 2015). Fourthly, IFN-induced tripartite motif 22 protein (TRIM22) inhibits HBV core promoter activity and gene expression *in vitro* and *in vivo* (Gao et al., 2009). Fifthly, many ISGs restrict viral transcription. For instance, zinc finger proteins trigger viral RNA decay *in vitro* and *in vivo* (Mao et al., 2013, Chen et al., 2015). Myeloid differentiation primary response protein 88 (MyD88) facilitates this decay (Li et al., 2010b). Myxoma resistance protein 1 (Mx1) impedes pgRNA encapsidation (Gordien et al., 2001, Li et al., 2012). APOBEC3G induces genome hyper-mutation and it is incorporated into cytosolic nucleocapsids to inhibit viral DNA replication (Noguchi et al., 2005, Nguyen et al., 2007, Nguyen and Hu, 2008). Sixthly, IFN-α upregulates RNA-dependent protein kinase (PKR) that inhibits the synthesis of viral proteins. Consequently, the intracellular level of capsid proteins is reduced (Park et al., 2011). Finally, IFN-α treatment enhances tetherin expression that blocks the egress of HBV particles. Tetherin colocalizes with virions at the multivesicular bodies and therefore reduces virus budding without affecting intracellular viral replication (Yan et al., 2015). In sum, IFN-α and ISGs almost target all the replicative steps in the HBV life cycle. Besides, IFN-α is a strong immunomodulator that stimulates adaptive immune responses. Recruited cytotoxic T cells are able to kill the HBV infected hepatocytes.

1.5.3. Nucleos(t)ide analogues

Beside IFN-α and pegylated IFN-α, six nucleoside and nucleotide analogues (NUCs) are licensed by FDA for treating chronic hepatitis B: Epivir (Lamivudine, approved in 1998), Hepsera (Adefovir dipivoxil, 2002), Baraclude (Entecavir, 2005), Tyzeka (Telbivudine, 2006), Viread (Tenofovir, 2008), and Vemlidy (Tenofovir alafenamide or TAF, November 2016). Lamivudine, Telbivudine and Entecavir are nucleoside analogues containing a nucleic acid

analogue and a sugar, whereas Adefovir dipivoxil, Tenofovir disoproxil fumarate and Tenofovir alafenamide are nucleotide analogues that contain a nucleic acid, a sugar and 1~3 phosphate groups (Fung et al., 2011, Lo and Wong, 2014). All six NUCs target the viral polymerase and potently inhibit minus-strand DNA synthesis by reverse-transcription mediated by the viral polymerase. However, they have their specific features.

Lamivudine (3TC, LAM), used to treat HIV infection, was the first nucleoside analogue approved for the treatment of chronic hepatitis B at a dose of 100 mg/day by oral administration. It is a broad reverse transcriptase inhibitor acting at HBV polymerase as well as HIV reverse transcriptase. It reduces viral DNA load, improves HBeAg seroconversion, normalizes ALT level and reverses fibrosis (Lai et al., 1998, Dienstag et al., 1999). Upon treatment, Lamivudine decreases the risk of hepatocellular carcinoma in cirrhotic patients when compared with the patients without treatment (Liaw et al., 2004, Yuen et al., 2007). However, the major drawback of Lamivudine therapy is frequent drug resistance mutation at the tyrosinemethionine-aspartate-aspartate (YMDD) motif in the catalytic domain of the viral polymerase. Emergence frequency of YMDD mutants arises from 15~32 % in the first year to 69 % in the fifth year of treatment (Lai et al., 2003). Other mutations responsible for drug resistance include rtM204V concomitantly occurring with rtL180M and rtM204I occurring alone or together with rtL180M (Allen et al., 1998). Nevertheless, Lamivudine is safe, moderately effective and improves liver function in patients (Kapoor et al., 2000, Yao et al., 2001).

Adefovir dipivoxil (ADV) was the second nucleotide analogue, approved for treating chronic hepatitis B at a dose of 10 mg/day. Adefovir leads to a thousand-fold reduction on HBV DNA titer, frequent HBeAg seroconversion, and normalization of ALT concentration compared with the placebo (Marcellin et al., 2003), although at 10 mg/day dose the speed of viral suppression was slow (>48 weeks). One great significance of Adefovir is that Lamivudine resistant rtM204V/I mutant is sensitive to Adefovir (Lampertico et al., 2005). However, upon Adevovir treatment two major mutations of viral polymerase rtA181V/T and rtN236T are emerging (Angus et al., 2003). 29 % resistance rate occurs in the fifth year of its treatment (Hadziyannis et al., 2006). Increased nephrotoxicity is associated with Adefovir treatment at higher doses. This nephrotoxicity with a decrease in serum phosphate and an increase in serum creatinine levels started from 4~12 months after therapy. Toxicity was disappeared when the treatment was terminated (Marcellin et al., 2008).

Entecavir (ETV) was licensed at a dose of 0.5 mg/day for treatment naïve patients and 1 mg/day for Lamivudine ineffective patients. As a guanosine analogue, Entecavir inhibits priming of viral polymerase involving guanosine and allows several additional nucleotides to

be incorporated prior to termination, in contrast to other NUCs that are obligate terminators (Langley et al., 2007, Tchesnokov et al., 2008). Compared to Lamivudine, Entecavir showed up to two thousand-fold efficacy in viral DNA reduction *in vitro*. The drug resistance of Entecavir was rare and only 1.2 % after 5-year treatment (Tenney et al., 2009, Chang et al., 2010), because three mutations are required before virus develops resistance. In addition to rtL180M and rtM204V mutations responsible for Lamivudine resistance, a third mutation of rcI169T, rcT184G, rtS202I or rtM250V is required (Baldick et al., 2008a, Baldick et al., 2008b).

Telbivudine (LdT), a thymidine analogue, was approved for treating chronic hepatitis B at a dose of 600 mg/day. Telbivudine has stoichiometric L-configuration opposite to natural nucleosides. It is incorporated into premature chain termination and competes with 5'-triphosphate thymidine and thereby inhibits viral polymerase. Telbivudine was much superior to Lamivudine in HBV suppression with the relative lower opportunity of drug resistance (Lai et al., 2007). After 24-week treatment, Telbivudine also showed better HBV suppression compared with Adefovir. However, mutations are high-frequent rtM204I with or without concomitant rtL180M and rtL80I/V and rare rtA181T/V and rtL229W/V. For side effect, peripheral neuropathy was also reported when patients have received a combination of Telbivudine and IFN-α, thus this combination is forbidden.

Tenofovir disoproxil fumarate (TDF) and its prodrug Tenofovir alafenamide (TAF) were approved for the treatment of chronic HBV infection at 300 mg/day and 25 mg/day, respectively. As chain terminator, both drugs compete for the natural substrate of deoxyadenosine 5'-triphosphate and inhibit viral polymerase, as a result, mediate HBV DNA reduction, HBeAg seroconversion and ALT normalization (Marcellin et al., 2008, Heathcote et al., 2011). So far, the sole documented primary resistance to Tenofovir occurred in two patients. A quadruple mutation of rtS106C, rtH126Y, rtD134E and rtL269I confers Tenofovir resistance (Park et al., 2019). Nephrotoxic side effect appears to be mild and less severe compared to Adefovir (Heathcote et al., 2011, Patterson et al., 2011).

Taken together, all approved inhibitors are potent in HBV DNA reduction and ALT normalization. However, long-term treatment of most of them leads to multiple drug resistance, except Tenofovir and Tenofovir alafenamide. This class inhibitors specifically target viral polymerase but not cccDNA. Therefore, they can suppress HBV replication but none of them is curative.

1.5.4. Entry inhibitors

The human NTCP gene is one of the members in the SLC10A family. NTCP protein is a 34 kD that can shift to 56 kD upon glycosylation. NTCP is mainly localized on the basolateral membrane of hepatocytes and it is a transporter of bile salts into hepatocytes (Hagenbuch and Meier, 1994). In 2012, human NTCP was identified as the HBV entry receptor (Yan et al., 2012). Constitutive expression of human NTCP renders non-susceptible hepatoma cells susceptible to HBV and HDV infections (Yan et al., 2012, Ni et al., 2014). Within NTCP, a key region (157~165 amino acids) is crucial for the binding of HBV preS1 protein and another region (84~87 amino acids) is responsible for post-binding processes (Yan et al., 2014, Ni et al., 2014). Later NTCP becomes a drug target.

Before the characterization of NTCP, Urban et al. identified that recombinant DHBV preS polypeptide inhibits DHBV infection in a dose-dependent manner. An 85-amino-acid preS peptide showed maximal inhibition (Urban et al., 1998). HBV infection also depends on the N-terminus of preS1 (3~77 amino acids) (Le Seyec et al., 1999). In the initial test, a myristoylated preS1 peptide at the large surface protein bound hepatocytes and blocked DHBV infection *in vitro* (Urban and Gripon, 2002). In the same year, differentiated HepaRG cell line was established as an *in vitro* HBV infection system (Gripon et al., 2002). Using PHH and HepaRG cultures, the myristoylated N-terminal 47 amino acids (2~48) of the HBV preS1 domain (genotype D) was found to specifically inhibit HBV infection with the EC_{50} value of 8 nM (Gripon et al., 2005). Amino acids (2~18) of the N-terminal preS1 efficiency blocked HBV infection and the amino acids (28~48) enhanced the inhibitory effect. Myristoylated 2~48 amino acids selectively bound primary tupaia hepatocytes (Glebe et al., 2005). Deletions and mutations between 11~21 amino acids led to the loss of inhibitory activity and finally key residues (amino acids 9~15, NPLGFFP) were confirmed. The peptide (2~48 amino acid) derived from the preS1 was further used to identify NTCP (Yan et al., 2012). Similarly, HDV infection is inhibited by the same peptide with the same specificity (Engelke et al., 2006, Schulze et al., 2010, Meier et al., 2013).

Myristoylated preS1-derived lipopeptides are promising candidates for antiviral therapy. In the preclinical study, the peptides permit subcutaneous delivery, accumulate in the liver and prevent HBV entry *in vivo*, when urokinase-type plasminogen activator and severe immunodeficient mice (USB) were repopulated with PHH or tupaia hepatocytes (Petersen et al., 2008). One of the peptides was officially designated as “Myrcludex B” (the myristoylated peptide excludes hepatitis B). Myrcludex B was solid-phase synthesized for preclinical use (Schieck et al., 2010). In HBV-infected USB mice that were superinfected with HDV, Myrcludex B treatment efficiently hinders the establishment of HDV infection (Lutgehetmann et al., 2012). Furthermore, in HBV mono-infection, Myrcludex B efficiently blocks HBV

spreading from initial infected human hepatocytes to naïve hepatocytes. Strikingly, Myrcludex B hinders amplification of the cccDNA pool (Volz et al., 2013).

In phase Ia clinical trial, Myrcludex B showed well tolerability and mild adverse effects at a dose of 20 mg by intravenous injection in healthy volunteers. Given by subcutaneous injection, 10 mg and higher doses reached a target saturation for at least 15 h (Blank et al., 2016). In phase Ib/IIa trials, 24 chronic hepatitis D patients were equally randomized (1:1:1) and received Myrcludex B, pegylated IFN-α-2a, or both. HDV RNA level is dramatically declined after 24-week treatment. HDV RNA becomes negative in two of eight patients that received either Myrcludex B or pegylated IFN-α, and in five of seven patients who have received both drugs. ALT levels are normalized in six of eight patients in the Myrcludex B group. Virus kinetic analysis suggests a synergistic effect of Myrcludex B and pegylated IFN-α on HDV (Bogomolov et al., 2016). Furthermore, a phase IIb trial compares Myrcludex B with Tenofovir and applies for co-treatment in chronic HDV patients. Another phase IIb trial with larger cohort amount confirms that HDV is eliminated in 40 % of the HBV/HDV co-infected patients upon co-treatment of Myrcludex B and IFN-α (Wedemeyer et al., AASLD Meeting 2018 & EASL ILC Meeting 2019). Besides its therapeutic potential, unlabelled and fluorescein-labeled Myrcludex B also serve as decent tools to study virus-receptor interaction after hNTCP identification (Ni et al., 2014, Urban et al., 2014, Li and Urban, 2016).

With weaker activity than Myrcludex B, small molecules can also inhibit HBV and HDV entry by targeting hNTCP. Cyclosporin A and its derivative SCYX1454139 show some NTCP-binding affinity (Nkongolo et al., 2014, Watashi et al., 2014, Shimura et al., 2017). Ezetimibe inhibits HBV entry (Lucifora et al., 2013) and lipase inhibitor Orlistat targets an early step in the HBV life cycle (Esser et al., 2018). However, none of them is as potent as Myrcludex B and has respective EC_{50} values at the micromolar range. HBV attachment before NTCP binding also becomes a drug target of surimin and heparin (Petcu et al., 1988, Schulze et al., 2007).

Table 1.3. Attachment and entry inhibitors.

Class	Name	Nature	Target	Clinical status	EC_{50} value*
Attachment	suramin	small molecule	L/M/S	approved§	25 μM
Inhibitor	heparin	glycoglycan	L/M/S	approved§	9.4 μg/mL
Entry	Myrcludex B	peptide	NTCP	phase III	8 nM
Inhibitor	Cyclosporin A	peptide	NTCP	approved§	1 μM
	SCYX1454139	peptide	NTCP	preclinical	0.17 μM
	Ezetimibe	small molecule	NTCP	approved§	18 μM

Orlistat	small molecule	unknown	approved§	50 μM

§: approved for other diseases but not chronic hepatitis B.

*: PHH or HepaRG cells. Adapted from (Lempp and Urban, 2014)

1.5.5. Capsid inhibitors

Core protein assembles with viral polymerase and pgRNA to form the nucleocapsid shell in which reverse transcription occurs as long as polymerase-bound pgRNA is encapsidated (Fletcher and Delaney, 2013). Interaction between core proteins or interference with core assembly is a target of capsid inhibitors. It has been shown that truncated core protein lacking its C-terminus retains the ability to assemble (Nassal, 1992). Therefore, mutants of the assembly domain have been used *in vitro* to screen modulators of capsid formation and assembly (Stray et al., 2006, Zlotnick et al., 2007).

Characterized capsid inhibitors are classified as heteroaryldihydropyrimidines (HAP), phenylpropenamides (AT) and sulfamoyl benzamides (SBA). The earliest HAP inhibitor is BAY 41-4109, which has an EC_{50} value of 120 nM and reduces the amounts of core protein in HepG2.2.15 cells (Deres et al., 2003, Klumpp et al., 2015). In HBV transgenic mice (Tg HBV1.3 fsX(-)3'5'), oral administration of BAY 41-4109 at 15 mg/kg for 28 d induced a significant reduction of viral DNA and cytoplasmic HBcAg levels in the liver (Weber et al., 2002). Moreover, BAY 41-4109 at 25 mg/kg for 5 d in humanized mice transplanted with PHH and infected with HBV led to a 10-fold drop in viral load (Brezillon et al., 2011). BAY 41-4109 has dual effects on capsid assembly. One BAY 41-4109 molecule is sufficient to induce every five capsid dimers to form non-capsid polymers (BAY: dimer = 1:5), and the formed capsids are stabilized by BAY 41-4109 at a ratio of one molecule per two dimers (BAY: dimer = 1:2). However, capsids are destroyed to generate large non-capsid polymers, when the ratio of BAY 41-4109 and capsid dimer is 1:1 or higher (BAY: dimer > 1:1). BAY 41-4109 may induce aberrant assembly at low concentrations when in excess misdirects assembly by reducing the stability of capsids (Stray et al., 2005, Stray and Zlotnick, 2006). HAP molecule binds the pocket of core protein at the dimer-dimer interface. Hence, a V124W core mutation at this pocket results in HAP resistance and confers HAP-like behaviors (Bourne et al., 2006, Tan et al., 2013). Further structural modification of the BAY 41-4109 identifies GLS4 (morphothiadine mesilate) which is more potent than BAY 41-4109 *in vitro* (Wang et al., 2012, Klumpp et al., 2015). GLS4 is 10-fold more potent with mean EC_{50} values of 15 nM (Klumpp et al., 2015). Compared to BAY 41-4109, GLS4 has no cytotoxicity up to 25 μM and shows a sustained decline of viral DNA in nude mice injected with HepAD38 cells. So far, GLS4 is in clinical evaluation in China (Wu et al., 2013).

The second class of capsid inhibitors is the AT series. AT-61 is a potent inhibitor of HBV replication *in vitro* (King et al., 1998) and its derivative AT-130 shows enhanced potency (Perni et al., 2000). Both derivatives are very effective against WT and NUC-resistant HBV mutants (Delaney et al., 2002). AT-130 blocks replication on the step of pgRNA packaging and nucleocapsid forming (Feld et al., 2007). Although structural studies have shown some differences between AT-130-bound and free capsids, co-structure of the capsid and AT-130 complex reveal that AT-130 binds the capsid and leads to tertiary and structural changes without disrupting the capsid structure (Katen et al., 2013). AT-130 locates mainly in the B-subunit pocket at the dimer-dimer interface, whereas HAP resides in the pocket of the C-subunit, which differs the two classes.

A third-class nucleocapsid assembly modulator is SBA, originally identified from high throughput screening using a murine AML12HBV10 cell line with stable HBV integration and pgRNA transcription (Campagna et al., 2013). Direct comparison of the SBA with BAY 41-4109 and AT-61 has shown that SBA inhibits HBV replication in a manner to form capsids devoid of nucleic acids. Interestingly, SBA showed selectivity against HBV, but not WHV or DHBV replication in HepG2 cells (Campagna et al., 2013). One of the representative SBA compounds, NVR 3-778, is the most advanced in development. Six-week NVR 3-778 treatment in humanized mice leads to the reduction of viral DNA that is comparable to Entecavir treatment. NVR 3-778 also shows a synergistic effect in combination with pegylated IFN-α and inhibits DNA levels to an undetectable level (Klumpp et al., 2018). NVR 3-778 is well-tolerated, pharmacologically effective and as efficient in phase Ia trial as *in vitro*. In phase Ib clinical trial, NVR 3-778 shows a marginal reduction in viral load when daily given at 400 mg. A 1.7-log decline in HBV DNA level, however, was observed at a higher dose of 600 mg/day (Yuen et al., 2019).

1.6. *In vitro* cell culture models

HBV has a narrow species and tissue tropism and thereby HBV study relies on a few *in vitro* cell culture models. Although hepatoma cell lines are widely used that support HBV replication and assembly, when they are transfected with cloned HBV genomes (Sells et al., 1988), transfection systems have no real cccDNA and thereby transcription from authentic cccDNA can not be studied (Slagle et al., 2015).

It was a long history when only PHH and primary tupaia hepatocytes (PTH) support the "pre-transcription" steps in the HBV life cycle that include receptor-mediated entry, uncoating, import of nucleocapsid in the nucleus, rcDNA repair, cccDNA formation (Gripon et al., 1988,

Kock et al., 2001). Gripon et al. demonstrated that the supplement of 1.5% DMSO in the culture medium efficiently enhanced HBV replication in PHH (Gripon et al., 1988). They further illustrated that the addition of polyethylene glycol increased viral adsorption and penetration (Gripon et al., 1993). So far PHH is still the gold model. However, once isolated and plated, primary hepatocytes *ex vivo* rapidly lose the differentiation state and HBV susceptibility. PHH also have a short life span of 1~2 weeks *in vitro* and it is not practical to study chronic HBV infection. In this year, the long-term functional maintenance of PHH over 4 weeks was achieved by using a combination of five chemicals in culture medium, whether this new system is the best physiologically relevant is under debate (Xiang et al., 2019).

In 2002, HepaRG, a progenitor cell line, which was isolated and colonized from the liver of a female HCV-infected patient, supported efficient *de novo* HBV infection when fully differentiated and infected. Cellular metabolism and innate immune responses in HepaRG cells are close to PHH. Similar to PHH, HepaRG cells show undetectable expression level of α-fetoprotein (AFP) but high levels of aldolase B, Cyp 2E1 and 3A4 liver enzymes (Gripon et al., 2002, Ni et al., 2014). However, a disadvantage of HepaRG cells includes low infectivity rate as only 5~10 % hepatocyte-like cells in the total cells could be infected. After differentiation processes, a majority of co-existing biliary cells are not susceptible to HBV and HDV infection. Besides, long-term maintenance of HepaRG cells is not available, as all viral markers including cccDNA stay stable up to 3 weeks p.i..

After another ten years, the HBV receptor NTCP was discovered (Yan et al., 2012), which provides a new direction to generate hepatoma cell lines reconstituted with human NTCP (hNTCP). Stable expression of hNTCP renders HepG2 and Huh7 hepatoma cells fully susceptible to HBV and HDV infection and enhances the infectivity rate in HepaRG cells (Ni et al., 2014). Different from Huh7^{hNTCP} cells with rather low infection rate (5 %) of HBV and deficiency in innate immunity, HepG2^{hNTCP} cells are more robust and supportive of high HBV infectivity (20~80 %). Moreover, HepG2^{hNTCP} cells are suitable for long-term cultivation after infection (eight weeks). Yet low levels of HBsAg secretion is a characteristic in HepG2^{hNTCP} cells when infected with cell culture (cc)-derived HBV. This low HBsAg level is partially caused by hNTCP overexpression and specific for HBV genotype D (Li et al., 2016a). Of special note, a slow proliferating HepG2^{hNTCP} cell clone, HepG2-NTCPsec+, supports viral spread to neighbor non-infected cells and multiple rounds of HBV infection (Konig et al., 2019)

Ectopic expression of hNTCP in cynomolgus macaque, rhesus macaque and swine hepatocytes permits HBV infection with comparable replication efficiencies to human hepatocytes, suggesting that hNTCP is the only limiting host factor in macaques and pigs

(Lempp et al., 2017). However, reconstitution of hNTCP did not provide HBV susceptibility in primary mouse, rat and dog hepatocytes, probably due to lack of other human-specific factors (Lempp et al., 2016a). Remarkably, the first and only mouse cell line, AML12, gains HBV susceptibility upon hNTCP expression, although the infection rate is rather low (<1 %) (Lempp et al., 2016b). In this special case, it is plausible that mature nucleocapsids are unstable in the $AML12^{hNTCP}$ cells and aberrantly released rcDNA converts to cccDNA (Cui et al., 2013, Cui et al., 2015, Cui et al., 2016).

To closer imitate the liver environment, hepatic co-culture systems have been established to allow more accurate and physiologically relevant HBV infection and virus-host interactions. Micropatterned co-culture of PHH and stromal cells support higher productive HBV infection that can be enhanced by blocking interferon-stimulated genes (e.g. using JAK inhibitor). This model offers a prolonged and productive infection and represents a new platform for investigating virus-host interactions and developing antiviral agents (Shlomai et al., 2014). Furthermore, the co-culture of PHH with mouse stromal cells delays PHH de-differentiation and thereby supports persistent infection for over 40 days. The platform can be miniaturized to 96-well plate format and also amenable to high throughput screening (Winer et al., 2017). Avoiding PHH de-differentiation seems important for its long-term infection, as shown in recent study PHH cultured with the five chemicals efficiently recapitulated HBV infection with constant levels of cccDNA and other viral markers (Xiang et al., 2019).

Stem cell-derived hepatocyte-like cells have been developed as a new model for viral hepatitis research (Wang et al., 2019). Pluripotent stem cells can be reprogrammed by co-expression of the Yamanaka factors (Oct3/4, Sox2, Klf4, c-Myc) in human fibroblasts (Takahashi and Yamanaka, 2006). The induced pluripotent stem cells (iPSC) can further be re-differentiated into hepatocyte-like cells (Sullivan et al., 2010). Similar to iPSC, human embryonic stem cells (hESC) resided in the liver or bone marrow can also be differentiated (Lavon et al., 2004). For both iPSC and hESC, the endodermal state is at first induced by introduction of Wnt3 and Activin A and finished by the expression of transcriptional factors FOX A2, GATA4 and Sox17. Secondly, DMSO and fibroblast growth factor are added to express hepatocyte markers, α-fetoprotein (AFP), cytokeratin 19 (CK19), hepatocyte nuclear factor (HNF) and epithelial cell adhesion molecules (EpCAM). During this process, endodermal culture turns to be the next state of the hepatic specification. Thirdly, these hepatoblasts are incubated with dexamethasone and hepatocyte growth factor. Hepatocyte maturation is associated with the expression of albumin, cytokeratin 18 (CK18) and Cyp 2E1 and 3A4 liver enzymes as shown in Figure 1.12. (Vosough et al., 2013).

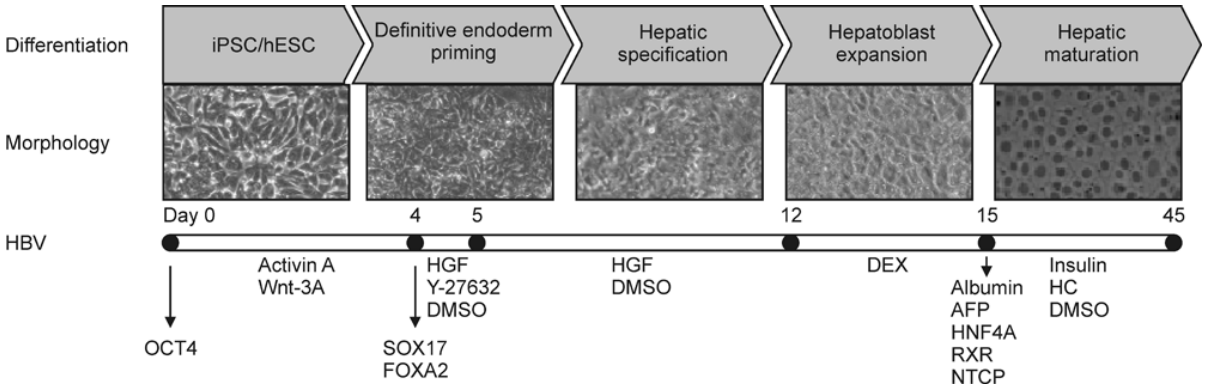

Figure 1.12. Stem cell-derived hepatocyte-like cells. The differentiation steps of iPSC or hESC contain definitive endoderm induction, hepatic specification, hepatoblast expansion and hepatic maturation to become HLC that is permissive for HBV infection. The cells are treated with activin A and Wnt-3A enhancer for 4 days, and HGF and Rock inhibitor Y-27632 for 1 day. Definitive endoderms are incubated with HGF alone for 1 week. Hepatoblast cells are treated with dexamethasone (DEX) for 3 days and can be infected with HBV at d 15 p.i.. Infected cells can be maintained in the presence of insulin, hydrocortisone (HC) and DMSO for another 1 month until d 45 post differentiation. Adapted from (Wang et al. 2019) with permission.

iPSC-derived hepatocyte-like cells support HBV replication, which is further enhanced by blocking the induction of interferon-stimulated genes (Shlomai et al., 2014). Compared to iPSC-derived hepatocyte-like cells (iPSC-HLC), immature proliferating hepatic progenitor-like cells (iPSC-HPC) are less efficient in HBV infection and the infection is dependent on the expression levels of human NTCP. Since long-term culture of iPSC-HLC is difficult, the persistence of cccDNA is established in iPSC-HPC further overexpressing human NTCP and down-regulating Janus kinase signaling (Kaneko et al., 2016). iPSC-HLC is further validated by antiviral agents Entecavir and Myrcludex B (Sakurai et al., 2017). Notably, both iPSC-derived and hESC-derived HLC gain efficient HBV infectivity. Xia et al. used an optimized protocol to differentiate the non-colony type monolayer culture of hESC and iPSC to HLC in 15 d. The HLC maintained its differentiated state and allowed HBV infection for more than 4 weeks. Importantly, the authors demonstrated that the optimized protocol for HLC differentiation provided the model capable of supporting HBV spread. Notably, the de-differentiation process occurred at a slower rate in HLC than PHH, as high expression levels of proviral factors including hNTCP, HNF4α and RXRα for more than 3 weeks, which makes HLC a suitable model for long-term HBV infection (Xia et al., 2017a). Taken together, all above *in vitro* models for HBV infection are summarized in Table 1.2..

In addition to the models that support *de novo* HBV infection, HepG2.2.15 cells are widely used in virion production and antiviral studies, despite HBV production is limited (Sells et al., 1987). Moreover, HepAD38 and HepG2.117 cells were generated. In both cells, the transcription of pgRNA is induced in a tetracycline-dependent manner (Ladner et al., 1997, Sun and Nassal, 2006). HBeAg production is cccDNA-dependent in HepAD38 cells, it is difficult

to reliably quantify HBeAg among excessive HBcAg from nucleocapsids during virus production. To solve this problem, a second-generation cccDNA reporter cell line, termed HepBHAe82, was developed in the principle that an HA tag was introduced into the N-terminus of PreCore ORF, so that only HBeAg generated from an HA encoding cccDNA but not HBcAg is tagged. The model is amenable to assess antiviral agents and identify host factors that regulate transcription from cccDNA (Cai et al., 2016).

Table 1.4. Feasible cell culture models for HBV infection.

Model	Infectivity rate	HBsAg	HBeAg	Advantages	Disadvantages
PHH	100%	++++	++++	the most physiological commercially available support innate sensing	donor variability, high cost, limited spread, short-term infection
HepaRG	5~10%	+++	++	close to PHH support innate sensing	long differentiation biliary cells included short-term infection low infectivity
HepaRG^{hNTCP}	10~20%	++++	+++	close to PHH support innate sensing	biliary cells included short-term infection long differentiation
HepG2^{hNTCP}	>50%	+	++++	robust, high throughput long-term infection	very low HBsAg secretion
Huh7^{hNTCP}	5%	+	++	support integration	low infectivity, unstable NTCP, deficient in innate sensing
AML12^{hNTCP}	1%	+	–	the sole mouse model	very low infectivity
iPSC-derived HLC	25~90%	+++	+++	physiological, close to PHH, support spread, long-term infection, personalized	ethical issue, high cost
hESC-derived HLC	50~90%	++++	++++	physiological, close to PHH, support spread, long-term infection, personalized	ethical concern, limited cell number, not available from adults

PHH: primary human hepatocytes; HLC: hepatocyte-like cells; iPSC: induced pluripotent stem cells; hESC: human embryonic stem cells. Antigen expression levels: ++++ high; +++

moderate; ++ low; + very low; - undetectable. NA: not applicable. Adapted from (Ni and Urban, 2017) with permission.

It is noteworthy to point out that most *in vitro* infection models support the formation of cccDNA, expression of HBx protein and show HBx-dependent HBV replication. All the models are listed in Table 1.3..

Table 1.5. Models for HBx-dependent HBV replication.

Model	Entry	cccDNA	assembly	secretion	HBx dependency§	Viremia	Immunity
PHH	+	+	+	+	Yes	NA	NA
HepaRG	+	+	+	+	Yes	NA	NA
$HepG2^{hNTCP}$	+	+	+	+	Yes	NA	NA
HepAD38	NA	+	+	+	ND	NA	NA
Transfected HepG2/Huh7	NA	No	+	+	Yes	NA	NA

NA: not applicable, ND: not determined. §: Efficient HBV replication in this model depends on HBx. Adapted from (Slagle et al., 2015) with permission.

1.7. Rationale and aims

The majority of HBx studies have been performed under experimental conditions in which hepatoma cells were transfected with plasmids encoding more-than-full-length HBV. Authentic functions of HBx on cccDNA could not be attained in this model, since the transcriptional template is plasmid but not cccDNA. Consistently, it has been studied that HBx stimulates HBV replication to less extent: when HBx is expressed from more-than-full-length constructs in transfected cells, HBV replication in the absence of HBx (introduction of two stop codons in the HBx ORF) is 2~3 fold reduced, which allows comparable production of Xd virions in these hepatoma cells with Xd plasmid in the absence of a helper HBx-encoding plasmid. This finding indicates that HBx is minimally required for transcription from a plasmid template. However, when susceptible cells (primary hepatocytes, etc.) were infected with Xd virus compared to an equal amount of WT virus, 50~100 fold weaker replication of Xd virus was observed. Indeed, replication of Xd virions are severely impaired in woodchucks (Zoulim et al., 1994) and bona fide infection in PHH and HepaRG cells (Lucifora et al., 2011)(Sonnabend J, thesis, 2013).

The pronounced effect observed in infection models compared to transfection systems can be hypothesized that a preference of functional HBx is selective on the cccDNA-dependent transcription of viral genes. The major differences between plasmid and cccDNA templates are that cccDNA may have relative low-copy numbers per cell, based on the knowledge of DHBV, and cccDNA has a tremendous transcriptional activity over time. Accurate quantification of

cccDNA copy number in infection models will provide new understandings on the nature of cccDNA. Using HBx-minus virus and HBx-encoding lentivirus, the effects of HBx on formation and transcription of cccDNA can be monitored.

Specific aim 1: Establishment of quantitative analysis of cccDNA numbers in its formation, maintenance and stability in *in vitro* infection systems.

To obtain a comprehensive overview, all susceptible hepatocytes and hepatoma cell lines will be infected with HBV. Except for HBx, all viral markers will be measured. cccDNA levels will be accurately quantified by reliable qPCR approach, which is specific for cccDNA. Referring to the percentage of infected cells, cccDNA numbers per infected cell are calculated.

Specific aim 2: Functional analysis of a minimal active domain and key residues for HBx transactivation in authentic infection.

Previous studies in our laboratory have shown that arginine-proline insertions into the HBx ORF resulted in significant loss of its transactivation activity. Lentiviral transcomplementation assay and extended mutational strategy using more truncations and deletions will be used to define key fragments. Whether HBx function is dependent on some binding proteins will be also investigated.

Specific aim 3: HBx-mediated formation and transcription of cccDNA and its inhibition.

Previous studies have shown that knockout of HBx within the viral genome profoundly impaired vial gene expression after infection with Xd virus. My early studies using stable DDB1 knockdown cells also showed that DDB1 plays an essential role and promotes transcription of cccDNA. Targeting the HBx-DDB1-CRL complex, new-class inhibitors will be identified and evaluated. Therapeutic perspectives of neddylation inhibition on HBV replication will be discussed.

2. MATERIALS AND METHODS

2.1. Materials

2.1.1. Organisms

2.1.1.1. Viruses

HBV:

Three types of HBV virions were prepared from (1) HepAD38, (2) HepG2-H1.3, and (3) Huh7 cells.

(1) HBV (subtype ayw) was isolated and originally cloned into plasmid pBR322 (pHBV-1) (Hirschman et al., 1980). Complementary DNA was subcloned at 3' terminus of the CMV-IE promoter of ptetHBV plasmid and stabilized in virus-producing HepAD38 cells (Ladner et al., 1997). The supernatant was collected from HepAD38 cells with the removal of doxycycline in culture medium and virus was further purified by heparin-affinity chromatography.

(2) A wild-type (WT) 1.3-fold-overlength HBV genome (subtype ayw) was PCR amplified from pHBV1.3 plasmid and subcloned in pTH1.3 plasmid (Sprinzl et al., 2001, Jost et al., 2007). In parallel, two stop codons within HBx opening reading frame were introduced in pTH1.3 to generate pTH1.3-ΔX. pTH1.3 or pTH1.3-ΔX together with pSV2neo plasmids were stably transfected in HepG2 cells and thereby HepG2-H1.3 and HepG2-H1.3-ΔX cell lines were generated (a kind gift from Ulrike Protzer). Secreted virions were PEG precipitated and 100-fold enriched.

(3) WT 1.1-fold-overlength HBV genome was cloned in pCHT-9/3091(WT) plasmid as previously described (Nassal, 1992). pCHT-9/3091(Xd) plasmid was generated by introducing two stop codons of Q8stop and Q87stop (C22T and C259T of the HBx coding region) within HBx opening reading frame without changing core and polymerase proteins (Jessica Sonnabend, unpublished). Huh7 hepatoma cells were transfected with pCHT-9/3091(WT) or pCHT-9/3091(Xd), and secreted WT and Xd virions were PEG precipitated and enriched. Section 2.2.2.2 describes more details of (2) and (3).

HDV:

HDV genomic-encoding plasmid pSVLD3 (genotype 1) (provided from John Taylor) and HBV envelope encoding pT7HB2.7 (a kind gift from Camille Sureau) plasmid were co-transfected in Huh7 cells. Secreted HDV viruses were purified by heparin affinity chromatography.

Lentivirus:

Second-generation recombinant lentiviruses were produced by a triple-transfection of HEK293T cells with pWPI-HBx/pInducer20-HBx, psPAX2 (expressing Gag and Pol of HIV) and pMD2.G (expressing VSV-G envelopes) (weight: weight: weight = 3: 3: 1). Supernatant between 24~72 hours post transfection was collected, pooled, filtered through 0.45 μM filter, ultracentrifuged, and resuspended. Section 2.2.2.5 describes more details.

2.1.1.2. Prokaryotic bacteria

E.coli strains DH5α and Top10 were used for molecular cloning. Competent cells for high-efficient transformation were home-made using rubidium chloride chemical sensitization according to Promega Protocols and Applications Guide.

2.1.1.3. Eukaryotic cell lines

Cell line	**Description**
Huh7	Differentiated hepatocyte-derived carcinoma cell line originally from a 57-year-old Japanese male HCC patient in 1982
HepG2	ATCC® HB-8065, a human hepatoma cell line from a 15-year-old Caucasian adolescent in 1979
$HepG2^{hNTCP}$	HepG2 cells stably expressing hNTCP (Ni et al., 2014)
HepaRG	Human hepatoma cell line isolated from a liver tumor of a female HCV and HCC patient (Gripon et al., 2002)
$HepaRG^{hNTCP}$	HepaRG cells stably expressing hNTCP (Ni et al., 2014)
HepAD38	HepG2-derived cell line with a tet-inducible integrate allowing pgRNA transcription and virus assembly in a tet-off manner (Ladner et al., 1997)
HepG2-H1.3(WT)	HepG2-derived cell line with an HBV 1.3-mer supporting constitutive pgRNA transcription and virus assembly (Jost et al., 2007)
HepG2-H1.3(ΔX)	HepG2-derived cell line with two stop codons in HBx ORF supporting generation of Xd virions (Lucifora et al., 2011)
HBx(WT)-$HepG2^{hNTCP}$	$HepG2^{hNTCP}$-derived cell line with an HA-tagged HBx for HBx(WT) expression in a tet-on manner (this thesis)
HBx(R96E)-$HepG2^{hNTCP}$	$HepG2^{hNTCP}$-derived cell line with an HA-tagged HBx for

	HBx(R96E) expression in a tet-on manner (this thesis)
HBx(WT)-HepaRG^{hNTCP}	HepaRG^{hNTCP}-derived cell line with an HA-tagged HBx for HBx(WT) expression in a tet-on manner (this thesis)
HBx(R96E)-HepaRG^{hNTCP}	HepaRG^{hNTCP}-derived cell line with an HA-tagged HBx for HBx(R96E) expression in a tet-on manner (this thesis)
PLC/PRF5	ATCC® CRL-8024, a human hepatoma cell line with natural HBs integrates and continuous HBsAg production (Daemer et al., 1980)
HEK293T	Human embryonic kidney cell line derived from HEK293 cell line expressing a mutated SV40 large T antigen (DuBridge et al., 1987).

2.1.1.4. Primary human hepatocytes (PHH)

PHH were isolated from liver specimens obtained after partial hepatectomy and following written informed consent of the patients (provided by Florian W.R. Vondran). The whole process was approved by the ethics commission of Hannover Medical School/Ethik-Kommission der MHH, no. 252-2008.

2.1.2. Inorganic consumables

2.1.2.1. Chemicals and compounds

Chemical	**Provider**	**Catalog number**
[α-^{32}P]-deoxyxytidine 5'-triphosphate (dCTP)	Hartmann Analytic GmbH	SRP-205(9.25 MBq)
Acetic acid (Ph.Eur.,>99.8%)	Sigma-Aldrich	33209-2.5L
Acrylamide/Bisacrylamide(30% w/v, 3.3% C)	Serva Electrophoresis GmbH	10687.01
Agarose, high melting temperature	Biozym Diagnostic GmbH	840004
Ampicillin	Life Technologies, Invitrogen	11593-027
Ammonium persulfate (AP)	Fisher Scientific GmbH	10744171
Bacto-Agar	Becton-Dickinson	214050
Bacto-Trypton	Becton-Dickinson	211705
Bacto-Yeast extract	Becton-Dickinson	212720
BAY41-4109	Bayer AG	
B.Braun Aqua (ddH2O), injektionszwecke	University Hospital Heidelberg	
Beta-Mercaptoethanol (2-ME)	Sigma-Aldrich GmbH	M6250-250ML
Blasticidin S	Life Technologies, Invitrogen	R210-01

Bovine serum albumin fraction V (>98%)	Carl Roth GmbH	Nr.8076.2
Caesium chloride (ultrapure)	Invitrogen	15507-023
Coelenterazine	PJK GmbH	102171
Diethyl pyrocarbonate (DEPC)	Sigma-Aldrich GmbH	D5758-50ML
Dimethylsulfoxide (DMSO)	EMD Millipore	1.02950.0500
Dithiothreitol (DTT) (>98%)	Sigma-Aldrich GmbH	D0632-1G
dNTPs (100 mM)	New England Biolabs	N0446S
Dulbecco's Modified Eagle Medium (DMEM)	Life Technologies, Invitrogen	41965-039
DMEM/F12 medium (v/v 1:1)	Life Technologies, Invitrogen	31330-038
Dulbecco's PBS (w/o Ca^{2+} and Mg^{2+})	Sigma-Aldrich GmbH	D8537-500ML
DNA loading dye (6×)	Fermentas	R0611
Doxycycline	Sigma-Aldrich GmbH	Y0001714
DRAQ5	Life Technologies, Invitrogen	62254
Ethanol absolute (Ph. Eur.,>99.8%)	Sigma-Aldrich GmbH	32205-2.5L-M
Ethidium bromide (EB)	Sigma-Aldrich GmbH	E7637-1G
Ethylenediaminetetraacetic acid (EDTA)	Serva Electrophoresis GmbH	39760.01
Fetal bovine serum gold (FBS)	PAA, GE Healthcare GmbH	A15-151
Fluoromount-G	Life Technologies, Invitrogen	00-4958-02
Formaldehyde (36.5-38%)	Sigma-Aldrich GmbH	F8775-500ML
GeneRuler 1kb DNA ladder	Fermantas	SM0312
GLS4 (morphothiadin)	Sunshine Lake Pharma Co., Ltd.	
Glycerol (99.9%)	Fisher Scientific	G/0650/15
Glycine	Sigma-Aldrich GmbH	G8898-1KG
Guanidine hydrochloride	Sigma-Aldrich GmbH	50950-1KG
Hank's balanced salt solution (HBSS)	Life Technologies, Invitrogen	14170-112
HEPES (1 M)	Life Technologies, Invitrogen	15630-080
Hydrochloric acid (>37% fuming)	Sigma-Aldrich GmbH	30721-2.5L
Hydrocortisone hemisuccinate	Sigma-Aldrich GmbH	H4881
Hoechst 33342	Life Technologies, Invitrogen	H3570
Illustra MicroSpin G-25 Column	GE Healthcare GmbH	27532501
Insulin	Sigma-Aldrich GmbH	91077C-1G
Interferon-α-2b (Intron A, injection use)	Schering-Plough	
Isopropanol (Ph. Eur.,>99.8%)	Sigma-Aldrich GmbH	33539-2.5L-M
Laemmli sample buffer (4×)	Bio-rad Laboratories	#161-0747
Lamivudine (3TC) (>98%)	Sigma-Aldrich GmbH	L1295-10MG
L-Glutamine (100×)	Life Technologies, Invitrogen	25030-024

Lipofectamine 3000 transfection reagent	Life Technologies, Invitrogen	L3000-001
Methanol (>99.9%)	Sigma-Aldrich GmbH	34860-2.5L-R
Milk powder (blocking grade)	Carl Roth GmbH	Nr.T145.2
Non-essential amino acids (100×)	Life Technologies, Invitrogen	11140-035
(N-morpholino) propane sulfonic acid (MOPS)	Serva Electrophoresis GmbH	29836.02
NP-40 (IGEPAL CA-630)	Sigma-Aldrich GmbH	I8896-50ML
PageRuler Plus prestained protein ladder	Fermentas	#26620
Paraformaldehyde (PFA)	Sigma-Aldrich GmbH	P6148-1KG
Penicillin, 10000 U/mL	Life Technologies, Invitrogen	15140-122
Peptone	Life Technologies, Invitrogen	211677
Polyethyleneimine (PEI), branched	Sigma-Aldrich GmbH	408727-100ML
Polyethylene glycol (PEG 8000) (ultrapure)	Sigma-Aldrich GmbH	89510-1KG-F
Potassium chloride	Sigma-Aldrich GmbH	31248-1KG
Protease inhibitor cocktail solution	Sigma-Aldrich GmbH	P8340-5ML
Protease/Phosphatase inhibitor cocktail(100×)	Cell Signaling Technology	#5872S
Puromycin	InvivoGen	ant-pr-1
RiboRuler High Range RNA Ladder	Fermentas	#SM1821
RNase Away reagent	Life Technologies, Invitrogen	10328-011
Sodium dodecyl sulfate (SDS)	Serva Electrophoresis GmbH	20765.03
Streptomycin, 10000 μg/mL	Life Technologies, Invitrogen	15140-122
Sodium bicarbonate	AppliChem GmbH	A3590,1000
Sodium citrate dihydrate (>99%)	AppliChem GmbH	A2403,1000
Sodium chloride (>99.5%)	Sigma-Aldrich GmbH	S7653-1KG
Sodium hydroxide	Sigma-Aldrich GmbH	30620-1KG-R
Tenofovir (TDF)	Sigma-Aldrich GmbH	SML1794-10MG
Tetramethylethylene-diamine (TEMED)	Carl Roth GmbH	Nr.2367.3
TransIT-LT1 transfection reagent	Mirus Bio GmbH	MIR2300
Tris (>99.9%)	Carl Roth GmbH	Nr.4855.2
Triton X-100	Merck	1.08603.1000
Trypan blue solution (0.4%)	Sigma-Aldrich GmbH	93595-50ML
Tween-20	Carl Roth GmbH	Nr.9127.1
William's Medium E	Life Technologies, Invitrogen	22551-022

2.1.2.2. Buffers and solutions (solvent is sterilized water if not specified)

For agarose gel electrophoresis:

TAE buffer (50×): 2 M Tris, 1 M glacial acetic acid, 0.05 M EDTA (pH = 8.0)

TE buffer (1×): 10 mM Tris, 1 mM EDTA (pH = 8.0)

For CsCl gradient ultracentrifugation and DNA dot-blot:

Caesium chloride gradients: 1.2 g/mL (28.9 g CsCl and 100 g H_2O); 1.3 g/mL (40.3 g CsCl and 100 g H_2O); 1.4 g/mL (54.5 g CsCl and 100 g H_2O), freshly prepared 20% sucrose in water (w/w).

Soak I buffer: 1.5 M NaCl, 0.5 M NaOH

Soak II buffer: 3 M NaCl, 0.5 M Tris (pH = 7.4)

SSC buffer (20×): 3 M NaCl, 0.3 M sodium citrate (pH = 7.0)

Denhardt's buffer (50×): 1 % BSA, 1 % Ficoll PM70, 1 % Polyvinvlpyrrolidone

Hybridization buffer: 10 μg/mL calf thymus DNA, 5× Denhardt's, 6× SSC, 0.5 % SDS

Dot-blot wash buffer: 1× SSC, 0.5 % SDS

For Northern blotting:

MOPS buffer (10×): 0.2 M MOPS free acid, 0.05 M sodium acetate anhydrous, 0.01 M Na_2EDTA (pH = 7.5), adjust pH value to 7.0 by adding NaOH. Avoid light at room temperature.

Northern blotting running buffer: 1× MOPS, 0.2 M formaldehyde in DEPC-treated H_2O.

1.2 % formaldehyde gel: 116 mL water, 16 mL 10× MOPS buffer, 1.92 gram agarose. Melting up this mixture and cooling it down to 60 degree, adding 28 mL 37% formaldehyde solution in a hood with gentle shaking. Casting the gel.

In-gel denature buffer: 0.05 M NaOH, 1.5 M NaCl

Hybridization buffer: QuikHyb Hybridization solution (Agilent), ready-to-use.

Low-stringency wash buffer: 2× SSC, 0.1 % SDS

High-stringency wash buffer: 0.1× SSC, 0.1 % SDS

For Southern blotting:

Southern blotting running buffer: 1× TAE buffer (see above)

Depurination buffer: 0.2 M HCl

Denaturing buffer: 0.5 M NaOH, 1.5 M NaCl

Neutralization buffer: 1.5 M NaCl, 1 M Tris-HCl (pH = 7.4)

Hybridization buffer: QuikHyb Hybridization solution (Agilent), ready-to-use.

Wash buffer: 1× SSC, 0.1 % SDS

For SDS-PAGE:

Resolving gel buffer (4×): 1.5 M Tris, 0.4 % SDS, 0.01 % NaN_3 (pH = 8.8)

Stacking gel buffer (4×): 0.5 M Tris, 0.4 % SDS, 0.01 % NaN_3 (pH = 6.8)

SDS running buffer (10×): 0.25 M Tris, 1.92 M glycine, 1 % SDS (pH = 8.3)

For Western blot:

RIPA lysis buffer: 25 mM Tris, 150 mM NaCl, 1 mM EDTA, 0.1 % NP-40, 1× protease/phosphatase inhibitor cocktail (pH = 7.4)

Blotting buffer: 48 mM Tris, 39 mM glycine, 0.04 % SDS, 10 % methanol

TBS buffer (10×): 0.2 M Tris, 1.37 M NaCl (pH = 8.0)

TBS-T wash buffer: 1× TBS, 0.05 % Tween-20

Blocking buffer: 5 % blocking-grade milk powder in 1× TBS-T buffer

Antibody dilution buffer: blocking buffer or 5 % BSA in 1× TBS-T buffer

For immunofluorescence and confocal microscopy:

Fixation buffer: 4 % paraformaldehyde in 1× PBS or ice-cold methanol

Permeabilization buffer: 0.25 % Triton X-100 in 1× PBS

Blocking buffer: 5 % blocking-grade milk powder in 1× PBS

Antibody dilution buffer: blocking buffer or 3 % goat serum in 1× PBS

Mounting buffer: Fluoromount G (Life Technologies)

For dual-luciferase assay:

Passive lysis buffer (5×): 125 mM glycyl glycine, 75 mM $MgSO_4$, 20 mM EGTA, 5 mM DTT, 0.5 % Triton X-100 (pH = 7.8)

Assay buffer: 25 mM glycyl glycine, 15 mM $MgSO_4$, 4 mM EGTA, 15 mM K_2PO_4 (pH = 7.8) in order to dilute coelenterazine (the substrate of renilla luciferase). For firefly luciferase, add 1 mM DTT and 1 mM ATP to the assay buffer prior to D-luciferin dilution.

2.1.2.3. Kits

Kit	**Provider**
GeneJET PCR purification kit	Fermentas, Thermo Fisher Scientific
GeneJET Gel extraction kit	Fermentas, Thermo Fisher Scientific
GeneJET plasmid mini-prep kit	Fermentas, Thermo Fisher Scientific
Plasmid plus midi kit	Qiagen
Plasmid maxi kit	Qiagen
Megaprime DNA Labeling System	Amersham, GE Healthcare GmbH
NucleoSpin RNA kit	Macherey-Nagel
NucleoSpin Tissue kit	Macherey-Nagel
NucleoSpin Blood kit	Macherey-Nagel
High Pure Viral Nucleic Acid Kit	Roche Life Science
CytoTox 96 NonRadioactive Cytotoxicity Assay	Promega
cDNA reverse transcription kit	ABI
NucBuster Protein Extraction kit	Merck Millipore
NE-PER Nuclear and Cytoplasmic Extraction Kit	Thermo Fisher Scientific

2.1.3. Biochemical consumables

2.1.3.1. Culture medium

Bacteria culture:

LB medium: 10 g/L trypton, 5 g/L yeast extract, and 10 g/L NaCl

TB medium: 12 g/L trypton, 24 g/L yeast extract, 0.35 % glycerol in 17 mM KH_2PO_4 and 72 mM K_2HPO_4

Cell culture:

Cell	**Medium**

Huh7, HepG2, HepG2^{hNTCP}, HEK293T, PLC/PRF5, HBx(WT&R96E)-HepG2^{hNTCP}(*) HepG2-H1.3 (WT&ΔX)	DMEM, 10 % FCS (heat-inactivated), 2 mM L-glutamine, 100 U/ml penicillin, 100 µg/ml streptomycin, 1 mM non-essential amino acids. *: 500 µg/mL G418 added
HepaRG, HepaRG^{hNTCP}, PHH HBx(WT&R96E)-HepaRG^{hNTCP}(*)	William's E, 10 % FCS (heat-inactivated), 2 mM L-glutamine, 100 U/ml penicillin, 100 µg/ml streptomycin, 1 mM non-essential amino acids, 5 µg/mL insulin, 50 µM hydrocortisone. During differentiation and HBV/HDV infection: 1.5 % DMSO added. *: 250 µg/mL G418 added
HepAD38	DMEM/F-12, 10 % FCS (non-heat inactivated), 2 mM L-glutamine, 100 U/ml penicillin, 100 µg/ml streptomycin, 400 µg/ml G418, 5 µg/ml insulin, 50 µg/ml hydrocortisone, 1 µg/ml doxycycline. For HBV production: doxycycline was removed.

2.1.3.2. Enzymes

Enzyme	**Provider**
Deep Vent DNA polymerase	New England Biolabs
Q5 Hot Start DNA polymerase	New England Biolabs
Restriction endonucleases	New England Biolabs
Calf Intestinal Alkaline Phosphatase	New England Biolabs
T4 DNA ligase	Fermentas, Thermo Fisher Scientific
T5 exonuclease	New England Biolabs
Plasmid-safe DNase	Epicentre, Lucigen
iTaq Universal SYBR Green Mix	Bio-rad
qScript XLT RT-qPCR Toughmix	Quanta Biosciences
PerfeCTa qPCR Toughmix	Quanta Biosciences
Trypsin	Life Technologies, Invitrogen

2.1.3.3. Antibodies

Primary antibody:

Antibody/Antisera	Species	Application	Provider
Anti-HBcAg	Rabbit polyclonal	IF: 1:3000	Dako
Anti-HBcAg (M312)	Mouse monoclonal	IF: 1:2000	Christa Kuhn
Anti-HBxAg (#641)	Rabbit polyclonal	WB/IF: 1:500	Christa Kuhn
Anti-HBxAg (#644)	Rabbit polyclonal	WB/IF: 1:500	Christa Kuhn
Anti-HDAg (GEAO)	Serum of an HBV/HDV co-infected patient	IF: 1:3000	Heiner Wedemeyer
Anti-HDAg (VUDA)	Serum of an HBV/HDV co-infected patient	IF: 1:3000	Heiner Wedemeyer
Anti-HBsAg (HBC34)	Human monoclonal	IF: 1:3000	Davide Corti
Anti-β-actin	Mouse monoclonal	WB: 1:2000	Sigma-Aldrich
Anti-HA tag	Rabbit monoclonal	WB: 1:1000	Cell Signaling Tech.
Anti-Flag tag (M2)	Mouse monoclonal	IP: 1:100; WB: 1:1000	Sigma-Aldrich
Anti-SMC6	Rabbit polyclonal	IF: 1:100	Sigma-Aldrich
Anti-SMC6 (M01)	Mouse monoclonal	WB: 1:500	Abgent
Anti-hnRNP K	Rabbit polyclonal	WB: 1:500	Proteintech

Secondary antibody:

Antibody	Species	Application	Provider
Alexa Fluor anti-rabbit 488	goat	IF: 1:500	Invitrogen
Alexa Fluor anti-rabbit 546	goat	IF: 1:500	Invitrogen
Alexa Fluor anti-mouse 488	goat	IF: 1:500	Invitrogen
Alexa Fluor anti-mouse 546	goat	IF: 1:500	Invitrogen
Alexa Fluor anti-human 488	goat	IF: 1:500	Invitrogen
Alexa Fluor anti-human 555	goat	IF: 1:500	Invitrogen
HRP anti-rabbit IgG	goat	WB: 1:10,000	Sigma-Aldrich
HRP anti-mouse IgG	goat	WB: 1:10,000	Sigma-Aldrich

2.1.3.4. Peptides

Myrcludex B (myr-preS1 2~48 amino acids)

myr-GTNLSVPNPLGFFPDHQLDPAFGANSNNPDWDFNPNKDHWPEANKVG

2.1.3.5. Plasmids

Plasmid	Description	Provider
pCHT-9/3091(WT)	Plasmid encoding overlength 1.1-mer HBV (genotype D, ayw) under CMV-IE promoter	(Nassal, 1992)
pCHT-9/3091(Xd)	Plasmid pCHT-9/3091(WT) with two stop mutations at Q8 (C22T) and Q87 (C259T) without alteration of polymerase	Jessica Sonnabend
pcDNA3.1-Zeo(-)-HBx	Plasmid pcDNA3.1 encoding full-length HBx under CMV-IE promoter	Jessica Sonnabend
pWPI-HBx-IRES-GFP	Bicistronic expression vector encoding HBx-IRES-GFP cassette under EF1α promoter	Jessica Sonnabend
psPAX2	Lentiviral packaging plasmid expressing HIV gag, pol, tat and rev proteins	Didier Trono
pMD2.G	VSV-G expressing plasmid for pseudo lentivirus packaging	Didier Trono
pWPI-HBx(WT)	Bicistronic lentiviral vector encoding HBx(1-154) and puromycin resistance gene	Jessica Sonnabend
pWPI-HBx(1-50)	Bicistronic lentiviral vector encoding HBx(1-50) and puromycin resistance gene	Bingqian Qu
pWPI-HBx(51-154)	Bicistronic lentiviral vector encoding HBx(51-154) and puromycin resistance gene	Bingqian Qu
pWPI-HBx(Δ51-142)	Bicistronic lentiviral vector encoding HBx(1-50 fused with 143-154) and puromycin resistance	Bingqian Qu
pWPI-HBx(51-142)	Bicistronic lentiviral vector encoding HBx (51-142) and puromycin resistance gene	Bingqian Qu
pWPI-HBx(58-142)	Bicistronic lentiviral vector encoding HBx (58-142) and puromycin resistance gene	Bingqian Qu
pWPI-HBx(R96E)	Bicistronic lentiviral vector encoding HBx(R96E) and puromycin resistance gene	Bingqian Qu
pWPI-HBx(R96A)	Bicistronic lentiviral vector encoding HBx(R96A) and puromycin resistance gene	Bingqian Qu
pWPI-GFP-puro	Bicistronic lentiviral vector encoding GFP	

	and puromycin resistance gene	Jessica Sonnabend
pInducer20-HBx(WT)	Lentiviral vector encoding HA-tagged HBx(WT) under TRE2 promoter and neomycin resistance gene after IRES	Emanuela Milani
pInducer20-HBx(R96E)	Lentiviral vector encoding HA-tagged HBx(R96E) under TRE2 promoter and neomycin resistance gene after IRES	Emanuela Milani
pUC18-HBx(WT)	Plasmid pUC18 encoding full-length HBx	Jessica Sonnabend
pSHH2.1	Plasmid pSV08 encoding a head-to-tail HBV dimer under SV40 promoter	(Cattaneo et al., 1983a)
pSVLD3	Plasmid containing a head-to-tail trimer of full-length HDV cDNA under SV40 promoter	Camille Sureau
pT7HB2.7	Plasmid encoding a 2700-bp HBV subgenomic fragment expressing envelopes and HBx under respective authentic promoters	Camille Sureau
pGL3-C-Fluc	Plasmid pGL3-Basic containing core promoter (1403-1817) to express firefly luciferase	(Tang et al., 2014)
pGL3-preS1-Fluc	Plasmid pGL3-Basic containing preS1 promoter (2710-2834) to express luciferase	(Tang et al., 2014)
pGL3-preS2-Fluc	Plasmid pGL3-Basic containing preS2 promoter (2966-152) to express luciferase	(Tang et al., 2014)
pGL3-X-Fluc	Plasmid pGL3-Basic containing X promoter (950-1310) to express firefly luciferase	(Tang et al., 2014)
pRL-SV40-Rluc	Plasmid pRL encoding renilla luciferase under SV40 promoter	Promega

2.1.3.6. Oligonucleotides

Name	**Sequence (5' to 3')**	**Reference**
cccDNA-F (p1040)	GTGGTTATCCTGCGTTGAT	
cccDNA-R (p1996)	GAGCTGAGGCGGTATCT	
cccDNA-probe (p1085)	FAM-AGTTGGCGAGAAAGTGAAAGCCTGC-TAMRA	This thesis
Total DNA-F (p466)	GTTGCCCGTTTGTCCTCTAATTC	

Total DNA-R (p541)	GGAGGGATACATAGAGGTTCCTTGA	(Lucifora et al., 2014)
Human β-globin-F	CAGGTACGGCTGTCATCACTTAGA	
Human β-globin-R	CATGGTGTCTGTTTGAGGTTGCTA	(Steinau et al., 2006)
pgRNA specific-F	CTCCTCCAGCTTATAGACC	
pgRNA specific-R	GTGAGTGGGCCTACAAA	(Lucifora et al., 2014)
HBs RNA specific-F	TGTACCAAACCTTCGGACGG	
HBs RNA specific-R	ATGCTGTACAGACTTGGCCC	This thesis
HBV total RNA-F	TCAGCAATGTCAACGACCGA	
HBV total RNA-R	TGCGCAGACCAATTTATGCC	This thesis
HDV RNA-F	GCGCCGGCYGGGCAAC	
HDV RNA-R	TTCCTCTTCGGGTCGGCATG	
HDV RNA-probe	FAM-CGCGGTCCGACCTGGGCATCCG -TAMRA	(Ferns et al., 2012)
SmaI-HBx-1-F	TCCCCCGGGATGGCTGCTAGGCTGTGCTG	This thesis
MluI-HBx-50-R	GCCGACGCGTTTACCCGTGGTCGGTCGGAA	This thesis
SmaI-HBx-51-F	CGCCCGGGATGGCGCACCTCTCTTTACGCG	This thesis
SmaI-HBx-58-F	CGCCCGGGATGCTCCCCGTCTGTGCCTTCTC	This thesis
MluI-HBx-142-R	CGACGCGTTTAGACCAATTTATGCCTACAGC	This thesis
MluI-HBx-154-R	GCCGACGCGTTTAGGCAGAGGTGAAAAAGTT GCA	This thesis
HBx-Δ51-142-R	**TGCTGGTGCGCACCCGTGGTCGGT**CGGAACG GCA (**Bold**: overlapped with HBx-Δ51-142-long-F)	This thesis
HBx-Δ51-142-long-F	***ACCGACCACGGGTGCGCACCAGCA****CCATGCA* *ACTTTTTCACCTCTGCC*TAAACGCGTCGGC	This thesis
HBx-Δ51-142-long-R	GCCGACGCGTTTA*GGCAGAGGTGAAAAAGTTG* *CATGGTGCTGGTGCGCACCCGTGGTCGGT* (*Italic*: annealed with HBx-Δ51-142-long-R)	This thesis
Internal-R96E-F	TCTTACATAAGGAGACTCTTGGAC	This thesis
Internal-R96E-R	GTCCAAGAGTCTCCTTATGTAAGA	This thesis
Internal-R96A-F	TCTTACATAAGGCGACTCTTGGAC	This thesis
Internal-R96A-R	GTCCAAGAGTCGCCTTATGTAAGA	This thesis

(underlined: SmaI or MluI cutting site; double underlined: the mutated 96th residue)

shRNA-DDB1-2C TGCTGTTGACAGTGAGCGCAAACACGAGATTAGAGATCTATAGTGAAGCCACAGATGTA TAGATCTCTAATCTCGTGTTTTTGCCTACTGCCTCGGA	
mature sense: AACACGAGAUUAGAGAUCU	
mature antisense: AGAUCUCUAAUCUCGUGUU	This thesis
shRNA-DDB1-3C TGCTGTTGACAGTGAGCGAAACGTTGACAGTAATGAACAATAGTGAAGCCACAGATGTA TTGTTCATTACTGTCAACGTTGTGCCTACTGCCTCGGA	
mature sense: ACGUUGACAGUAAUGAACA	
mature antisense: UGUUCAUUACUGUCAACGU	This thesis

2.1.4. Software

Name	**Application**	**Provider**
Adobe Illustrator 6.0	Vector-based graphic editing	Adobe Systems
Adobe Photoshop 6.0	Graphic editing	Adobe Systems
Ascent 2.4	Luminescence reading	Thermo Scientific
CFX Manager	Real-time qPCR signal collection	Bio-rad
CorelDRAW Graphics Suite X3	Vector-based graphic editing	Corel Cooperations
CorelDRAW Graphics Suite X5	Graphic export to images	Corel Cooperations
Endnote X7	Reference management	Clarivate Analytics
Fiji (ImageJ updated)	Image processing	Open source
FlowJo V10	FACS raw-data analyses	Becton-Dickinson
GraphPad PRISM 5	Graphic and statistic raw-data	Graphpad, Inc
Leica Application Suite	Confocal microscopy	Leica Inc.
Microsoft Excel	Statistic software	Microsoft
Microsoft Word/Powerpoint	Thesis writing and presentation	Microsoft
Nanodrop 2000 1.6	Nucleic acid contents	Thermo Scientific
Odyssey Software	Western blot analyses	Li-COR Biosciences
Quantity One 1-D analysis	Northern/southern blot analyses	Bio-Rad
Vector NTI Software 11	Sequence bioinformatics	Life Technologies

2.2. Methods

2.2.1. Molecular cloning

2.2.1.1. Overlapping PCR and mutagenesis

Mutagenesis is based on two rounds of PCR amplification. The first PCR amplifies two fragments with overlapping part carrying the mutation introduced by primers. Products of the first PCR are annealed and become the template of a second PCR reaction. In this thesis, the eventual PCR product carrying each mutation was inserted back to the original construct to replace WT HBx. For pWPI-HBx(R96E) generation shown as an example, HBx-1-F and internal HBx-R96E-R primers amplified N-terminal fragment containing R96E mutation, and internal HBx-R96E-F and HBx-154-R primers amplified C-terminal fragment with the same mutation. Two products were purified, mixed in a molar ratio 1:1 and subjected to the template of a second PCR using HBx-1-F and HBx-154-R primers to generate a full-length HBx(R96E) insert for ligation. For truncation, one direct PCR reaction was sufficient. For pWPI-HBx(1-50) shown as an example, HBx-1-F and HBx-50-R amplified a 150 bp product directly used as the insert. Specifically, the insert of pWPI-HBx(Δ51-142) was the product of one PCR reaction using HBx-1-F and a long primer HBx-Δ51-142 with a 36 bp tail encoding the 143~154 residues of HBx.

Every 50 μL of PCR reaction using Q5 Hot Start High-Fidelity DNA polymerase included 10 μL of 5× Q5 reaction buffer, 1 μL of 10 mM dNTPs, 2.5 μL of forward primer (10 μM), 2.5 μL of reverse primer (10 μM), 10 ng of pWPI-HBx(WT) plasmid or 100 ng of a mixture of two fragments (molar ratio 1:1), 10 μL of 5× Q5 High GC Enhancer, 0.5 μL of Q5 DNA polymerase, and water to 50 μL. PCR program was set up as follows: 98℃ 3 min, [98℃ 10 sec, 54℃ 30 sec, 72℃ 60 sec] for 36 cycles, 72℃ 5 min, 4℃ hold. All PCR products were subjected to agarose gel electrophoresis.

2.2.1.2. Restriction digestion

After gel electrophoresis, all size-characterized PCR products (c.a. 5 μg) were purified and subjected to a 50 μL reaction containing 20 U of each restrictive endonucleases; On the other hand, 5 μg of pWPI-HBx(WT) was incubated with 20 U of each endonuclease in a 50 μL reaction. All digestions were performed at 37℃ for 1 h and endonuclease activity was heat-inactivated at 70~80℃ for 15-20 min. Insert DNA was silica-column purified and backbone DNA was purified by agarose gel electrophoresis.

2.2.1.3. Dephosphorylation of vector DNA

Self-ligation of the partially linearized vector is highly reduced by dephosphorylation of 5' ends of the vector. Linearized products of vector by restriction digestion were incubated with 10 U of calf intestinal alkaline phosphatase in CutSmart buffer at 37℃ for 1 h. Phosphatase activity was heat-inactivated at 65℃ for 20 min and column-purified before ligation.

2.2.1.4. Agarose and formaldehyde gel electrophoresis

For molecular cloning, PCR products of HBx (c.a.500 bp) were mixed with DNA loading dye and separated in a 2 % agarose gel (0.01% ethidium bromide, v/v) soaked in 1× TAE buffer. Likewise, pWPI plasmid backbone was separated in a 1 % agarose gel. For 28S/18S ribosomal RNA visualization, 2 μg of total RNA samples were mixed with RNA loading dye and separated in a 1 % native agarose gel. Electrophoresis was performed at 140 V for 20~30 min and signals inside gels were visualized under UV light.

For Southern blotting, DNA samples were separated in a 1.2 % agarose gel without ethidium bromide. Electrophoresis was performed at 125 V (5 V per centimeter between anode and cathode electrodes) for approximate 3 h until indicating blue dye went to the edge of the gel.

For northern blotting, RNA samples were separated in a 1.2% formaldehyde gel (shown in session 2.1.2.2) without ethidium bromide in pre-cooled 1× MOPS buffer. The formaldehyde gel was pre-run at 70 V for 30 min and later on RNA samples were loaded and run. Electrophoresis was performed at 125 V for approximate 3~4 h.

2.2.1.5. Ligation and transformation

Backbone and insert (HBx fragments, amount calculated) were mixed at a molar ratio of 1:5 and incubated with 2 U (sticky end) or 10 U (blunt end) of T4 ligase in 1× T4 ligase buffer at room temperature for 1 h. Specifically, 10% of PEG4000 was added to blunt-end reactions to enhance ligation efficiency. One reaction with backbone alone was set up as control.

Competent *E.coli* DH5α or Top10 cells were ice-thawed. 5 μL of ligation product was mixed with 50 μL of competent cells. The mixture pipetted up and down and incubated on ice for 30 min. Afterward, it was heat-shocked at 42℃ for 90 sec and immediately chilled on ice

for 3 min. 500 µL of antibiotic-free pre-warmed LB or TB medium was added and the recovery of transformed bacteria was at 37℃ for 50 min on a heater with gentle shaking. Bacteria were dispersed on LB-agar plates containing 100 µg/mL Ampicillin and incubated at 37℃ overnight.

2.2.1.6. Colony characterization

The next day after transformation, three colonies on each plate with the recombinant product and one colony on the control plate were picked up and propagated in Ampicillin-containing LB medium overnight at 37℃. Recombinant plasmids were extracted using a mini preparation kit. These plasmids were either characterized by restriction digestion (choose one endonuclease on the insert and the other on the backbone) or by PCR amplification using Deep Vent DNA polymerase. Validated recombinant plasmids were further expanded by midi plus or maxi prep.

2.2.1.7. Sanger sequencing

5 µL of mini-prep recombinant plasmid (80-100 ng/µL) were mixed with 5 µL of pWPI-seq-F sequencing primer (5 µM). Sequencing reactions were sent to GATC Company. Two days later, results of Sanger sequencing were aligned with expected correct sequences and read sequence by sequence using Vector NTI software. Successful plasmids were used for cell culture experiments.

2.2.2. Cell culture

2.2.2.1. Maintenance, thawing and freezing of cells

All eukaryotic cells used in this thesis were cultivated in 37℃ incubator with 5% CO_2 supply and 95% humidity. During maintenance, cells were split twice or three times per week, except HBx(WT)-HepaRG^{hNTCP} cells once every two weeks. In detail, cells were rinsed once with 1× PBS and incubated with trypsin (e.g. 700 µL/T75 flask) at 37℃ for 3~10 min. When detached, the cells were resuspended in complete culture medium by pipetting up and down to obtain single cell suspension. The splitting factor for one passage was 1:5 ~ 1:20. Mycoplasma tests were randomly performed using PCR Mycoplasma Test Kit (Promokine) according to the instructions.

HepaRG and HepaRG^{hNTCP} cells were seeded (2×10^5 cells/12-well format or 1×10^5 cells/24-well format) in the absence of DMSO. After two-week maintenance, they were

cultivated with differentiation medium containing 1.5 % DMSO for another two weeks to become susceptible for HBV and HDV infection. For MLN4924 experiments, HepAD38 cells were seeded as a monolayer and maintained for 7 d in the presence of 1 μg/mL of doxycycline. Later on, cells were washed with PBS for three times and cultivated with the same medium depleting doxycycline, which allows robust pgRNA transcription and virus assembly.

To thaw cells, frozen aliquots in -80℃ or liquid nitrogen were immediately thrown in 37℃ water bath with shaking. As soon as they were thawed, the cells were suspended with complete medium and centrifuged at 500 rpm for 5 min. Pellets were resuspended in medium and cells were seeded in a culture flask. One day later, the medium was changed in order to remove the remaining DMSO.

To freeze cells, cells in the proliferating phase were trypsinized and suspended in complete medium. Survival rate was determined by trypan blue staining and cells more than 95% survival were considered to be frozen. The cells were centrifuged at 500 rpm for 5 min and pellets were resuspended in 90 % FCS and 10 % DMSO and aliquoted in cryotubes. Aliquots were kept in freezing box containing isopropanol at -80℃ overnight before further transferred in liquid nitrogen.

2.2.2.2. Production and enrichment of HBV mutants

As shown in session 2.1.1.1, HepAD38 cells were cultivated as a monolayer in a multi-layer flask for two weeks in the presence of tetracycline. After removal of tetracycline, the supernatant was collected twice every week from week 2 to 8. Every 400 mL of supernatant was filtered and subjected to heparin affinity chromatography. The heparin-sepharose binding virus was eluted in 15.5 mL of Tris-NaCl buffer and immediately supplemented with 1.8 mL of pure FCS. This WT HBV virus was aliquoted and kept at -80℃.

For WT and Xd virus production, HepG2-H1.3 (WT) and HepG2-H1.3 (Xd) cells were seeded in 15-cm petridish as a monolayer. The supernatant was collected twice every week from week 1 to 5. Alternately, these viruses were produced by transfection of Huh7 cells in 15-cm petridish with pCHT-9/3091(WT) or pCHT-9/3091(Xd) using the PEI reagent (see 2.2.2.7 transfection). Two days post transfection, cells were washed with PBS for three times and supernatant from d 2~7, d 7~12, and d 12~17 was collected. Supernatant from each preparation was centrifuged at 4000 rpm for 15 min and filtered sterile. The supernatant was mixed with PEG8000 at a final concentration of 6% and incubated at 4℃ overnight. The next day, the

supernatant was centrifuged at 10,000 rpm at 4℃ for 1 h and the pellet was resuspended in 1% of the original volume with PBS supplemented with 10% FCS. The resuspension was rotated at 4℃ overnight and centrifuged at 8000 rpm for 10 min. Clear supernatant containing concentrated WT or Xd virions was kept at -80℃.

2.2.2.3. HBV and HDV infection

Before infection, produced HBV virus from stable cells was titrated using HBV real-time PCR, whereas virus from plasmid-transfected Huh7 cells was titrated by CsCl gradient ultracentrifugation and DNA dot-blot. PHH, HepaRG, HepaRG^{hNTCP}, HepG2^{hNTCP} cells were seeded in 24-well plates at a density of 2×10^5 PHH, HepaRG, HepaRG^{hNTCP}/well or 4×10^5 HepG2^{hNTCP}/well. For infection, 540 µL of medium (PHH, HepaRG, differentiated HepaRG^{hNTCP} supplemented with 1.5% DMSO; HepG2^{hNTCP} without DMSO) was mixed with 60 µL of 40% PEG8000 and then HBV virus (mge/cell ranging from 100 to 3000). The infection inoculate was added onto the cells and cells were incubated at 37℃ overnight. The next day, cells were washed twice with PBS and complete medium (PHH, HepaRG, differentiated HepaRG^{hNTCP} with 1.5% DMSO; HepG2^{hNTCP} with 2% DMSO) was added. The medium was changed every 2~3 days until the end of experiments. For entry inhibition, the cells were pre-treated with 1 µM of MyrB for 15 min at 37℃ and MyrB was included in inoculates during the infection.

Before HDV infection, the virus was titrated using HDV-specific real-time PCR. Differentiated HepaRG^{hNTCP} cells were inoculated with 540 µL of medium supplemented with 1.5% DMSO, 60 µL of 40% PEG8000 and HDV virus (mge/cell = 100) at 37℃ overnight. Later on, cells were washed and medium with 1.5% DMSO was changed every 2~3 days.

2.2.2.4. Production and concentration of lentivirus

Pseudo-lentivirus were produced in HEK293T cells by triple-transfection of the plasmids: (i) HBx-encoding pWPI-HBx or pIncuder20-HBx or shRNA-expressing pAPM, all of which were compatible with packaging helpers (ii) and (iii); (ii) psPAX2 encoding HIV genes (gag, pol, tat and rev) that support lentivirus replication; (iii) pMD2.G encoding VSV-G glycoproteins for lentivirus entry.

Six million HEK293T cells were seeded in a 15-cm petridish on one day before co-transfection. 27 µg of HBx-expressing plasmid, 27 µg of psPAX2 and 9 µg of pMD2.G were co-transfected (as shown in session 2.2.2.7). 24 h post transfection, the medium was gently changed. Supernatant from 24~48 h and 48~72 h post transfection was collected, pooled, centrifuged at 4000 rpm for 15 min at 4 ℃ and filtered sterile. The clear supernatant was ultracentrifuged at 20,000 rpm for 2 h at 4℃. After this centrifugation, the supernatant was discarded and the pellet was resuspended in 500 µL of William's E medium supplemented with 10 % FCS and rotated for 2 h at 4℃. After final centrifugation at 8000 rpm for 10 min, the supernatant was kept at -80℃.

2.2.2.5. Lentivirus transduction

Before transduction, lentivirus was titrated by real-time PCR using primers that bind to the woodchuck Hepatitis Virus posttranscriptional regulatory element (WPRE) within packaging plasmids. For transient lentiviral trans-complementation assay, HepG2^{hNTCP} and HepaRG^{hNTCP} cells in 24-well plates were transduced with 25 µL of concentrated lentivirus per well (mge/cell = 50) in the medium supplemented with 8 µg/mL of polybrene, which enhances transduction efficiency in retroviral infection. The next day, inoculates were discarded and fresh medium was added.

2.2.2.6. Generation of HBx-HepaRG^{hNTCP} and HBx-HepG2^{hNTCP} cells

HepG2^{hNTCP} and undifferentiated HepaRG^{hNTCP} cells were seeded at 50% density in 6-well plates and transduced with 100 µL of concentrated lentivirus that either encodes WT or HBx R96E mutant. On d 1 post transduction, inoculates were discarded and fresh medium was added. On d 3 post transduction, the cells were split and cultivated in complete medium supplemented with 1 mg/mL of G418. Untransduced cells were treated similarly as antibiotics selection control. Between 7 and 10 days post transduction, when all untransduced cells were killed and detached, transduced cells were trypsinized and transferred in a T75 flask with 1 mg/mL of G418 until d 14. The cells were maintained with 0.5 mg/mL of G418 from d 14 to 28. Most cells were frozen in liquid nitrogen for long-term storage and the rest was maintained. To characterize, 1 µg/ml of doxycycline was added in the medium for 72 h and inducible HBx expression was confirmed by western blot and immunofluorescence.

2.2.2.7. Transfection

Cells were seeded one day ago to achieve 60-70% density at the moment of transfection. For plasmid transfection, TransIT-LT1 and lipofectamine 3000 reagents were used. Specifically, one transfection mixture was prepared (0.5 μg of plasmid, 1.5 μL of TransIT-LT1, 50 μL of antibiotic-free serum-reduced Opti-MEM, 24-well format), while lipofectamine 3000 preparation required two mixtures (mixture A: 0.5 μg of plasmid, 1 μL of P3000, 50 μL of Opti-MEM; mixture B: 1 μL of lipofectamine 3000 in 50μL of Opti-MEM), which were mixed later. Each transfection mixtures was incubated at room temperature for 15~30 min and dropwise added onto the cells.

For HBV and lentivirus production, affordable PEI reagent was used as similar as lipofectamine but with different amount rates of plasmid and PEI (w/w = 1:1 in Huh7 cells; w/w = 1:3 in HEK293T cells)

For siRNA, a reverse transfection protocol was adapted according to manufacturer's instructions. Firstly, siRNA was diluted to 50 nM concentration in 100 μL of Opti-MEM medium and then 1 μL of lipofectamine RNAiMAX was added in this one transfectant. The transfection mixture was directly added into the plate for 20 min at room temperature prior to cell seeding. Secondly, during this 20 min, HepG2 cells were trypsinated, counted and adjusted to 1×10^5 per well. Finally, the cell suspension was added on the top of the transfection mixture. 3 d post transfection, knockdown efficiency of target genes was analyzed by real-time PCR or western blot.

2.2.3. Assays

2.2.3.1. DNA and RNA extraction

HBV virion DNA was extracted from heparin-purified virus stocks or unpurified supernatant of HepAD38 cells using the High Pure Viral Nucleic Acid Kit according to the manufacturer's instructions. 200 μL of virus or supernatant, 200 μL of freshly prepared working solution supplemented with carrier RNA and 50 μL of proteinase K solution was mixed and incubated for 10 min at 72℃. 100 μL of binding buffer afterward was added and thoroughly mixed. This mixture was transferred to a High Pure Filter tube and centrifuged at 8000 g for 1 min. Binding to the column, DNA was washed by 500 μL of inhibitor removal buffer once and 450 μL of wash buffer twice. DNA was eluted in 50 μL of pre-warmed water.

HBV DNA from infected hepatocytes was extracted using the NucleoSpin Tissue Kit according to the manufacturer's manuals. Briefly, cells were washed with PBS for three times and immediately lysed in 200 μL of buffer T1 to obtain total lysates. The lysates were mixed with 25 μL of proteinase K and 200 μL of buffer B3 and incubated at 70℃ for 1 h. The product was mixed with 210 μL of ethanol and loaded to silica columns, washed by 500 μL of buffer BW once and 600 μL of buffer B5 twice. Eventually, DNA was eluted in 50~100 μL of pre-warmed water. DNA content and A260/A280 absorbance values were measured using NanoDrop 2000 spectrophotometer.

HBV virion RNA was extracted from the supernatant of HepAD38 cells using the High Pure Viral Nucleic Acid Kit. Viral RNA extraction was performed similarly as described above and eluted in 50 μL of RNase-free water. The eluate was digested by RNase-free DNase at 37℃ for 30 min.

HBV total RNA from infected hepatocytes was extracted using the NucleoSpin RNA kit. Infected cells were lysed in 350 μL of buffer RA1 containing 3.5 μL of β-mercaptoethanol at room temperature for 5 min with gentle shaking. Viscose lysates were applied through the NucleoSpin Filter and centrifuged at 11,000 g for 1 min. The flow-through was mixed with the same volume of 70% ethanol by pipetting up and down. Then samples were loaded onto the silica columns and desalted by one wash of 350 μL of MDB. To remove cellular DNA, bound RNA was in-column incubated with 100 μL of reconstituted RNase-free rDNase for 15 min at room temperature. Columns were washed by adding 200 μL of RAW2 buffer once and 600 μL of RA3 buffer twice. Finally, RNA was eluted in 30 μL of RNase-free water. RNA content and A260/280 absorbance values were measured using a spectrophotometer. For northern blotting use, the concentration of RNA samples must be more than 1 μg/μL.

2.2.3.2. T5 exonuclease hydrolysis

Prior to cccDNA quantification, total DNA extracted from *in vitro* infected hepatocytes was incubated with T5 exonuclease, in this step, rcDNA, dslDNA as well as genomic DNA were hydrolyzed to dNTPs and cccDNA was intact, since total lysates containing high copy numbers of rcDNA provided false positive signals in cccDNA quantification. Among a panel of exonucleases, T5 exonuclease but not plasmid-safe DNase was identified to be the most efficient one that removes rcDNA in the presence of genomic DNA (Figure 2.1.A). The

combination of T5 exonuclease treatment and cccDNA-selective primers allowed specific quantification of cccDNA in *in vitro* infected hepatocytes (Figure 2.1.B).

To be specific, 5 μL of DNA eluate was incubated with 3.5 μL of water, 1 μL of 10× reaction buffer #4 and 0.5 μL of T5 exonuclease (5 U) at 37℃ for 1 h and 70℃ for 20 min. Digestion products were frozen at -20℃ or directly subjected to cccDNA-specific qPCR quantification.

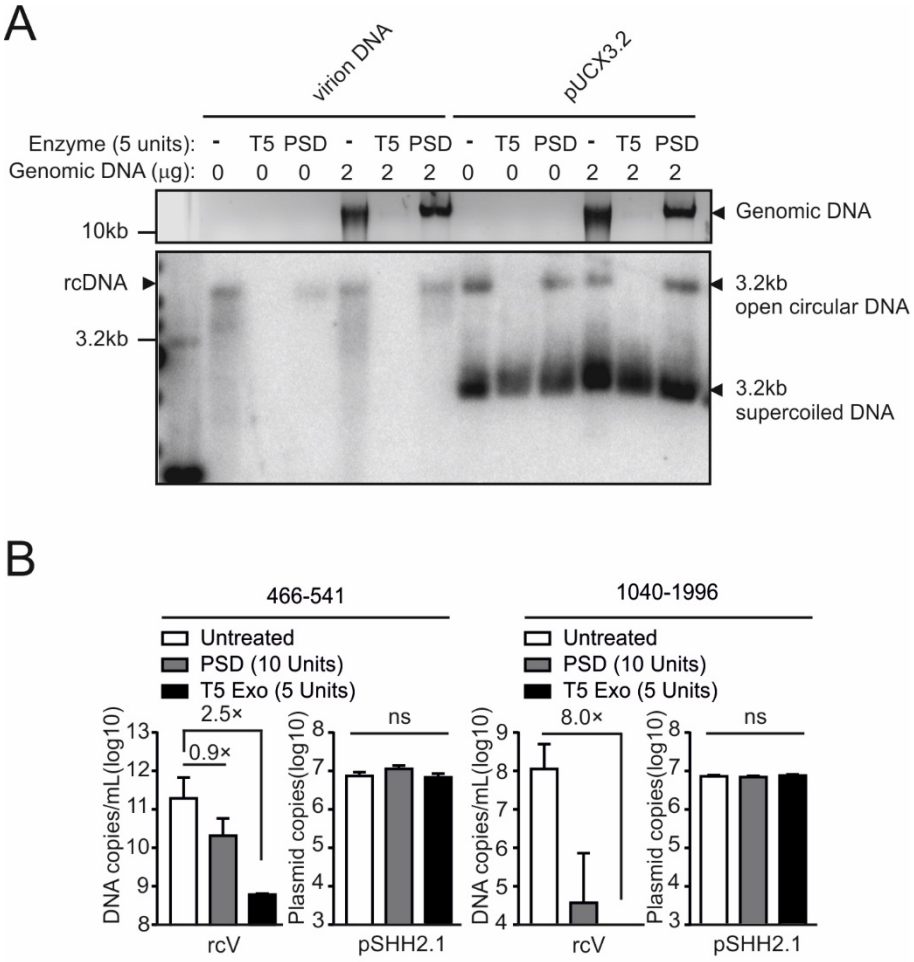

Figure 2.1. T5 exonuclease preserves cccDNA and efficiently removes rcDNA and genomic DNA. (A) Virion DNA or pUC18-HBx plasmid (3.2 kb) was digested with T5 exonuclease (T5 Exo, 5 U) or plasmid-safe DNase (PSD, 5 U) in the absence or presence (2 μg) of genomic DNA (top panel) at 37°C for 1 h and the products were loaded to Southern blotting (lower panel). (B) Virion DNA (rcV) or pSHH2.1 plasmid was incubated with T5 Exo (5 U) or PSD (10 U) at 37°C for 1 hour, and the products were further analyzed by total DNA primers (pp466-541, left) or cccDNA primers (pp1040-1996, right), respectively. ns: no significance.

2.2.3.3. cccDNA Taqman quantitative PCR (qPCR)

After comparison of a series of master mixes provided from several companies (Bio-rad, Qiagen, and Quanta Biosciences), one of them, the PerfeCTa qPCR Toughmix (95112-012), was chosen and used in the Bio-rad CFX96 TouchTM Real-time PCR thermocycler (data not shown).

Real-time quantitative PCR reaction was set up by mixing 2 µL of T5 exonuclease-digested DNA sample, 0.6 µL of p1040, 0.6 µL of p1996, 0.6 µL of probe p1085, 7.5 µL of PerfeCTa qPCR Toughmix and 3.7 µL of water (total volume 15 µL). Optimized two-step qPCR program was established: 95℃ for 15 min, followed by 95℃ for 5 seconds (denaturation) and 63℃ for 70 seconds (annealing, elongation) for 50 cycles. Relative fluorescence unit was read after each of the cycles. pSHH2.1 plasmid carrying a head-to-tail HBV dimer was 1:10 serial diluted to generate a standard curve. For low-copy standards (10^3, 10^2, 10^1 copies), 10-fold serial dilutions were specifically performed using a solvent (Tris 10 mM, EDTA 0.1 mM, yeast tRNA 10 ng/ml, and Tween-20 0.01%) instead of water (Quanta Biosciences, personal communication). Samples that were not digested by T5 exonuclease were used for human β-globin quantifications. Levels of β-globin, a single-copy gene, were used to normalize the input signals. For data analysis, "cccDNA copies/well" was primarily determined by measuring total cccDNA copies in all eluates and it was further calculated to "cccDNA copies/cell" by dividing cell numbers in one well. Finally, the number of "cccDNA copies/infected cell" was determined by using "cccDNA copies/cell" to infectivity rate. Besides, HBV total DNA numbers were quantified in undigested samples using p466 and p541 primers by SYBR-green based real-time PCR described in session 2.2.3.5. Scheme of 2.2.3.2 and 2.2.3.3 is shown (Figure 2.2).

2.2.3.4. Reverse transcription of total RNA

Total RNA samples with HBV transcripts in HBV infection or HDV genomes in HDV infection were extracted as described above. Reverse transcription was performed using the High-capacity cDNA Reverse Transcription Kit and reaction was prepared by mixing 3 µL of RNA (< 1 µg), 2 µL of 10× buffer, 2 µL of random primer, 0.8 µL of dNTP (100 mM), 1 µL of RNase inhibitor, 1 µL of RTase, and 10.2 µL of RNase-free water (total volume 20 µL). The mixture afterwards was subjected to RT-PCR using the program: 25℃ for 10 min (annealing of random primer and RNA template), 37℃ for 2 h (reverse transcription), and 85℃ for 5 min (RTase heat inactivation), 4℃ hold. Complementary DNA products were 1:10 diluted.

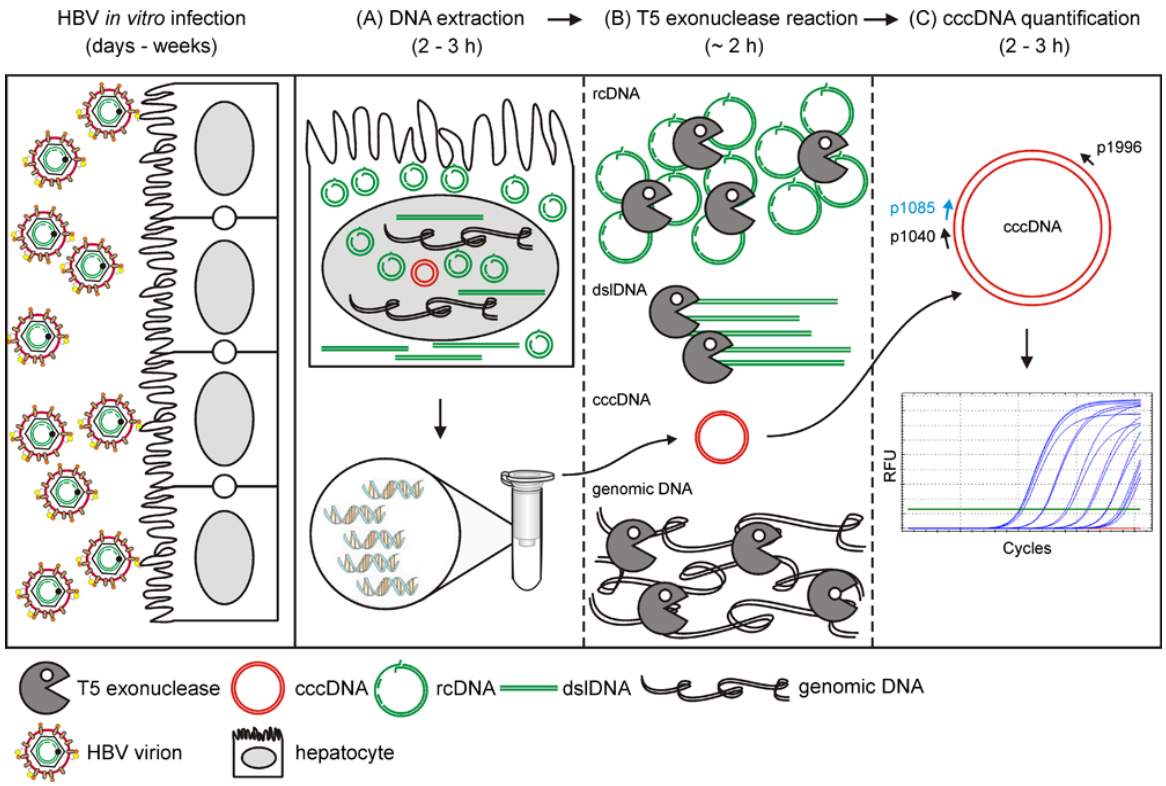

Figure 2.2. Working flowchart of cccDNA quantification. Susceptible cells (PHH, HepaRG^{NTCP}, HepG2^{NTCP}) infected with high mges (> 300) of HBV are lysed. (A) Lysates are incubated at 70 °C in the presence of proteinase K and later loaded on a silica column and eluted. (B) T5 exonuclease (5 U/1 h) removes host genomic DNA (black) and HBV replicative intermediates (rcDNA, dslDNA, *etc.*) (green) and preserves cccDNA intact (red). (C) cccDNA is amplified by p1040/p1996 primers and detected by probe p1085.

2.2.3.5. Quantitative PCR of HBV transcripts and HDV RNA

Expression levels of pgRNA, HBs and total transcripts were quantified using specific primers shown in session 2.1.3.6. PCR reaction contained 2 µL of diluted complementary DNA, 7.5 µL of 2× SYBR green mix, 0.6 µL of forward primer, 0.6 µL of reverse primer and 4.3 µL of water (total volume 15 µL). The qPCR was performed as follows: 95℃ × 5 min, [95℃ × 10 sec, 60℃ ×30 sec, plate read] × 40 cycles. As standard, pSHH2.1 plasmid was 1:10 serial diluted to obtain standard samples with 10^9, 10^8, 10^7, 10^6, 10^5, 10^4, 10^3 copies/µL and loaded aside in the same plate.

Reverse-transcribed HDV complementary DNA was quantified using the "Ferns" primers in a reaction including 2 µL of diluted DNA, 7.5 µL of 2× SYBR green mix, 0.6 µL of forward primer, 0.6 µL of reverse primer and 4.3 µL of water (total volume 15 µL) using the above program. Besides, copies of HDV RNA could be directly quantified using one-step qScript XLT RT-qPCR Toughmix in a reaction with 2 µL of the RNA template, 7.5 µL of 2× qScript XLT Toughmix, 0.6 µL of forward primer, 0.6 µL of reverse primer, 0.3 µL of probe and 4 µL

of water. RT-qPCR program was 50℃ × 10 min (reverse transcription), 95℃ × 3 min, [95℃ × 10 sec, 60℃ × 30 sec, plate read] × 40 cycles. For both HDV qPCR, overlength HDV pJC126 plasmid was 1:10 serial diluted to 10^8, 10^7, 10^6, 10^5, 10^4, 10^3, 10^2 copies/μL and loaded as standard aside.

2.2.3.6. CsCl gradient ultracentrifugation

CsCl density gradients were prepared by slowly one-by-one loading 500 μL of 1.4 g/mL CsCl at the bottom of ultracentrifugation tube, 500 μL of 1.3 g/mL CsCl, 500 μL of 1.2 g/mL CsCl and freshly prepared 500 μL of 20 % sucrose. Finally, 2.3 mL of virus supernatant or 2.3 mL of medium containing 50 μL of the concentrated virus was carefully loaded on the top without interference of CsCl layers. Ultracentrifugation tubes were accurately balanced (weight difference < 0.01 g). Ultracentrifugation was performed at 58,000 rpm for 3.5 h at 20℃. Later on, fractions were collected using Beckman Fraction Recovery System in a 96-well plate (7~8 drops of the first fraction, 6 drops of the second to the twelfth fractions). The fractions were immediately subjected to DNA dot blot or frozen at -20℃ overnight.

2.2.3.7. DNA dot blot

For quantification of HBV DNA amounts in the fractions collected from CsCl density ultracentrifugation, PBS pre-wet positive-charged nylon membrane on the top of two pieces of Whatman papers were assembled on the vacuum-based 96-well dot-blot system. Standard DNA samples were prepared by 1:20 diluting the H0 stock (1×10^{11} copies/50 μL of pCHT-9/3091 plasmid) to obtain H1 (5×10^9 copies/50 μL), which was further 1:5 serial diluted to H2 (1×10^9 copies/50 μL), H3 (2×10^8 copies/50 μL), H4 (4×10^7 copies/50 μL), H5 (8×10^6 copies/50 μL) and H6 (1.6×10^6 copies/50 μL). Standards and fractions were loaded onto the nylon membrane and washed twice with PBS. The membrane was air-dried, rapidly incubated with Soak I buffer (1.5 min, twice) and afterward Soak II buffer (1 min, four times). It was air-dried again and DNA was crosslinked twice under UV crosslinker.

To develop DNA signal on the membrane, radioactive HBV-specific DNA probe was produced using the Megaprime DNA labeling kit. In detail, 5 μL of template (SacI-linearized pCHT-9/3091 plasmid, 5 ng/μL) was mixed with 5 μL of random 9-mer oligonucleotide and 16 μL of water. This mixture was denatured at 95℃ for 10 min and immediately chilled on ice

for 3 min. Pre-cooled 4 μL of dATP, 4 μL of dGTP, 4 μL of dTTP and 5 μL of reaction buffer were added to the mixture. Bringing this mixture to the iso-lab, 2 μL of Klenow fragment (1 U/μL) and 5 μL of [α-^{32}P]-dCTP were added. The mixture was incubated at 37℃ for 15 min with gentle shaking. The product was purified using a MicroSpin G25 column to remove free radioactive labeled nucleotides and thereby the flow-through contained 15~30 bp radioactive incorporated double-strand oligos, which were denatured at 95℃ for 10 min and immediately chilled on ice again and ready for hybridization use.

The membrane with crosslinked DNA was pre-hybridized with home-made hybridization buffer at 68℃ for 1 h. The denatured probe was then dropwise added into the buffer and hybridization was performed by rotating the membrane and incubating with the probe at 68℃ overnight. The next day, the membrane was washed twice with prewarmed wash buffer for 30 min each, air-dried. After washes, radioactivity value on the membrane was measured by a counter (usually the value is 100~500). The membrane was incubated with a β-radiation ^{32}P-sensitive film (Fuji) in a locked cassette overnight. The third day, the signal on the film was read by a phosphorimager (Fuji Typhoon FLA-7000).

Using Quantify One software, a standard curve was created based on the signals from standards. Accordingly, signals of other dots were calculated into absolute HBV DNA copies. Specifically for the virus produced in transfected Huh7 cells, virus titer was the sum of DNA copies in three consensus dots representing only enveloped virions but not naked nucleocapsids.

2.2.3.8. Southern blotting

Southern blotting allows the detection of DNA samples with different sizes and structures. DNA samples extracted using the High Pure Viral Nucleic Acid Kit or the Hirt method were loaded on a 1.2% agarose gel. Gel electrophoresis was at 125 V for approximate 3 h until the bromophenol blue dye went to the boundary of the gel.

After running, the gel was soaked with 0.2 M HCl and gently agitated for 10 min at room temperature to depurinate DNA. The gel was shortly rinsed in water for three times, soaked in denaturing buffer with gentle agitation for 1 h at room temperature. Rinsed for three times in water, the gel was soaked in neutralizing buffer for 1 h at room temperature. Shortly rinsed in water, the gel was agitated and balanced for 15 min in 20× SSC buffer. To blot DNA onto nylon membrane, the transfer apparatus was assembled as follows:

Lay two pieces of Whatman 3MM paper on a scaffold chamber higher than the surface of 20× SSC buffer. Soak tails of Whatman papers in the buffer and completely wet the papers, get rid of the bubbles between papers using a plastic roller.

Lay the gel on the top of Whatman papers, remove bubbles.

Place pre-soaked positive-charged nylon membrane on the top of the gel, remove bubbles between the gel and the membrane.

Lay two pieces of Whatman papers on the top of the membrane, remove bubbles. Seal the boundaries of the gel with parafilm.

Put a stack of dry paper towels on the top of Whatman papers, avoid connection to the buffer.

Add some ballast (1000 gram) on top of the whole apparatus and let the capillary transfer running overnight.

The next day, disassemble the blotting apparatus, air dry the membrane, and crosslink it twice under UV crosslinker or bake it up to 80℃ for 1 h (both steps stabilize DNA onto the membrane). Probe production, (pre-)hybridization and signal development are the same as those described in DNA dot blot.

2.2.3.9. Northern blotting

Owing to RNA instability and its self-complementary, RNA samples were pre-denatured before gel electrophoresis and kept denature conditions relying on formaldehyde in the gel. 1.2 % formaldehyde gel was pre-run in 1× MOPS buffer supplemented with 0.2 M formaldehyde at 70 V for at least 15 min. During the pre-run process, 10 μL of total RNA (1 μg/μL) was mixed with 30 μL of Formaldehyde Loading Dye (Ambion) by pipetting up and down. This mixture was heated up to 65℃ for 15 min to denature RNA secondary structures and chilled on ice for 5 min. In the cool room, denatured RNA samples were loaded into the formaldehyde gel and electrophoresis was performed at 120 V for about 3.5 h until the dyes went to the edge of the gel. After running, the gel was rapidly rinsed with water twice and soaked in denaturing buffer (0.05 M NaOH) for 20 min at room temperature. The gel was rinsed with water for three times, further soaked in DEPC-treated 20× SSC buffer for 15 min before blotted using the facility as described above (Figure 2.3.) and transferred to nylon membrane overnight. After blotting, the membrane was crosslinked and hybridized as described above in session 2.2.3.7.

2.2.3.10. LDH cytotoxicity assay

Released lactate dehydrogenase (LDH) was measured using a CytoTox 96 Non-Radioactive Cytotoxicity kit (G1780, Promega) according to the protocol. Briefly, collected supernatant was centrifuged at 400 g for 5 minutes to remove cell debris. 50 µl of the supernatant was incubated with 50 µl of CytoTox96 reagent for 30 min with protection from light. Then, 50 µl of stop solution was added, and the colorimetric absorbance at 490 nm was measured. The untreated group was set up as 100% and viability for all the groups was normalized.

2.2.3.11. WST-1 cytotoxicity assay

PHH, HepG2^{hNTCP} and HepaRG^{hNTCP} cells treated with MLN4924 were washed twice with PBS and incubated with medium freshly supplemented with 1:15 diluted WST-1 stock (Roche 11644807001) at 37℃ for 15 min. The absorbance at 450 nm was measured using an EnVision multilabel reader (Perkin-Elmer). The untreated group was set up as 100% and the relative survival rate was calculated.

2.2.3.12. HBsAg and HBeAg measurement

The culture medium of HBV infected cells was collected and centrifuged at 4000 rpm for 5 min. Depending on distinct cell types, the supernatant was undiluted or 1:2 ~1:20 diluted with PBS. Absolute HBsAg and/or HBeAg levels were detected by commercial assays, HBsAg was measured by an Architect assay (Abbott), while HBeAg was quantified by an ADVIA Centaur XP Immunoassay System (Siemens Diagnostic). Values more than 0.05 IU/mL for HBsAg or 1.0 index for HBeAg were regarded as positive.

2.2.3.13. Immunofluorescence

Infected cells were washed twice with PBS, fixed with 4% paraformaldehyde for 30 min at room temperature. After PBS washes, cells were permeabilized with 0.25% Triton X-100 for 30 min at room temperature. Afterward, the cells were blocked with 5% milk in PBS for 1 h at room temperature and incubated with primary antibody at 4℃ overnight (dilution factor summarized in session 2.1.3.3). The next day, after three five-minute washes, the cells were incubated with 1:500 diluted Alexa Fluor 488/546/555-conjugated goat anti-rabbit/mouse/human IgG (H+L) antibody and 1 µg/mL of Hoechst 33342 dye at room temperature for 1 h. After three washes, images were taken under a DFC350 FX microscope

(Leica) and analyzed using the Fiji software. Moreover, in order to calculate the infectivity rate, both HBcAg-positive and Hoechst-positive cell numbers were counted by eyes in twenty random views under a microscope, and HBcAg-positive cell number in every 100 Hoechst-positive cells was shown.

2.2.3.14. Confocal microscopy

Confocal microscopy for SMC6 and HBcAg co-staining according to a Gilead's protocol with minor modifications. HBV infected cells grew on coverslips were fixed with 4 % PFA supplemented with 1 % sucrose for 10 minutes at room temperature. The cells were washed by PBS for three times and permeabilized with 1% Triton X-100 for 30 minutes at room temperature. Because of the instability of SMC6 epitope, fixed cells were immediately stained on the same day. The cells were blocked with 3% goat serum in PBS at 4℃ for 1 h and then co-stained with rabbit anti-SMC6 antibody (Sigma-Aldrich HPA042733, 1:100 diluted) and mouse anti-HBcAg antibody (homemade M312, 1:1000 diluted) for 1 h at room temperature. As shown in Figure 2.4., the anti-SMC6 antibody was validated and very specific. After washes with PBS for eight times, the cells were co-incubated with Alexa Fluor 488 anti-rabbit IgG and 546 anti-mouse antibody and 5 μM of DRAQ5 nuclear dye for 1 h at room temperature. After eight washes with PBS, coverslips were rinsed by pure water and air-dried for 30 min at room temperature protected from light. Finally, the mounting reagent was dropped on the slides and coverslips were faced down and attached on the slides. The next day, high-resolution images were taken under Leica confocal microscope (excitation wavelength: 488 nM SMC6, 546 nM HBcAg, 647 nM nucleus. All images were colorized, analyzed and merged by the Fiji software.

Figure 2.3. Validation of the anti-SMC6 antibody by siRNA transfection and intracellular staining. HepG2^{hNTCP} cells were mock-transfected or reverse-transfected with siRNA against EGFP (red) and SMC6 (blue). 48 h post transfection, the cells were fixed, permeabilized, and subjected to intracellular SMC6 staining using the Sigma-Aldrich antibody (1:200 diluted). SMC6 expression levels were analyzed by flow cytometry and shown in this histogram. Black curve: unspecific background staining; yellow curve: endogenous SMC6 level; red curve: EGFP negative control; blue curve: SMC6 knockdown by specific siRNA. Flow cytometry analysis was assisted by Pascal Mutz.

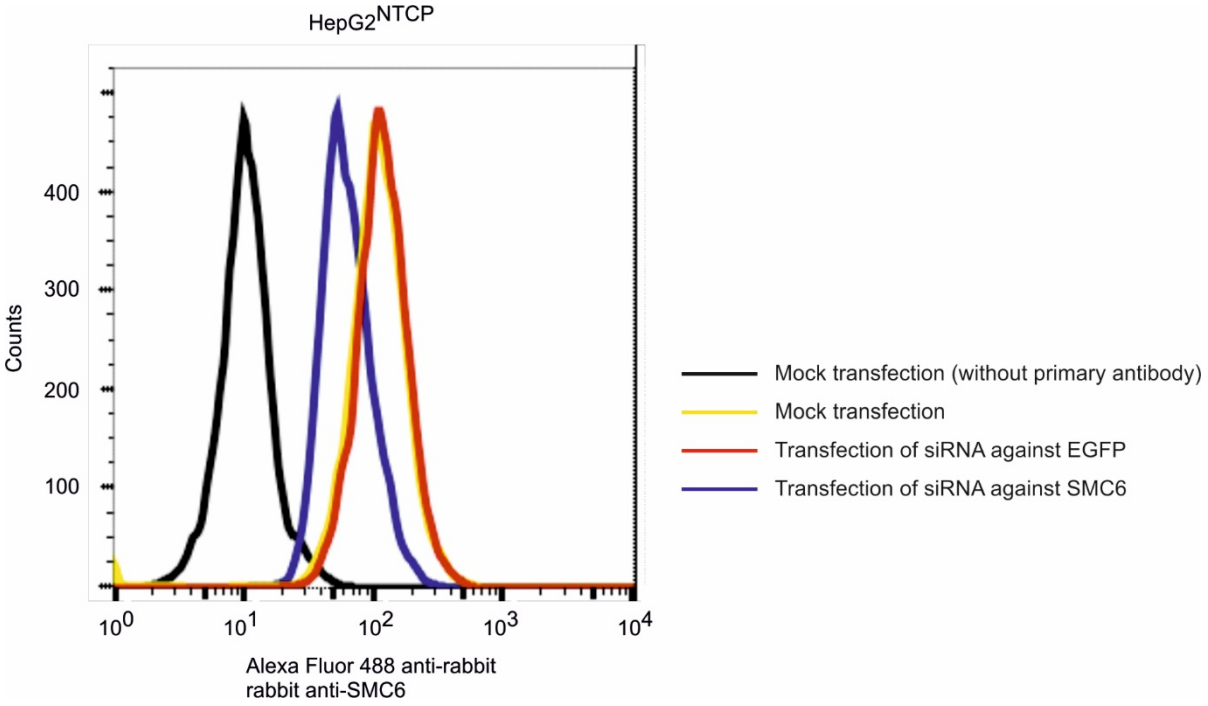

2.2.3.15. Western blotting

HBx(WT)- and HBx(R96E)-HepG2^{hNTCP} cells were lysed with 1× Laemmli buffer (Bio-rad #161-0747) supplemented with 1% protease/phosphatase inhibitors (Cell Signalling Technology #5872S) on ice for 20 min. Total cell lysates were denatured at 98℃ for 10 min and chilled on ice for 3 min. After short-time centrifugation, the lysates were loaded into a 4-20 % SDS gel for protein separation at 80 V in the stacking part and 120 V in resolving part. Proteins were blotted onto methanol-activated PVDF membrane, which was further blocked with 5% milk in TBS buffer and incubated with anti-HA antibody (1:1000) (Cell Signalling Technology #3724S) or anti-β-actin antibody (1:2000) (Sigma-Aldrich A1978) at 4℃ overnight. Membranes were washed by TBS-T buffer for 10 min for three times and incubated with HRP-conjugated secondary antibody (1:10,000) (Sigma-Aldrich A0545 and A9044) at room temperature for 1.5 h. After washes for three times, membranes were incubated with enhanced ECL substrate (Perkin-Elmer NEL104001EA) and the chemical signal was developed by an ECL chemocam imager (Intas).

Especially for SMC6 detection, nuclei of infected cells were isolated, washed and lysed to obtain nuclear lysates using the NucBuster Protein Extraction kit according to the manufacturer's instructions. The nuclear lysates were loaded into an SDS gel, wet blotted at 30 V overnight. Following steps were the same as described above.

2.2.3.16. Co-immunoprecipitation (co-IP)

To perform the co-IP assay, HBx(WT)- and HBx(R96E)-HepG2^{hNTCP} cells were transiently transfected with pcDNA3-Flag-DDB1 plasmid. 24 h post transfection, the cells were washed with PBS twice and MLN4924 was added for 48 h in the medium in the presence or absence of 1 μg/mL of doxycycline. The cells were lysed in modified RIPA buffer (50 mM Tris-HCl, 150 mM NaCl, 0.1 % NP-40) with 1 % protease/phosphatase inhibitors and 1 mM of PMSF on ice for 30 min. The lysates were centrifuged at 12,000 rpm for 10 min at 4℃ and the clear supernatant was transferred to new tubes, where proteins were incubated with mouse anti-Flag M2 antibody (Sigma-Aldrich F1804, 2 μL of antibody per 200 μL of supernatant) at 4℃ on a rotator overnight. The next day, protein G sepharose beads (GE Healthcare 10164015) were added at 4℃ for 2 h to capture Flag-DDB1 and HA-HBx(WT or R96E) complex. The beads were centrifuged down, washed with ice-cold lysis buffer for 5 cycles and finally resuspended with 1× Laemmli buffer. After 98℃ denaturation, samples were subjected to western blot.

2.2.3.17. Dual luciferase assay

Huh7 cells seeded in 24-well plates were co-transfected with 50 ng of pRL-SV40-Rluc plasmid as well as 450 ng of pGL3-HBV-promoter-Fluc plasmid overnight. The cells were treated with 5 μM of MLN4924 or 5 μM of Lamivudine for another 48 h. Later on, cells were washed with PBS for three times and lysed with 100 μL of 1× passive lysis buffer for 20 min at room temperature. 20 μL of the lysates were transferred into a white-wall 96-well plate. Using luminometer, 100 μL of coelenterazine substrate in assay buffer was automatically added to the lysate and 5 seconds later renilla luciferase unit was read. Furthermore, 100 μL of luciferin substrate in assay buffer supplemented with DTT and ATP was added and firefly luciferase unit was measured in the luminometer. Relative luciferase unit was calculated as the rate of firefly unit and renilla unit.

3. RESULTS

3.1. Kinetics of cccDNA establishment and evaluation of inhibitors on cccDNA stability

3.1.1. Raising the mge results in an increase of infected cells and cccDNA copies

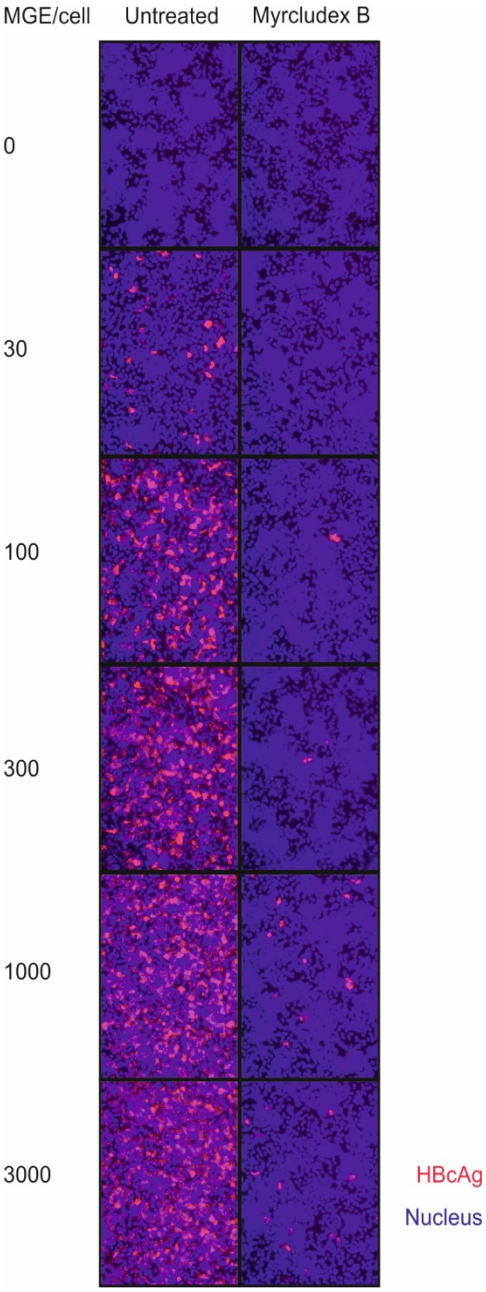

Using the method of T5 exonuclease digestion of total DNA samples followed by cccDNA-specific qPCR, the kinetics of cccDNA formation was firstly analyzed in the HepG2^{hNTCP} cells infected at different mge's. By rising the mge of HBV in inoculates, the accumulation of cccDNA in the HepG2^{hNTCP} cells was measured. Using mge's of 30, 100, 300, 1000 and 3000 per cell as shown in Figure 3.1., expression levels of intracellular HBcAg confirmed productive infection. At mge from 30 to 1000, evidently more HBcAg positive cells were observed, however the infection at the highest mge 3000 did not lead to a further increase of HBcAg^{+} cells. On the other hand, at mge >1000 the entry inhibitor MyrB profoundly reduced HBcAg expression, suggesting that HBV replication under those conditions is exclusively initiated by the receptor-mediated entry of virions and therefore HBcAg expression is cccDNA-dependent.

Figure 3.1. HBcAg expression levels in infections with increasing mge. HepG2^{hNTCP} cells were infected with different amounts of virus inoculates (mge/cell = 30, 100, 300, 1000, 3000). As control MyrB (1 μM) was co-administered during the infection to verify NTCP-mediated entry of the virus. On d 10 p.i., intracellular HBcAg expression levels (red) were visualized. Nuclei were indicated by Hoechst staining (blue).

The rise of mge per cell from 30 to 1000 led to not only an increase of infected cells but a correlative increase of total cccDNA copies per well. Similarly, the level of total DNA was also increased in a linear manner. However, at an mge of 3000 no proportional increase of cccDNA and total DNA numbers was observed (Figure 3.2.A). Therefore, cccDNA copy numbers show saturated when very high mge of the virus is used under conditions when the majority of cells have been infected, although the mechanism how the host controls cccDNA copy number is still unknown. Consistently, the correlation of mge with HBeAg and HBsAg secretion and an increased number of infected cells was

observed previously in HepaRG cells and PHH (Schulze et al., 2012). Indeed, at mge's from 30 to 1000, both HBeAg and HBsAg levels were accordingly increased. From mge's 1000 to 3000, the increase of HBsAg level was not proportional but HBeAg level was greatly inclined, probably due to the cross-detection of nucleocapsids at such a high mge (Figure 3.2.B).

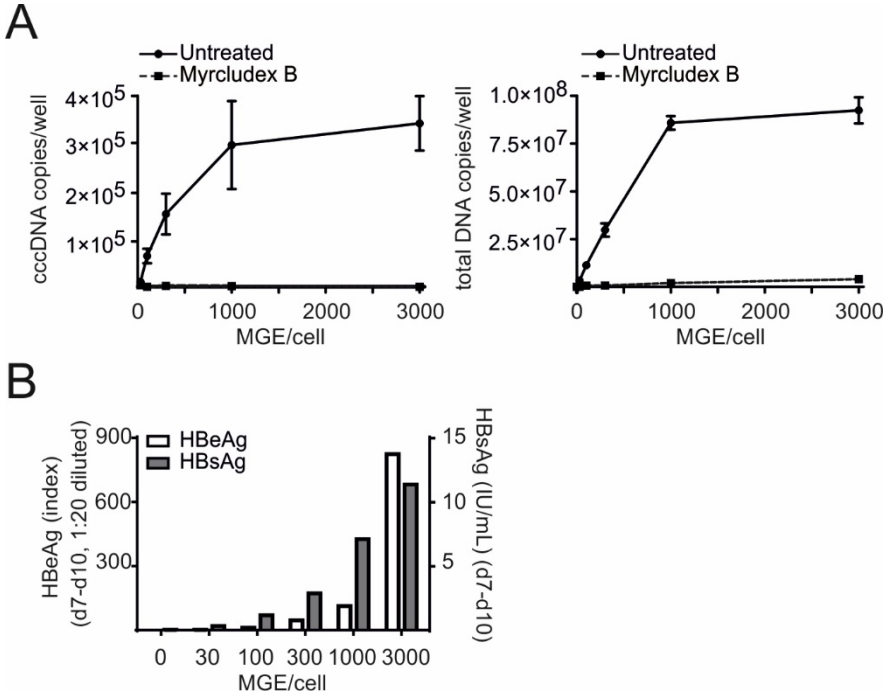

Figure 3.2. cccDNA and secreted antigen levels in infections with increasing mge. (A) HepG2^{hNTCP} cells were infected with different amounts of virus inoculates (mge/cell = 30, 100, 300, 1000, 3000) in parallel and total DNA samples were prepared on d 10 p.i.. Samples were hydrolyzed by T5 Exo (5 U/60 min) at 37°C for 1 h, and cccDNA level was determined using pp1040-1996 primers. Total DNA copy numbers were determined in undigested samples using pp466-541 primers. (B) Within the same infections, extracellular replicative markers, secreted HBsAg (grey) and HBeAg (white) values from d 7 to 10 p.i., were measured.

3.1.2. Comprehensive kinetics of cccDNA establishment in infected hepatocytes

To achieve moderate infection rates, an mge of 300 was used for infection. The cccDNA formation over time p.i. in PHH, HepaRG, HepaRG^{hNTCP}, and HepG2^{hNTCP} cells was analyzed. Under the same infection conditions, infection rates of HepG2^{hNTCP}, HepaRG^{hNTCP}, HepaRG cells and PHH were 24%, 8.6%, 5.3% and 16.7%, respectively, which were determined by counting HBcAg^{+} cells at d 7 p.i. as shown in Figure 3.3..

It was observed that 24.0 % of HepG2^{hNTCP} cells were infected, which provides the maximal infectivity among all models. To my surprise, the infectivity rate in HepG2^{hNTCP} cells was even higher than PHH with physiological hNTCP expression. However, differentiated HepaRG^{hNTCP} (8.6%) and HepaRG cells (5.3%) at the same mge value were less infected, suggesting that HBV has a strict hepatocyte-specific tropism and in these models co-existing

biliary cells can not be infected. This was confirmed by the observation that cytokeratin 18 protein, a hepatocyte-specific marker (Wells et al., 1997), was expressed in 7.8% of total differentiated HepaRG^{hNTCP} cells, which was very close to the infectivity rate 8.6%.

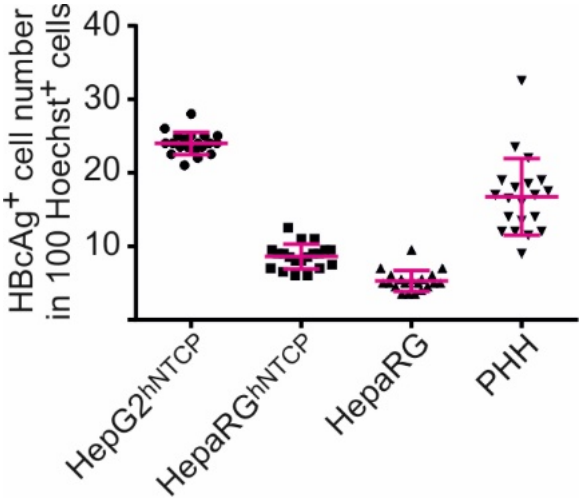

Figure 3.3. Infectivity of infected hepatocytes at an mge value of 300. Infectivity rates (d 7 p.i., mge/cell = 300) in indicated cultures were determined by counting HBcAg-positive and Hoechst-positive cell numbers from twenty random views under a microscope.

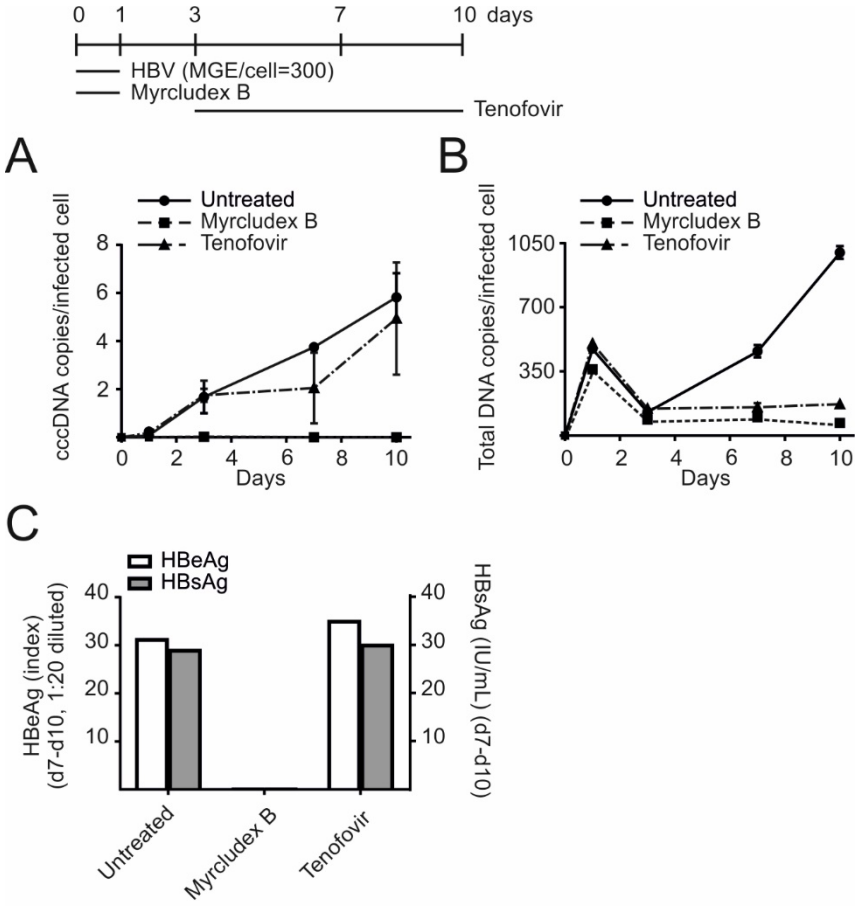

Figure 3.4. cccDNA formation and accumulation in infected PHH. PHH were infected at an mge of 300. MyrB (1 μM) and Tenofovir (15 μM) were used as controls shown in the timeline.

(A) Total DNA was extracted on d 1, 3, 7, 10 p.i.. T5 exonuclease treatment (37°C, 5 U/60 min) was performed prior to cccDNA quantification (left). cccDNA copy number was normalized by a factor derived from β-globin level to eliminate variation from inputs and further calculated to "cccDNA copies/cell". Finally, the value of "cccDNA copies/infected cell" was determined by using "cccDNA copies/cell" to divide the elution rate and infectivity rate (Figure 3.3.). (B) Undigested DNA samples were used for quantification of total HBV DNA (right). (C) Productive infection in this infection was validated by measuring secreted HBeAg (white) and HBsAg (grey) values during d 7 to 10 p.i..

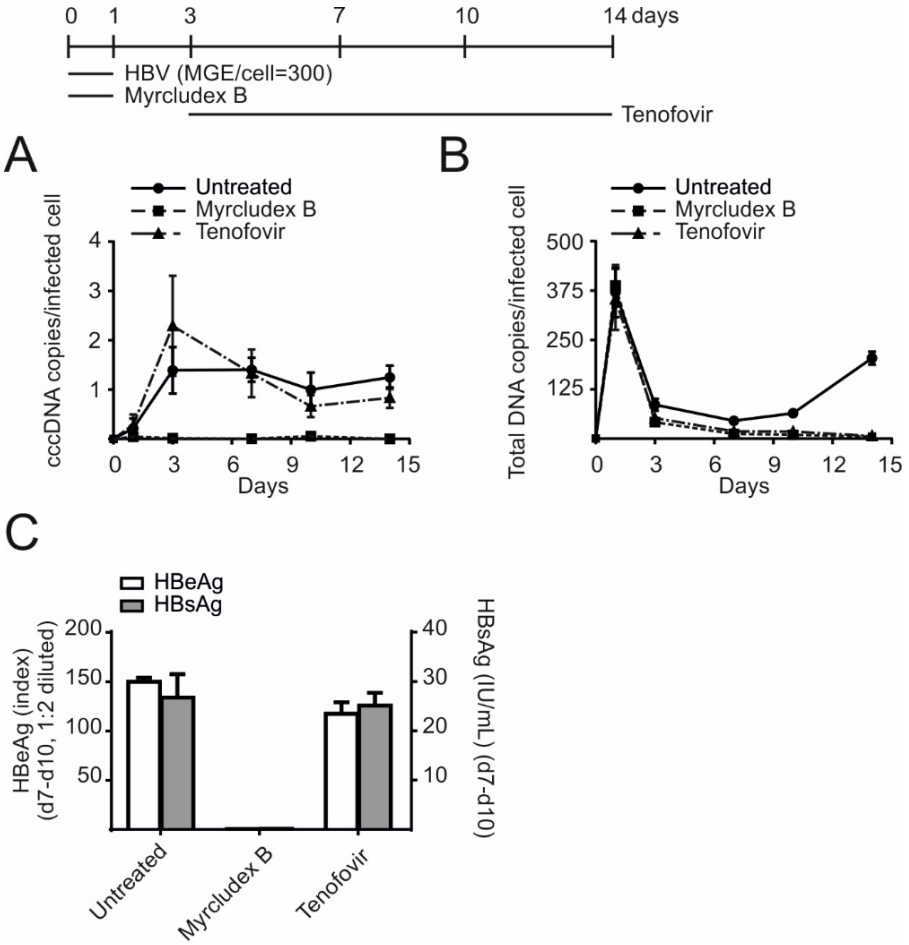

Figure 3.5. cccDNA formation and accumulation in differentiated HepaRG cells. Differentiated HepaRG cells were infected at an mge of 300, MyrB (1 μM) and Tenofovir (15 μM) were used as controls shown in the timeline. (A) Total DNA was extracted on d 1, 3, 7, 10, 14 p.i.. T5 exonuclease treatment (37°C, 5 U/60 min) was performed prior to cccDNA quantification (left). (B) Undigested DNA samples were used for quantification of total HBV DNA (right). (C) Productive infection in this infection was validated by measuring secreted HBeAg (white) and HBsAg (grey) values during d 7 to 10 p.i..

Next, the kinetics of cccDNA formation was comprehensively analyzed in all infection models. In PHH, cccDNA was hardly detectable on d 1 p.i. but accumulated swiftly to an average of 5.8 copies per infected cell at d 10 p.i. (Figure 3.4.A). Mean copy numbers of cccDNA in PHH from three donors ranged from 2.5 to 10.5 (data not shown). As expected, cccDNA formation was blocked by MyrB but not Tenofovir treatment. Input virion DNA was detected on d 1 p.i. and total HBV DNA (rcDNA and cccDNA) produced from viral replication rapidly increased at later time courses (> d 3), suggesting pgRNA synthesis and its reverse

transcription. Total DNA synthesis was sensitive to Tenofovir treatment (Fig. 3.4.B). In differentiated HepaRG^{hNTCP} and HepaRG cells, cccDNA was detectable on d 1 p.i. A unique feature was that cccDNA copy numbers increased rapidly until d 3 and remained at a stable level of 1~4 copies per infected cell until d 14, which suggests that most of the cccDNA molecules are formed simultaneously and do not undergo amplification after d 3 p.i. (Figure 3.5. and 3.6.). CccDNA formation in infected HepG2^{hNTCP} cells was similar to that in PHH with a linear increase from 0.5 copy per cell at d 3 p.i to approximate 1 copy per cell at d 14 (Figure 3.7.). Furthermore, although the kinetics of cccDNA formation differs in PHH and other cell lines, the mean values of cccDNA numbers in all the models are generally low (< 6 copies per infected cell). The cccDNA pool does not undergo intracellular amplification during two weeks after infection, which implies that significant amplification of cccDNA after the first-round establishment does not occur in all those models (Qu et al., 2018)

Regarding total HBV DNA, hundreds of copy numbers representing input virions were detected in all the systems on d 1 p.i.. Later on, a steady increase of total DNA levels representing the majority of rcDNA inside progeny nucleocapsids could be observed in all the models. However, even after two weeks p.i., there were merely 3-fold more progeny DNA than the inoculated DNA in PHH. Likewise, replicative HBV DNA produced in HepaRG^{hNTCP} and HepG2^{hNTCP} cell models was never more than the inoculates (Figure 3.4.~3.7.B). This *in vitro* data contrast the concept that HBV successful infection in chimpanzees requires inoculated dosage as low as 10 mge per animal.

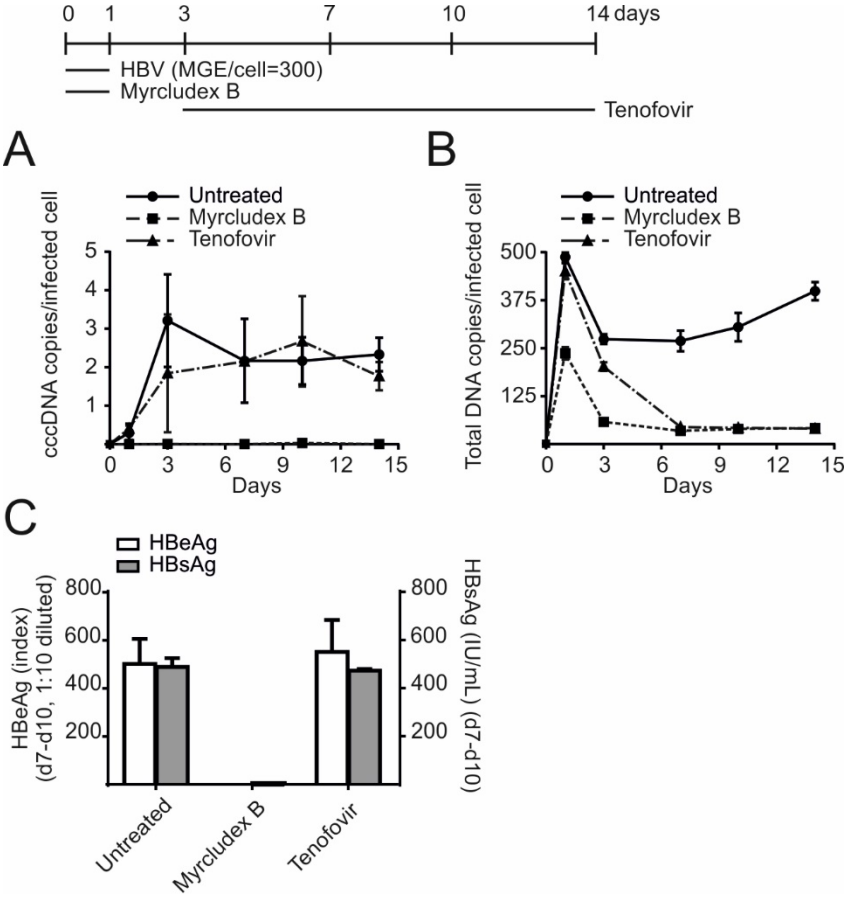

Figure 3.6. cccDNA formation and accumulation in differentiated HepaRG^{hNTCP} cells. Differentiated HepaRG^{hNTCP} cells were infected at an mge of 300 as shown in the timeline. (A) Total DNA was extracted on d 1, 3, 7, 10, 14 p.i. and cccDNA levels were quantified (left). (B) Level of total HBV DNA (right) was measured similarly as shown in Figure 3.5.. (C) Productive infection was validated by measuring secreted HBeAg (white) and HBsAg (grey) values during d 7 to 10 p.i..

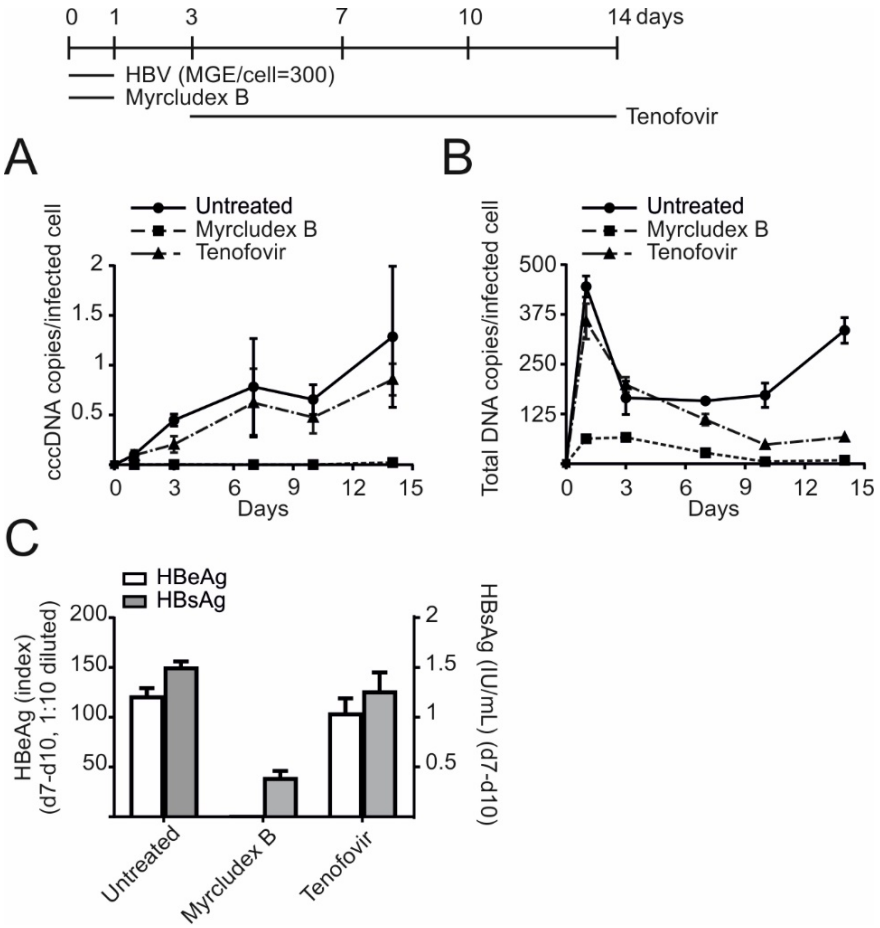

Figure 3.7. cccDNA formation and accumulation in infected HepG2^{hNTCP} cells. HepG2^{hNTCP} cells were infected at an mge of 300 as shown in the timeline. (A) Total DNA was extracted on d 1, 3, 7, 10, 14 p.i. and cccDNA levels were quantified (left). (B) Level of total HBV DNA (right) was measured similarly as shown in Figure 3.5..(C) Productive infection was validated by measuring secreted HBeAg (white) and HBsAg (grey) values during d 7 to 10 p.i.. MyrB (1 μM) and Tenofovir (15 μM) were used as controls.

3.1.3. Effects of different drugs on cccDNA formation

As shown above, the kinetics of cccDNA accumulation in HepG2^{hNTCP} cells is very close to that in PHH. Hence HepG2^{hNTCP} cells were further used for evaluation of the effect of representative drugs on cccDNA formation, which act at different steps of the HBV life cycle. The inhibitors tested were interferon-α-2b (Intron-A, Schering-Plough), two nucleos(t)ide analogues Lamivudine and Tenofovir, two entry inhibitors Myrcludex B (MyrB) and cyclosporine, and two capsid inhibitors GLS4 and BAY41-4109.

First, IFN-α, MyrB and cyclosporine were co-administered with the virus whereas nucleos(t)ide analogues and capsid inhibitors were treated p.i.. Compared to the untreated group, IFN-α did not lead to a considerable reduction of HBcAg at 100 IU/mL however moderately reduced its level at 1000 IU/mL. MyrB blocked viral entry and subsequent HBcAg expression,

whereas cyclosporine as a weaker entry inhibitor slightly reduced it. Lamivudine and Tenofovir failed to reduce HBcAg level. In contrast as capsid inhibitors, both BAY41-4109 and GLS4 profoundly reduced HBcAg at 1 μM (Figure 3.8.).

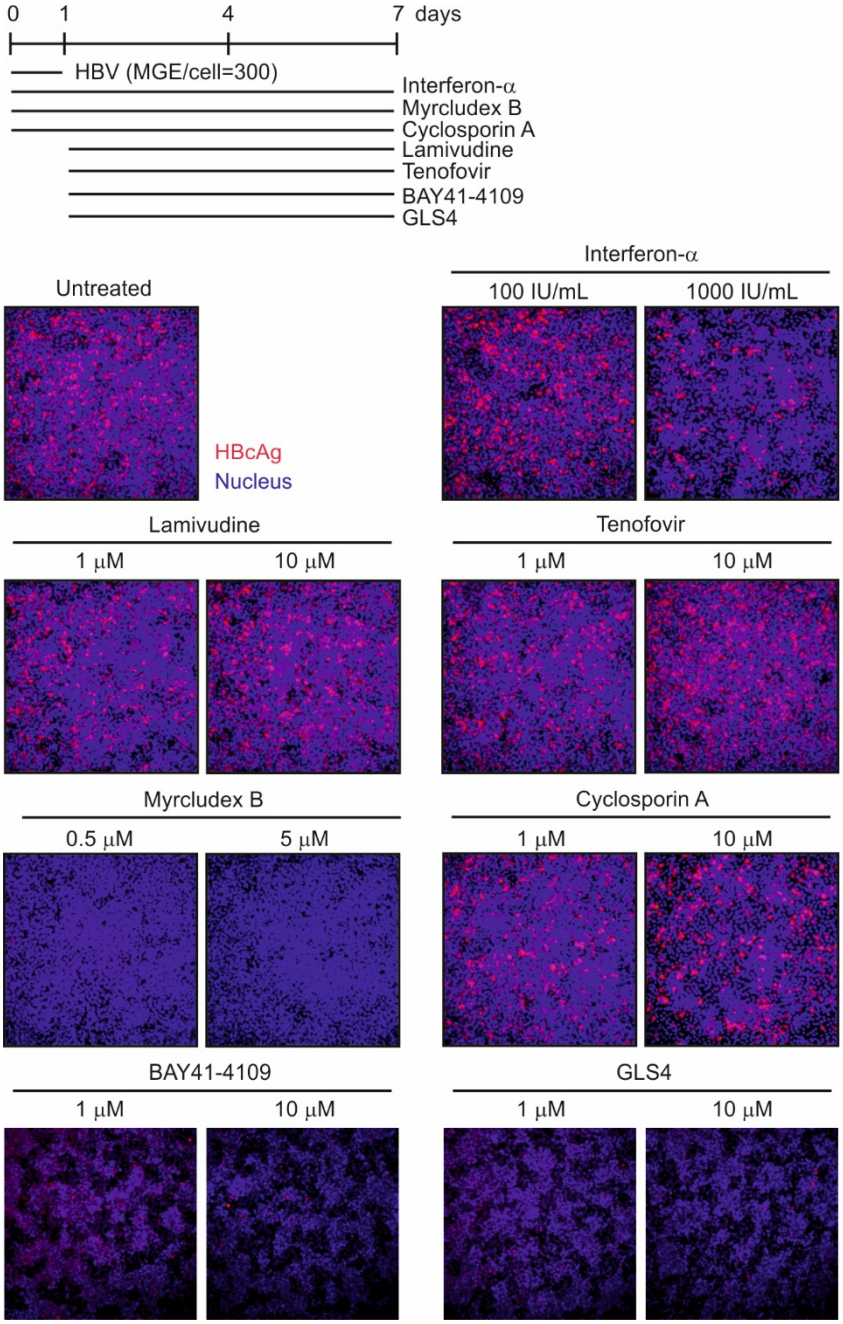

Figure 3.8. Effect of antiviral drugs on HBcAg expression. Infected HepG2^{hNTCP} cells (mge/cell = 300) were treated with interferon-α-2b (100 and 1000 IU/mL), Lamivudine (1 and 10 μM), Tenofovir (1 and 10 μM), MyrB (0.5 and 5 μM), and Cyclosporine A (1 and 10 μM) for six days or one week as shown. On d 7 p.i., cells were fixed and HBcAg staining was performed by an immunofluorescence assay (red). Hoechst staining indicates nuclei (blue).

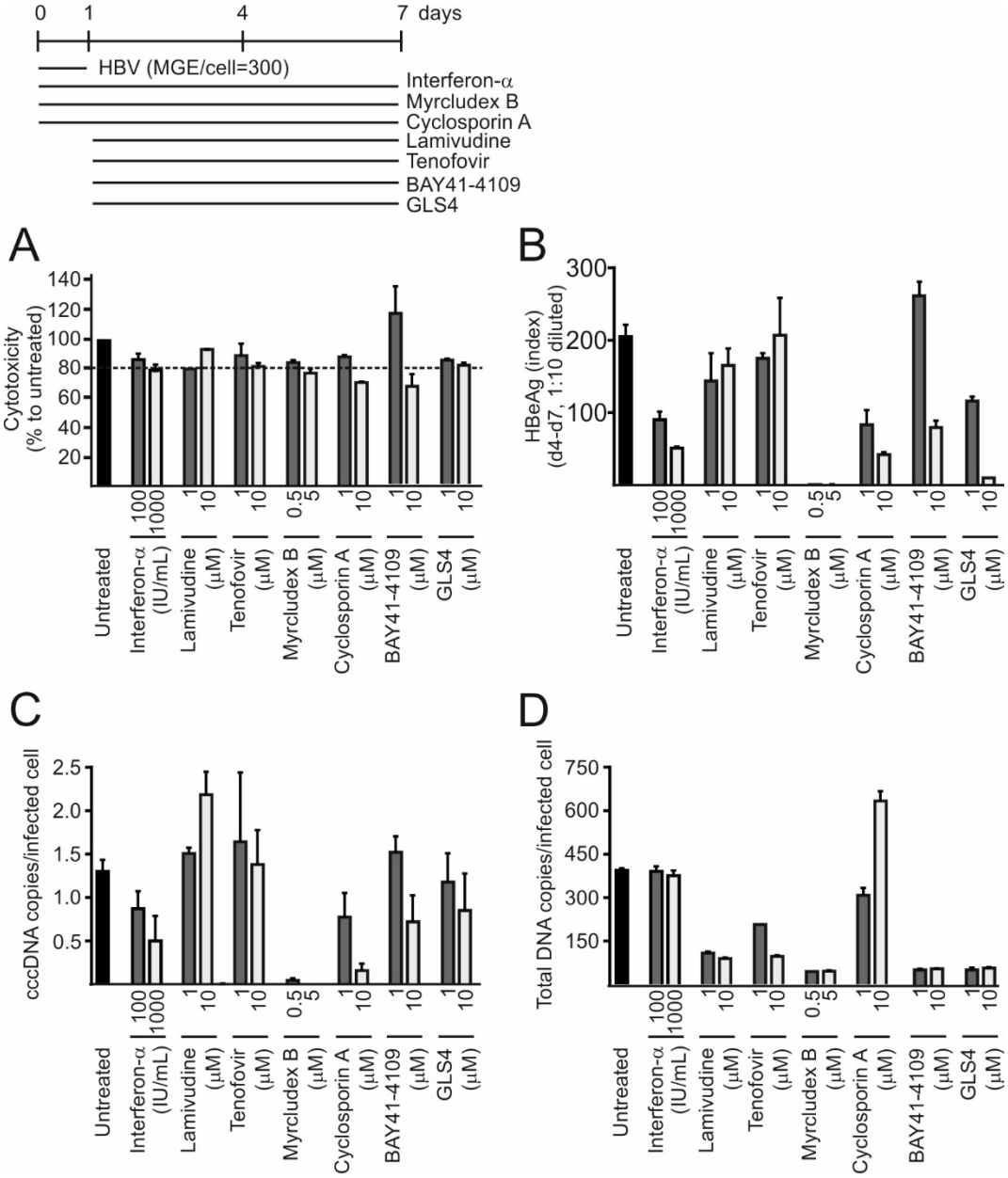

Figure 3.9. Effect of antiviral drugs on cccDNA establishment and maintenance. IFN-α-2b, entry inhibitor MyrB and cyclosporine (entry inhibition activity via NTCP binding), were co-administered with HBV inoculates during infection in HepG2^{hNTCP} cells. The drugs were maintained in cell culture medium for one week. Lamivudine, Tenofovir, BAY41-4109, and GLS4 were added from d 1 to 7 p.i. (A) Cell viability was determined by an LDH release assay. Survival rate: % to untreated set as 100 %. Dashline: 80 %. (B) Secreted HBeAg values, (C) calculated cccDNA (left) and (D) total DNA copies (right) per infected HepG2^{hNTCP} cell were shown.

Except 10 μM of BAY41-4109 and cyclosporine A, all treatments did not induce more than 20% cell death as shown in Figure 3.9.A. IFN-α inhibited cccDNA formation and HBeAg secretion in a dose-dependent manner when it was administered up to 1000 IU/mL, which is consistent with a recent report (Shen et al., 2018). MyrB completely blocked viral entry, cccDNA formation and subsequent HBeAg secretion, when it was co-administered with the virus. A similar but weaker effect was observed for cyclosporine that also prevents HBV entry

by interacting NTCP (EC_{50} = 8 μM). Nucleos(t)ide analogues hardly affected cccDNA levels when they were applied at d 1 p.i.. At 1 μM, neither GLS4 nor BAY41-4109 affected cccDNA copy numbers when they were administered at d 1 p.i.. However, a 30% reduction of cccDNA copy numbers was observed at 10 μM (Figure 3.9.C).

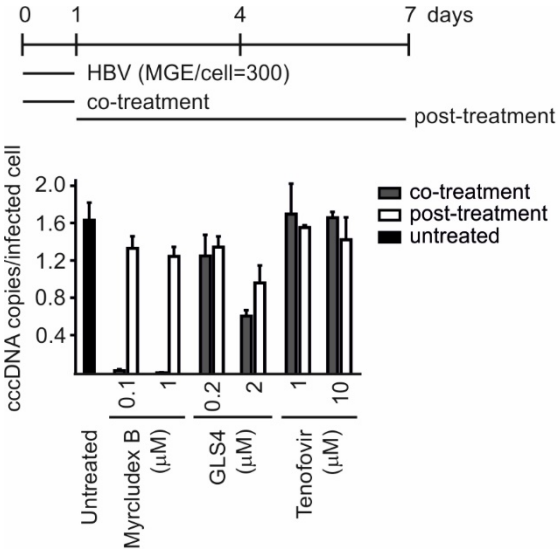

Figure 3.10. Co-treatment of MyrB or GLS4 with virus blocks cccDNA formation. MyrB (0.1 and 1 μM), GLS4 (0.2 and 2 μM), and Tenofovir (1 and 10 μM) were co-administered with HBV (mge/cell = 300) during infection (co-treatment) or p.i. from d 1 to 7. (post-treatment). CccDNA expression levels were measured on d 7 p.i..

The second experiment was set up to compare MyrB, capsid inhibitor GLS4 and nucleotide analogue Tenofovir. This data revealed that MyrB as entry inhibitor was functional in blocking cccDNA formation when it was co-administered with the virus, but not post treated. Indeed, MyrB profoundly reduced cccDNA levels at an EC_{50} value of 10 nM and an EC_{90} value of 100 nM (Qu et al., 2018). To less extent, co-administration of GLS4 at a high dose of 2 μM with virus, affected early cccDNA formation, however post treatment of GLS4 seldom reduced cccDNA level, which is consistent with the observation that such capsid inhibitors can directly act on already assembled capsids and functionally alter their structures (Guo et al., 2017, Schlicksup et al., 2018). However, the concentrations required for this activity are far exceeding the EC_{50} values for interference with virus assembly (Figure 3.10.). This data shed light on dual functions of capsid inhibitors, including the destruction of nucleocapsids during infection and interference of virus assembly p.i. (Berke et al., 2017).

Taken together, the results in this session demonstrate that (I) not only HepaRG but the recently developed NTCP-transduced cell lines, are suitable systems to study cccDNA early formation and medium-term accumulation, (II) absolute cccDNA copy numbers are extremely low (less than 6 copies per infected cell) in all *in vitro* infection models, (III) entry inhibitor MyrB blocks cccDNA formation and to less extent GLS4 interferes with cccDNA formation.

3.2. Nuclear HBx promotes transcription from cccDNA

3.2.1. HBx expressed by its authentic promoter is located in the nucleus

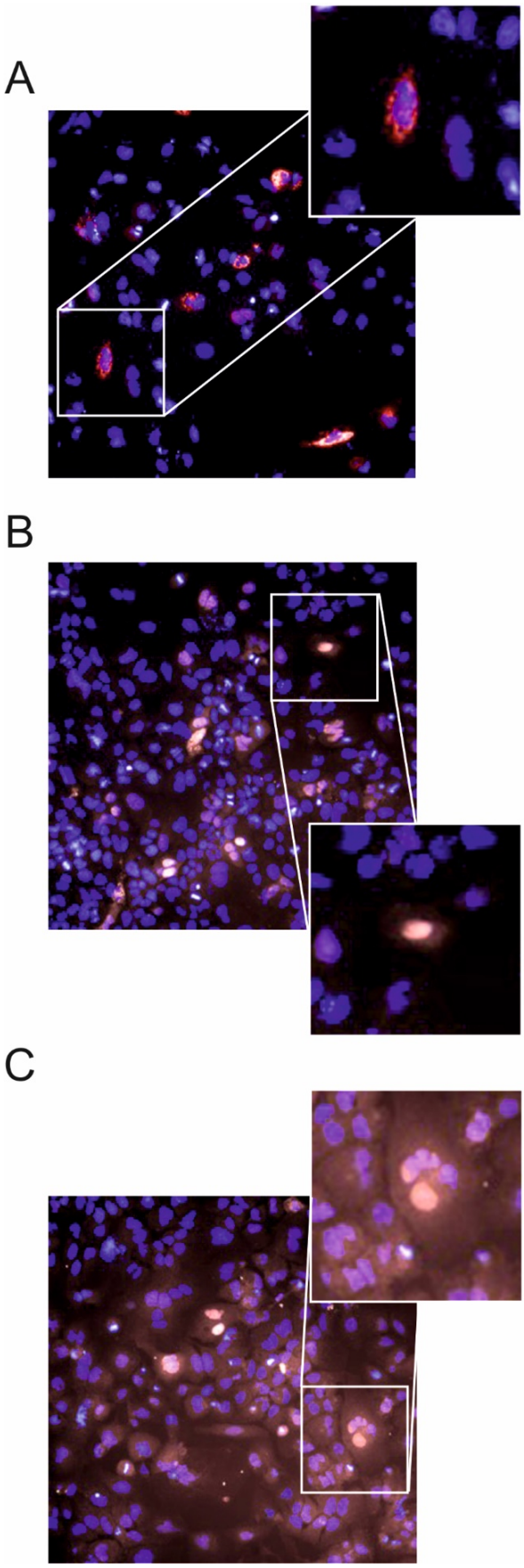

As depicted in the introduction, HBx is regarded as a multi-functional non-structural protein involved in many nuclear and cytoplasmic cellular processes. The first scientific question I thought was whether HBx is expressed in the nucleus, cytoplasm, or both. In terms of reliable detection of HBx protein in authentic HBV infection, there are two major problems: low expression level of HBx protein and long-term restriction of an antibody with the maximal sensitivity. All commercial anti-HBx antibodies and homemade anti-HBx sera were tested in order to visualize HBx expression in real HBV infection in various models (PHH, HepG2^{hNTCP} and Huh7^{hNTCP} cells) and at multiple mge's (mge/cell = 300, 1000, 3000). However, over years none of these attempts gave rise to one reliable visualization of HBx protein measured by either western blot or immunofluorescence (data were not shown). In order to study HBx localization, I stepped backward to perform transient transfection using conditions that are closer to virus infection. Therefore, Huh7 hepatoma cells were transfected with several formats of plasmid encoding HBx by different promoters (pcDNA3.1-HBx; pWPI-HBx; pCH-9/3091-HBV-1.1mer) and in each case HBx subcellular localization was monitored.

To my surprise, HBx localizations diversified. As shown in Figure 3.11.A, HBx protein was mostly located within cytoplasm when it was expressed by the CMV promoter

(pcDNA3.1-HBx). It was observed that HBx aggregated and formed speckles in the cytoplasm when its expression level was extremely high by a strong promoter like CMV. Only a small proportion of HBx appeared in the nucleus. Besides, loss of cells that was shown by reduced nuclear staining was correlated with HBx expression at such high level, suggesting that cell death might be induced in the presence of aberrantly high expression of HBx.

In contrast, when HBx was expressed by the EF1α promoter (pWPI-HBx) that is weaker than CMV promoter, HBx became mostly nuclear while a minor proportion was located in the cytoplasm. Unlike cytosolic HBx, nuclear HBx proteins were all diffused in the whole nucleus without forming any visible aggregates (Figure 3.11.B). Remarkably, when Huh7 cells were transfected with overlength HBV genome (pCH-9/3091-WT) in which HBx was expressed by its authentic X promoter, only background unspecific signals were found in cytoplasm due to the least expression of HBx protein leading to less antibody binding specificity, again, HBx protein was exclusively located and diffused expressed in the nucleus, which was very similar to what was shown in the panel B (Figure 3.11.C).

Furthermore, the amounts of HBx expression correlate with HBx subcellular localization. Driven by the strong CMV promoter, HBx is cytosolic however this situation is artificial and not physiological. By weaker EF1α or X promoter, HBx becomes nuclear but seems not co-localized with nucleolus and any nuclear bodies (Figure 3.11.). Assuming that HBx protein expressed from cccDNA in the authentic infection is less transcriptional efficient but similar to the case of transfection with overlength HBV plasmid containing the same X promoter, it is speculated that therefore HBx expression level is pretty low and HBx is also localized in nucleus of infected cells, although it remains not traceable by current methods. Additionally, it is further expected that the majority of HBx proteins arise in the nucleus and thus regulate nuclear events during HBV replication. These findings are consistent with insights presented by experienced HBx researchers (Slagle et al., 2015).

With this, for the first time, this observation suggested that at least HBx protein could be involved in the nuclear games of HBV replication, mostly meaning cccDNA formation and its transcription. Therefore, two following scientific questions were raised up: (I) whether HBx protein is indispensable in cccDNA formation and maintenance of cccDNA stability and (II) whether HBx modulates cccDNA transcription.

Figure 3.11. HBx is a nuclear protein when it is expressed by the authentic promoter. Huh7 cells were transiently transfected with plasmids (A) pcDNA3.1-HBx; (B) pWPI-HBx-IRES-GFP and (C) pCH-9/3091-HBV-1.1mer (WT) (0.5 μg plasmid per well in 24-well plate). 48 hours post transfection, the cells were fixed and stained with anti-HBx rabbit serum (#644,

1:500 diluted) (red). Hoechst staining indicates nuclei (blue). Magnification factor = 200; For zoom-in images, magnification factor = 400.

3.2.2. HBx transactivates cccDNA transcription but not affects its formation

To investigate exact roles of HBx in formation and transcription of cccDNA, WT virions together with HBx-minus (Xd) virions (HBx expression is null by introducing two stop codons within X ORF without altering polymerase and core ORFs) were generated. Since HBx is not detectable in infection, virion DNA of Xd stock was amplified by PCR and the PCR product was Sanger sequenced to confirm stop mutations on HBx (data not shown). As shown in Figure 3.12.A, when HepG2^{hNTCP} cells were infected with the same mge of WT and Xd virions produced in two independent preparations, comparable cccDNA kinetics over time was observed, suggesting that HBx is dispensable for the formation of cccDNA and maintenance of cccDNA stability. Moreover, during d 1 to 3 p.i., levels of pregenomic RNA and total transcripts were hardly affected. In contrast, compared to Xd, transcription of WT virus was significantly enhanced in the presence of HBx and this difference started from d 3 to 7 and sustained from d 7 to 10, when transcription is initiated by newly synthesized cccDNA, implying that maximal HBV transcription of cccDNA requires HBx and HBx also maintains transcription (Figure 3.12.B and C).

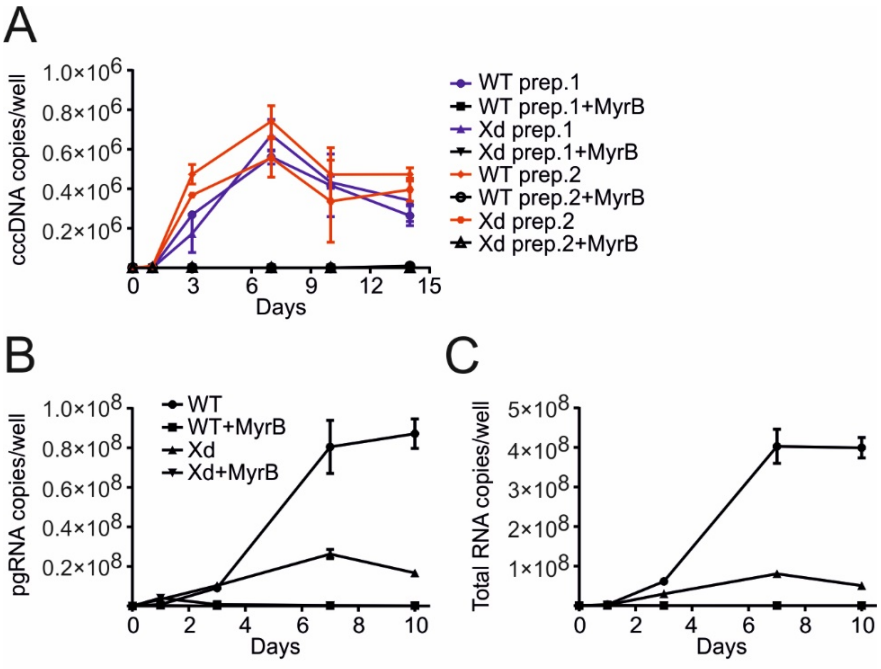

Figure 3.12. HBx is not essential in cccDNA formation but required in cccDNA transcription in HepG2^{hNTCP} cells. WT and Xd virions were generated by transfection of Huh7 cells and enriched by PEG precipitation. Prior to infection, virus titers were determined by CsCl gradient ultracentrifugation and DNA dot-blot. HepG2^{hNTCP} cells were infected with the same mge of WT and Xd virions (mge/cell = 100). (A) At d 1, 3, 7, 10, 14 p.i., total DNA was extracted and cccDNA expression levels were measured. prep.: independent preparations of each virus.

(B) At d 1, 3, 7, 10 p.i., total RNA was extracted and pgRNA genome copies were measured. (C) At d 1, 3, 7, 10 p.i., copies of total HBV transcripts were determined. As a control, MyrB (1 μM) was co-treated during each infection.

A previous study has demonstrated that HBx is a key regulator to initiate and maintain HBV replication in differentiated HepaRG cells (Lucifora et al., 2011). To confirm it, this function of HBx protein on cccDNA was further studies in differentiated HepaRG^{hNTCP} cells. When infected with WT and Xd virions, both viruses replicated similarly during d 1 and 3 p.i., except some more pgRNA signals from Xd virion on d 1 was detected. However again WT virion showed enhanced transcriptional activity over time until d 21. The transcription of the WT virus was declined after d 14, probably due to loss of differentiation status in HepaRG^{hNTCP} cells (Figure 3.13.). Moreover, these data implied that functional HBx protein might be translated very early, as transcription of WT virus started exceeding that of Xd virus at d 3 p.i., and the expression of HBx protein could be sustained at least during the first two weeks p.i..

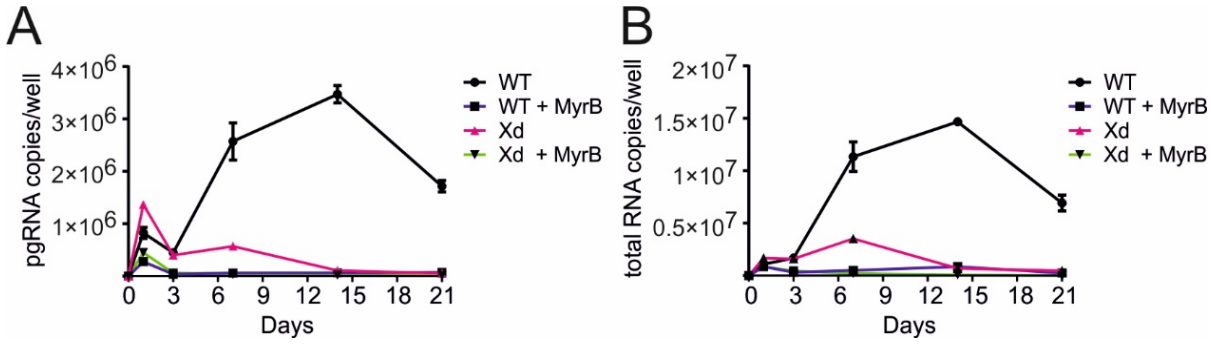

Figure 3.13. HBx enhances cccDNA transcription in differentiated HepaRG^{hNTCP} cells. Differentiated HepaRG^{hNTCP} cells were infected with the same mge of WT and Xd. virions side by side (mge/cell = 100). (A) At d 1, 3, 7, 14, 21 p.i., total RNA was extracted and genome copies of pgRNA were determined. (B) Total HBV transcripts in the same RNA samples were shown. MyrB (1 μM) was co-treated during infection.

3.2.3. C-terminal mini-HBx is sufficient and indispensable in transactivation

Next, the molecular determinants within HBx protein that mediate regulation of cccDNA transcription were characterized. Overlapping with ORFs of polymerase and core, HBx is not suitable for engineering within its genome for virus production, however, the combination of Xd infection and lentiviral trans-complementation encoding HBx mutants allows genetic modification of HBx protein.

Firstly, lentiviruses encoding truncation and deletion forms of HBx protein were generated and validated. When HepG2^{hNTCP} cells were infected with WT virus and superinfected with lentivirus expressing either GFP or full-length HBx (1-154), cccDNA transcription was not affected further inclined, indicating that basal level of HBx expressed from the WT virus is

sufficient to maintain its transcription and redundant ectopic HBx could not further elevate transcription of cccDNA. Nevertheless, when Xd virus-infected HepG2^{hNTCP} cells were subsequently transduced with lentivirus expressing full-length HBx (1-154), the transcription level was fully enhanced to the exact level of WT virus, illustrating that the cccDNA templates of Xd virus stay transcriptional inactive as long as they encounter HBx (1-154) and immediately become active, even though the HBx proteins are ectopic and late expressed. Most importantly, when Xd virus-infected cells were transduced with lentivirus expressing HBx truncations, entire C-terminal HBx (51-154) showed the same enhancing activity of cccDNA transcription as full-length HBx, the N-terminal HBx (1-50) and a deletion mutant (Δ51-142), however, showed no activity anymore on the cccDNA of Xd virus. In addition, two shorter truncations (HBx 51-142 and 58-142) were partially functional and rescued transcriptional degree of Xd virus to 50~70 % of the level of WT virus (Figure 3.14.A). Taken together, these data suggested that C-terminal HBx is sufficient and indispensable to rescue cccDNA transcription of Xd virus. In the experiments, patterns of secreted HBeAg were very consistent with corresponding transcription (Figure 3.14. B). Similar to Figure 3.12., no significant alteration of cccDNA during transduction and expression of these HBx mutants was observed, except that HBx (58-142) showed a two-fold decrease at the cccDNA level compared to the untransduced group (Figure 3.14.C).

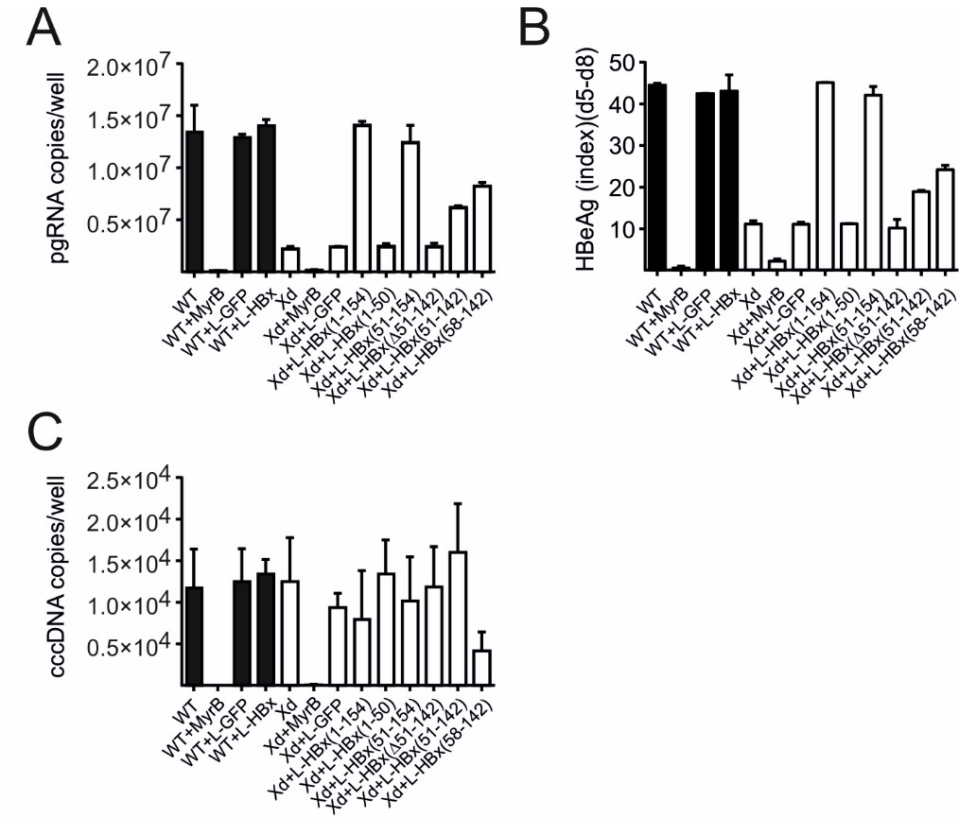

Figure 3.14. C-terminal HBx is sufficient and indispensable in cccDNA transactivation. HepG2^{hNTCP} cells were infected with WT and Xd virions (mge/cell = 100). On d 2 p.i., infected

cells were transduced with lentiviruses expressing GFP, HBx (1-154), HBx (1-50), HBx (51-154), HBx (Δ51-142), HBx (51-142) and HBx (58-142) (mge/cell = 50) overnight and afterward medium was changed every 2~3 days. On d 8 p.i., (A) pgRNA and (C) cccDNA expression levels were determined. (B) Supernatant from d 5 to 8 p.i. was collected and HBeAg values were measured.

Secondly, attentions were paid on the DDB1-binding deficient mutant, HBx (R96E). Xd virus-infected HepG2^{hNTCP} cells were transduced with lentiviruses expressing HBx (WT), HBx (R96E) and HBx (R96A). Two types of lentivirus vectors, constitute expression vector pWPI-HBx, and inducible expression vector pInducer20-HBx (kind gift provided by Bernd Wollscheid, ETH Zürich), were devised. As a positive control, transduction of HBx (WT) rescued transcription of Xd virus to the level of WT virus. For both transductions, HBx (R96E) was not able to enhance the transcription. However, HBx (R96A) still showed 80% rescue activity as shown (Figure 3.15.).

Since the arginine 96 residue is crucial to HBx-DDB1 binding, it was thereby confirmed that DDB1-binding function of HBx, or in another word, the HBx-DDB1 complex is responsible for HBx's transactivation in authentic infection setting, which provides a forward step consistent with previous study using plasmid system (Leupin et al., 2003). The R96E mutation that alters a basic residue to an acidic residue, may inactivate HBx-DDB1 binding activity. Unlike R96E, R96A mutation itself may cause a mild biochemical change and not affect the binding activity (Li et al., 2010c).

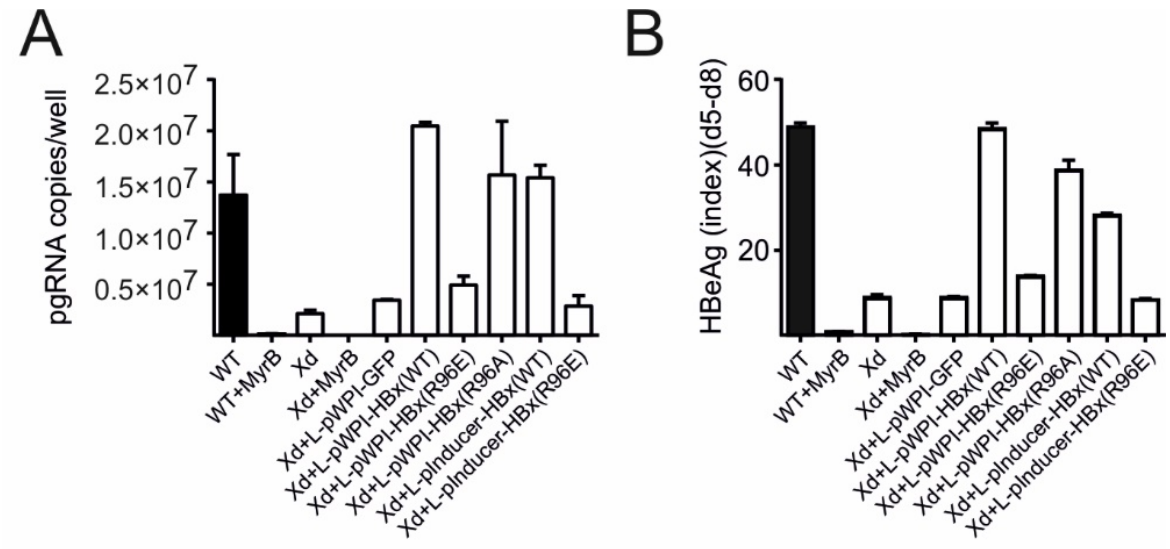

Figure 3.15. R96E single-point mutation on HBx abolishes its transactivation activity. HepG2^{hNTCP} cells were infected with WT or Xd viruses (mge/cell = 100). For Xd infection, infected cells were transduced with lentivirus (pWPI-HBx and pInducer20-HBx formats, mge/cell = 50) on d 2 p.i.. After pInducer20-HBx transduction, doxycycline (1 μg/mL) was added on d 5 p.i. to induce HBx expression. (A) On d 8 p.i., total RNA was extracted and pgRNA expression levels were examined. (B) For both transductions, supernatant from d 5 to 8 was collected and HBeAg values were measured.

To sum up this chapter, HBx is a nuclear protein when it is expressed by authentic X promoter and nuclear HBx functions as a modulator at the cccDNA level. Experiments with comparison of WT and Xd infections demonstrated that HBx protein is a transcriptional enhancer *in trans* but not essential in cccDNA formation. These data suggest the nature of HBx as a nuclear transactivator *in trans*. Furthermore, relying on the lentivirus-based trans-complementation assay, I confirmed that entire C-terminal HBx is sufficient but indispensable to enhance cccDNA transcription, presumably because generalized DDB1-binding region covers the whole C-terminus (61-154) but not the minimal binding motif (88-101) in the middle of the C-terminus, although the minimal motif is core component responsible for HBx-DDB1 binding. This has been proved by the fact that HBx (R96E) could not rescue the transcription of Xd virus, indicating that one of the functions of HBx, DDB1 binding, is the major mechanism for enhancing cccDNA transcription. Entire C-terminal HBx (51-154), termed “mini-HBx”, plays the same role as WT HBx in modulating HBV replication at the cccDNA level. However, what is the exact role of its N-terminus (1-50) is still largely unknown.

3.3. Neddylation blockage inhibits transcription from persistent cccDNA

Recently, two independent groups identified SMC5 and SMC6 as major restriction factors that are ubiquitinated and degraded during HBV replication (Decorsiere et al., 2016, Murphy et al., 2016), which provides a new direction that the prevention of this degradation may become a drug target. From HBV side, HBx protein binds DDB1 and recruits host E3 ubiquitin ligase Cullin 4A and this complex mediates SMC5/6 degradation. So far, no regimen is available to interfere with HBx-DDB1 interaction or HBx itself. Given that neddylation is required for the activation of Cullin 4A, subsequent degradation of SMC5/6 and initiation of cccDNA transcription, neddylation inhibitor may break down the HBx-DDB1-Cullin 4A complex at the Cullin 4A level.

3.3.1. MLN4924 selectively inhibits HBV but not HDV replication

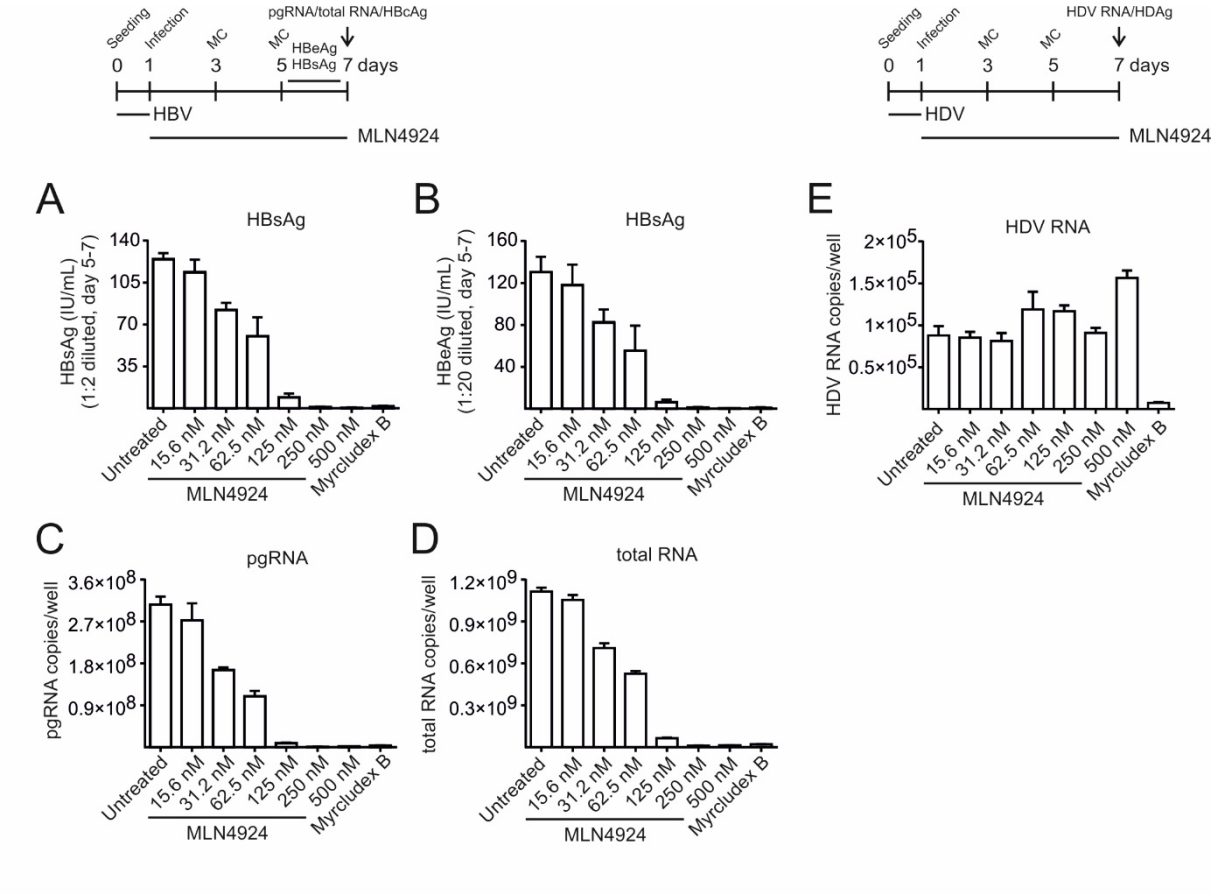

Figure 3.16. MLN4924 inhibits HBV replication and does not affect HDV RNA replication. Differentiated HepaRG^{hNTCP} cells were infected with HBV and treated with two-fold serial diluted MLN4924 (15.6, 31.2, 62.5, 125, 250, 500 nM) from d 1 to 7. (A) Secreted HBsAg and (B) HBeAg levels from d 5 to 7 were measured. On d 7 p.i., total RNA was extracted and (C) pgRNA and (D) total RNA genome copies were determined. (E) The same batch of differentiated HepaRG^{hNTCP} cells was infected with HDV and treated with the same indicated doses of MLN4924 from d 1 to 7. On d 7 p.i., total RNA was extracted and copies of HDV RNA genome were measured. MyrB (1 μM) was co-treated during infection.

As shown in Figure 3.16., six-day MLN4924 treatment reduced all HBV transcripts (pgRNA and total RNA) and secreted viral proteins (HBeAg, HBsAg) in a dose-dependent manner starting from a very low dose of 30 nM. At higher doses (> 250 nM), the inhibitory effects were comparable to the levels by MyrB treatment. In contrast, HDV replication at RNA genome level was not altered up to 250 nM. Since HBV and HDV shared the same envelopes and strategies of virus entry via NTCP receptor, this data suggested that MLN4924 does not interfere with attachment and entry steps. It also implied that neddylation is of importance specific in HBV but not HDV replication.

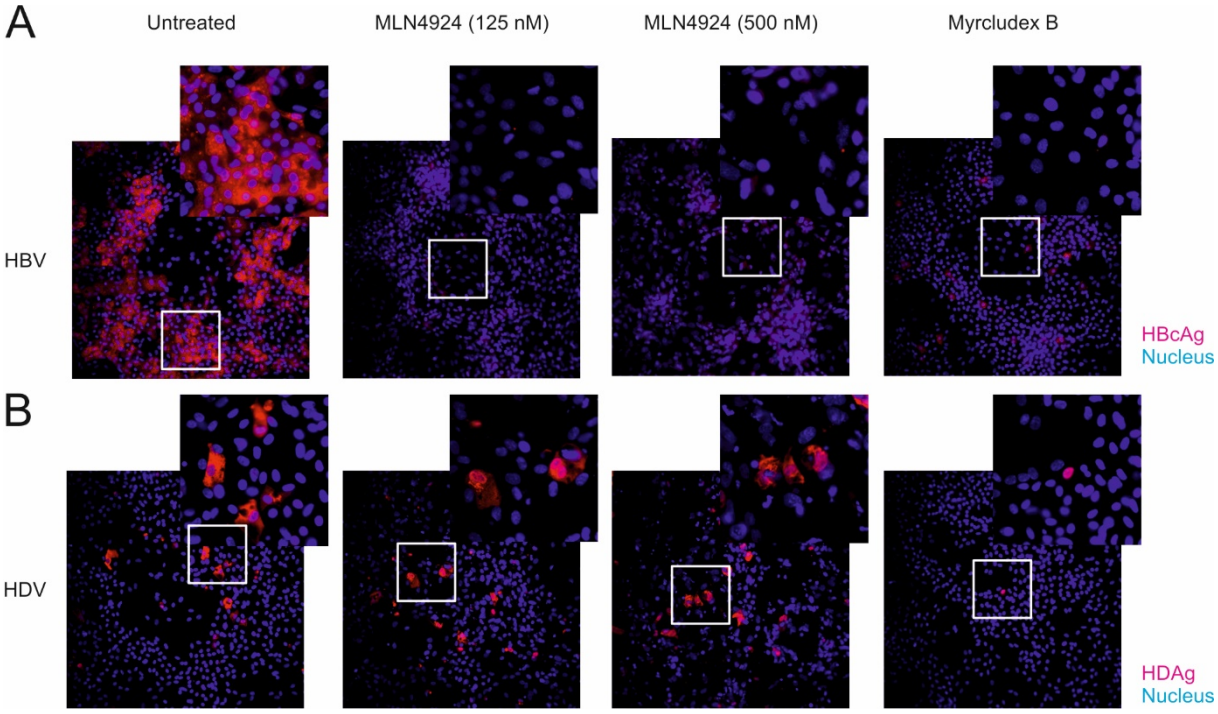

Figure 3.17. MLN4924 reduces intracellular HBcAg level but not HDAg expression. (A) Differentiated HepaRG^{hNTCP} cells were infected with HBV and administered with MLN4924 from d 1 to 7 p.i.. On d 7, cells were fixed, stained and HBcAg expression levels were visualized. (B) Differentiated HepaRG^{hNTCP} cells were infected with HDV and treated with MLN4924 from d 1 to 7 p.i.. On d 7, infected cells were fixed and HDAg levels were determined. For both infections, MyrB (1 μM) was co-treated during infection.

The other piece of evidence proving that selective effect upon MLN4924 treatment was the expression levels of HBV and HDV intracellular viral antigens. For HBV infection, HBcAg was present in all infected hepatocytes in the untreated group and its expression was diminished at 125 nM and 500 nM of MLN4924. Combining with the data in Figure 3.16, MLN4924 led to the reduction of all RNA and protein markers during HBV replication. In contrast, HDAg levels were not affected up to 500 nM in HDV infection. Besides, although cell death occurred in a small proportion of cells, either the HDAg expression in alive cells or total rate of HDAg

positive cells was not changed (Figure 3.17.). Hence, in HBV replication MLN4924 at least targets exactly on the step of RNA production or at the upstream of transcription.

3.3.2. MLN4924 reduces the production of HBV DNA- and RNA-containing virions

In recent three years, an emerging concept is the identification of pgRNA-containing particles that are enriched during nucleos(t)ide treatment. RNA-containing virions are infectious and become a new clinical marker in antiviral therapy (Wang et al., 2016, Wang et al., 2017, Wang et al., 2018). As shown in Figure 3.17., MLN4924 potentiated inhibition of intracellular pgRNA expression, one of the follow-up questions was whether MLN4924 also inhibits the production of RNA-containing virions. To test this possibility, HepAD38, the virus-producing cell that generates pgRNA and secrets a great number of virions, was incubated with MLN4924 during virus production and the amounts of RNA- as well as DNA-containing virions were measured.

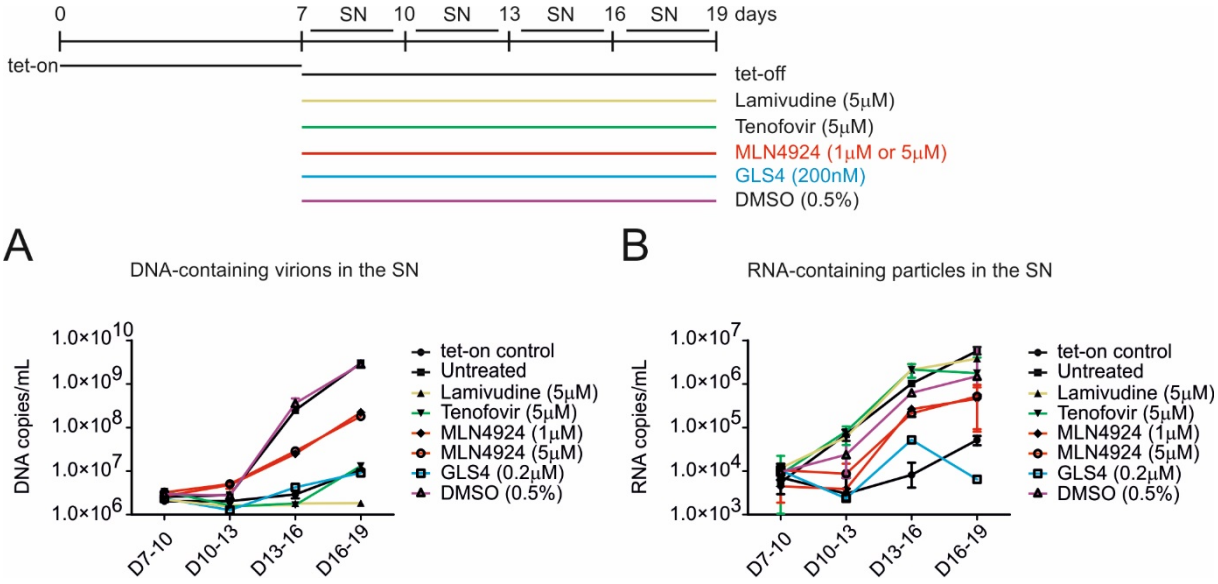

Figure 3.18. MLN4924 prevents the secretion of DNA- and RNA-containing virions. HepAD38 cells were seeded at a confluent density and maintained with supplemented doxycycline (1 μg/mL) as shown in the timeline (tet-on phase). On d 7 post seeding, doxycycline was removed and Lamivudine (5 μM), Tenofovir (5 μM), MLN4924 (1 μM or 5 μM), GLS4 (0.2 μM) and DMSO (0.5%) were added. The supernatant (SN) was collected every 3 days until d 19. Before nucleic acid extraction, the supernatant was centrifuged at 4000 rpm for 10 min to remove any cellular components. (A) Total DNA was extracted and eluates were digested with RNase (10 U/60 min) and DNA copies in the product were measured. (B) Total RNA was extracted and eluates were digested with RNase-free DNase (10 U/60 min) then RNA copies in the product were determined.

As expected, Lamivudine as well as Tenofovir, resulted in 300-fold (approximate 2.5 log-scale) less encapsidated DNA in the supernatant during d 16 to 19. Interestingly, Lamivudine showed unexpected better inhibitory effect on DNA secretion than Tenofovir, which is more potent in patients. As a positive control, the capsid inhibitor GLS4 led to a reduction of virus

production to the same extent as that induced by nucleos(t)ide inhibitors. Upon MLN4924 treatment, 30-fold (1.5 log-scale) less DNA-containing viruses in the supernatant were detected (Figure 3.18.A). On the other hand, GLS4 showed a similar 300-fold reduction of RNA-containing particles as DNA-containing particles at the late time course, demonstrating that GLS4 decreases production of RNA- and DNA-containing viruses in common probably due to the inhibition of capsid assembly independent on pgRNA conversion to rcDNA. However, Lamivudine and Tenofovir treatments failed to decline RNA amounts, compared to the untreated group, which is consistent with their modes of action that block reverse transcription of pgRNA but do not affect pgRNA itself. Remarkedly, MLN4924 treatment resulted in 10-fold less production of RNA-containing particles (Figure 3.18.B). Unlike nucleos(t)ides selective to DNA inhibition, MLN4924 showed no selectivity on the RNA- and DNA-containing viruses, although both inhibitory effects were less efficient than GLS4. These data implied that the mechanism of MLN4924 might be (I) prevention of pgRNA production as shown in Figure 3.16. and/or (II) blockage of capsid assembly similar but less efficient to GLS4. Nevertheless, the mechanism (I) is distinct from modes of action of nucleos(t)ide inhibitors and capsid modulators.

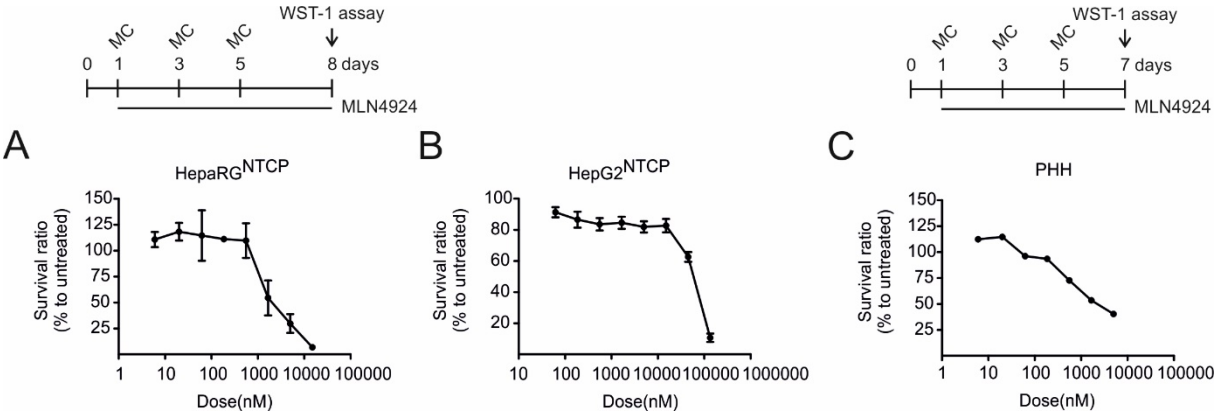

Figure 3.19. CC_{50} values of MLN4924 in HepaRG^{hNTCP}, HepG2^{hNTCP} cells and PHH. (A) Differentiated HepaRG^{hNTCP} and (B) HepG2^{hNTCP} cells were treated with 1:3 serial doses of MLN4924 (HepaRG^{hNTCP}: 6.7 nM, 20 nM, 67 nM, 200 nM, 667 nM, 2 μM, 6.67 μM, 20 μM; HepG2^{hNTCP}: 67 nM, 200 nM, 667 nM, 2 μM, 6.67 μM, 20 μM, 66.7 μM, 200 μM) from d 1 to 8 post seeding. On d 8, WST-1 assay was performed and survival rates were calculated (untreated: 100%). (C) PHH were treated with different doses of MLN4924 (6.7 nM, 20 nM, 67 nM, 200 nM, 667 nM, 2 μM, 6.67 μM) from d 1 to 7 post seeding. On d 7, WST-1 assay was performed and survival rates were calculated (untreated: 100%).

3.3.3. Transcripts of all HBV promoters on cccDNA are declined upon treatment

Furthermore, pharmacologic index values of MLN4924 in all models were measured. CC_{50} values in PHH and HepaRG^{hNTCP} cells were comparable, however, HepG2^{hNTCP} cells were much more tolerant with a CC_{50} value of 70 μM (Figure 3.19.). Next, EC_{50} values of MLN4924 were measured in those infection systems. HBV infected HepaRG^{hNTCP} and HepG2^{hNTCP} cells

were treated with MLN4924 for 7 days and infected PHH for 6 days. Comprehensive documentation at secreted HBsAg/HBeAg, total transcripts as well as cccDNA was made. In HepaRG^{hNTCP} cells, the EC_{50} value of HBsAg was 26.9 nM and the value of HBeAg was 15 nM, while the EC_{50} value of transcription was 30.2 nM. Except for 2 μM leading to cytotoxicity and loss of cccDNA numbers, MLN4924 never induced more than 30% reduction on the cccDNA numbers, suggesting that MLN4924 is a transcriptional inhibitor (Figure 3.20. A~D).

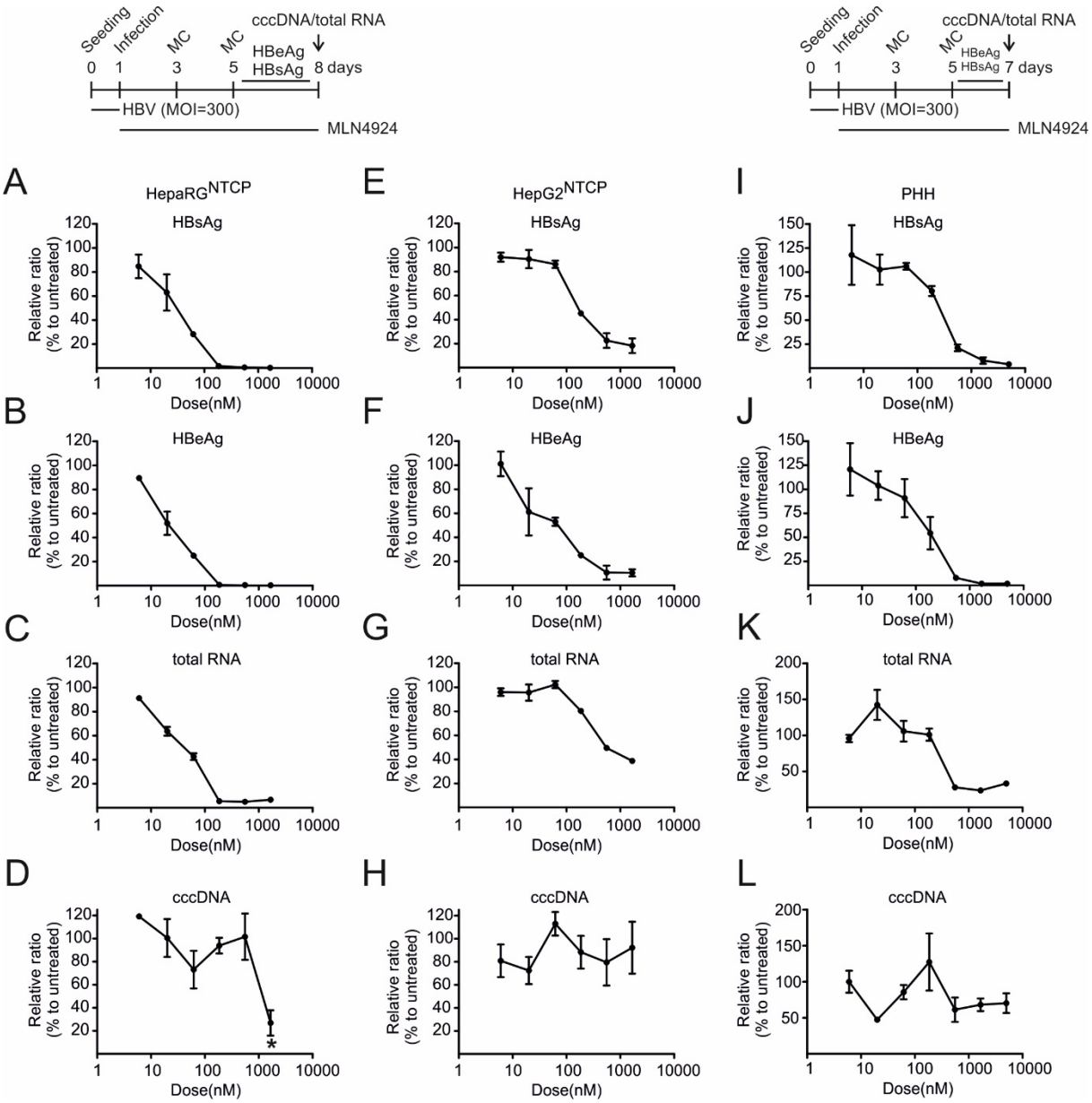

Figure 3.20. EC_{50} values of MLN4924 in HepaRG^{hNTCP}, HepG2^{hNTCP} cells and PHH. Differentiated HepaRG^{hNTCP} cells were HBV infected and treated with MLN4924 (6.7 nM, 20 nM, 67 nM, 200 nM, 667 nM, 2 μM) from d 1 to 8 p.i.. (A) HBsAg and (B) HBeAg levels in the supernatant from d 5 to 8 were determined. (C) On d 8, total RNA was extracted and total transcripts were measured and (D) cccDNA level in total lysates was determined. *: cytotoxicity at 2 μM. HepG2^{hNTCP} cells were infected and treated with MLN4924 (6.7 nM, 20 nM, 67 nM, 200 nM, 667 nM, 2 μM) from d 1 to 8 p.i.. (E) HBsAg and (F) HBeAg levels in the supernatant from d 5 to 8 were determined. (G) On d 8, total transcripts were measured and (H) cccDNA level was examined. PHH were infected and treated with MLN4924 (6.7 nM, 20 nM, 67 nM,

200 nM, 667 nM, 2 μM, 6.67 μM) from d 1 to 7 p.i.. (I) HBsAg and (J) HBeAg levels in the supernatant from d 5 to 7 were determined. (K) On d 7, total transcripts were measured and (L) cccDNA level was examined.

In HepG2^{hNTCP} cells, the EC_{50} value of HBsAg was 175 nM and the value of HBeAg was 30.2 nM, but the EC_{50} value of transcription was much higher at 484.7 nM. cccDNA level, however, was quite stable upon MLN4924 treatment (Figure 3.20. E~H). In PHH, the EC_{50} value of HBsAg was 293.4 nM, the value of HBeAg was 143.7 nM and the value of transcription was 292.4 nM (Figure 3.20. I~L). Overall, all EC_{50} values in all three models were in the nanomolar range (< 1 μM). Besides, HBV replication in HepaRG^{hNTCP} and HepG2^{hNTCP} cells, compared to PHH, was more sensitive in responding to MLN4924 treatment according to the EC_{50} values.

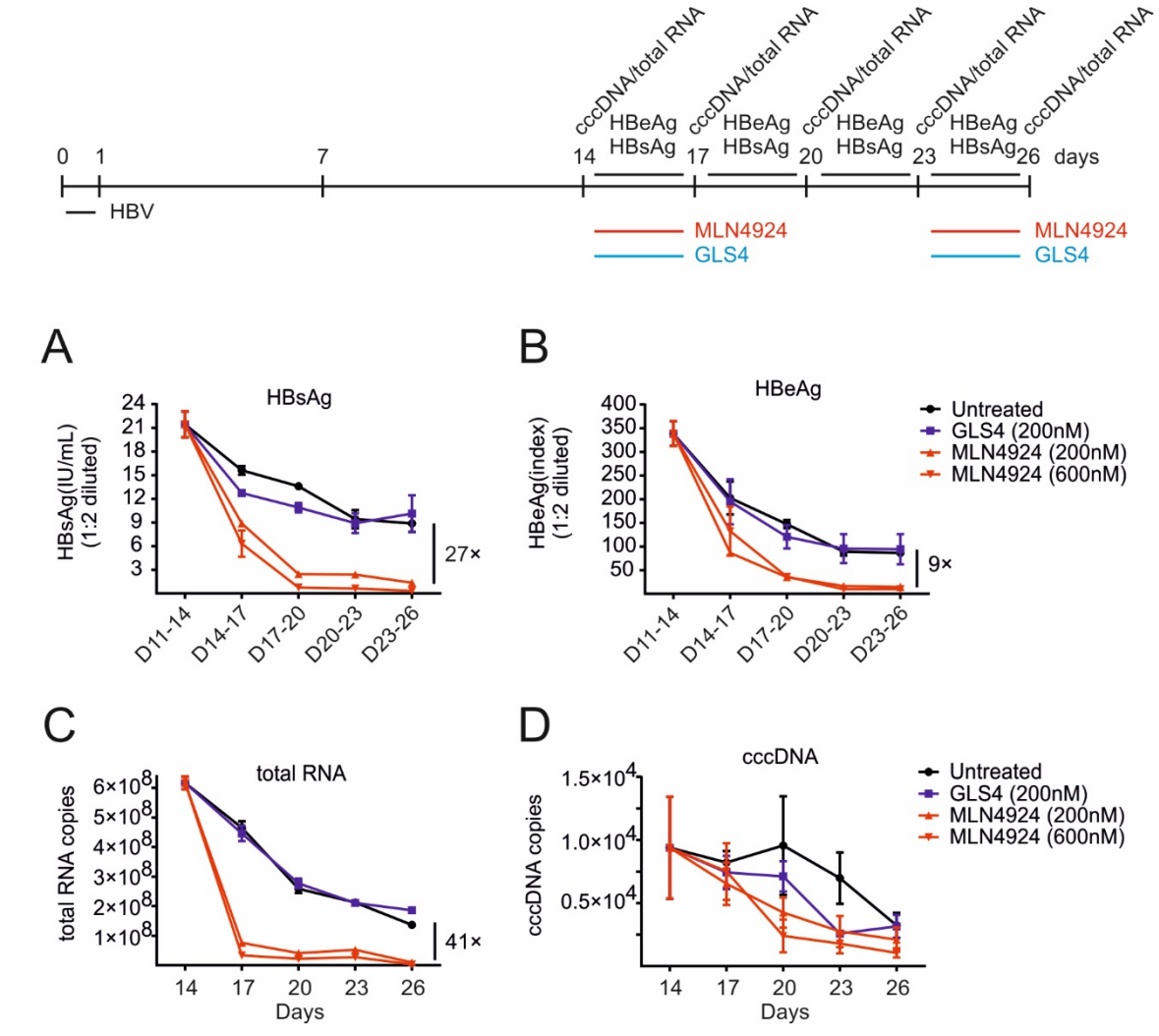

Figure 3.21. MLN4924 mediates irreversible transcriptional inhibition from persistent cccDNA in HepaRG^{hNTCP} cells. Differentiated HepaRG^{hNTCP} cells were infected with HBV and maintained until d 14, when cells were pulse-treated with MLN4924 (200 nM and 600 nM) or GLS4 (200 nM) from d 14 to 17 and d 23 to 26. During d 17 to 23, MLN4924 was removed. Starting from d 11 p.i., the supernatant was collected every 3 days and (A) HBsAg and (B) HBeAg values were determined. On d 14, 17, 20, 23, and 26, (C) total RNA was extracted and total transcripts were examined. (D) cccDNA levels were also measured.

As shown in Figure 3.20., MLN4924 is a transcriptional inhibitor without interference with cccDNA. Since cccDNA reservoir has been established in chronic HBV patients, it is meant to address whether transcription remains hampered upon MLN4924 treatment when the cccDNA pool has been fully formed. I therefore conducted long-term infection in differentiated HepaRG^{hNTCP} cells and maintained them for 14 d which was followed by a pulse treatment (3-day on, 6-day off and 3-day on of MLN4924). Transcription from persistent cccDNA was rapidly inhibited upon the first round 3-day treatment and sustained inhibition of transcription was observed during withdrawal of MLN4924. In addition, the second round of 3-day treatment achieved a 41-fold reduction of transcription. As a result, 27-fold reduced HBsAg and 9-fold reduced HBeAg levels were observed by the end of the second round treatment. In contrast, capsid inhibitor GLS4, neither affected transcripts nor HBsAg secretion. Loss of cccDNA numbers occurred spontaneously in the untreated HepaRG^{hNTCP} cells after 20 d p.i. (7 weeks post cultivation) and in this case, MLN4924 speeded up cccDNA decay but this acceleration effect was minimal (approximate 2 fold) (Figure 3.21.). Besides not only cccDNA numbers, after 14 d long-term infection, levels of transcripts and secreted HBsAg/HBeAg were also declined without any treatments in differentiated HepaRG^{hNTCP} cells, meaning that the cellular environment of HepaRG^{hNTCP} cells becomes worse and worse to support stable HBV replication over time.

Since differentiated HepaRG^{hNTCP} cells are not the best model supporting stable HBV replication for more than three weeks, the HepG2^{hNTCP} cells, which allow long-term infection were infected (Yi Ni & Bingqian Qu, 2016 international HBV meeting) and pulse-treated with MLN4924 from 14 d p.i. on. During initial 3-day treatment, MLN4924 inhibited cccDNA transcription as well as antigen secretion. To my surprise, a rebound of transcription occurred during the removal of MLN4924. Especially during d 3 to 6 post withdrawal (d 20 to 23 p.i.), the number of transcripts came back to the same level of untreated group, meaning that cccDNA transcription is completely recovered. Interestingly, the rebound transcription was immediately inhibited again compared to the untreated by the second round of MLN4924 treatment, suggesting that MLN4924 can inhibit reactivated transcription from cccDNA being activated after transcriptional silence (Figure 3.22.A~C). In this model, the cccDNA pool was much more stable. Except for one outlier (MLN4924, 3 μM, d 20), MLN4924 did not affect cccDNA stability and thereby this “switch on-and-off” of cccDNA transcription was independent on cccDNA destruction but relying on its transcriptional manipulation (Figure 3.22.D). The findings clearly demonstrated that MLN4924 blockage of transcription is reversible in

HepG2^{hNTCP} cells and suggested that modes of the exact action of cccDNA transcription in HepG2^{hNTCP} and HepaRG^{hNTCP} cells might be distinct.

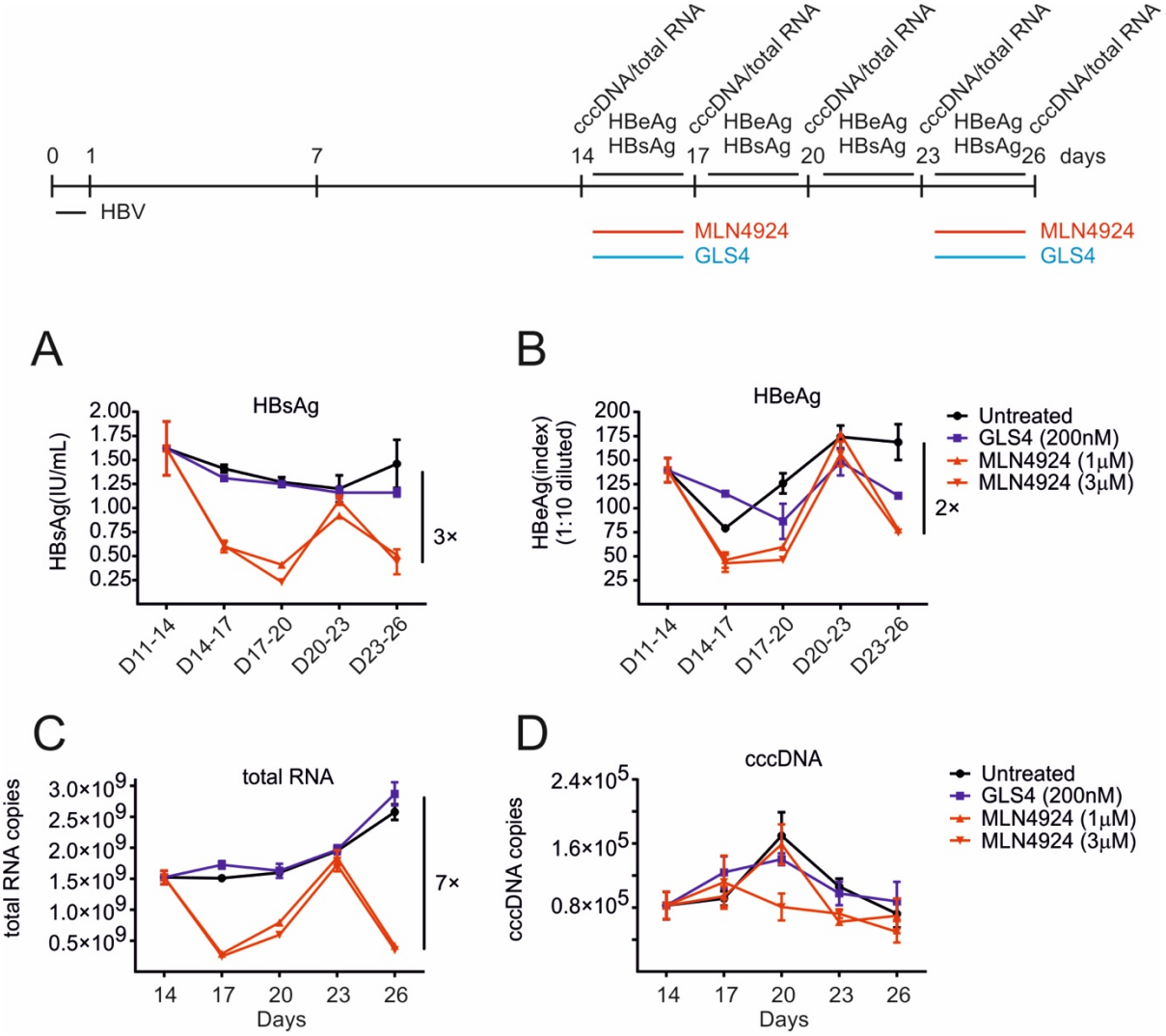

Figure 3.22. Rebound of cccDNA transcription after MLN4924 withdrawal is prompt in HepG2^{hNTCP} cells. HepG2^{hNTCP} cells were infected with HBV and maintained until d 14 when cells were pulse-treated with MLN4924 (1 μM and 3 μM) or GLS4 (200 nM) from d 14 to 17 and d 23 to 26 (3-day on, 6-day off and 3-day on of MLN4924). From d 11 p.i., the supernatant was collected every 3 days and (A) HBsAg and (B) HBeAg values were determined. On d 14, 17, 20, 23, and 26, (C) total RNA was extracted and total transcripts were examined. (D) cccDNA level was also quantified.

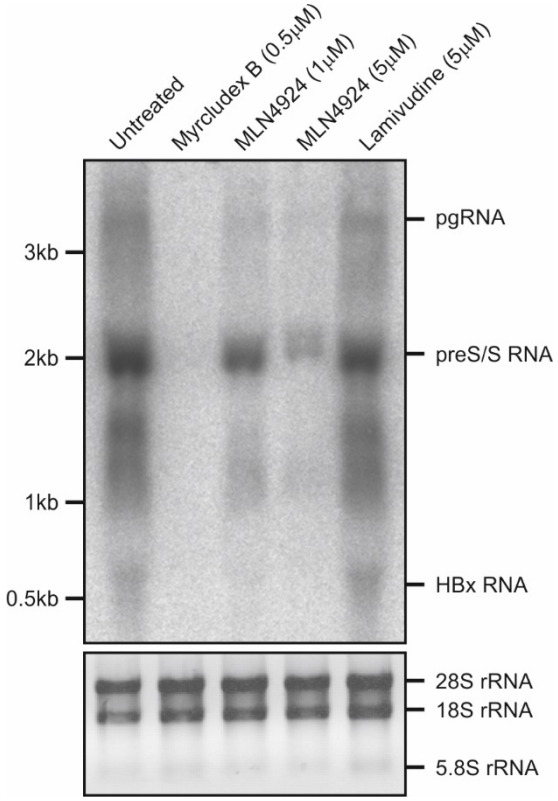

Figure 3.23. Transcription from all HBV promoters is inhibited upon MLN4924 treatment. HBV-infected HepG2^{hNTCP} cells (mge/cell = 500) were treated with MLN4924 from d 2 to 7 or Lamivudine from d 3 to 7 p.i.. On d 7, cellular total RNA was extracted.

10 μg of each RNA samples were analyzed by northern blotting (upper) and 2 μg of the same samples were shown on a native 1 % agarose gel (lower).

As previously shown, MLN4924 is a potent transcriptional inhibitor (Figure 3.20., 3.21. and 3.22), however it is unclear whether MLN4924 can solely reduce the level of one subgenomic RNA, or whether it inhibits general transcription of all HBV promoters, including core, preS1, preS2 and X promoters. The northern blotting analysis showed that MyrB blocked virus entry and profoundly reduced all transcriptions due to less formed cccDNA. In contrast, Lamivudine targeting at the reverse transcription of pgRNA, had no effect on transcription. MLN4924 induced decrease of all the transcripts in a dose-dependent manner, which showed pronounced effects on pgRNA and X RNA levels at 1 μM and further strongly reduced preS/S RNA levels at 5 μM. Although the reduction of preS/S RNA requires a higher concentration, overall MLN4924 did not show any selectivity on transcription from a specific promoter. Therefore, this data suggested that MLN4924 is a pan-transcriptional inhibitor targeting at all HBV promoters (Figure 3.23.).

In chronic HBV infection, HBsAg generation is not only relying on transcription from episomal cccDNA but also from integration into the host genome (Wooddell et al., 2017). Since MLN4924 inhibits transcription from all promoters located on cccDNA, I further evaluated whether MLN4924 also affected transcription of HBV integrants HBV by studying PLC/PRF5 the “Alexander” cell, which carries 7~8 natural HBs integrants (without full-length pgRNA

sequence). When PLC/PRF5 cells were treated with MLN4924 for 6 days, no significant reduction of HBs transcription was observed at increasing concentrations up to 3 μM (higher concentrations e.g. 10 μM, induced cytotoxicity, not shown) (Figure 3.24.). Besides, the same test was performed using another hepatoma cell, Hep3B, with fewer copies of integrants per cell. MLN4924 also did not show any alterations at HBs transcripts in the Hep3B cells (data not shown).

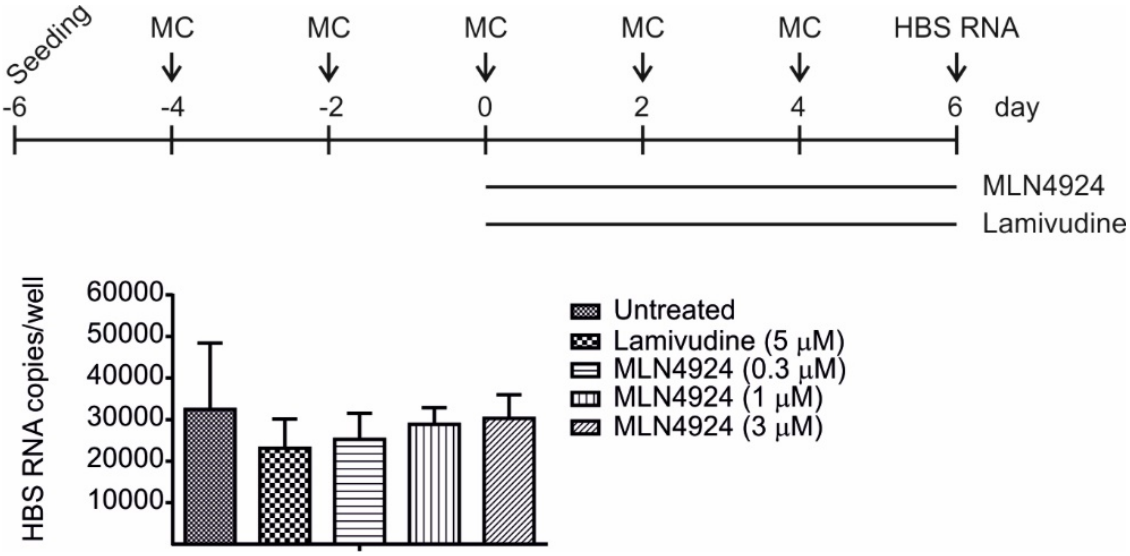

Figure 3.24. MLN4924 does not reduce HBs transcription in PLC/PRF5 cells. PLC/PRF5 cells were seeded and maintained until they formed a monolayer (d 4~6 post seeding) when MLN4924 (0.3 μM, 1 μM, 3 μM) was treated onto the cells for 6 days. On d 6, total RNA was extracted and HBs transcripts were measured. Lamivudine (5 μM) was added as a negative control.

Unlike that HBsAg present in the supernatant of Hep3B cells is unmeasurable, PLC/PRF5 cells produce and secret considerable amounts of HBsAg. The HBsAg levels of PLC/PRF5 cells upon MLN4924 treatment were measured. As shown in Figure 3.25.A, over time post seeding intracellular HBsAg was accumulated. Compared to the untreated, 0.3 μM of MLN4924 showed no reduction on HBsAg, however 1 μM and 3 μM of MLN4924 led to a slight reduction. For extracellular HBsAg, at d 0~2 post treatment, MLN4924 induced a 35% decrease and later on d 2~4 and d 4~6, the reduction degree was enlarged up to 70%, indicating that continuous MLN4924 treatment results in translational inhibition, although transcription level as previously shown in this model was not changed at all (Figure 3.25.B).

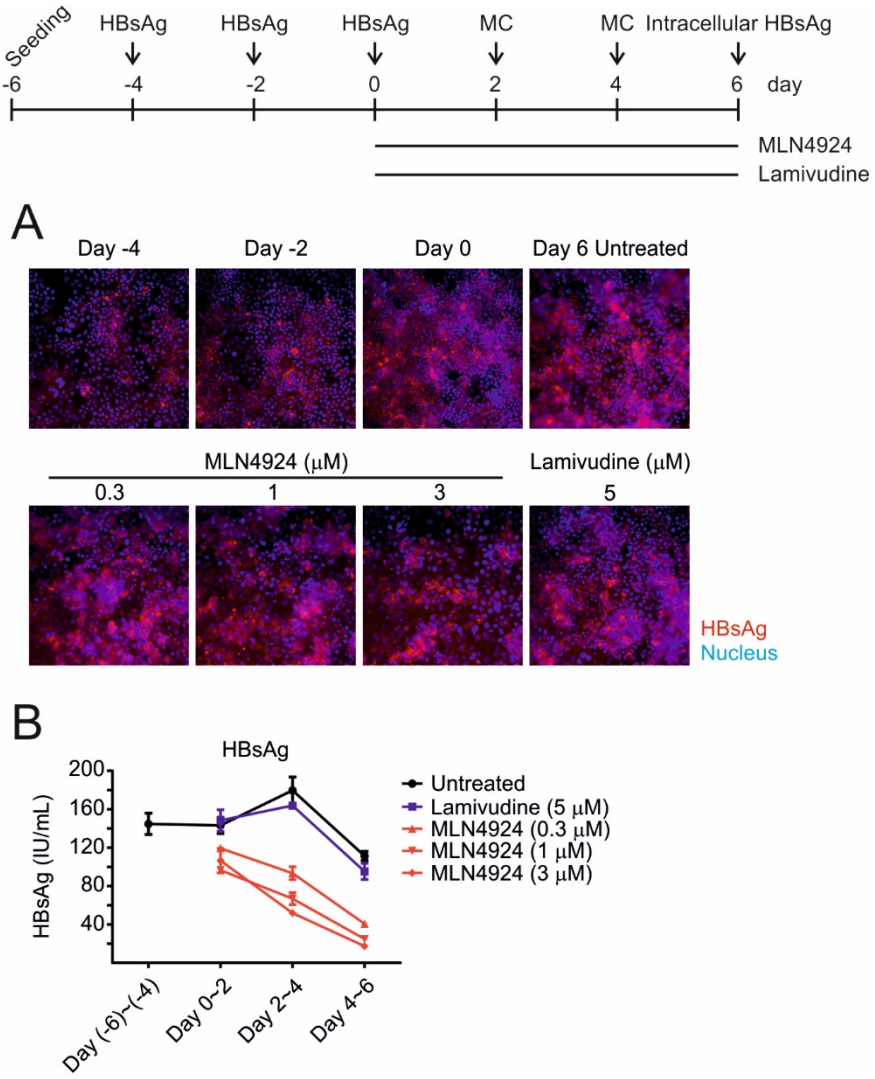

Figure 3.25. MLN4924 inhibits HBsAg production in PLC/PRF5 cells. (A) PLC/PRF5 cells were seeded and secreted HBsAg level was measured every two days before treatment and when MLN4924 (0.3 μM, 1 μM, 3 μM) was treated onto the cells for 6 days. On d 6 post treatment, intracellular HBsAg was visualized by IF staining (HBC34 anti-HBsAg, 1: 3000 diluted). (B) On d (-6)~(-4), d 0~2, d 2~4 and d 4~6, the supernatant was collected and HBsAg level was measured, respectively. Lamivudine (5 μM) was used as a negative control.

To summarize this session, MLN4924 was characterized as a transcriptional inhibitor with determined EC_{50} and CC_{50} values in PHH, $HepG2^{hNTCP}$ and differentiated $HepaRG^{hNTCP}$ cells. As a consequence of transcriptional inhibition, MLN4924 reduced amounts of both DNA- and RNA-containing particles in the supernatant of virus-producing HepAD38 cells. By pulse-treatment experiment, a discrepancy that MLN4924 showed the irreversible effect on $HepaRG^{hNTCP}$ cells and reversible effect on $HepG2^{hNTCP}$ cells was shown. MLN4924 did not show any promoter specificity but minimized transcription from all four HBV promoters located at cccDNA. Furthermore, MLN4924 did not inhibit transcription from the same preS1 and preS2 promoters when they are integrated, however MLN4924 showed a moderate inhibition on HBsAg production probably by targeting at its translation and post-translational modification.

3.4. MLN4924 inhibits cccDNA transcription in an HBx-dependent manner

3.4.1. MLN4924 does not decrease HBx expression or interfere with HBx-DDB1 binding

To investigate whether MLN4924 effect is dependent on HBx, this hypothesis was firstly tested in an HBx-null system by performing HBV reporter assay. As shown in Figure 3.26., when pGL3-HBVpromoter-Fluc (a kind gift from Dongyan Jin, University of Hong Kong) and pGL3-SV40-Rluc plasmids were co-transfected in normal Huh7 cells, Lamivudine treatment showed no difference in expression levels of firefly and renilla luciferases. MLN4924 treatment in the transfected cells also did not change in relative firefly luciferase levels expressed by preS1 and X promoters. However, MLN4924 even induced 3-fold and 4-fold more luciferase levels expressed by core and preS2 promoters, respectively, compared to the mock-treated. Nevertheless, MLN4924 did not inhibit luciferase transcription driven by any of the four HBV promoters in the absence of HBx protein.

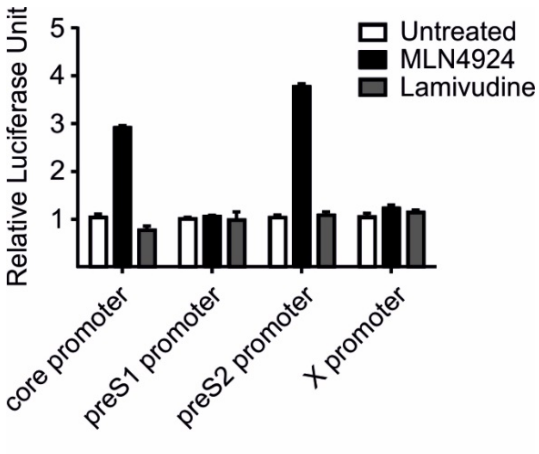

Figure 3.26. MLN4924 does not inhibit transcription in the absence of HBx. Huh7 cells were co-transfected with 450 ng of pGL3-core promoter-Fluc, pGL3-preS1 promoter-Fluc, pGL3-preS2 promoter-Fluc, pGL3-X promoter-Fluc and 50 ng of pRL-SV40-Rluc (w/w = 9: 1). 24 hours post transfection, the cells were treated with MLN4924 (5 μM) and Lamivudine (5 μM) for another 48 hours. Cells were lysed and total lysates were used for two-step dual-luciferase measurements by determining firefly and renilla readouts. Relative luciferase unit was calculated as firefly/renilla rate and further normalized as fold change to the mock-treated (set up as 1).

To elucidate the accurate role of HBx upon MLN4924 treatment requires more authentic systems, two stable cell lines expressing HA-tagged HBx fusion protein under inducible tet-mini-CMV promoter were generated. As shown in the scheme, integration of the HBx(WT) cassette was introduced by lentiviral transduction and stabilized by G418 selection in HepG2^{hNTCP} and HepaRG^{hNTCP} cells. In parallel, HepG2^{hNTCP} and HepaRG^{hNTCP} cells with stable expression of HBx (R96E) mutant (indicated by red asterisks) that has almost no transactivation function and impaired DDB1-binding activity were also generated (Figure 3.27.). Unexpectedly, the proliferation of the HBx(WT)-HepaRG^{hNTCP} cells was extremely slow compared to parental HepaRG^{hNTCP} cells, and it took more than two weeks for one splitting. Therefore, it was not comparable at all since HBx(R96E)-HepaRG^{hNTCP} cells proliferated as normal as parental cells (data not shown). The HBx(WT)-HepG2^{hNTCP} and HBx(R96E)-

HepG2^{hNTCP} cells, however, grew at the same speed. For this reason, the HepG2^{hNTCP} cells were selected for further experiments.

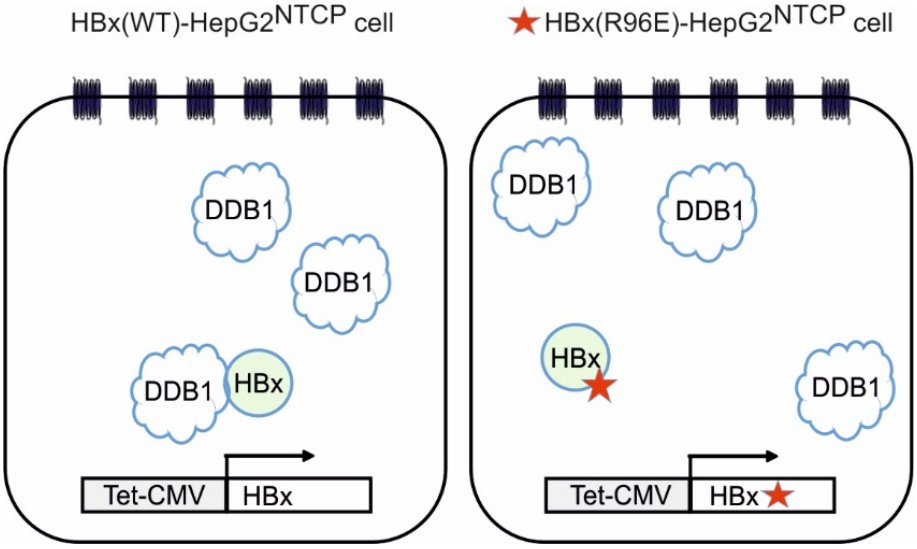

Figure 3.27. Generation of stable HBx(WT)- and HBx(R96E)-HepG2^{hNTCP} cells. (Left) HepG2^{hNTCP} cell line with endogenous expression of DDB1 was transduced with lentivirus generated from pInducer20-HA-HBx(WT) plasmid that expresses WT HBx in a tetracycline-/doxycycline-dependent manner. Lentiviral integration was stabilized by G418 (1 mg/mL) selection for two weeks and reinforced by adding G418 (0.5 mg/mL) for another two weeks. (Right) The same parental HepG2^{hNTCP} cell was transduced with lentivirus expressing R96E HBx mutant (red asterisks) with impaired binding activity to DDB1. After transduction, the HBx(R96E)-HepG2^{hNTCP} cell was G418 selected and maintained similarly.

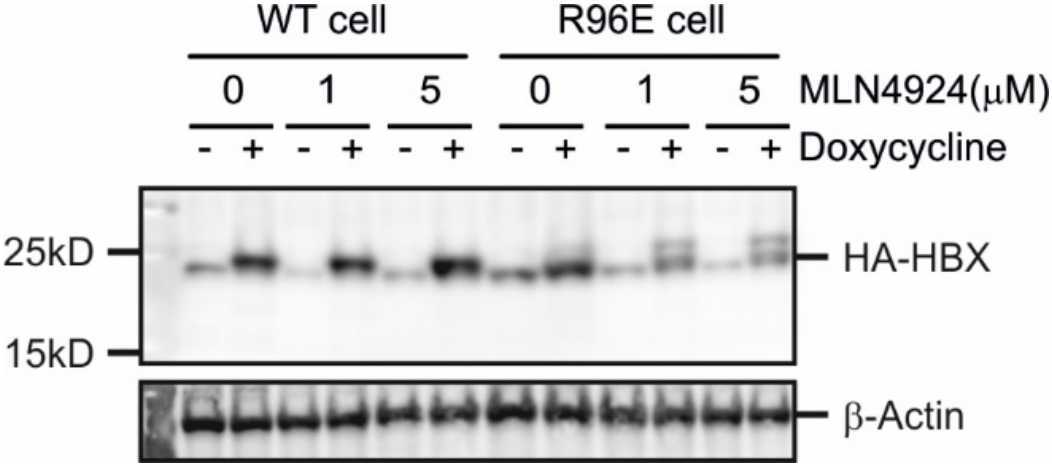

Figure 3.28. MLN4924 does not reduce HBx expression. HBx(WT)-HepG2^{hNTCP} cell (WT cell) and HBx(R96E)-HepG2^{hNTCP} cell (R96E cell) were seeded at the same numbers in parallel, doxycycline (1 μg/mL) and MLN4924 (mock, 1 μM, 5 μM) were co-treated for 3 d. Total lysates of these cells were analyzed by western blot to show HBx expression.

The HBx(WT)-HepG2^{hNTCP} (WT cell) and HBx(R96E)-HepG2^{hNTCP} cells (R96E cell) allowed investigation of HBx functions upon MLN4924 treatment in authentic infection. HBx expression was measured in both cells. When MLN4924 was not treated, both cells showed doxycycline-inducible expression levels of HBx proteins, compared to the background expression in the absence of doxycycline, and the final levels of WT and R96E proteins were

almost the same. HBx expression was very stable in the presence of MLN4924 in the WT cell. To my surprise, MLN4924 treatment split HBx(R96E) protein to two bands, including one with the same size as HBx(WT) and the other larger. Since MLN4924 is a neddylation inhibitor, the larger band was definitely not the neddylated HBx(R96E) but a possible phosphorylation form of HBx(R96E), when dephosphorylation of the glutamic acid was somehow blocked upon MLN4924 treatment. Nevertheless, total amounts of the two bands remained equal to the original amount when MLN4924 was not added. At least, MLN4924 treatment did not alter HBx expression in the WT cell (Figure 3.28.).

Next, a Flag-tagged DDB1 fusion protein was transiently overexpressed in those cells, the Flag-DDB1 protein was pulled-down and HBx that binds DDB1 was detected. Ectopic DDB1 fusion bound to HBx protein in the WT cell and MLN4924 treatment could not reduce DDB1-HBx interaction (rates of [IP: DDB1; IB: HBx]/[IP: DDB1; IB: DDB1] were unchanged). The detection of HBx protein in pulled-down DDB1 complex represented authentic HBx-DDB1 binding, since (i) without doxycycline induction this interaction was hardly visualized and (ii) in the control R96E cell this interaction was profoundly impaired (Figure 3.29.). Consistent with a previous report (Leupin et al., 2003), the arginine residue was regarded as the major determinant responsible for HBx-DDB1 interaction, HBx(R96E) protein had a weak binding activity to DDB1 and the R96 cell represented a situation where HBx was present but not functional in transactivation (Figure 3.15.). More importantly, I confirmed that MLN4924 neither reduced HBx(WT) expression nor interfered with HBx-DDB1 association in WT and R96E cells, which are reliable models allowing an authentic infection to further explore HBx functions.

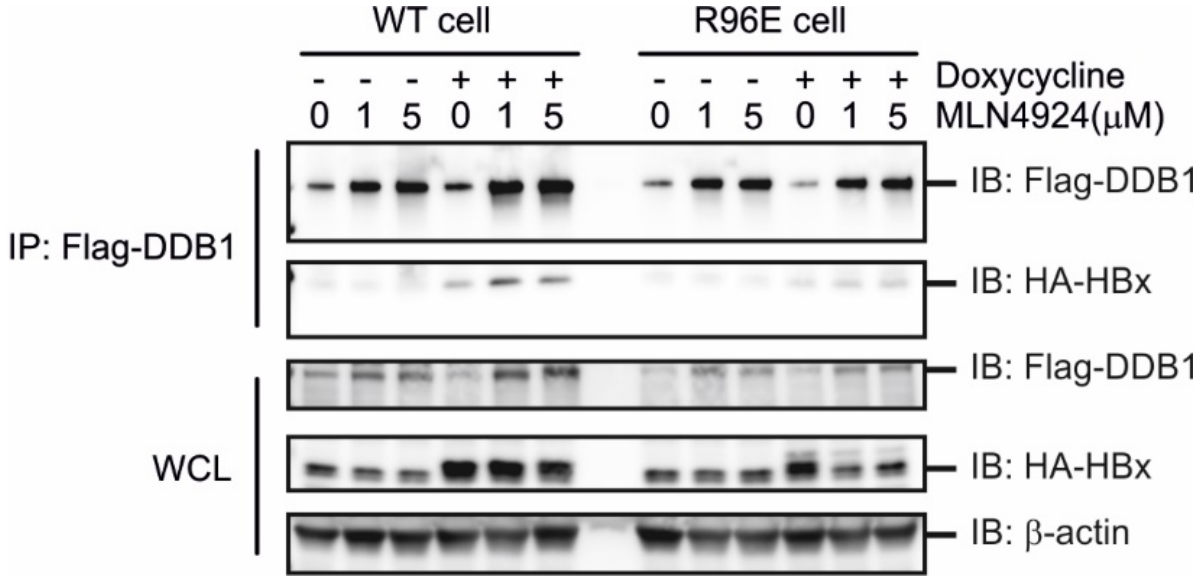

Figure 3.29. MLN4924 does not interfere with HBx-DDB1 interaction. WT and R96E cells were transiently transfected with a pcDNA3 plasmid expressing Flag-DDB1 fusion protein. 24 h post transfection, transfectants were removed, cells were washed by PBS twice and treated

with MLN4924 (mock, 1 μM, 5 μM) for another 48 h in medium without or with doxycycline (1 μg/mL). In the end, cells were lysed in modified RIPA buffer (50 mM Tris-HCl, 150 mM NaCl, 0.1% NP-40) and lysates were centrifuged at 12,000 rpm for 10 minutes, the supernatant was collected and used for the co-IP assay. IP: immunoprecipitation, IB: western blotting, WCL: whole cell lysates.

3.4.2. MLN4924 restricts cccDNA transcription in an HBx-dependent manner

Since full-length HBx has been integrated into the host genome of WT and R96E cells, one drawback is that when the cells are infected total transcripts from cccDNA can not be reliably detected by PCR because of a great amount of HBx transcripts generated from integrates. However, pgRNA expressed only from cccDNA but not from integrated HBx is a decent marker to reflect the real transcriptional activity from cccDNA. Therefore, WT and R96E cells were infected with Xd virions, HBx expression was induced by adding doxycycline and pgRNA levels, as well as HBeAg, were evaluated. PgRNA expression levels were 10-fold enhanced in WT cell when HBx(WT) was present and MLN4924 treatment could cut off this HBx-dependent enhancement to the background level. In contrast, HBx(R96E) protein induced a less than 2-fold increase of pgRNA expression and even this slight enhancement was reduced by MLN4924 to the basal level (Figure 3.30.A). Similarly, HBeAg value was 4-fold inclined in the presence of HBx(WT) and MLN4924 completely eliminated enhanced its value to the baseline level of Xd virus, whereas HBeAg value was not enhanced by HBx(R96E) yet MLN4924 further declined it by 50% (Figure 3.30.B). As expected, cccDNA was not reduced in both WT and R96E cells (Figure 3.30.C).

To further illustrate this HBx dependency, in addition to the stable HBx-expressing cells, Xd infection was combined with lentiviral transcomplementation to study whether MLN4924 showed similar phenotype when HBx was transiently provided *in trans*. HepaRG^{hNTCP} and HepG2^{hNTCP} cells were infected with Xd virus, transduced with lentivirus expressing GFP, HBx(WT) and HBx(R96E) proteins on d 2 p.i., and further treated with MLN4924 on d 5. Similar to Figure 3.15., HBx(WT), but not GFP or HBx(R96E) fully enhanced pgRNA levels in both cells. In HepaRG^{hNTCP} cells, MLN4924 but not Lamivudine, completely repressed transcription from cccDNA back to the level of Xd infection. MLN4924 performance in HepG2^{hNTCP} cells was not as potent as that in HepaRG^{hNTCP} cells but remained functional. Again HBx(R96E) protein could not enhance transcription of Xd virus but MLN4924 displayed a 2-fold reduction of transcription in both cells (Figure 3.31.). Using two different models as shown in Figure 3.30 and 3.31, mode of MLN4924 action was confirmed in an HBx-dependent manner. MLN4924 selectivity on HBx(WT) but not HBx(R96E) also suggested that the mechanism of MLN4924 was highly relying on the HBx-DDB1 complex.

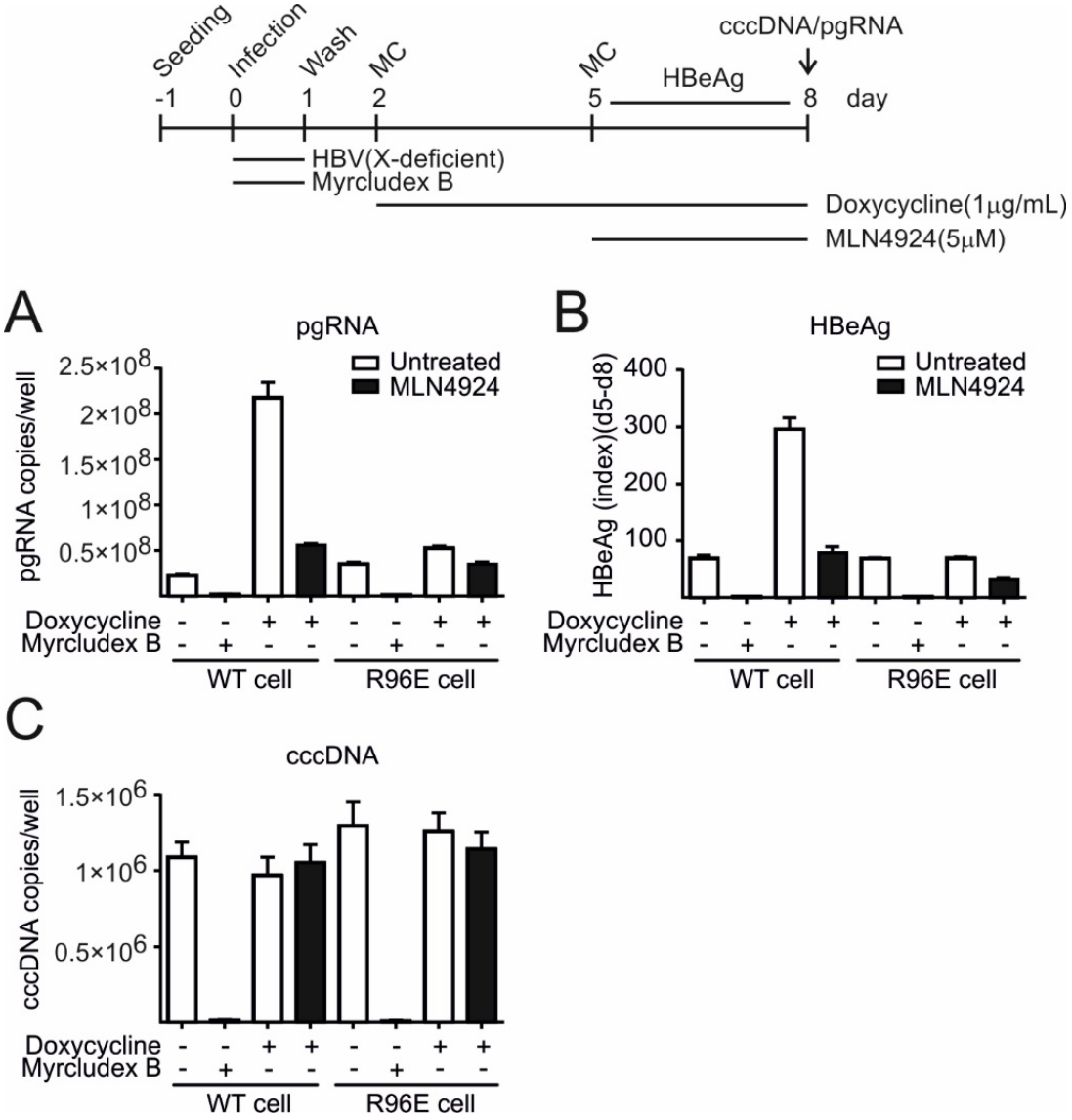

Figure 3.30. MLN4924 inhibits transcription from cccDNA in an HBx-dependent manner in two stable cells. WT cell and R96E cell were infected with Xd virions (mge/cell = 100). Two days p.i., doxycycline (1 μg/mL) was administered on d 2~5 and later MLN4924 (5 μM) was added during d 5~8 p.i.. (A) Viral pgRNA and (B) HBeAg secretion were examined, and (C) cccDNA levels were measured. MyrB (1 μM) was used to show NTCP-mediated virus entry.

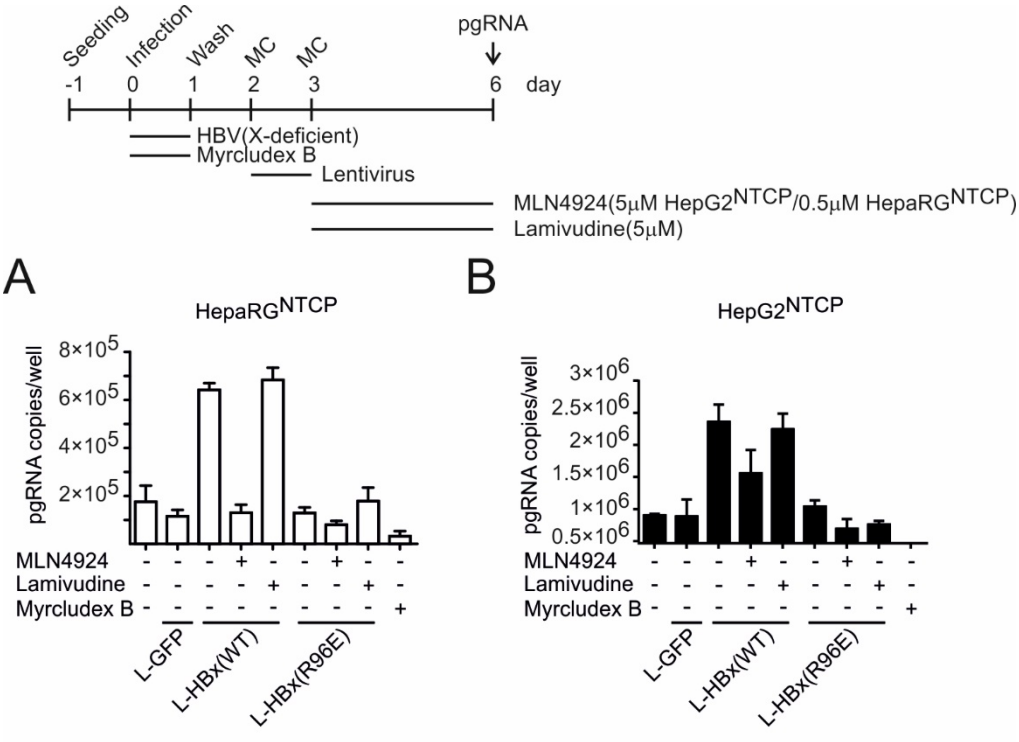

Figure 3.31. MLN4924 inhibits transcription from cccDNA in an HBx-dependent manner when HBx is expressed *in trans*. (A) Differentiated HepaRG^{hNTCP} and (B) HepG2^{hNTCP} cells were infected with Xd virions and transiently transduced with indicating lentiviruses encoding GFP, HBx(WT) and HBx(R96E) proteins as shown on d 2 p.i.. Transduced cells were further treated with MLN4924 (5 μM in HepG2^{hNTCP} cells/0.5 μM in HepaRG^{hNTCP} cells) or Lamivudine (5 μM in both cells). On d 8 p.i., pgRNA levels were determined by qPCR.

3.4.3. MLN4924 restores HBx-mediated SMC6 degradation

Recently, SMC5 and SMC6 proteins were identified as major restriction factors that prevent maximal transcription from cccDNA. HBx protein binds DDB1 and bridges E3 ubiquitin ligase Cullin 4A and this functional complex induces SMC5/6 degradation. If MLN4924 indeed serves as a transcriptional inhibitor in an HBx-DDB1-dependent manner but does not reduce HBx amounts or interfere with HBx-DDB1 association, it makes sense to speculate that MLN4924 deactivates the function of HBx-DDB1 complex, which mediates SMC5/6 degradation.

Two-color confocal microscopy allowed visualization of SMC6 and HBcAg at the single infected HepaRG^{hNTCP} cells. SMC6 proteins showed exclusive nuclear expression and very specific nuclear localization as bright dots in the uninfected hepatocytes, which was consistent with the recent finding showing co-localization of SMC6 protein and PML nuclear bodies (Niu et al., 2017). During infection, HBV replication diminished SMC6 signals in HBcAg high-expressing hepatocytes (Figure 3.32.A). Since long-term MLN4924 treatment resulted in loss of HBcAg as shown in Figure 3.17., I had to shorten MLN4924 treatment time, focus on cells with accumulated lower HBcAg level (meaning that the cells have been infected) and seek for moderate SMC6 expression, which was expected as newly synthesized SMC6 protein upon MLN4924 treatment, after all old SMC6 proteins were eliminated during the former 6-day HBV replication. The re-emergence of SMC6 signals evidenced that MLN4924 deactivated HBx-DDB1 machinery and as a consequence, newly synthesized SMC6 proteins were restored. However, Lamivudine was not able to restore SMC6 expression in HBcAg-positive cells (Figure 3.32.B and C).

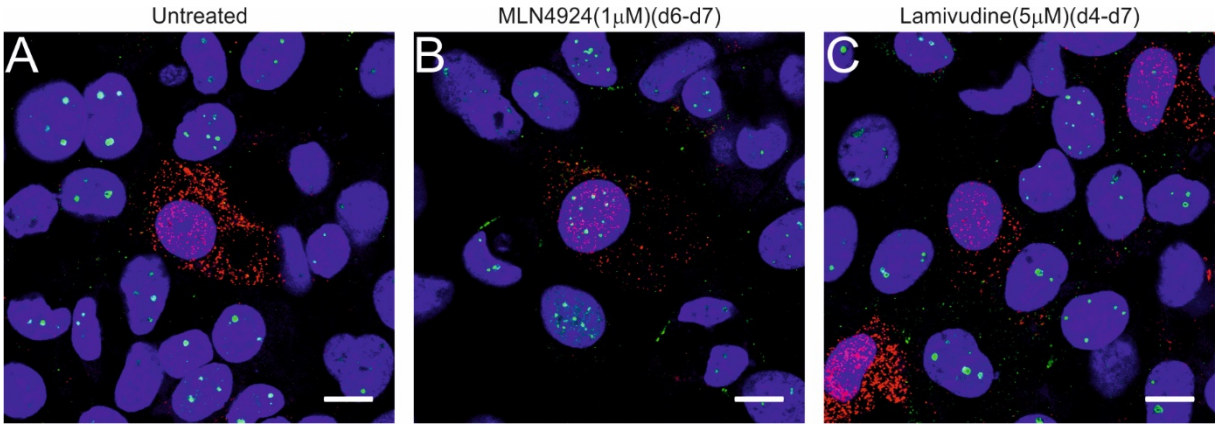

Figure 3.32. MLN4924 prevents HBx-mediated SMC5/6 degradation in infected HepaRG^{hNTCP} cells. Differentiated HepaRG^{hNTCP} cells were infected with HBV virions (mge/cell = 500) and (A) mock-treated, or (B) treated with MLN4924 (1 μM) from d 6~7 p.i., or (C) Lamivudine (5 μM) from d 4~7 p.i.. The cells were fixed and freshly fixed SMC6 epitopes were detected by immunofluorescence on the same day of fixation using a validated antibody (green: anti-SMC6). HBcAg (red: anti-HBcAg) was co-stained. Representative images were taken under confocal microscopy. Bar: 10 μM.

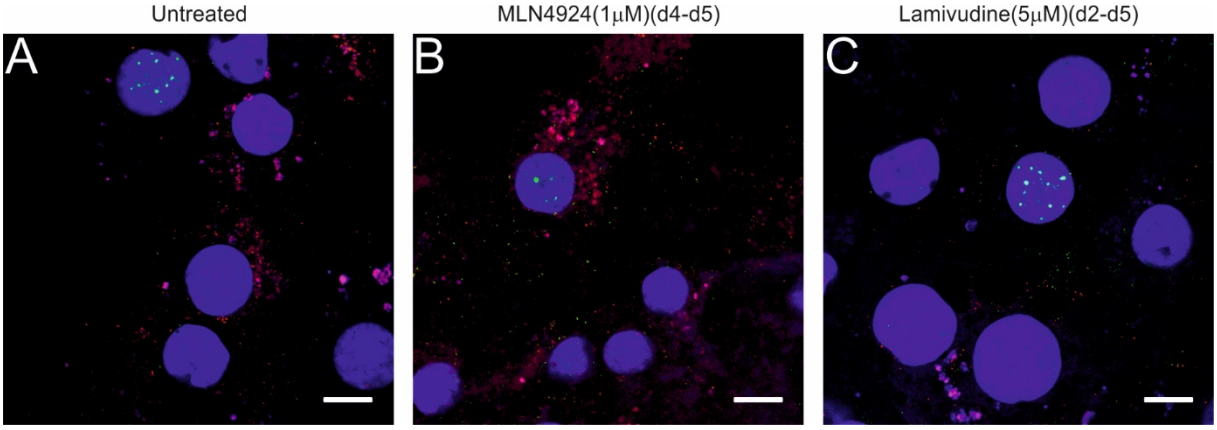

Figure 3.33. MLN4924 prevents HBx-mediated SMC5/6 degradation in infected PHH. PHH were infected with HBV virions (mge/cell = 500) and (A) mock-treated, or (B) treated with MLN4924 (1 μM) from d 4~5, or (C) Lamivudine (5 μM) from d 2~5 p.i.. The cells were fixed and fresh SMC6 epitopes (green: anti-SMC6) were detected by immunofluorescence on the same day of fixation. HBcAg (red: anti-HBcAg) was co-stained. Images were taken under confocal microscopy. Bar: 10μM.

Moreover, more physiological PHH were infected. In HBV infection, most cells were HBcAg positive that was correlated with complete loss of SMC6 signals. Upon MLN4924 treatment, cells with robust HBcAg and detectable SMC6 expression were found, although the restoration of SMC6 signals was not as nice as that in infected HepaRG^{hNTCP} cells (Figure 3.33.).

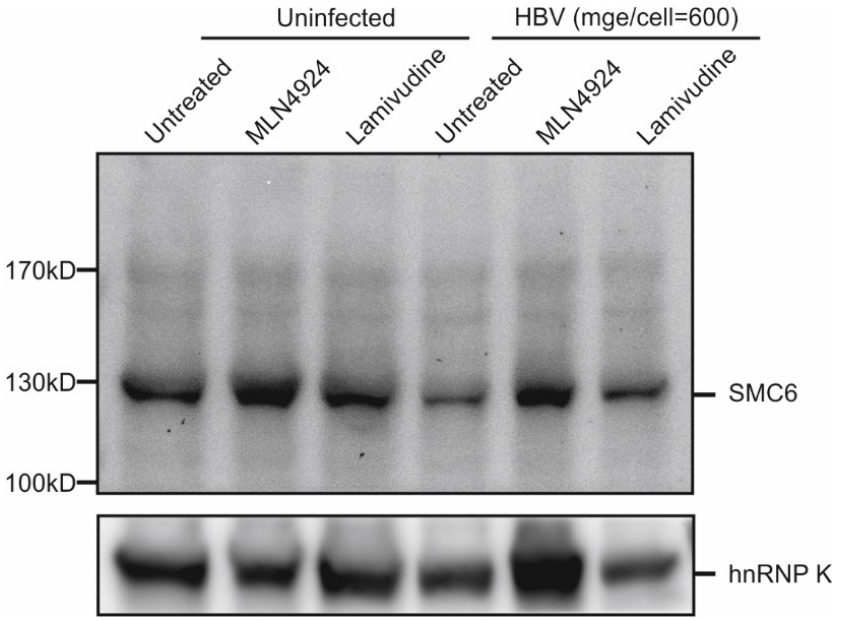

Figure 3.34. HBV replication induces SMC6 degradation. HepG2^{hNTCP} cells were infected with HBV (mge/cell = 600). On d 4 p.i., MLN4924 (5 μM) and Lamivudine (5 μM) treatments were initiated. On d 7, nuclei of infected cells were isolated, washed and lysed. Nuclear lysates were subjected to western blotting. levels of SMC6 and hnRNPk were determined.

Detection of SMC6 protein level by western blotting provided an overview beyond single-cell confocal analysis. When HepG2^{hNTCP} cells were infected with HBV at a moderate mge (mge/cell = 600) and SMC6 levels in nuclear fraction were measured, HBV replication induced 3-fold reduction of SMC6 protein level compared to the uninfected, indicating that SMC6

proteins were largely degraded during infection (considering that at such mge, not all cells were infected and SMC6 proteins were not eliminated in the uninfected cells). Distinct from Lamivudine, MLN4924 treatment led to enhanced SMC6 expression level during infection. However, it seems that the level of another HBx-binding protein hnRNP K was also elevated. (Figure 3.34.). This issue is still under investigation.

To summarize, endogenous SMC6 is not a specific target of host ubiquitination machinery in natural condition. In HBV infection, HBx protein at very low expression level hijacks host ubiquitin ligase via direct DDB1 binding and potential SMC6 association. The complex induces SMC5/6 degradation. SMC5/6 degradation enables the maximal transcriptional activity of cccDNA and facilitates robust HBV replication. On the other hand, the neddylation inhibitor MLN4924 neither reduces the amounts of HBx protein nor disturbs HBx-DDB1 association. Instead, MLN4924 probably deactivates the function of this complex by blocking neddylation of downstream Cullin 4A. Consequently, newly synthesized SMC5/6 proteins can not be degraded and in turn, the presence traps cccDNA in "transcriptional silence".

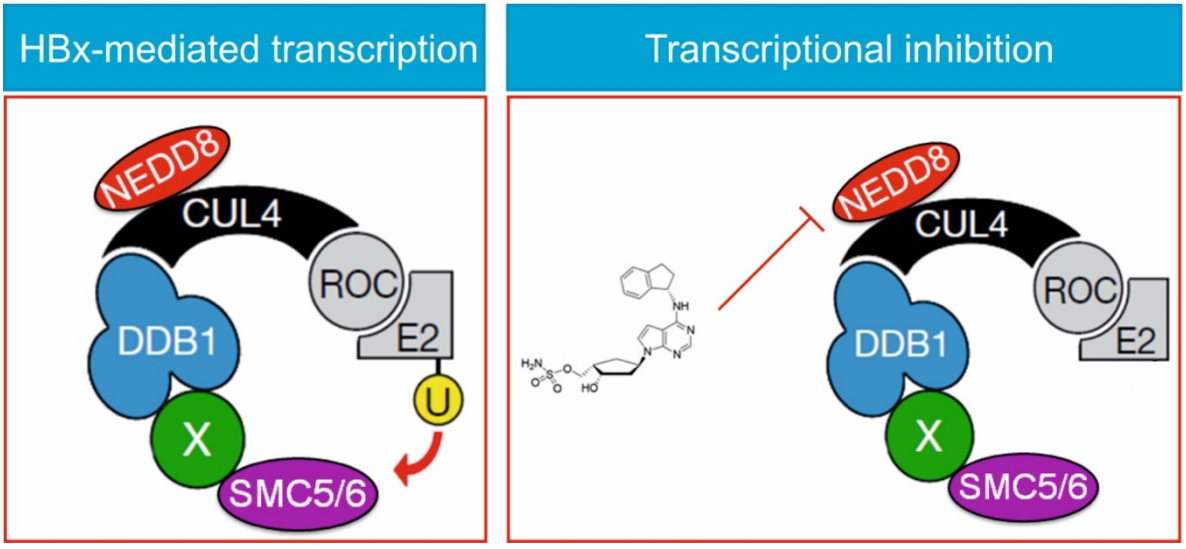

Figure 3.35. HBx-mediated transcription from cccDNA and its inhibition by MLN4924. Left panel: In HBV infection that expresses HBx protein, it binds DDB1 and bridges host Cullin 4A (CUL4) ligase complex with SMC5/6 proteins and thereby mediates SMC5/6 ubiquitination and degradation. As a result, cccDNA shifts to a "transcriptional active" status to support robust HBV replication. Adapted from (Decorsiere et al., 2016).

Right panel: Neither HBx amount nor HBx-DDB1 interaction is affected by MLN4924. MLN4924 blocks CUL4 neddylation and full activation and thereby SMC5/6 degradation is prevented to some extent. In the presence of MLN4924, infected cells synthesize new batch of SMC5/6, which traps cccDNA in "transcriptional silence".

4. DISCUSSION

4.1. New insights of cccDNA in HBV biology

Formation and transcription of cccDNA are two of the most mysterious topics in HBV biology. However, due to the scarcity of susceptible models, knowledge of cccDNA was largely adapted from studies of other hepadnaviruses, like DHBV and WHV. DHBV cccDNA persists within hepatocytes with its half-life comparable to that of the host cell, where numbers of 50 or higher cccDNA molecules are present, especially when L envelope protein is depleted (Summers et al., 1990, Wu et al., 1990, Kajino et al., 1994, Zhu et al., 2001). In contrast, the copy number of HBV cccDNA in human hepatocytes seems much lower, although excessive numbers of replicative intermediates are present, which could replenish and amplify the cccDNA pool (Nassal, 2015). Indeed, although in the DHBV system cccDNA is rapidly formed and the pool can be efficiently amplified upon nuclear re-import of newly formed rcDNA-containing nucleocapsids (Wu et al., 1990), there is no strong evidence whether and to what extent intracellular amplification of cccDNA in HBV-infected human hepatocytes occurs, especially in *in vitro* infection.

So far, efficient *in vitro* infection in all susceptible cell lines requires inoculation with a high amount of virions for certain hours (> 4 h) in the additional presence of PEG, as shown in Figure 3.1 and 3.3. (e.g. 10% infected cells at an mge of 300). Unlike that many viruses require lower moi of 0.1~1, this unusual infection feature in HBV virology is possibly due to a slow transition of naive virions to a mature hNTCP-binding competent state that is required for infection, after sufficient cellular association with HSPG. This profound association of virions and subviral particles occurs even in non-susceptible cells (Qu et al., 2018). Furthermore, virus stocks from cell culture supernatants contain rcDNA-containing naked nucleocapsids if not properly purified by heparin affinity chromatography (Seitz et al., 2016). These naked capsids also show a strong tendency to attach to different types of cells in the absence of NTCP. Therefore, on early days after virus inoculation when cccDNA is being formed, the rcDNA/cccDNA rate is extremely high compared to the *in vitro* samples harvested at later time points p.i. or the *in vivo* samples of patients or humanized mouse livers. The problem of accurate cccDNA quantification has been solved in this thesis using T5 exonuclease that removes cellular DNA and all HBV intermediates via its exonuclease activity targeting free ends of rcDNA and dslDNA but leaves cccDNA intact (Qu et al., 2018). Applying the method to this study, comprehensive cccDNA kinetics in all models was determined and these findings answered some scientific questions related to cccDNA biology:

First, it compares the kinetics of cccDNA accumulation in different infection models, including PHH, HepaRG, HepaRG^{hNTCP} and HepG2^{hNTCP} cells. The results demonstrated that copy numbers are relatively low in all models (<6 per infected cell)(Figure 3.4.~3.7.)(Qu et al., 2018). The numbers are consistent with previous studies depicted in PHH and HepaRG cells (Miller and Robinson, 1984, Laras et al., 2006) but contrast earlier studies in the liver of DHBV infected ducks and primary duck hepatocytes, or WHV infected woodchuck hepatocytes with the numbers in the range of 10~100 (Mason et al., 1982, Zhang et al., 2003). Of note, Zhang et al found that using single-cell analysis 90% of the nuclei in chronically DHBV infected duck had 1~17 cccDNA numbers and the rest of nuclei contained significantly more cccDNA (Zhang et al., 2003). In this thesis, it is clear that absolute cccDNA numbers in HBV infection were far less than average cccDNA numbers in DHBV infection as previously reported. This difference can be partially explained by a direct comparison of DHBV and HBV in transfected HepG2 cells showing that DHBV rcDNA to cccDNA conversion was more efficient than HBV (Kock et al., 2010). This unique characteristic enables higher cccDNA numbers in DHBV replication. Unlike DHBV, cccDNA copy number was approximate 1.5 per cell in chronic hepatitis B patients. Remarkably, the cccDNA level in HBeAg-negative patients was even 10-fold lower than that in HBeAg-positive ones. This cccDNA level was comparable with that in *in vitro* infected HepaRG and HepG2^{hNTCP} cells and slightly lower than the average level in PHH. However, so far due to detection sensitivity, HBV cccDNA copy number at the single-cell level is largely unknown. Recently, one report suggested that nuclear DNA level determined by fluorescent *in situ* hybridization assay in HepAD38 cells meets the Normal distribution (Li et al., 2018b). However, the method can not show cccDNA in a specific way in a nuclear pool containing protein-free rcDNA. In the future, the exact cccDNA number and its heterogeneity at the single-cell level need to be further investigated.

Second, cccDNA copy numbers can not be further increased by raising the mge when all cells are infected (Figure 3.2.)(Qu et al., 2018). This data indicates that there is an intracellular restriction for the unstoppable conversion of rcDNA to cccDNA. It is consistent with our earlier observation that depicted a saturation of HBV antigen level at mge/cell above 8000, when 100% of PHH were almost infected at this mge (Schulze et al., 2012). In this study, raising mge from 30 to 1000 associates with a linear incline of accumulated cccDNA level. At mge >1000, however, no further proportional increase of cccDNA and total DNA levels was observed (Figure 3.2.). The harsh control of cccDNA generation at high mge's limits HBV cccDNA numbers lower than the DHBV cccDNA numbers. This unique feature might be explained by two theories. Firstly, some host factor(s) involved in the processes of cccDNA formation (nuclear import of capsids, removal of the covalently-bound polymerase, etc.) can be used at

lower mge's but completely occupied at mge >1000, which therefore limits rcDNA to cccDNA conversion. These factor(s) may be HBV specific, since DHBV rcDNA converts much more efficiently to cccDNA than HBV in the same HepG2 cells in cross-species transfection experiments (Kock et al., 2010). Secondly, established cccDNA episomes may induce nuclear innate immune responses to shut-off the host machinery for excessive cccDNA formation. At lower mge's, low numbers of cccDNA evade the defense pathway. Once accumulated cccDNA copies in the nucleus exceed the threshold of sensing (e.g. > 6 copies per infected cell), the host cell elicits feedback, in turn, locking the nucleus and avoids further cccDNA formation.

Third, the effects of representative inhibitors on cccDNA formation and maintenance were analyzed. Once established, numbers of cccDNA do not further amplify during late days of infection, which is in line with the kinetics of cccDNA formation leading to the saturation of copy numbers (Figure 3.4.~3.7.)(Qu et al., 2018). Staying stable, cccDNA is difficult to be eliminated. In patients resolved in acute HBV infection, cccDNA is even not completely cleared for decades although adaptive immunity has been activated (Rehermann et al., 1996). For approved antivirals, Lamivudine and Tenofovir barely affected cccDNA levels, while IFN-α at high dose induced cccDNA reduction with low efficacy, suggesting that first-line therapies are poorly effective in the elimination of cccDNA pool (Figure 3.9.). The best entry inhibitor, MyrB (available on market in 2019~2020), has shown drastically inhibitory effect on *de novo* establishment of cccDNA when it was pre- and co-administered. In the liver, MyrB protects uninfected hepatocytes from being secondarily infected by the viruses released from infected cells (Volz et al., 2013). Post treatment of capsid modulator GLS4 at high dose also led to cccDNA decline, but co-treatment of GLS4 was more efficient probably due to direct action on nucleocapsids before rcDNA to cccDNA conversion (Figure 3.10.). This finding is in agreement with that other capsid assembly modulators upon co-treatment also have interference with capsids and effect on cccDNA (Berke et al., 2017, Lahlali et al., 2018).

4.2. Transcriptional promotion is the major function of HBx

Using the plasmid transfection system, researchers have revealed that HBx presumably interacts with a great number of host factors and is required for maximal HBV replication. However, the exact role of HBx in authentic HBV infection is obscure. All the attempts were restricted for over twenty years for two major reasons: (I) absence of convenient *in vitro* infection systems (Table 1.3.); (II) scarcity of HBx detection in infected cells due to the low expression level of HBx protein and lack of a specific antibody with sufficient detection sensitivity. In addition, the biology of HBx protein is partially related to cccDNA, which was also not reliably detected.

The first issue has been overcome in the era of the discovery of HBV receptor, human NTCP (Yan et al., 2012) and subsequent generation of a series of stable hepatoma cells with human NTCP reconstitution that allows HBV entry, cccDNA formation, and replication (Ni et al., 2014). Later on, reliable cccDNA detection in these cell lines was established, including handy qPCR assay (Figure 3.2.~3.10.). With these tools, the potential functions of HBx on cccDNA can be investigated. However, the second problem has not been solved. In all models, most of the HBV replication markers were well detected, except HBx and polymerase. Overexpression of tagged HBx protein was widely used in hundreds of studies, although fusing tags with HBx may alter its conformation (Slagle et al., 2015). In our previous studies, seventeen home-made anti-sera and commercial HBx antibodies were screened by immunofluorescence and western blot analysis using hepatoma cells with HBx overexpression. It was disappointed that only three out of the seventeen anti-sera/antibodies showed enough detection specificity. Even worse, none of them detected HBx in authentic *in vitro* infection (Sonnabend J, thesis, 2013). Detection failure may be caused by its low expression abundancy or short half-life (approximate 3 h) (Beran et al., the International Liver Congress, 2018).

As shown in Figure 3.11., the expression level of HBx correlated with its subcellular localization. It was believed that HBx was a cytoplasmic mediator involved in many pathways and a nuclear transcriptional activator (Doria et al., 1995). When HBx was overexpressed by a CMV promoter, HBx showed rarely nuclear but exclusively cytoplasmic localization (Figure 3.11.A). In contrast, when HBx was overexpressed by mammalian EF1α promoter or expressed by its own X promoter from the overlength HBV genome, HBx almost became a nuclear protein (Figure 3.11.B and C). The alteration of HBx distribution, which is likely of determination by its expression amount, is consistent with an early study showing that HBx was predominantly localized in the nuclei in weakly expressing cells (Henkler et al., 2001). Of note, HBx protein - in physiological occasion- is expressed by the X promoter using either cccDNA or directly translated from a low amount of virion HBx transcripts (Niu et al., 2017). Therefore, it is concluded that HBx has an exclusive or at least predominant nuclear localization in authentic infection. The possibility can not be excluded that HBx protein shuttles between nucleus and cytoplasm since HBx has both nuclear localization signal and nuclear export signal (Cha et al., 2009). Nevertheless, nuclear localization of HBx suggests that the biggest function of HBx, from HBV side of view, takes place in the nucleus and thereby narrows to formation or transcription of cccDNA.

HBx protein is essential to maintain HBV replication but not for the generation of cccDNA in infected HepaRG cells (Lucifora et al., 2011). This finding was confirmed in HepaRG^{hNTCP} and the new model HepG2^{hNTCP} cells in which Xd virus showed reduced transcriptional activity

than WT virion starting from d 3 p.i.. In addition, persistent HBx expression maintained HBV transcription over weeks after infection (Figure 3.12~3.13.). The transcriptional enhancement can be explained by two DDB1-mediated mechanisms (Hodgson et al., 2012): HBx-DDB1-cccDNA binding model that requires transcriptional factors recruited directly by HBx binding to the cccDNA via DDB1. This has been partially supported by an HBx chromatic IP validation in HBV transfected cells (Belloni et al., 2009), and HBx-DDB1 displacement model that requires HBx association with SMC5/6 and DDB1 recruitment of host ubiquitin machinery to induce degradation of these restriction factors (Decorsiere et al., 2016).

Essential domains located on HBx are essential for this function. Since HBV genome is too compact to be edited and HBx is undetectable in *in vitro* infection, a lentiviral-based trans-complementation assay to restore the transcription of Xd virus to the level of WT infection was applied. This system is feasible and flexible to introduce HBx truncations and single point mutations. Using this method, it was proved that the whole C-terminal HBx is sufficient and functional (Figure 3.14.). Compared to the full-length HBx(1-154), the N-terminal HBx(1-50) did not rescue transcription of Xd virus, meaning that the N-terminal has no transcriptional enhancing activity or it is poorly expressed due to its smaller size (6 kD). C-terminal HBx(51-154) alone was completely functional as HBx(WT) so that the HBx(1-50) could be dispensible, which was consistent with two previous reports (Murakami et al., 1994, Misra et al., 2004). Furthermore, deletion of the residues 51-142 led to a complete loss of function, suggesting that this region at least is essential. Two shorter truncations HBx (51-142) and (58-142) were only partially functional, indicating that not only 51-142 but 143-154 residues played a role in transactivation. Overall, the data revealed that transcriptional activation of HBx is not relying on one short and continuous motif but dependent on the whole C-terminus, or at least three fragments 51-57, 58-142, and 143-154 at the same time. These findings fit an early study when separate domains of HBx (around residue 68 and residues 110-139) are both necessary for its function that was determined by co-transfecting HepG2 cells with an HBx-minus genome plasmid and the other plasmid expressing mutated HBx (Runkel et al., 1993). It is also consistent with another finding that residues 58-140 retain transactivation function but with less activity (Kumar et al., 1996).

In the past twenty years, researchers focused on identifying HBx-interacting proteins. The trend was initiated when HBx was found to interfere with cellular DNA repair machinery by binding DDB1, which is one of the authentic binding proteins again characterized in this thesis (Becker et al., 1998). Of note, DDB1 is the major but not sole determinant with HBx interaction and the binding is responsible for transactivation properties of HBx protein (Wentz et al., 2000). Nevertheless, later one structural study ensured the authentic association of recombinant DDB1

protein and a promiscuous α-helical HBx peptide and showed that HBx residue 88-101 is the key motif responsible for DDB1 binding (Li et al., 2010c). The results in this thesis showed that the HBx(R96E) mutant completely lost its transactivation activity, meaning DDB1 dependency in the transactivation. Interestingly, the HBx(R96A) mutant was still functional (Figure 3.15.). One of the explanations is that R96E mutation results in a major charge turnover and conformational change of HBx protein that is fierce enough to break up the HBx-DDB1 interaction, whereas R96A mutation alters the protein to a weaker extent -in this case- allowing the partial association of HBx and DDB1. As a promising binding partner, DDB1 is absolutely involved in the process of HBx-mediated transactivation. Since DDB1 has two major functions including DNA repair via formation of DDB1-DDB2 complex (Nag et al., 2001, Leupin et al., 2005) and recruitment of host ubiquitin-proteasome system (Minor and Slagle, 2014). Regarding that no evidence has shown that DNA repair is required in cccDNA maintenance and HBx is not required in cccDNA formation (Figure 3.12.), it is concluded that HBx-DDB1 complex hijacks ubiquitin-proteasome machinery and unlocks SMC5/6 restriction on the transcription of cccDNA. Overall, transcriptional promotion is the major function of HBx after HBV infection.

4.3. Co-evolutionary strategies of HBx, cccDNA and its transcriptional capacity

Except one report insisted that a regulatory protein, allegedly termed DHBx, exists and is expressed by a hidden reading frame in DHBV genomes (Chang et al., 2001), most researchers have believed that DHBV lacks a homologue of the X protein. On the other hand, cccDNA copy number per infected cell in HBV infection is far less than the DHBV cccDNA number. If the major function of HBx acts only on transactivation of cccDNA, from DHBV to HBV, a hypothesis comes out that specific evolutionary emergence of HBx in WHV and HBV infection largely enhances the transcriptional capacity of cccDNA. Compared to DHBV, HBV has more transcriptional active cccDNA and therefore the cccDNA numbers evolve to fewer copies to hide in the nucleus and better fits the host.

The SMC5/6 complex serves as a host restriction factor and HBx-induced degradation of SMC5/6 enhances HBV transcription (Decorsiere et al., 2016, Murphy et al., 2016). In HBV infection, the internal connection of HBx protein and cccDNA is exclusively dependent on the SMC5/6 complex. During HBV human adaptation, it is likely that the driven force of HBx emergence was to degrade SMC5/6 complex, enhance cccDNA transcription. At the very beginning of HBV replication in human hepatocytes, the first virion evolved HBx protein and showed significantly enhanced replication efficiency. Over time, the virus encoding HBx

protein became evolutionarily dominant. Later on, the virus lowered cccDNA copy number. This hypothesis was supported by a recent study showing that highly divergent GSHBx, WHx, bat X and HBx were able to degrade mammalian SMC6 protein. Importantly, the HBx-induced degradation among all X proteins was the most efficient. Vice versa, SMC6 protein is the least conserved component of the SMC5/6 complex (Abdul et al., 2018). This virus-host "arms race" suggests that HBx has evolved in several species and eventually becomes completely functional in transactivation. In addition, whether avian (duck, chicken, etc.) SMC5/6 complex prevents DHBV cccDNA transcription, becomes a very interesting topic. If duck complex has no or low restrictive activity on the transcription of DHBV cccDNA, correspondingly, the "DHBx" is not required.

Colocalization of SMC6 protein and PML nuclear bodies may hint the specific residence of cccDNA and explain why cccDNA maintains at low copy numbers. Two recent publications and our data of SMC6 staining pattern showed that SMC6 was mostly colocalized in the nuclear bodies (Figure 3.32~3.33) (Niu et al., 2017, Livingston et al., 2017). Niu et al showed that knockdown of SMC6 fully restored transcription of Xd virus to the level of WT virus, implying that a majority of active cccDNA transcription (> 95%) is restricted by SMC6 or depends on HBx-mediated counteraction of this restriction. Therefore, SMC6 protein has to capture the few copy cccDNA and silence its transcription inside or close to the nuclear bodies where SMC6 is located. It is further expected that formation and /or transcription of cccDNA prefer to occur in the nuclear bodies for genomic loci. The interplay among HBx, cccDNA and SMC6 in PML nuclear bodies will be investigated in future studies. Table 4.1. summarizes properties of HBx, SMC6 and cccDNA.

Table 4.1. Properties of X proteins, SMC6 and cccDNA among viruses.

Virus	cccDNA copy per infected cell	X protein	SMC6 restriction	X-induced SMC6 degradation
HBV	+ (1~6)	HBx	Yes	Yes
WHV	ND	WHx	ND	Yes
DHBV	++ (50~100)	NA	ND	No

NA: not available; ND: not determined; +: low copy; ++: high copy.

4.4. MLN4924 is a new-class antiviral with dual targets

MLN4924 is a new-class antiviral. As shown in Figure 1.10., most steps in the HBV life cycle have been considered as drug targets except HBx. In drug discovery, viral proteins with enzymatic activity or known crystal structure are prone to be developed as targets of small

molecules. For instance, HCV that encodes a batch of viral enzymes (NS3, NS5A and NS5B) served as candidates of direct-acting antivirals (Sofosbuvir, etc.) (Gotte and Feld, 2016). HBV encodes only one polymerase with RTase and RNase H activities. However, NUCs have a major limitation since they selectively block one of the branches in HBV replication, reverse transcription of pgRNA. Upon NUC treatment, HBeAg translated by precore mRNA derived from cccDNA and HBsAg translated by preS/S integrates are actively expressed (Wooddell et al., 2017), although prolonged treatment (median 126 months) may lead to cccDNA decline (Lai et al., 2017). In this thesis, MLN4924 was identified as a transcriptional inhibitor that decreases transcription (pgRNA, preS/S RNA and X RNA) from all four HBV promoters (Figure 3.23.), which further leads to a reduction on HBsAg and HBeAg. Transcription inhibition of cccDNA is the most promising target of MLN4924.

MLN4924 not only acts as a new antiviral but becomes a tool in modulating HBx-mediated transcription in *in vitro* experiments. Six-day removal of MLN4924 led to HBV rebound in long-term infected HepG2^{hNTCP} cells but not in HepaRG^{hNTCP} cells (Figure 3.21.~3.22.). Since it was also reported that MLN4924-mediated inhibition of Cullin 4A neddylation and Vpx-induced degradation of SAMHD1 in HIV infection is reversible (Hofmann et al., 2013), it is consistent that MLN4924 acts as a reversible transcriptional inhibitor in HepG2^{hNTCP} cells and serves as a modulator at the transcriptional level upon pulse treatment, which provides a simple way to switch on and off transcription and will facilitate future studies on transcription of cccDNA. However, what causes the discrepancy between HepG2^{hNTCP} and HepaRG^{hNTCP} cells is still unclear. One possible explanation is due to the different metabolic kinetics in these cells. As shown in Table 4.2., differentiated HepaRG^{hNTCP} cells have the lowest EC_{50} values and the most sensitive upon MLN4924 treatment. Regarding their non-proliferating status, HepaRG^{hNTCP} cells may not completely decay MLN4924 after six-day removal (Gripon et al., 2002). Remaining intracellular MLN4924 inhibits the rebound of HBV replication. In contrast, HepG2^{hNTCP} cells with proliferation may be able to dilute out MLN4924 to a concentration that is much lower than its respective EC_{50} values and in this occasion, HBV replication is reactivated after six days.

Table 4.2. Summary of MLN4924 EC_{50} and CC_{50} values in three models.

EC_{50}/CC_{50} (nM)	**PHH**	**HepaRG^{hNTCP}**	**HepG2^{hNTCP}**
EC_{50} of HBsAg	293.4 [102~860]*	26.9 [9~66]	175.1 [40~910]
EC_{50} of HBeAg	143.7 [68~298]	15.0 [5~33]	30.2 [0~235]
EC_{50} of transcription	292.4 [18~11596]	30.2 [5~113]	484.7 [>80]
CC_{50}	857.0 [245~3607]	2442 [1025~6545]	>50000

*Best-fit values [95% CI (profile likelihood) calculated based on independent experiments];
EC_{50}: half maximum of effective dose; CC_{50}: half maximum of cytotoxicity

MLN4924's second target is blockage of HBsAg translation and secretion. In chronic infection, integrated HBV DNA is another source of HBsAg production (Wooddell et al., 2017, Tu et al., 2017). My work also revealed the inhibition of HBsAg secretion upon MLN4924 treatment in PLC/PRF5 cells with natural HBs integration. The mechanism for the inhibition of HBsAg secretion is probably distinct from that for the inhibition of transcription. Targeting neddylation inhibits transcription from cccDNA in *de novo* infection but not from integrated DNA in the PLC/PRF5 cells (Figure 3.24.). This phenotype is consistent with the fact that HBx protein enhances gene transcription selectively from extrachromosomal DNA templates but shows no effect lentiviral mediated insertion DNA in the host genome (van Breugel et al., 2012). Indeed, MLN4924 treatment seems no inhibitory effect on the transcription from natural integrates. Remarkably, MLN4924 treatment induced a 3-fold reduction on HBsAg secretion, although HBs transcription was not affected (Figure 3.25.). Given that the first mode of MLN4924 action is selective transcriptional inhibition from cccDNA, in addition to that MLN4924 reduces HBsAg expression or interferes with HBsAg stability at the translational level. It is totally unknown whether HBsAg can be a direct neddylation target, but HBx protein itself may require HDM2-mediated neddylation to maintain its function and stability. Mass spectrometry analysis in HEK293T cells transfected with HBx identified that lysine 91 and 95 are two major neddylation sites (Liu et al., 2017). In conclusion, MLN4924 has dual targets: (1) prevention of HBx-mediated degradation of SMC5/6 complex components, as a result, inhibition of transcription from cccDNA; (2) reduction of HBsAg at the translational or post-translational level. So far, point (1) was proved in this thesis and (2) requires further experiments.

As shown in Figure 3.27~3.31., it is confirmed that the mode of MLN4924 action at the transcriptional level is dependent on HBx-DDB1 complex, using stable cell lines and lentiviral transcomplementation assay. These findings not only support the authentic availability of HBx-DDB1-Cullin 4A interaction in HBV replication but suggest this complex as a novel drug target. MLN4924 is not a direct-acting antiviral yet since it mainly targets the NAE1-mediated neddylation that is downstream of HBx-DDB1 complex but not HBx-DDB1 interaction, although HBx neddylation might be a direct target. Targeting HBx or HBx-DDB1 complex must be much more specific and lead to better efficiency and less toxicity on host cells. A major bottleneck is the lack of structures of HBx protein or HBx-DDB1 complex. At this stage, an alternative is an efficient and rapid system for assaying HBx-mediated transactivation (Zhou et al., 2017), which is the only available model to initiate drug screening and investigate small molecules interfering with HBx-DDB1 complex.

All the attempts in this thesis shed light on the topic that targeting the HBx-DDB1-Cullin complex inhibits transcription from HBV cccDNA in susceptible hepatoma cells and the complex is absolutely druggable (Qu et al., the International Liver Congress 2019). To achieve this aim, either depleting HBx as shown in Figure 3.13., knocking down DDB1 (data not shown), interfering with HBx-DDB1 association, or blocking Cullin 4 neddylation result in remarkable inhibition at the transcriptional level. Figures 3.32~3.34 showed that HBV replication almost diminished SMC6 signals in infected PHH and HepaRG^{hNTCP} cells and MLN4924 treatment restored the expression of SMC6 probably by switching off HBx function. The SMC6 mediated transcriptional silence of cccDNA seems HBV specific and not universal to foreign episomal genomes of other DNA viruses, since a recent study has shown that SMC6 protein is not required at all for the E2-mediated transcriptional activation or E1/E2-mediated transient replication in human papillomavirus infection, despite its binding activity to viral E2 protein (Bentley et al., 2018). Perhaps, SMC6 binds cccDNA and this binding recruits other transcriptional repressors to control the epigenetic status of cccDNA, which would be further characterized (Belloni et al., 2009).

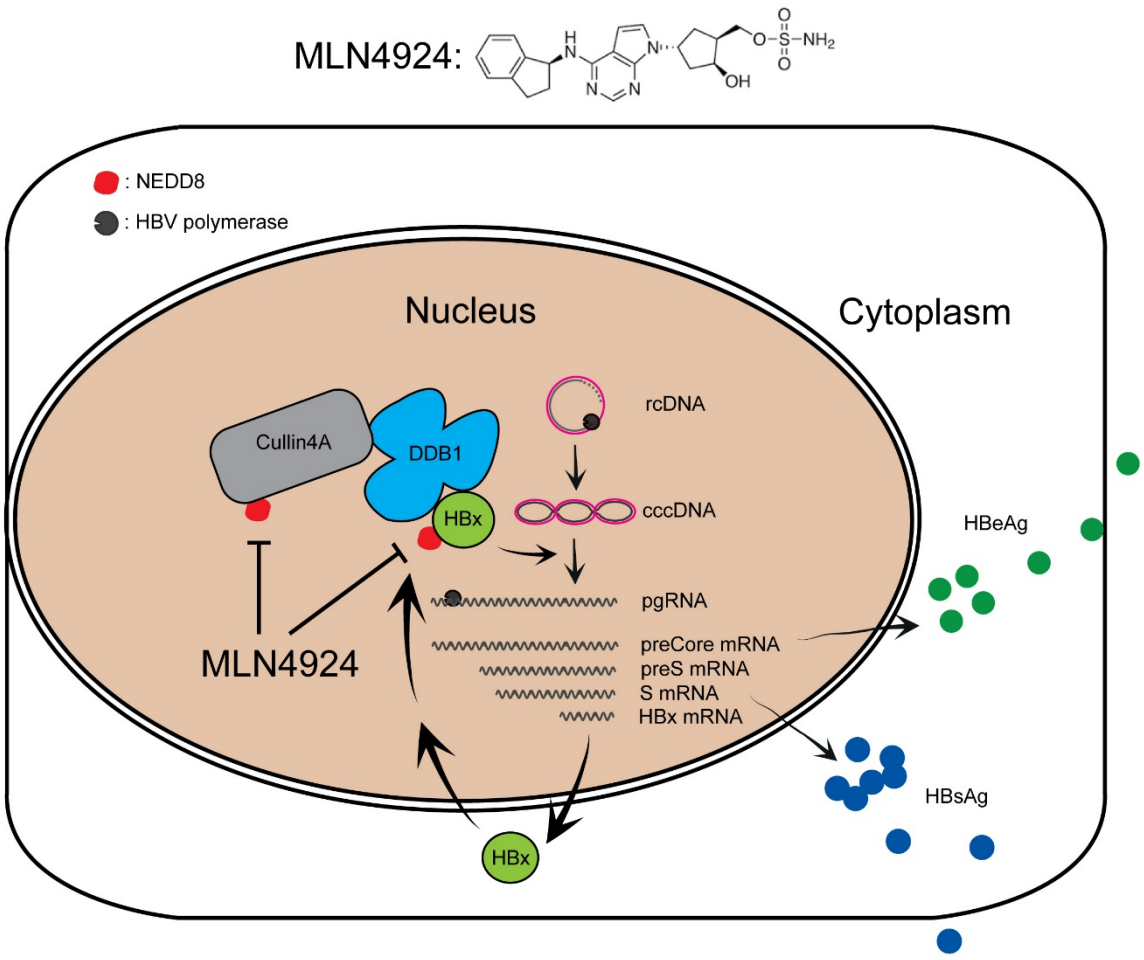

Figure 4.1. Proposed working model of MLN4924. In HBV replication, HBx protein is expressed and located in the nucleus. HBx binds DDB1 and recruits Cullin 4A E3 ubiquitin ligase, in order to counteract host restrictions on cccDNA and then transactivates cccDNA

transcription. HBx-mediated cccDNA transcription is the major target of a neddylation inhibitor, MLN4924, which inhibits Cullin 4A activation and probable neddylation of HBx protein. Consequently, MLN4924 mediates transcriptional inhibition in an HBx-dependent manner. In addition, MLN4924 reduces HBsAg production directly at the translational or post-translational level.

4.5. Comparison of MLN4924 and other transcriptional inhibitors

Given that MLN4924 is not the only HBV transcriptional inhibitors, other prodrugs are under development and investigation. For instance, 640 FDA-approved drugs were screened for the ability to inhibit HBV transcription from a reporter plasmid cotransfected with HBx in HEK293T cells. Some compounds inhibited HBV transcription in the presence of HBx. These drugs (Terbinafine etc.) also interfered with HBx-mediated transcription in HepG2.2.15 and transfected HepG2 cells (van de Klundert et al., 2016b). However, using the models that do not form authentic cccDNA, whether the validated drugs target HBx-mediated cccDNA transcription is unclear. Overexpressed HBx may have artificial effects.

Using HepG2^{hNTCP} infection model, several HBV transcriptional inhibitors were also identified. 1827 FDA-approved drugs were validated by a recombinant HBV-based NanoLuc assay and KX2-391, an inhibitor of Src kinase and tubulin polymerization, was identified as a leading candidate. KX2-391 suppressed HBV replication in PHH and HepG2^{hNTCP} cells in a dose-dependent manner and inhibited HBV transcription from precore promoter in an HBx-independent manner but not other promoters (Harada et al., 2017). Distinct from MLN4924 that inhibits transcription from all four HBV promoters (Figure 3.23.), KX2-391 relies on a specific host factor, hepatocyte nuclear factor 4α (HNF4α), selective on precore promoter as proposed in the paper. This suggests that transcriptional factors and co-factors may act on a specific promoter and could be targets of transcriptional inhibitors. As an example, retinoid X receptor alpha (RXRα) modulates transcriptional network and controls hepatic lipid metabolism. The RXR-specific agonist bexarotene inhibits HBV transcription in HepaRG cells, HepG2^{hNTCP} cells and primary tupaia hepatocytes (Song et al., 2018). Later on, retinoic acid receptor (RAR) agonists were also identified as transcriptional inhibitors. To be specific, among the agonists Tazarotene repressed cccDNA transcription in PHH and HepaRG cells and showed the most potent inhibitory effect on HBsAg secretion in PHH (EC_{50}: ~30nM). RNA sequencing analysis confirmed that Tazarotene altered the expression level of genes in RAR and metabolic pathways and inhibited HBV in part through RARβ but not RARα (Li et al., 2018a). In our group, we also have screened 1181 FDA-approved drugs and identified RARα-specific agonist Am80 (tamibarotene) potent in inhibition of transcription from cccDNA. HBV genotypes B, D and E

were equally inhibited, showing a general role of RARα in HBV replication (Nkongolo et al., 2019). None of the studies above evaluated HBx dependency of the drugs in infection settings. Although nuclear HBx targets the SMC5/6 complex, it could not be excluded that HBx also binds and modulates transcriptional cofactors like HNF4a, RARα/β and RXR onto the cccDNA and transactivates its transcription.

Beside small molecules that can repress transcription from cccDNA, RNAi-based therapeutics have the potential to clear existing HBV transcripts (Wooddell et al., 2013). One of the siRNA regimens under development, ARC-520, has shown a dramatical reduction on HBsAg in treatment-näive HBeAg positive patients but much less reduction in HBeAg negative or NUC-treated patients (Wooddell et al., 2017). Many integrants in infected chimpanzees lacked targeting sites of ARC-520 and produced mRNA that was difficult to be targeted. MLN4924 also showed profound inhibition of transcription from cccDNA but not integrants, because of the HBx selectivity only on cccDNA templates (Figure 3.24.) (van Breugel et al., 2012). The selectivity of both ARC-520 and MLN4924 on cccDNA limits their future applications. Different from ARC-520, MLN4924 showed an additional effect on HBsAg stability or assembly (Figure 3.25.). However, this effect is too weak to efficiently block a great amount of HBsAg produced from integrants.

Nevertheless, MLN4924 is the first available antiviral targeting the HBx-DDB1-Cullin 4A complex, although at this stage it is not conclusive whether MLN4924 is also a direct-acting antiviral if MLN4924 inhibits neddylation of HBx protein and stability of HBsAg. At present, this finding ensures the HBx-DDB1 complex as a prerequisite in cccDNA transcription and a promising antiviral target. After two years of my finding (Qu et al., 2016 International HBV Meeting), one group identified MLN4924 (Pevonedistat) as a potent HBV inhibitor (Sekiba et al., 2019a). Very recently, the authors also proposed Nitazoxanide (NTZ), a thiazolidine anti-infective agent, as an inhibitor of transcription from cccDNA by targeting the HBx-DDB1 interaction (Sekiba et al., 2019b). However, the drugs in both studies showed less pronounced inhibitory effects on transcription (2~3 fold) compare to my study. More importantly, they lack key evidence showing HBx dependency in authentic infection (e.g. using Xd virus). Additionally, the same effects of MLN4924 and Nitazoxanide in two studies are contradictory to the scientific concept that the effect of Nitazoxanide targeting HBx-DDB1 association should be more specific and effective than that of MLN4924 targeting downstream Cullin 4A adaptor. Therefore, one direction in drug discovery is to seek for or re-design small molecules with better efficacy that directly deactivate HBx protein or disturb HBx-DDB1 binding. For this view, either HBx crystal structure (if it exists) or HBx-DDB1 complex structure will be helpful. The

second way is to further unravel the HBx protein and its new and authentic functions. For instance, what is the exact function of the N-terminal HBx (1~50 amino acids)? Consistent with my study as shown in Figure 3.14. and 3.15. (Qu et al., 2017 International HBV Meeting), functional analysis revealed that highly conserved residues, the CCCH motif (C61, C69, C137, and H139), are required for HBx function and HBx exhibits stoichiometric zinc binding in the presence of DDB1 (Fletcher et al., 2017 International HBV Meeting). HBx as a zinc-finger protein that is highly active in general transcriptional processes, are definitely worthy to be further studied and new functions are expected to be translated into novel antiviral targets.

4.6. Final summary

240 million people worldwide are chronically infected with HBV. Thus, the urgent need for curative therapies is unquestionable. To achieve a sterilizing or functional cure, eliminating cccDNA or silencing its transcription becomes the ultimate goal. In this thesis, a quantitative and comprehensive analysis of the dynamics and stability of cccDNA in *in vitro* infected hepatocytes allows more understandings of cccDNA biology. Accurate quantification of cccDNA is meaningful to judge clinical endpoint under conventional therapies (pegylated IFNα, NUCs) in patients when cccDNA level is reduced and also helpful for evaluation of the outcomes of novel regimens (e.g. phase III trials of Myrcludex B and capsid inhibitors). Additionally, cccDNA turnover determined based on current and ongoing experimental data in long-term infection can be translated and built up to mathematical models, which predict whether and how long elimination of cccDNA occurs and provide a message of the endpoint in future HBV therapy.

HBx is a nuclear protein and makes use of its entire C-terminus to associate with DDB1. This complex recruits Cullin 4A unlocks the restriction of SMC5/6 complex on the cccDNA and maximize its transcription. This virus-host interaction enables and maintains cccDNA transcription and, as a consequence, guarantees extremely efficient transcription from a few copies of cccDNA template and lowers the copy number in the long-term evolution. Persistence of cccDNA transcription highly relies on HBx expression. Therefore, depletion of HBx or loss of its transactivation function traps cccDNA to a “latent” status, which is frequently occurred in other DNA viruses (HSV, HPV, etc.). As the sole viral protein acting on transcription from cccDNA, targeting HBx is much more specific, compared to epigenetic modulators (histone methylation, acetylation, etc.), which show no selectivity between cccDNA and genomic DNA.

Targeting HBx-mediated transcription by a neddylation inhibitor, MLN4924, is not only a decent tool switching on and off transcription in basic research but a direction of new-class

antivirals. In this direction HBx, DDB1 and Cullin 4A can be targeted. Blockage of HBx-mediated transcription from cccDNA may open novel translational therapeutic approaches allowing the functional cure of chronic hepatitis B. In future, these include: (1) evaluation of MLN4924 and other neddylation inhibitors towards *in vivo* models and (2) identification of other HBx inhibitors by targeting HBx zinc-binding activity and HBx-DDB1 interaction.

5. PUBLICATIONS AND PATENTS

5.1. Peer-reviewed publications (2016~2019)

1. A novel method to precisely quantify Hepatitis B Virus covalently closed circular (ccc)DNA formation, maintenance, and loss.

Tu T, Zehnder B, Qu B, Main N, Allweiss L, Dandri M, Shackel N, Urban S.

J Hepatol. Submitted.

2. Stem cell-derived polarized hepatocytes.

Dao Thi VL, Wu X, Belote R, Andreo U, Takacs C, Fernandez J, Vale-Silva L, Prallet S, Decker C, Fu RM, Qu B, Uryu K, Molina H, Saeed M, Steinmann E, Urban S, Singaraja R, Schneider W, Simon S, Rice C.

Nat Commun. Minor revision.

3. Stem Cell-Derived Hepatocyte-Like Cells as Model for Viral Hepatitis Research.

Wang J, Qu B, Zhang F, Zhang C, Deng W, Dao Thi VL, Xia Y.

Stem Cells Int. 2019 Jun 12: 9605252. DOI: 10.1155/2019/9605252.

4. Quantification of Hepatitis B Virus Covalently Closed Circular DNA in Infected Cell Culture Models by Quantitative PCR.

Qu B, Urban S.

Bio-protocol. 2019 Apr; 9(7), e3202. DOI: 10.21769/BioProtoc.3202.

5. T5 Exonuclease Hydrolysis of Hepatitis B Virus Replicative Intermediates Allows Reliable Quantification and Fast Drug Efficacy Testing of Covalently Closed Circular DNA by PCR.

Qu B, Ni Y, Lempp FA, Vondran FWR, Urban S.

J Virol. 2018 Nov 12; 92(23). DOI: 10.1128/JVI.01117-18.

6. HBV Bypasses the Innate Immune Response and Does not Protect HCV From Antiviral Activity of Interferon.

Mutz P, Metz P, Lempp FA, Bender S, Qu B, Schöneweis K, Seitz S, Tu T, Restuccia A, Frankish J, Dächert C, Schusser B, Koschny R, Polychronidis G, Schemmer P, Hoffmann K, Baumert TF, Binder M, Urban S, Bartenschlager R.

Gastroenterology. 2018 May; 154(6): 1791-1804.e22. DOI: 10.1053/j.gastro.2018.01.044.

7. Critical Role of HAX-1 in Promoting Avian Influenza Virus Replication in Lung Epithelial Cells.

Li X*, Qu B*, He G, Cardona CJ, Song Y, Xing Z.

Mediators Inflamm. 2018 Jan; 2018: 3586132. DOI: 10.1155/2018/3586132.

*: equally contributed

8. Sodium Taurocholate Cotransporting Polypeptide Is the Limiting Host Factor of Hepatitis B Virus Infection in Macaque and Pig Hepatocytes.

Lempp FA, Wiedtke E, Qu B, Roques P, Chemin I, Vondran FWR, Le Grand R, Grimm D, Urban S.

Hepatology. 2017 Sep; 66(3): 703-716. DOI: 10.1002/hep.29112.

9. Restrictive Influence of SAMHD1 on Hepatitis B Virus Life Cycle.

Sommer AF, Rivière L, Qu B, Schott K, Riess M, Ni Y, Shepard C, Schnellbächer E, Finkernagel M, Himmelsbach K, Welzel K, Kettern N, Donnerhak C, Münk C, Flory E, Liese J, Kim B, Urban S, König R.

Sci Rep. 2016 May; 27; 6: 26616. DOI: 10.1038/srep26616.

10. Hepatitis B Virus Infection of A Mouse Hepatic Cell Line Reconstituted with Human Sodium Taurocholate Cotransporting Polypeptide.

Lempp FA, Qu B, Wang YX, Urban S.

J Virol. 2016 Apr; 90(9): 4827-31. DOI: 10.1128/JVI.02832-15.

5.2. Oral presentations at conferences (first authorship) (2016~2019)

1. The NEDD8-activating enzyme inhibitor MLN4924 potently inhibits transcription from covalently closed circular DNA in a Hepatitis B Virus X protein-dependent manner.

Qu B, Leuthold M, Mutz P, Nebioglu F, Bartenschlager R, Urban S.

31st International Conference on Antiviral Research (ICAR). Session: Hepatitis and Retroviruses, number 201. Presented on June 13th 2018, Porto, Portugal.

2. The NEDD8-activating enzyme (NAE) inhibitor MLN4924 potently interferes with HBV infection.

Qu B, Leuthold M, Urban S.

2016 International HBV Meeting. O-7. Presented on September 21th 2016, Seoul, Korea.

5.3. Poster presentations at conferences (2015~2019)

1. Targeting the HBx-DDB1-Cullin complex inhibits transcription from HBV covalently closed circular DNA in susceptible hepatoma cells.

Qu B, Leuthold MM, Sonnabend J, Urban S.

The International Liver Congress 2019; 70(1), e712-e713. Presented on April 13th 2019, Vienna.

DOI: 10.1016/S0618-8278(19)31427-6

2. A comparative evaluation of antiviral inhibitors and HBc-deficient HBV on cccDNA formation and stability.

Qu B, Zehnder B, Tu T, Ni Y, Urban S.

2018 International HBV Meeting. Presented on October 5th 2018, Taormina.

3. HBx: Hepatitis B Virus Swiss Army Knife enabling successful infection.

Milani E, Qu B, Urban S, Wollscheid B.

17th Human Proteome Organization World Congress-HUPO 2018. Presented on October 1st 2018, Orlando.

4. Functional analysis identifies key fragments and residues to promote HBx transactivation.

Qu B, Leuthold M, Sonnabend J, Urban S.

2017 International HBV Meeting. *P-46*. Presented on September 4th 2017, Washington DC.

5. Selective digestion of HBV rcDNA by T5 exonuclease allows reliable PCR-based quantification of cccDNA in in vitro infection systems.

Qu B, Ni Y, Lempp FA, Urban S.

2015 International HBV Meeting. P-35. Presented on October 6th 2015, Dolce Bad Nauheim.

6. Myrcludex B and GLS4 interfere with the formation of HBV covalently closed circular DNA.

Qu B, Zehnder B, Tu T, Ni Y, Urban S.

28th Annual Meeting of the Society for Virology. *P-295*. Presented on March 15th 2018, Wuerzburg.

7. The NEDD8-activating enzyme inhibitor MLN4924 potently inhibits HBV transcription in an HBx-dependent manner.

Qu B, Leuthold M, Urban S.

27th Annual Meeting of the Society for Virology. *P-221*. Presented on March 23th 2017, Marburg.

8. DNA damage-binding protein 1 promotes transcription from covalently closed circular DNA in Hepatitis B Virus infection.

Qu B, Sonnabend J, Hezel P, Urban S.

26th Annual Meeting of the Society for Virology. *P-328*. Presented on April 8th 2016, Muenster.

5.4. Patents

1. Compounds and combinations thereof for preventing and/or treating HBV and/or HDV infections

Inventors: Florian Lempp, Stephan Urban, Yi Ni, Lea Nussbaum, Bingqian Qu

Patent number: WO2018054891A1

Application number: PCT/EP2017/073608

6. REFERENCES

ABDUL, F., FILLETON, F., GEROSSIER, L., PATUREL, A., HALL, J., STRUBIN, M. & ETIENNE, L. 2018. Smc5/6 Antagonism by HBx Is an Evolutionarily Conserved Function of Hepatitis B Virus Infection in Mammals. *J Virol,* 92.

ALLEN, M. I., DESLAURIERS, M., ANDREWS, C. W., TIPPLES, G. A., WALTERS, K. A., TYRRELL, D. L., BROWN, N. & CONDREAY, L. D. 1998. Identification and characterization of mutations in hepatitis B virus resistant to lamivudine. Lamivudine Clinical Investigation Group. *Hepatology,* 27**,** 1670-7.

ALLWEISS, L., VOLZ, T., GIERSCH, K., KAH, J., RAFFA, G., PETERSEN, J., LOHSE, A. W., BENINATI, C., POLLICINO, T., URBAN, S., LUTGEHETMANN, M. & DANDRI, M. 2018. Proliferation of primary human hepatocytes and prevention of hepatitis B virus reinfection efficiently deplete nuclear cccDNA in vivo. *Gut,* 67**,** 542-552.

ANGUS, P., VAUGHAN, R., XIONG, S., YANG, H., DELANEY, W., GIBBS, C., BROSGART, C., COLLEDGE, D., EDWARDS, R., AYRES, A., BARTHOLOMEUSZ, A. & LOCARNINI, S. 2003. Resistance to adefovir dipivoxil therapy associated with the selection of a novel mutation in the HBV polymerase. *Gastroenterology,* 125**,** 292-7.

ASSELAH, T., BOYER, N., SAADOUN, D., MARTINOT-PEIGNOUX, M. & MARCELLIN, P. 2016. Direct-acting antivirals for the treatment of hepatitis C virus infection: optimizing current IFN-free treatment and future perspectives. *Liver Int,* 36 Suppl 1**,** 47-57.

BALDICK, C. J., EGGERS, B. J., FANG, J., LEVINE, S. M., POKORNOWSKI, K. A., ROSE, R. E., YU, C. F., TENNEY, D. J. & COLONNO, R. J. 2008a. Hepatitis B virus quasispecies susceptibility to entecavir confirms the relationship between genotypic resistance and patient virologic response. *J Hepatol,* 48**,** 895-902.

BALDICK, C. J., TENNEY, D. J., MAZZUCCO, C. E., EGGERS, B. J., ROSE, R. E., POKORNOWSKI, K. A., YU, C. F. & COLONNO, R. J. 2008b. Comprehensive evaluation of hepatitis B virus reverse transcriptase substitutions associated with entecavir resistance. *Hepatology,* 47**,** 1473-82.

BALSANO, C., BILLET, O., BENNOUN, M., CAVARD, C., ZIDER, A., GRIMBER, G., NATOLI, G., BRIAND, P. & LEVRERO, M. 1993. The hepatitis B virus X gene product transactivates the HIV-LTR in vivo. *Arch Virol Suppl,* 8**,** 63-71.

BARTENSCHLAGER, R., KUHN, C. & SCHALLER, H. 1992. Expression of the P-protein of the human hepatitis B virus in a vaccinia virus system and detection of the nucleocapsid-associated P-gene product by radiolabelling at newly introduced phosphorylation sites. *Nucleic Acids Res,* 20**,** 195-202.

BARTENSCHLAGER, R. & SCHALLER, H. 1988. The amino-terminal domain of the hepadnaviral P-gene encodes the terminal protein (genome-linked protein) believed to prime reverse transcription. *Embo j,* 7**,** 4185-92.

BARTENSCHLAGER, R. & SCHALLER, H. 1992. Hepadnaviral assembly is initiated by polymerase binding to the encapsidation signal in the viral RNA genome. *Embo j,* 11**,** 3413-20.

BAZINET, M., PANTEA, V., CEBOTARESCU, V., COJUHARI, L., JIMBEI, P., ALBRECHT, J., SCHMID, P., LE GAL, F., GORDIEN, E., KRAWCZYK, A., MIJOCEVIC, H., KARIMZADEH, H., ROGGENDORF, M. & VAILLANT, A. 2017. Safety and efficacy of REP 2139 and pegylated interferon alfa-2a for

treatment-naive patients with chronic hepatitis B virus and hepatitis D virus co-infection (REP 301 and REP 301-LTF): a non-randomised, open-label, phase 2 trial. *Lancet Gastroenterol Hepatol,* 2**,** 877-889.

BECKER, S. A., LEE, T. H., BUTEL, J. S. & SLAGLE, B. L. 1998. Hepatitis B virus X protein interferes with cellular DNA repair. *J Virol,* 72**,** 266-72.

BELLONI, L., ALLWEISS, L., GUERRIERI, F., PEDICONI, N., VOLZ, T., POLLICINO, T., PETERSEN, J., RAIMONDO, G., DANDRI, M. & LEVRERO, M. 2012. IFN-alpha inhibits HBV transcription and replication in cell culture and in humanized mice by targeting the epigenetic regulation of the nuclear cccDNA minichromosome. *J Clin Invest,* 122**,** 529-37.

BELLONI, L., POLLICINO, T., DE NICOLA, F., GUERRIERI, F., RAFFA, G., FANCIULLI, M., RAIMONDO, G. & LEVRERO, M. 2009. Nuclear HBx binds the HBV minichromosome and modifies the epigenetic regulation of cccDNA function. *Proc Natl Acad Sci U S A,* 106**,** 19975-9.

BENTLEY, P., TAN, M. J. A., MCBRIDE, A. A., WHITE, E. A. & HOWLEY, P. M. 2018. The SMC5/6 complex interacts with the papillomavirus E2 protein and influences maintenance of viral episomal DNA. *J Virol*.

BERGAMETTI, F., SITTERLIN, D. & TRANSY, C. 2002. Turnover of hepatitis B virus X protein is regulated by damaged DNA-binding complex. *J Virol,* 76**,** 6495-501.

BERKE, J. M., DEHERTOGH, P., VERGAUWEN, K., VAN DAMME, E., MOSTMANS, W., VANDYCK, K. & PAUWELS, F. 2017. Capsid Assembly Modulators Have a Dual Mechanism of Action in Primary Human Hepatocytes Infected with Hepatitis B Virus. *Antimicrob Agents Chemother,* 61.

BLANK, A., MARKERT, C., HOHMANN, N., CARLS, A., MIKUS, G., LEHR, T., ALEXANDROV, A., HAAG, M., SCHWAB, M., URBAN, S. & HAEFELI, W. E. 2016. First-in-human application of the novel hepatitis B and hepatitis D virus entry inhibitor myrcludex B. *J Hepatol,* 65**,** 483-9.

BLOOM, K., ELY, A., MUSSOLINO, C., CATHOMEN, T. & ARBUTHNOT, P. 2013. Inactivation of hepatitis B virus replication in cultured cells and in vivo with engineered transcription activator-like effector nucleases. *Mol Ther,* 21**,** 1889-97.

BLUMBERG, B. S., ALTER, H. J. & VISNICH, S. 1965. A "NEW" ANTIGEN IN LEUKEMIA SERA. *Jama,* 191**,** 541-6.

BOCK, C. T., SCHRANZ, P., SCHRODER, C. H. & ZENTGRAF, H. 1994. Hepatitis B virus genome is organized into nucleosomes in the nucleus of the infected cell. *Virus Genes,* 8**,** 215-29.

BOCK, C. T., SCHWINN, S., LOCARNINI, S., FYFE, J., MANNS, M. P., TRAUTWEIN, C. & ZENTGRAF, H. 2001. Structural organization of the hepatitis B virus minichromosome. *J Mol Biol,* 307**,** 183-96.

BOGOMOLOV, P., ALEXANDROV, A., VORONKOVA, N., MACIEVICH, M., KOKINA, K., PETRACHENKOVA, M., LEHR, T., LEMPP, F. A., WEDEMEYER, H., HAAG, M., SCHWAB, M., HAEFELI, W. E., BLANK, A. & URBAN, S. 2016. Treatment of chronic hepatitis D with the entry inhibitor myrcludex B: First results of a phase Ib/IIa study. *J Hepatol,* 65**,** 490-8.

BONTRON, S., LIN-MARQ, N. & STRUBIN, M. 2002. Hepatitis B virus X protein associated with UV-DDB1 induces cell death in the nucleus and is functionally antagonized by UV-DDB2. *J Biol Chem,* 277**,** 38847-54.

BOUCHARD, M. J. & SCHNEIDER, R. J. 2004. The enigmatic X gene of hepatitis B virus. *J Virol,* 78**,** 12725-34.

BOUCHARD, M. J., WANG, L. H. & SCHNEIDER, R. J. 2001. Calcium signaling by HBx protein in hepatitis B virus DNA replication. *Science,* 294**,** 2376-8.

BOURNE, C. R., FINN, M. G. & ZLOTNICK, A. 2006. Global structural changes in hepatitis B virus capsids induced by the assembly effector HAP1. *J Virol,* 80**,** 11055-61.

BREZILLON, N., BRUNELLE, M. N., MASSINET, H., GIANG, E., LAMANT, C., DASILVA, L., BERISSI, S., BELGHITI, J., HANNOUN, L., PUERSTINGER, G., WIMMER, E., NEYTS, J., HANTZ, O., SOUSSAN, P., MOROSAN, S. & KREMSDORF, D. 2011. Antiviral activity of Bay 41-4109 on hepatitis B virus in humanized Alb-uPA/SCID mice. *PLoS One,* 6**,** e25096.

BRINGAS, R. 1997. Folding and assembly of hepatitis B virus core protein: a new model proposal. *J Struct Biol,* 118**,** 189-96.

BROWNELL, J. E., SINTCHAK, M. D., GAVIN, J. M., LIAO, H., BRUZZESE, F. J., BUMP, N. J., SOUCY, T. A., MILHOLLEN, M. A., YANG, X., BURKHARDT, A. L., MA, J., LOKE, H. K., LINGARAJ, T., WU, D., HAMMAN, K. B., SPELMAN, J. J., CULLIS, C. A., LANGSTON, S. P., VYSKOCIL, S., SELLS, T. B., MALLENDER, W. D., VISIERS, I., LI, P., CLAIBORNE, C. F., ROLFE, M., BOLEN, J. B. & DICK, L. R. 2010. Substrate-assisted inhibition of ubiquitin-like protein-activating enzymes: the NEDD8 E1 inhibitor MLN4924 forms a NEDD8-AMP mimetic in situ. *Mol Cell,* 37**,** 102-11.

BRUNETTO, M. R., RODRIGUEZ, U. A. & BONINO, F. 1999. Hepatitis B virus mutants. *Intervirology,* 42**,** 69-80.

BRUSS, V. & GERLICH, W. H. 1988. Formation of transmembraneous hepatitis B e-antigen by cotranslational in vitro processing of the viral precore protein. *Virology,* 163**,** 268-75.

CAI, C. W., LOMONOSOVA, E., MORAN, E. A., CHENG, X., PATEL, K. B., BAILLY, F., COTELLE, P., MEYERS, M. J. & TAVIS, J. E. 2014. Hepatitis B virus replication is blocked by a 2-hydroxyisoquinoline-1,3(2H,4H)-dione (HID) inhibitor of the viral ribonuclease H activity. *Antiviral Res,* 108**,** 48-55.

CAI, D., MILLS, C., YU, W., YAN, R., ALDRICH, C. E., SAPUTELLI, J. R., MASON, W. S., XU, X., GUO, J. T., BLOCK, T. M., CUCONATI, A. & GUO, H. 2012. Identification of disubstituted sulfonamide compounds as specific inhibitors of hepatitis B virus covalently closed circular DNA formation. *Antimicrob Agents Chemother,* 56**,** 4277-88.

CAI, D., WANG, X., YAN, R., MAO, R., LIU, Y., JI, C., CUCONATI, A. & GUO, H. 2016. Establishment of an inducible HBV stable cell line that expresses cccDNA-dependent epitope-tagged HBeAg for screening of cccDNA modulators. *Antiviral Res,* 132**,** 26-37.

CAMPAGNA, M. R., LIU, F., MAO, R., MILLS, C., CAI, D., GUO, F., ZHAO, X., YE, H., CUCONATI, A., GUO, H., CHANG, J., XU, X., BLOCK, T. M. & GUO, J. T. 2013. Sulfamoylbenzamide derivatives inhibit the assembly of hepatitis B virus nucleocapsids. *J Virol,* 87**,** 6931-42.

CASCIANO, J. C. & BOUCHARD, M. J. 2018. Hepatitis B virus X protein modulates cytosolic Ca(2+) signaling in primary human hepatocytes. *Virus Res,* 246**,** 23-27.

CATTANEO, R., WILL, H., DARAI, G., PFAFF, E. & SCHALLER, H. 1983a. Detection of an element of the SV40 late promoter in vectors used for expression studies in COS cells. *Embo j,* 2**,** 511-4.

CATTANEO, R., WILL, H., HERNANDEZ, N. & SCHALLER, H. 1983b. Signals regulating hepatitis B surface antigen transcription. *Nature,* 305**,** 336-8.

CATTANEO, R., WILL, H. & SCHALLER, H. 1984. Hepatitis B virus transcription in the infected liver. *Embo j,* 3**,** 2191-6.

CHA, M. Y., RYU, D. K., JUNG, H. S., CHANG, H. E. & RYU, W. S. 2009. Stimulation of hepatitis B virus genome replication by HBx is linked to both nuclear and cytoplasmic HBx expression. *J Gen Virol,* 90**,** 978-86.

CHAMI, M., FERRARI, D., NICOTERA, P., PATERLINI-BRECHOT, P. & RIZZUTO, R. 2003. Caspase-dependent alterations of Ca2+ signaling in the induction of apoptosis by hepatitis B virus X protein. *J Biol Chem,* 278**,** 31745-55.

CHANG, L. J., HIRSCH, R. C., GANEM, D. & VARMUS, H. E. 1990. Effects of insertional and point mutations on the functions of the duck hepatitis B virus polymerase. *J Virol,* 64**,** 5553-8.

CHANG, S. F., NETTER, H. J., HILDT, E., SCHUSTER, R., SCHAEFER, S., HSU, Y. C., RANG, A. & WILL, H. 2001. Duck hepatitis B virus expresses a regulatory HBx-like protein from a hidden open reading frame. *J Virol,* 75**,** 161-70.

CHANG, T. T., LAI, C. L., KEW YOON, S., LEE, S. S., COELHO, H. S., CARRILHO, F. J., POORDAD, F., HALOTA, W., HORSMANS, Y., TSAI, N., ZHANG, H., TENNEY, D. J., TAMEZ, R. & ILOEJE, U. 2010. Entecavir treatment for up to 5 years in patients with hepatitis B e antigen-positive chronic hepatitis B. *Hepatology,* 51**,** 422-30.

CHEN, E. Q., DAI, J., BAI, L. & TANG, H. 2015. The efficacy of zinc finger antiviral protein against hepatitis B virus transcription and replication in tansgenic mouse model. *Virol J,* 12**,** 25.

CHEN, M., HIENG, S., QIAN, X., COSTA, R. & OU, J. H. 1994. Regulation of hepatitis B virus ENI enhancer activity by hepatocyte-enriched transcription factor HNF3. *Virology,* 205**,** 127-32.

CHEN, Y. & MARION, P. L. 1996. Amino acids essential for RNase H activity of hepadnaviruses are also required for efficient elongation of minus-strand viral DNA. *J Virol,* 70**,** 6151-6.

CONDREAY, L. D., WU, T. T., ALDRICH, C. E., DELANEY, M. A., SUMMERS, J., SEEGER, C. & MASON, W. S. 1992. Replication of DHBV genomes with mutations at the sites of initiation of minus- and plus-strand DNA synthesis. *Virology,* 188**,** 208-16.

COURTOIS, G., BAUMHUETER, S. & CRABTREE, G. R. 1988. Purified hepatocyte nuclear factor 1 interacts with a family of hepatocyte-specific promoters. *Proc Natl Acad Sci U S A,* 85**,** 7937-41.

CUI, X., CLARK, D. N., LIU, K., XU, X. D., GUO, J. T. & HU, J. 2016. Viral DNA-Dependent Induction of Innate Immune Response to Hepatitis B Virus in Immortalized Mouse Hepatocytes. *J Virol,* 90**,** 486-96.

CUI, X., GUO, J. T. & HU, J. 2015. Hepatitis B Virus Covalently Closed Circular DNA Formation in Immortalized Mouse Hepatocytes Associated with Nucleocapsid Destabilization. *J Virol,* 89**,** 9021-8.

CUI, X., LUDGATE, L., NING, X. & HU, J. 2013. Maturation-associated destabilization of hepatitis B virus nucleocapsid. *J Virol,* 87**,** 11494-503.

DAEMER, R. J., FEINSTONE, S. M., ALEXANDER, J. J., TULLY, J. G., LONDON, W. T., WONG, D. C. & PURCELL, R. H. 1980. PLC/PRF/5 (Alexander) hepatoma cell line: further characterization and studies of infectivity. *Infect Immun,* 30**,** 607-11.

DANE, D. S., CAMERON, C. H. & BRIGGS, M. 1970. Virus-like particles in serum of patients with Australia-antigen-associated hepatitis. *Lancet,* 1**,** 695-8.

DECORSIERE, A., MUELLER, H., VAN BREUGEL, P. C., ABDUL, F., GEROSSIER, L., BERAN, R. K., LIVINGSTON, C. M., NIU, C., FLETCHER, S. P., HANTZ, O. & STRUBIN, M. 2016. Hepatitis B virus X protein identifies the Smc5/6 complex as a host restriction factor. *Nature,* 531**,** 386-9.

DELANEY, W. E. T., EDWARDS, R., COLLEDGE, D., SHAW, T., FURMAN, P., PAINTER, G. & LOCARNINI, S. 2002. Phenylpropenamide derivatives AT-61 and AT-130 inhibit replication of wild-type and lamivudine-resistant strains of hepatitis B virus in vitro. *Antimicrob Agents Chemother,* 46**,** 3057-60.

DERES, K., SCHRODER, C. H., PAESSENS, A., GOLDMANN, S., HACKER, H. J., WEBER, O., KRAMER, T., NIEWOHNER, U., PLEISS, U., STOLTEFUSS, J., GRAEF, E., KOLETZKI, D., MASANTSCHEK, R. N., REIMANN, A., JAEGER, R., GROSS, R., BECKERMANN, B., SCHLEMMER, K. H., HAEBICH, D. & RUBSAMEN-WAIGMANN, H. 2003. Inhibition of hepatitis B virus replication by drug-induced depletion of nucleocapsids. *Science,* 299**,** 893-6.

DIAO, J., KHINE, A. A., SARANGI, F., HSU, E., IORIO, C., TIBBLES, L. A., WOODGETT, J. R., PENNINGER, J. & RICHARDSON, C. D. 2001. X protein of hepatitis B virus inhibits Fas-mediated apoptosis and is associated with up-regulation of the SAPK/JNK pathway. *J Biol Chem,* 276**,** 8328-40.

DIENSTAG, J. L., SCHIFF, E. R., WRIGHT, T. L., PERRILLO, R. P., HANN, H. W., GOODMAN, Z., CROWTHER, L., CONDREAY, L. D., WOESSNER, M., RUBIN, M. & BROWN, N. A. 1999. Lamivudine as initial treatment for chronic hepatitis B in the United States. *N Engl J Med,* 341**,** 1256-63.

DORIA, M., KLEIN, N., LUCITO, R. & SCHNEIDER, R. J. 1995. The hepatitis B virus HBx protein is a dual specificity cytoplasmic activator of Ras and nuclear activator of transcription factors. *Embo j,* 14**,** 4747-57.

DRYDEN, K. A., WIELAND, S. F., WHITTEN-BAUER, C., GERIN, J. L., CHISARI, F. V. & YEAGER, M. 2006. Native hepatitis B virions and capsids visualized by electron cryomicroscopy. *Mol Cell,* 22**,** 843-50.

DUDA, D. M., BORG, L. A., SCOTT, D. C., HUNT, H. W., HAMMEL, M. & SCHULMAN, B. A. 2008. Structural insights into NEDD8 activation of cullin-RING ligases: conformational control of conjugation. *Cell,* 134**,** 995-1006.

DURANTEL, D. & ZOULIM, F. 2016. New antiviral targets for innovative treatment concepts for hepatitis B virus and hepatitis delta virus. *J Hepatol,* 64**,** S117-S131.

ECKHARDT, S. G., MILICH, D. R. & MCLACHLAN, A. 1991. Hepatitis B virus core antigen has two nuclear localization sequences in the arginine-rich carboxyl terminus. *J Virol,* 65**,** 575-82.

ELMORE, L. W., HANCOCK, A. R., CHANG, S. F., WANG, X. W., CHANG, S., CALLAHAN, C. P., GELLER, D. A., WILL, H. & HARRIS, C. C. 1997. Hepatitis B virus X protein and p53 tumor suppressor interactions in the modulation of apoptosis. *Proc Natl Acad Sci U S A,* 94**,** 14707-12.

EMBADE, N., FERNANDEZ-RAMOS, D., VARELA-REY, M., BERAZA, N., SINI, M., GUTIERREZ DE JUAN, V., WOODHOO, A., MARTINEZ-LOPEZ, N., RODRIGUEZ-IRURETAGOYENA, B., BUSTAMANTE, F. J., DE LA HOZ, A. B., CARRACEDO, A., XIRODIMAS, D. P., RODRIGUEZ, M. S., LU, S. C., MATO, J. M. & MARTINEZ-CHANTAR, M. L. 2012. Murine double minute 2 regulates Hu antigen R stability in human liver and colon cancer through NEDDylation. *Hepatology,* 55**,** 1237-48.

ENCHEV, R. I., SCHULMAN, B. A. & PETER, M. 2015. Protein neddylation: beyond cullin-RING ligases. *Nat Rev Mol Cell Biol,* 16**,** 30-44.

ENGELKE, M., MILLS, K., SEITZ, S., SIMON, P., GRIPON, P., SCHNOLZER, M. & URBAN, S. 2006. Characterization of a hepatitis B and hepatitis delta virus receptor binding site. *Hepatology,* 43**,** 750-60.

ESSER, K., LUCIFORA, J., WETTENGEL, J., SINGETHAN, K., GLINZER, A., ZERNECKE, A. & PROTZER, U. 2018. Lipase inhibitor orlistat prevents hepatitis B virus infection by targeting an early step in the virus life cycle. *Antiviral Res,* 151**,** 4-7.

FAVRE, M., BREITBURD, F., CROISSANT, O. & ORTH, G. 1977. Chromatin-like structures obtained after alkaline disruption of bovine and human papillomaviruses. *J Virol,* 21**,** 1205-9.

FELD, J. J., COLLEDGE, D., SOZZI, V., EDWARDS, R., LITTLEJOHN, M. & LOCARNINI, S. A. 2007. The phenylpropenamide derivative AT-130 blocks HBV replication at the level of viral RNA packaging. *Antiviral Res,* 76**,** 168-77.

FERNS, R. B., NASTOULI, E. & GARSON, J. A. 2012. Quantitation of hepatitis delta virus using a single-step internally controlled real-time RT-qPCR and a full-length genomic RNA calibration standard. *J Virol Methods,* 179**,** 189-94.

FLETCHER, S. P. & DELANEY, W. E. T. 2013. New therapeutic targets and drugs for the treatment of chronic hepatitis B. *Semin Liver Dis,* 33**,** 130-7.

FORGUES, M., MARROGI, A. J., SPILLARE, E. A., WU, C. G., YANG, Q., YOSHIDA, M. & WANG, X. W. 2001. Interaction of the hepatitis B virus X protein with the Crm1-dependent nuclear export pathway. *J Biol Chem,* 276**,** 22797-803.

FUNG, J., LAI, C. L., SETO, W. K. & YUEN, M. F. 2011. Nucleoside/nucleotide analogues in the treatment of chronic hepatitis B. *J Antimicrob Chemother,* 66**,** 2715-25.

GAO, B., DUAN, Z., XU, W. & XIONG, S. 2009. Tripartite motif-containing 22 inhibits the activity of hepatitis B virus core promoter, which is dependent on nuclear-located RING domain. *Hepatology,* 50**,** 424-33.

GARCIA, P. D., OU, J. H., RUTTER, W. J. & WALTER, P. 1988. Targeting of the hepatitis B virus precore protein to the endoplasmic reticulum membrane: after signal peptide cleavage translocation can be aborted and the product released into the cytoplasm. *J Cell Biol,* 106**,** 1093-104.

GAREAU, J. R. & LIMA, C. D. 2010. The SUMO pathway: emerging mechanisms that shape specificity, conjugation and recognition. *Nat Rev Mol Cell Biol,* 11**,** 861-71.

GEARHART, T. L. & BOUCHARD, M. J. 2010. The hepatitis B virus X protein modulates hepatocyte proliferation pathways to stimulate viral replication. *J Virol,* 84**,** 2675-86.

GENG, X., HARRY, B. L., ZHOU, Q., SKEEN-GAAR, R. R., GE, X., LEE, E. S., MITANI, S. & XUE, D. 2012a. Hepatitis B virus X protein targets the Bcl-2 protein CED-9 to induce intracellular Ca2+ increase and cell death in Caenorhabditis elegans. *Proc Natl Acad Sci U S A,* 109**,** 18465-70.

GENG, X., HUANG, C., QIN, Y., MCCOMBS, J. E., YUAN, Q., HARRY, B. L., PALMER, A. E., XIA, N. S. & XUE, D. 2012b. Hepatitis B virus X protein targets Bcl-2 proteins to increase intracellular calcium, required for virus replication and cell death induction. *Proc Natl Acad Sci U S A,* 109**,** 18471-6.

GERLICH, W. H. & ROBINSON, W. S. 1980. Hepatitis B virus contains protein attached to the 5' terminus of its complete DNA strand. *Cell,* 21**,** 801-9.

GISH, R. G., GIVEN, B. D., LAI, C. L., LOCARNINI, S. A., LAU, J. Y., LEWIS, D. L. & SCHLUEP, T. 2015. Chronic hepatitis B: Virology, natural history, current management and a glimpse at future opportunities. *Antiviral Res,* 121**,** 47-58.

GLEBE, D., URBAN, S., KNOOP, E. V., CAG, N., KRASS, P., GRUN, S., BULAVAITE, A., SASNAUSKAS, K. & GERLICH, W. H. 2005. Mapping of the hepatitis B virus attachment site by use of infection-inhibiting preS1 lipopeptides and tupaia hepatocytes. *Gastroenterology,* 129**,** 234-45.

GORDIEN, E., ROSMORDUC, O., PELTEKIAN, C., GARREAU, F., BRECHOT, C. & KREMSDORF, D. 2001. Inhibition of hepatitis B virus replication by the interferon-inducible MxA protein. *J Virol,* 75**,** 2684-91.

GOTTE, M. & FELD, J. J. 2016. Direct-acting antiviral agents for hepatitis C: structural and mechanistic insights. *Nat Rev Gastroenterol Hepatol,* 13**,** 338-51.

GRIPON, P., CANNIE, I. & URBAN, S. 2005. Efficient inhibition of hepatitis B virus infection by acylated peptides derived from the large viral surface protein. *J Virol,* 79**,** 1613-22.

GRIPON, P., DIOT, C. & GUGUEN-GUILLOUZO, C. 1993. Reproducible high level infection of cultured adult human hepatocytes by hepatitis B virus: effect of polyethylene glycol on adsorption and penetration. *Virology,* 192**,** 534-40.

GRIPON, P., DIOT, C., THEZE, N., FOUREL, I., LOREAL, O., BRECHOT, C. & GUGUEN-GUILLOUZO, C. 1988. Hepatitis B virus infection of adult human hepatocytes cultured in the presence of dimethyl sulfoxide. *J Virol,* 62**,** 4136-43.

GRIPON, P., RUMIN, S., URBAN, S., LE SEYEC, J., GLAISE, D., CANNIE, I., GUYOMARD, C., LUCAS, J., TREPO, C. & GUGUEN-GUILLOUZO, C. 2002. Infection of a human hepatoma cell line by hepatitis B virus. *Proc Natl Acad Sci U S A,* 99**,** 15655-60.

GUO, F., ZHAO, Q., SHERAZ, M., CHENG, J., QI, Y., SU, Q., CUCONATI, A., WEI, L., DU, Y., LI, W., CHANG, J. & GUO, J. T. 2017. HBV core protein allosteric modulators differentially alter cccDNA biosynthesis from de novo infection and intracellular amplification pathways. *PLoS Pathog,* 13**,** e1006658.

GUO, L., WANG, X., REN, L., ZENG, M., WANG, S., WENG, Y., TANG, Z., WANG, X., TANG, Y., HU, H., LI, M., ZHANG, C. & LIU, C. 2014. HBx affects CUL4-DDB1 function in both positive and negative manners. *Biochem Biophys Res Commun,* 450**,** 1492-7.

GUO, W., CHEN, M., YEN, T. S. & OU, J. H. 1993. Hepatocyte-specific expression of the hepatitis B virus core promoter depends on both positive and negative regulation. *Mol Cell Biol,* 13**,** 443-8.

HADZIYANNIS, S. J., TASSOPOULOS, N. C., HEATHCOTE, E. J., CHANG, T. T., KITIS, G., RIZZETTO, M., MARCELLIN, P., LIM, S. G., GOODMAN, Z., MA, J., BROSGART, C. L., BORROTO-ESODA, K., ARTERBURN, S. & CHUCK, S. L. 2006. Long-term therapy with adefovir dipivoxil for HBeAg-negative chronic hepatitis B for up to 5 years. *Gastroenterology,* 131**,** 1743-51.

HAGENBUCH, B. & MEIER, P. J. 1994. Molecular cloning, chromosomal localization, and functional characterization of a human liver Na+/bile acid cotransporter. *J Clin Invest,* 93**,** 1326-31.

HARADA, K., NISHITSUJI, H., UJINO, S. & SHIMOTOHNO, K. 2017. Identification of KX2-391 as an inhibitor of HBV transcription by a recombinant HBV-based screening assay. *Antiviral Res,* 144**,** 138-146.

HARTMANN-STUHLER, C. & PRANGE, R. 2001. Hepatitis B virus large envelope protein interacts with gamma2-adaptin, a clathrin adaptor-related protein. *J Virol,* 75**,** 5343-51.

HEATHCOTE, E. J., MARCELLIN, P., BUTI, M., GANE, E., DE MAN, R. A., KRASTEV, Z., GERMANIDIS, G., LEE, S. S., FLISIAK, R., KAITA, K., MANNS, M., KOTZEV, I., TCHERNEV, K., BUGGISCH, P., WEILERT, F., KURDAS, O. O., SHIFFMAN, M. L., TRINH, H., GUREL, S., SNOW-LAMPART, A., BORROTO-ESODA, K., MONDOU, E., ANDERSON, J., SORBEL, J. & ROUSSEAU, F. 2011. Three-year efficacy and safety of tenofovir disoproxil fumarate treatment for chronic hepatitis B. *Gastroenterology,* 140**,** 132-43.

HEERMANN, K. H., GOLDMANN, U., SCHWARTZ, W., SEYFFARTH, T., BAUMGARTEN, H. & GERLICH, W. H. 1984. Large surface proteins of hepatitis B virus containing the pre-s sequence. *J Virol,* 52**,** 396-402.

HEERMANN, K. H., KRUSE, F., SEIFER, M. & GERLICH, W. H. 1987. Immunogenicity of the gene S and Pre-S domains in hepatitis B virions and HBsAg filaments. *Intervirology,* 28**,** 14-25.

HENKLER, F., HOARE, J., WASEEM, N., GOLDIN, R. D., MCGARVEY, M. J., KOSHY, R. & KING, I. A. 2001. Intracellular localization of the hepatitis B virus HBx protein. *J Gen Virol,* 82**,** 871-82.

HIRSCH, R. C., LAVINE, J. E., CHANG, L. J., VARMUS, H. E. & GANEM, D. 1990. Polymerase gene products of hepatitis B viruses are required for genomic RNA packaging as wel as for reverse transcription. *Nature,* 344**,** 552-5.

HIRSCHMAN, S. Z., PRICE, P., GARFINKEL, E., CHRISTMAN, J. & ACS, G. 1980. Expression of cloned hepatitis B virus DNA in human cell cultures. *Proc Natl Acad Sci U S A,* 77**,** 5507-11.

HODGSON, A. J., HYSER, J. M., KEASLER, V. V., CANG, Y. & SLAGLE, B. L. 2012. Hepatitis B virus regulatory HBx protein binding to DDB1 is required but is not sufficient for maximal HBV replication. *Virology,* 426**,** 73-82.

HOFMANN, H., NORTON, T. D., SCHULTZ, M. L., POLSKY, S. B., SUNSERI, N. & LANDAU, N. R. 2013. Inhibition of CUL4A Neddylation causes a reversible block to SAMHD1-mediated restriction of HIV-1. *J Virol,* 87**,** 11741-50.

HORI, T., OSAKA, F., CHIBA, T., MIYAMOTO, C., OKABAYASHI, K., SHIMBARA, N., KATO, S. & TANAKA, K. 1999. Covalent modification of all members of human cullin family proteins by NEDD8. *Oncogene,* 18**,** 6829-34.

HU, Y., CHENG, X., CAO, F., HUANG, A. & TAVIS, J. E. 2013. beta-Thujaplicinol inhibits hepatitis B virus replication by blocking the viral ribonuclease H activity. *Antiviral Res,* 99**,** 221-9.

HUANG, D. T., AYRAULT, O., HUNT, H. W., TAHERBHOY, A. M., DUDA, D. M., SCOTT, D. C., BORG, L. A., NEALE, G., MURRAY, P. J., ROUSSEL, M. F. & SCHULMAN, B. A. 2009. E2-RING expansion of the NEDD8 cascade confers specificity to cullin modification. *Mol Cell,* 33**,** 483-95.

HUANG, D. T., HUNT, H. W., ZHUANG, M., OHI, M. D., HOLTON, J. M. & SCHULMAN, B. A. 2007. Basis for a ubiquitin-like protein thioester switch toggling E1-E2 affinity. *Nature,* 445**,** 394-8.

HUANG, D. T., PAYDAR, A., ZHUANG, M., WADDELL, M. B., HOLTON, J. M. & SCHULMAN, B. A. 2005. Structural basis for recruitment of Ubc12 by an E2 binding domain in NEDD8's E1. *Mol Cell,* 17**,** 341-50.

HUANG, M. J. & SUMMERS, J. 1991. Infection initiated by the RNA pregenome of a DNA virus. *J Virol,* 65**,** 5435-9.

HUOVILA, A. P., EDER, A. M. & FULLER, S. D. 1992. Hepatitis B surface antigen assembles in a post-ER, pre-Golgi compartment. *J Cell Biol,* 118**,** 1305-20.

JANSSEN, H. L., VAN ZONNEVELD, M., SENTURK, H., ZEUZEM, S., AKARCA, U. S., CAKALOGLU, Y., SIMON, C., SO, T. M., GERKEN, G., DE MAN, R. A., NIESTERS, H. G., ZONDERVAN, P., HANSEN, B. & SCHALM, S. W. 2005. Pegylated interferon alfa-2b alone or in combination with lamivudine for HBeAg-positive chronic hepatitis B: a randomised trial. *Lancet,* 365**,** 123-9.

JIANG, T., LIU, M., WU, J. & SHI, Y. 2016. Structural and biochemical analysis of Bcl-2 interaction with the hepatitis B virus protein HBx. *Proc Natl Acad Sci U S A,* 113**,** 2074-9.

JILBERT, A. R., FREIMAN, J. S., GOWANS, E. J., HOLMES, M., COSSART, Y. E. & BURRELL, C. J. 1987. Duck hepatitis B virus DNA in liver, spleen, and pancreas: analysis by in situ and Southern blot hybridization. *Virology,* 158**,** 330-8.

JOST, S., TURELLI, P., MANGEAT, B., PROTZER, U. & TRONO, D. 2007. Induction of antiviral cytidine deaminases does not explain the inhibition of hepatitis B virus replication by interferons. *J Virol,* 81**,** 10588-96.

KAJINO, K., JILBERT, A. R., SAPUTELLI, J., ALDRICH, C. E., CULLEN, J. & MASON, W. S. 1994. Woodchuck hepatitis virus infections: very rapid recovery after a prolonged viremia and infection of virtually every hepatocyte. *J Virol,* 68**,** 5792-803.

KAMITANI, T., KITO, K., NGUYEN, H. P. & YEH, E. T. 1997. Characterization of NEDD8, a developmentally down-regulated ubiquitin-like protein. *J Biol Chem,* 272**,** 28557-62.

KANEKO, S., KAKINUMA, S., ASAHINA, Y., KAMIYA, A., MIYOSHI, M., TSUNODA, T., NITTA, S., ASANO, Y., NAGATA, H., OTANI, S., KAWAI-KITAHATA, F., MURAKAWA, M., ITSUI, Y., NAKAGAWA, M., AZUMA, S., NAKAUCHI, H., NISHITSUJI, H., UJINO, S., SHIMOTOHNO, K., IWAMOTO, M., WATASHI, K., WAKITA, T. & WATANABE, M. 2016. Human induced pluripotent stem cell-derived hepatic cell lines as a new model for host interaction with hepatitis B virus. *Sci Rep,* 6**,** 29358.

KANN, M., SODEIK, B., VLACHOU, A., GERLICH, W. H. & HELENIUS, A. 1999. Phosphorylation-dependent binding of hepatitis B virus core particles to the nuclear pore complex. *J Cell Biol,* 145**,** 45-55.

KAPOOR, D., GUPTAN, R. C., WAKIL, S. M., KAZIM, S. N., KAUL, R., AGARWAL, S. R., RAISUDDIN, S., HASNAIN, S. E. & SARIN, S. K. 2000. Beneficial effects of lamivudine in hepatitis B virus-related decompensated cirrhosis. *J Hepatol,* 33**,** 308-12.

KATEN, S. P., TAN, Z., CHIRAPU, S. R., FINN, M. G. & ZLOTNICK, A. 2013. Assembly-directed antivirals differentially bind quasiequivalent pockets to modify hepatitis B virus capsid tertiary and quaternary structure. *Structure,* 21**,** 1406-16.

KING, R. W., LADNER, S. K., MILLER, T. J., ZAIFERT, K., PERNI, R. B., CONWAY, S. C. & OTTO, M. J. 1998. Inhibition of human hepatitis B virus replication by AT-61, a phenylpropenamide derivative, alone and in combination with (-)beta-L-2',3'-dideoxy-3'-thiacytidine. *Antimicrob Agents Chemother,* 42**,** 3179-86.

KLUMPP, K., LAM, A. M., LUKACS, C., VOGEL, R., REN, S., ESPIRITU, C., BAYDO, R., ATKINS, K., ABENDROTH, J., LIAO, G., EFIMOV, A., HARTMAN, G. & FLORES, O. A. 2015. High-resolution crystal structure of a hepatitis B virus replication inhibitor bound to the viral core protein. *Proc Natl Acad Sci U S A,* 112**,** 15196-201.

KLUMPP, K., SHIMADA, T., ALLWEISS, L., VOLZ, T., LUTGEHETMANN, M., HARTMAN, G., FLORES, O. A., LAM, A. M. & DANDRI, M. 2018. Efficacy of NVR 3-778, Alone and In Combination With Pegylated Interferon, vs Entecavir In uPA/SCID Mice With Humanized Livers and HBV Infection. *Gastroenterology,* 154**,** 652-662 e8.

KOCK, J., NASSAL, M., MACNELLY, S., BAUMERT, T. F., BLUM, H. E. & VON WEIZSACKER, F. 2001. Efficient infection of primary tupaia hepatocytes with purified human and woolly monkey hepatitis B virus. *J Virol,* 75**,** 5084-9.

KOCK, J., ROSLER, C., ZHANG, J. J., BLUM, H. E., NASSAL, M. & THOMA, C. 2010. Generation of covalently closed circular DNA of hepatitis B viruses via intracellular recycling is regulated in a virus specific manner. *PLoS Pathog,* 6**,** e1001082.

KONIG, A., YANG, J., JO, E., PARK, K. H. P., KIM, H., THAN, T. T., SONG, X., QI, X., DAI, X., PARK, S., SHUM, D., RYU, W. S., KIM, J. H., YOON, S. K., PARK, J. Y., AHN, S. H., HAN, K. H., GERLICH, W. H. & WINDISCH, M. P. 2019. Efficient long-term amplification of hepatitis B virus isolates after infection of slow proliferating HepG2-NTCP cells. *J Hepatol,* 71**,** 289-300.

KONIGER, C., WINGERT, I., MARSMANN, M., ROSLER, C., BECK, J. & NASSAL, M. 2014. Involvement of the host DNA-repair enzyme TDP2 in formation of the covalently closed circular DNA persistence reservoir of hepatitis B viruses. *Proc Natl Acad Sci U S A,* 111**,** E4244-53.

KUMAR, M., JUNG, S. Y., HODGSON, A. J., MADDEN, C. R., QIN, J. & SLAGLE, B. L. 2011. Hepatitis B virus regulatory HBx protein binds to adaptor protein IPS-1 and inhibits the activation of beta interferon. *J Virol,* 85**,** 987-95.

KUMAR, V., JAYASURYAN, N. & KUMAR, R. 1996. A truncated mutant (residues 58-140) of the hepatitis B virus X protein retains transactivation function. *Proc Natl Acad Sci U S A,* 93**,** 5647-52.

LADNER, S. K., OTTO, M. J., BARKER, C. S., ZAIFERT, K., WANG, G. H., GUO, J. T., SEEGER, C. & KING, R. W. 1997. Inducible expression of human hepatitis B virus (HBV) in stably transfected hepatoblastoma cells: a novel system for screening potential inhibitors of HBV replication. *Antimicrob Agents Chemother,* 41**,** 1715-20.

LAHLALI, T., BERKE, J. M., VERGAUWEN, K., FOCA, A., VANDYCK, K., PAUWELS, F., ZOULIM, F. & DURANTEL, D. 2018. Novel Potent Capsid Assembly Modulators Regulate Multiple Steps of the Hepatitis B Virus Life Cycle. *Antimicrob Agents Chemother,* 62.

LAI, C. L., CHIEN, R. N., LEUNG, N. W., CHANG, T. T., GUAN, R., TAI, D. I., NG, K. Y., WU, P. C., DENT, J. C., BARBER, J., STEPHENSON, S. L. & GRAY, D. F. 1998. A one-year trial of lamivudine for chronic hepatitis B. Asia Hepatitis Lamivudine Study Group. *N Engl J Med,* 339**,** 61-8.

LAI, C. L., GANE, E., LIAW, Y. F., HSU, C. W., THONGSAWAT, S., WANG, Y., CHEN, Y., HEATHCOTE, E. J., RASENACK, J., BZOWEJ, N., NAOUMOV, N. V., DI BISCEGLIE, A. M., ZEUZEM, S., MOON, Y. M., GOODMAN, Z., CHAO, G., CONSTANCE, B. F. & BROWN, N. A. 2007. Telbivudine versus lamivudine in patients with chronic hepatitis B. *N Engl J Med,* 357**,** 2576-88.

LAI, C. L., RATZIU, V., YUEN, M. F. & POYNARD, T. 2003. Viral hepatitis B. *Lancet,* 362**,** 2089-94.
LAI, C. L., WONG, D., IP, P., KOPANISZEN, M., SETO, W. K., FUNG, J., HUANG, F. Y., LEE, B., CULLARO, G., CHONG, C. K., WU, R., CHENG, C., YUEN, J., NGAI, V. & YUEN, M. F. 2017. Reduction of covalently closed circular DNA with long-term nucleos(t)ide analogue treatment in chronic hepatitis B. *J Hepatol,* 66**,** 275-281.

LAMPERTICO, P., VIGANO, M., MANENTI, E., IAVARONE, M., LUNGHI, G. & COLOMBO, M. 2005. Adefovir rapidly suppresses hepatitis B in HBeAg-negative patients developing genotypic resistance to lamivudine. *Hepatology,* 42**,** 1414-9.

LAN, Y. T., LI, J., LIAO, W. & OU, J. 1999. Roles of the three major phosphorylation sites of hepatitis B virus core protein in viral replication. *Virology,* 259**,** 342-8.

LANFORD, R. E., NOTVALL, L., LEE, H. & BEAMES, B. 1997. Transcomplementation of nucleotide priming and reverse transcription between independently expressed TP and RT domains of the hepatitis B virus reverse transcriptase. *J Virol,* 71**,** 2996-3004.

LANGLEY, D. R., WALSH, A. W., BALDICK, C. J., EGGERS, B. J., ROSE, R. E., LEVINE, S. M., KAPUR, A. J., COLONNO, R. J. & TENNEY, D. J. 2007. Inhibition of hepatitis B virus polymerase by entecavir. *J Virol,* 81**,** 3992-4001.

LARAS, A., KOSKINAS, J., DIMOU, E., KOSTAMENA, A. & HADZIYANNIS, S. J. 2006. Intrahepatic levels and replicative activity of covalently closed circular hepatitis B virus DNA in chronically infected patients. *Hepatology,* 44**,** 694-702.

LAVON, N., YANUKA, O. & BENVENISTY, N. 2004. Differentiation and isolation of hepatic-like cells from human embryonic stem cells. *Differentiation,* 72**,** 230-8.

LE DUFF, Y., BLANCHET, M. & SUREAU, C. 2009. The pre-S1 and antigenic loop infectivity determinants of the hepatitis B virus envelope proteins are functionally independent. *J Virol,* 83**,** 12443-51.

LE SEYEC, J., CHOUTEAU, P., CANNIE, I., GUGUEN-GUILLOUZO, C. & GRIPON, P. 1999. Infection process of the hepatitis B virus depends on the presence of a defined sequence in the pre-S1 domain. *J Virol,* 73**,** 2052-7.

LE-TRILLING, V. T., MEGGER, D. A., KATSCHINSKI, B., LANDSBERG, C. D., RUCKBORN, M. U., TAO, S., KRAWCZYK, A., BAYER, W., DREXLER, I., TENBUSCH, M., SITEK, B. & TRILLING, M. 2016. Broad and potent antiviral activity of the NAE inhibitor MLN4924. *Sci Rep,* 6**,** 19977.

LEMPP, F. A., MUTZ, P., LIPPS, C., WIRTH, D., BARTENSCHLAGER, R. & URBAN, S. 2016a. Evidence that hepatitis B virus replication in mouse cells is limited by the lack of a host cell dependency factor. *J Hepatol,* 64**,** 556-64.

LEMPP, F. A., QU, B., WANG, Y. X. & URBAN, S. 2016b. Hepatitis B Virus Infection of a Mouse Hepatic Cell Line Reconstituted with Human Sodium Taurocholate Cotransporting Polypeptide. *J Virol,* 90**,** 4827-4831.

LEMPP, F. A. & URBAN, S. 2014. Inhibitors of hepatitis B virus attachment and entry. *Intervirology,* 57**,** 151-7.

LEMPP, F. A., WIEDTKE, E., QU, B., ROQUES, P., CHEMIN, I., VONDRAN, F. W. R., LE GRAND, R., GRIMM, D. & URBAN, S. 2017. Sodium taurocholate cotransporting polypeptide is the limiting host factor of hepatitis B virus infection in macaque and pig hepatocytes. *Hepatology,* 66**,** 703-716.

LENHOFF, R. J. & SUMMERS, J. 1994. Coordinate regulation of replication and virus assembly by the large envelope protein of an avian hepadnavirus. *J Virol,* 68**,** 4565-71.

LEUPIN, O., BONTRON, S., SCHAEFFER, C. & STRUBIN, M. 2005. Hepatitis B virus X protein stimulates viral genome replication via a DDB1-dependent pathway distinct from that leading to cell death. *J Virol,* 79**,** 4238-45.

LEUPIN, O., BONTRON, S. & STRUBIN, M. 2003. Hepatitis B virus X protein and simian virus 5 V protein exhibit similar UV-DDB1 binding properties to mediate distinct activities. *J Virol,* 77**,** 6274-83.

LEVRERO, M., POLLICINO, T., PETERSEN, J., BELLONI, L., RAIMONDO, G. & DANDRI, M. 2009. Control of cccDNA function in hepatitis B virus infection. *J Hepatol,* 51**,** 581-92.

LEWELLYN, E. B. & LOEB, D. D. 2011. The arginine clusters of the carboxy-terminal domain of the core protein of hepatitis B virus make pleiotropic contributions to genome replication. *J Virol,* 85**,** 1298-309.

LI, B., WANG, Y., SHEN, F., WU, M., LI, Y., FANG, Z., YE, J., WANG, L., GAO, L., YUAN, Z. & CHEN, J. 2018a. Identification of Retinoic Acid Receptor Agonists as Potent Hepatitis B Virus Inhibitors via a Drug Repurposing Screen. *Antimicrob Agents Chemother*.

LI, H. C., HUANG, E. Y., SU, P. Y., WU, S. Y., YANG, C. C., LIN, Y. S., CHANG, W. C. & SHIH, C. 2010a. Nuclear export and import of human hepatitis B virus capsid protein and particles. *PLoS Pathog,* 6**,** e1001162.

LI, J., LIN, S., CHEN, Q., PENG, L., ZHAI, J., LIU, Y. & YUAN, Z. 2010b. Inhibition of hepatitis B virus replication by MyD88 involves accelerated degradation of pregenomic RNA and nuclear retention of pre-S/S RNAs. *J Virol,* 84**,** 6387-99.

LI, J., ZONG, L., SUREAU, C., BARKER, L., WANDS, J. R. & TONG, S. 2016a. Unusual Features of Sodium Taurocholate Cotransporting Polypeptide as a Hepatitis B Virus Receptor. *J Virol,* 90**,** 8302-13.

LI, M., SOHN, J. A. & SEEGER, C. 2018b. Distribution of Hepatitis B Virus Nuclear DNA. *J Virol,* 92.

LI, N., ZHANG, L., CHEN, L., FENG, W., XU, Y., CHEN, F., LIU, X., CHEN, Z. & LIU, W. 2012. MxA inhibits hepatitis B virus replication by interaction with hepatitis B core antigen. *Hepatology,* 56**,** 803-11.

LI, S. K., HO, S. F., TSUI, K. W., FUNG, K. P. & WAYE, M. Y. 2008. Identification of functionally important amino acid residues in the mitochondria targeting sequence of hepatitis B virus X protein. *Virology,* 381**,** 81-8.

LI, T., ROBERT, E. I., VAN BREUGEL, P. C., STRUBIN, M. & ZHENG, N. 2010c. A promiscuous alpha-helical motif anchors viral hijackers and substrate receptors to the CUL4-DDB1 ubiquitin ligase machinery. *Nat Struct Mol Biol,* 17**,** 105-11.

LI, W., LI, M., LIAO, D., LU, X., GU, X., ZHANG, Q., ZHANG, Z. & LI, H. 2016b. Carboxyl-terminal truncated HBx contributes to invasion and metastasis via deregulating metastasis suppressors in hepatocellular carcinoma. *Oncotarget,* 7**,** 55110-55127.

LI, W. & URBAN, S. 2016. Entry of hepatitis B and hepatitis D virus into hepatocytes: Basic insights and clinical implications. *J Hepatol,* 64**,** S32-s40.

LI, Y., XIA, Y., HAN, M., CHEN, G., ZHANG, D., THASLER, W. E., PROTZER, U. & NING, Q. 2017. IFN-alpha-mediated Base Excision Repair Pathway Correlates with Antiviral Response Against Hepatitis B Virus Infection. *Sci Rep,* 7**,** 12715.

LIAO, W. & OU, J. H. 1995. Phosphorylation and nuclear localization of the hepatitis B virus core protein: significance of serine in the three repeated SPRRR motifs. *J Virol,* 69**,** 1025-9.

LIAW, Y. F., SUNG, J. J., CHOW, W. C., FARRELL, G., LEE, C. Z., YUEN, H., TANWANDEE, T., TAO, Q. M., SHUE, K., KEENE, O. N., DIXON, J. S., GRAY, D. F. & SABBAT, J. 2004. Lamivudine for patients with chronic hepatitis B and advanced liver disease. *N Engl J Med,* 351**,** 1521-31.

LIEN, J. M., ALDRICH, C. E. & MASON, W. S. 1986. Evidence that a capped oligoribonucleotide is the primer for duck hepatitis B virus plus-strand DNA synthesis. *J Virol,* 57**,** 229-36.

LIU, F., CAMPAGNA, M., QI, Y., ZHAO, X., GUO, F., XU, C., LI, S., LI, W., BLOCK, T. M., CHANG, J. & GUO, J. T. 2013. Alpha-interferon suppresses hepadnavirus transcription by altering epigenetic modification of cccDNA minichromosomes. *PLoS Pathog,* 9**,** e1003613.

LIU, N., ZHANG, J., YANG, X., JIAO, T., ZHAO, X., LI, W., ZHU, J., YANG, P., JIN, J., PENG, J., LI, Z. & YE, X. 2017. HDM2 Promotes NEDDylation of Hepatitis B Virus HBx To Enhance Its Stability and Function. *J Virol,* 91.

LIU, Y., LI, J., CHEN, J., LI, Y., WANG, W., DU, X., SONG, W., ZHANG, W., LIN, L. & YUAN, Z. 2015. Hepatitis B virus polymerase disrupts K63-linked ubiquitination of STING to block innate cytosolic DNA-sensing pathways. *J Virol,* 89**,** 2287-300.

LIVINGSTON, C. M., RAMAKRISHNAN, D., STRUBIN, M., FLETCHER, S. P. & BERAN, R. K. 2017. Identifying and Characterizing Interplay between Hepatitis B Virus X Protein and Smc5/6. *Viruses,* 9.

LIZZANO, R. A., YANG, B., CLIPPINGER, A. J. & BOUCHARD, M. J. 2011. The C-terminal region of the hepatitis B virus X protein is essential for its stability and function. *Virus Res,* 155**,** 231-9.

LO, A. O. & WONG, G. L. 2014. Current developments in nucleoside/nucleotide analogues for hepatitis B. *Expert Rev Gastroenterol Hepatol,* 8**,** 607-22.

LOMONOSOVA, E., DAW, J., GARIMALLAPRABHAKARAN, A. K., AGYEMANG, N. B., ASHANI, Y., MURELLI, R. P. & TAVIS, J. E. 2017. Efficacy and cytotoxicity in cell culture of novel alpha-hydroxytropolone inhibitors of hepatitis B virus ribonuclease H. *Antiviral Res,* 144**,** 164-172.

LONG, Q., YAN, R., HU, J., CAI, D., MITRA, B., KIM, E. S., MARCHETTI, A., ZHANG, H., WANG, S., LIU, Y., HUANG, A. & GUO, H. 2017. The role of host DNA ligases in hepadnavirus covalently closed circular DNA formation. *PLoS Pathog,* 13**,** e1006784.

LOPEZ-CABRERA, M., LETOVSKY, J., HU, K. Q. & SIDDIQUI, A. 1990. Multiple liver-specific factors bind to the hepatitis B virus core/pregenomic promoter: trans-activation and repression by CCAAT/enhancer binding protein. *Proc Natl Acad Sci U S A,* 87**,** 5069-73.

LU, G., LOMONOSOVA, E., CHENG, X., MORAN, E. A., MEYERS, M. J., LE GRICE, S. F., THOMAS, C. J., JIANG, J. K., MECK, C., HIRSCH, D. R., D'ERASMO, M. P., SUYABATMAZ, D. M., MURELLI, R. P. & TAVIS, J. E. 2015. Hydroxylated tropolones inhibit hepatitis B virus replication by blocking viral ribonuclease H activity. *Antimicrob Agents Chemother,* 59**,** 1070-9.

LUCIFORA, J., ARZBERGER, S., DURANTEL, D., BELLONI, L., STRUBIN, M., LEVRERO, M., ZOULIM, F., HANTZ, O. & PROTZER, U. 2011. Hepatitis B virus X protein is essential to initiate and maintain virus replication after infection. *J Hepatol,* 55**,** 996-1003.

LUCIFORA, J., ESSER, K. & PROTZER, U. 2013. Ezetimibe blocks hepatitis B virus infection after virus uptake into hepatocytes. *Antiviral Res,* 97**,** 195-7.

LUCIFORA, J., XIA, Y., REISINGER, F., ZHANG, K., STADLER, D., CHENG, X., SPRINZL, M. F., KOPPENSTEINER, H., MAKOWSKA, Z., VOLZ, T., REMOUCHAMPS, C., CHOU, W. M., THASLER, W. E., HUSER, N., DURANTEL, D., LIANG, T. J., MUNK, C., HEIM, M. H., BROWNING, J. L.,

DEJARDIN, E., DANDRI, M., SCHINDLER, M., HEIKENWALDER, M. & PROTZER, U. 2014. Specific and nonhepatotoxic degradation of nuclear hepatitis B virus cccDNA. *Science,* 343**,** 1221-8.

LUO, N., CAI, Y., ZHANG, J., TANG, W., SLAGLE, B. L., WU, X. & HE, S. 2012. The C-terminal region of the hepatitis B virus X protein is required for its stimulation of HBV replication in primary mouse hepatocytes. *Virus Res,* 165**,** 170-8.

LUTGEHETMANN, M., MANCKE, L. V., VOLZ, T., HELBIG, M., ALLWEISS, L., BORNSCHEUER, T., POLLOK, J. M., LOHSE, A. W., PETERSEN, J., URBAN, S. & DANDRI, M. 2012. Humanized chimeric uPA mouse model for the study of hepatitis B and D virus interactions and preclinical drug evaluation. *Hepatology,* 55**,** 685-94.

LUTGEHETMANN, M., VOLZ, T., KOPKE, A., BROJA, T., TIGGES, E., LOHSE, A. W., FUCHS, E., MURRAY, J. M., PETERSEN, J. & DANDRI, M. 2010. In vivo proliferation of hepadnavirus-infected hepatocytes induces loss of covalently closed circular DNA in mice. *Hepatology,* 52**,** 16-24.

LUTWICK, L. I. & ROBINSON, W. S. 1977. DNA synthesized in the hepatitis B Dane particle DNA polymerase reaction. *J Virol,* 21**,** 96-104.

MAC, C. F. 1946. Homologous serum hepatitis. *Proc R Soc Med,* 39**,** 655-7.

MAO, R., NIE, H., CAI, D., ZHANG, J., LIU, H., YAN, R., CUCONATI, A., BLOCK, T. M., GUO, J. T. & GUO, H. 2013. Inhibition of hepatitis B virus replication by the host zinc finger antiviral protein. *PLoS Pathog,* 9**,** e1003494.

MARCELLIN, P., CHANG, T. T., LIM, S. G., SIEVERT, W., TONG, M., ARTERBURN, S., BORROTO-ESODA, K., FREDERICK, D. & ROUSSEAU, F. 2008. Long-term efficacy and safety of adefovir dipivoxil for the treatment of hepatitis B e antigen-positive chronic hepatitis B. *Hepatology,* 48**,** 750-8.

MARCELLIN, P., CHANG, T. T., LIM, S. G., TONG, M. J., SIEVERT, W., SHIFFMAN, M. L., JEFFERS, L., GOODMAN, Z., WULFSOHN, M. S., XIONG, S., FRY, J. & BROSGART, C. L. 2003. Adefovir dipivoxil for the treatment of hepatitis B e antigen-positive chronic hepatitis B. *N Engl J Med,* 348**,** 808-16.

MARTIN-LLUESMA, S., SCHAEFFER, C., ROBERT, E. I., VAN BREUGEL, P. C., LEUPIN, O., HANTZ, O. & STRUBIN, M. 2008. Hepatitis B virus X protein affects S phase progression leading to chromosome segregation defects by binding to damaged DNA binding protein 1. *Hepatology,* 48**,** 1467-76.

MASON, W. S., ALDRICH, C., SUMMERS, J. & TAYLOR, J. M. 1982. Asymmetric replication of duck hepatitis B virus DNA in liver cells: Free minus-strand DNA. *Proc Natl Acad Sci U S A,* 79**,** 3997-4001.

MCCLAIN, S. L., CLIPPINGER, A. J., LIZZANO, R. & BOUCHARD, M. J. 2007. Hepatitis B virus replication is associated with an HBx-dependent mitochondrion-regulated increase in cytosolic calcium levels. *J Virol,* 81**,** 12061-5.

MEIER, A., MEHRLE, S., WEISS, T. S., MIER, W. & URBAN, S. 2013. Myristoylated PreS1-domain of the hepatitis B virus L-protein mediates specific binding to differentiated hepatocytes. *Hepatology,* 58**,** 31-42.

MEIER, P., SCOUGALL, C. A., WILL, H., BURRELL, C. J. & JILBERT, A. R. 2003. A duck hepatitis B virus strain with a knockout mutation in the putative X ORF shows similar infectivity and in vivo growth characteristics to wild-type virus. *Virology,* 317**,** 291-8.

MILLER, R. H. & ROBINSON, W. S. 1984. Hepatitis B virus DNA forms in nuclear and cytoplasmic fractions of infected human liver. *Virology,* 137**,** 390-9.

MINOR, M. M. & SLAGLE, B. L. 2014. Hepatitis B virus HBx protein interactions with the ubiquitin proteasome system. *Viruses,* 6**,** 4683-702.

MIRANDA, M. & SORKIN, A. 2007. Regulation of receptors and transporters by ubiquitination: new insights into surprisingly similar mechanisms. *Mol Interv,* 7**,** 157-67.

MISRA, K. P., MUKHERJI, A. & KUMAR, V. 2004. The conserved amino-terminal region (amino acids 1-20) of the hepatitis B virus X protein shows a transrepression function. *Virus Res,* 105**,** 157-65.

MOLNAR-KIMBER, K. L., SUMMERS, J., TAYLOR, J. M. & MASON, W. S. 1983. Protein covalently bound to minus-strand DNA intermediates of duck hepatitis B virus. *J Virol,* 45**,** 165-72.

MOLNAR-KIMBER, K. L., SUMMERS, J. W. & MASON, W. S. 1984. Mapping of the cohesive overlap of duck hepatitis B virus DNA and of the site of initiation of reverse transcription. *J Virol,* 51**,** 181-91.

MUELLER, H., WILDUM, S., LUANGSAY, S., WALTHER, J., LOPEZ, A., TROPBERGER, P., OTTAVIANI, G., LU, W., PARROTT, N. J., ZHANG, J. D., SCHMUCKI, R., RACEK, T., HOFLACK, J. C., KUENG, E., POINT, F., ZHOU, X., STEINER, G., LUTGEHETMANN, M., RAPP, G., VOLZ, T., DANDRI, M., YANG, S., YOUNG, J. A. T. & JAVANBAKHT, H. 2018. A novel orally available small molecule that inhibits hepatitis B virus expression. *J Hepatol,* 68**,** 412-420.

MURAKAMI, S. 2001. Hepatitis B virus X protein: a multifunctional viral regulator. *J Gastroenterol,* 36**,** 651-60.

MURAKAMI, S., CHEONG, J. H. & KANEKO, S. 1994. Human hepatitis virus X gene encodes a regulatory domain that represses transactivation of X protein. *J Biol Chem,* 269**,** 15118-23.

MURPHY, C. M., XU, Y., LI, F., NIO, K., RESZKA-BLANCO, N., LI, X., WU, Y., YU, Y., XIONG, Y. & SU, L. 2016. Hepatitis B Virus X Protein Promotes Degradation of SMC5/6 to Enhance HBV Replication. *Cell Rep,* 16**,** 2846-2854.

NAG, A., DATTA, A., YOO, K., BHATTACHARYYA, D., CHAKRABORTTY, A., WANG, X., SLAGLE, B. L., COSTA, R. H. & RAYCHAUDHURI, P. 2001. DDB2 induces nuclear accumulation of the hepatitis B virus X protein independently of binding to DDB1. *J Virol,* 75**,** 10383-92.

NASSAL, M. 1992. The arginine-rich domain of the hepatitis B virus core protein is required for pregenome encapsidation and productive viral positive-strand DNA synthesis but not for virus assembly. *J Virol,* 66**,** 4107-16.

NASSAL, M. 2008. Hepatitis B viruses: reverse transcription a different way. *Virus Res,* 134**,** 235-49.

NASSAL, M. 2015. HBV cccDNA: viral persistence reservoir and key obstacle for a cure of chronic hepatitis B. *Gut,* 64**,** 1972-84.

NEWBOLD, J. E., XIN, H., TENCZA, M., SHERMAN, G., DEAN, J., BOWDEN, S. & LOCARNINI, S. 1995. The covalently closed duplex form of the hepadnavirus genome exists in situ as a heterogeneous population of viral minichromosomes. *J Virol,* 69**,** 3350-7.

NGUYEN, D. H., GUMMULURU, S. & HU, J. 2007. Deamination-independent inhibition of hepatitis B virus reverse transcription by APOBEC3G. *J Virol,* 81**,** 4465-72.

NGUYEN, D. H. & HU, J. 2008. Reverse transcriptase- and RNA packaging signal-dependent incorporation of APOBEC3G into hepatitis B virus nucleocapsids. *J Virol,* 82**,** 6852-61.

NI, Y., LEMPP, F. A., MEHRLE, S., NKONGOLO, S., KAUFMAN, C., FALTH, M., STINDT, J., KONIGER, C., NASSAL, M., KUBITZ, R., SULTMANN, H. & URBAN, S. 2014. Hepatitis B and D viruses exploit sodium taurocholate co-transporting polypeptide for species-specific entry into hepatocytes. *Gastroenterology,* 146**,** 1070-83.

NI, Y., SONNABEND, J., SEITZ, S. & URBAN, S. 2010. The pre-s2 domain of the hepatitis B virus is dispensable for infectivity but serves a spacer function for L-protein-connected virus assembly. *J Virol,* 84**,** 3879-88.

NI, Y. & URBAN, S. 2017. Stem cell-derived hepatocytes: A promising novel tool to study hepatitis B virus infection. *J Hepatol,* 66**,** 473-475.

NIU, C., LIVINGSTON, C. M., LI, L., BERAN, R. K., DAFFIS, S., RAMAKRISHNAN, D., BURDETTE, D., PEISER, L., SALAS, E., RAMOS, H., YU, M., CHENG, G., STRUBIN, M., DELANEY, W. I. & FLETCHER, S. P. 2017. The Smc5/6 Complex Restricts HBV when Localized to ND10 without Inducing an Innate Immune Response and Is Counteracted by the HBV X Protein Shortly after Infection. *PLoS One,* 12**,** e0169648.

NKONGOLO, S., NI, Y., LEMPP, F. A., KAUFMAN, C., LINDNER, T., ESSER-NOBIS, K., LOHMANN, V., MIER, W., MEHRLE, S. & URBAN, S. 2014. Cyclosporin A inhibits hepatitis B and hepatitis D virus entry by cyclophilin-independent interference with the NTCP receptor. *J Hepatol,* 60**,** 723-31.

NKONGOLO, S., NUSSBAUM, L., LEMPP, F. A., WODRICH, H., URBAN, S. & NI, Y. 2019. The retinoic acid receptor (RAR) alpha-specific agonist Am80 (tamibarotene) and other RAR agonists potently inhibit hepatitis B virus transcription from cccDNA. *Antiviral Res*.

NOGUCHI, C., ISHINO, H., TSUGE, M., FUJIMOTO, Y., IMAMURA, M., TAKAHASHI, S. & CHAYAMA, K. 2005. G to A hypermutation of hepatitis B virus. *Hepatology,* 41**,** 626-33.

OLSEN, S. K., CAPILI, A. D., LU, X., TAN, D. S. & LIMA, C. D. 2010. Active site remodelling accompanies thioester bond formation in the SUMO E1. *Nature,* 463**,** 906-12.

ORI, A. & SHAUL, Y. 1995. Hepatitis B virus enhancer binds and is activated by the Hepatocyte nuclear factor 3. *Virology,* 207**,** 98-106.

OU, J. H., LAUB, O. & RUTTER, W. J. 1986. Hepatitis B virus gene function: the precore region targets the core antigen to cellular membranes and causes the secretion of the e antigen. *Proc Natl Acad Sci U S A,* 83**,** 1578-82.

OU, J. H., YEH, C. T. & YEN, T. S. 1989. Transport of hepatitis B virus precore protein into the nucleus after cleavage of its signal peptide. *J Virol,* 63**,** 5238-43.

PARK, E. S., LEE, A. R., KIM, D. H., LEE, J. H., YOO, J. J., AHN, S. H., SIM, H., PARK, S., KANG, H. S., WON, J., HA, Y. N., SHIN, G. C., KWON, S. Y., PARK, Y. K., CHOI, B. S., LEE, Y. B., JEONG, N., AN, Y., JU, Y. S., YU, S. J., CHAE, H. B., YU, K. S., KIM, Y. J., YOON, J. H., ZOULIM, F. & KIM, K. H. 2019. Identification of a quadruple mutation that confers tenofovir resistance in chronic hepatitis B patients. *J Hepatol,* 70**,** 1093-1102.

PARK, I. H., BAEK, K. W., CHO, E. Y. & AHN, B. Y. 2011. PKR-dependent mechanisms of interferon-alpha for inhibiting hepatitis B virus replication. *Mol Cells,* 32**,** 167-72.

PATTERSON, S. J., GEORGE, J., STRASSER, S. I., LEE, A. U., SIEVERT, W., NICOLL, A. J., DESMOND, P. V., ROBERTS, S. K., LOCARNINI, S., BOWDEN, S. & ANGUS, P. W. 2011. Tenofovir disoproxil fumarate rescue therapy following failure of both lamivudine and adefovir dipivoxil in chronic hepatitis B. *Gut,* 60**,** 247-54.

PATZER, E. J., NAKAMURA, G. R. & YAFFE, A. 1984. Intracellular transport and secretion of hepatitis B surface antigen in mammalian cells. *J Virol,* 51**,** 346-53.

PERNI, R. B., CONWAY, S. C., LADNER, S. K., ZAIFERT, K., OTTO, M. J. & KING, R. W. 2000. Phenylpropenamide derivatives as inhibitors of hepatitis B virus replication. *Bioorg Med Chem Lett,* 10**,** 2687-90.

PERSING, D. H., VARMUS, H. E. & GANEM, D. 1987. The preS1 protein of hepatitis B virus is acylated at its amino terminus with myristic acid. *J Virol,* 61**,** 1672-7.

PETCU, D. J., ALDRICH, C. E., COATES, L., TAYLOR, J. M. & MASON, W. S. 1988. Suramin inhibits in vitro infection by duck hepatitis B virus, Rous sarcoma virus, and hepatitis delta virus. *Virology,* 167**,** 385-92.

PETERSEN, J., DANDRI, M., MIER, W., LUTGEHETMANN, M., VOLZ, T., VON WEIZSACKER, F., HABERKORN, U., FISCHER, L., POLLOK, J. M., ERBES, B., SEITZ, S. & URBAN, S. 2008. Prevention of hepatitis B virus infection in vivo by entry inhibitors derived from the large envelope protein. *Nat Biotechnol,* 26**,** 335-41.

POLARIS OBSERVATORY, C. 2018. Global prevalence, treatment, and prevention of hepatitis B virus infection in 2016: a modelling study. *Lancet Gastroenterol Hepatol,* 3**,** 383-403.

POLLICINO, T., BELLONI, L., RAFFA, G., PEDICONI, N., SQUADRITO, G., RAIMONDO, G. & LEVRERO, M. 2006. Hepatitis B virus replication is regulated by the acetylation status of hepatitis B virus cccDNA-bound H3 and H4 histones. *Gastroenterology,* 130**,** 823-37.

PRANGE, R. & STREECK, R. E. 1995. Novel transmembrane topology of the hepatitis B virus envelope proteins. *Embo j,* 14**,** 247-56.

PROPST, T., PROPST, A., LHOTTA, K., VOGEL, W. & KONIG, P. 1998. Reinforced intradermal hepatitis B vaccination in hemodialysis patients is superior in antibody response to intramuscular or subcutaneous vaccination. *Am J Kidney Dis,* 32**,** 1041-5.

QI, Y., GAO, Z., XU, G., PENG, B., LIU, C., YAN, H., YAO, Q., SUN, G., LIU, Y., TANG, D., SONG, Z., HE, W., SUN, Y., GUO, J. T. & LI, W. 2016. DNA Polymerase kappa Is a Key Cellular Factor for

the Formation of Covalently Closed Circular DNA of Hepatitis B Virus. *PLoS Pathog,* 12**,** e1005893.

QU, B., NI, Y., LEMPP, F. A., VONDRAN, F. W. R. & URBAN, S. 2018. T5 exonuclease hydrolysis of Hepatitis B Virus replicative intermediates allows reliable quantification and fast drug efficacy testing of covalently closed circular DNA by PCR. *J Virol*.

QUASDORFF, M. & PROTZER, U. 2010. Control of hepatitis B virus at the level of transcription. *J Viral Hepat,* 17**,** 527-36.

RABE, B., DELALEAU, M., BISCHOF, A., FOSS, M., SOMINSKAYA, I., PUMPENS, P., CAZENAVE, C., CASTROVIEJO, M. & KANN, M. 2009. Nuclear entry of hepatitis B virus capsids involves disintegration to protein dimers followed by nuclear reassociation to capsids. *PLoS Pathog,* 5**,** e1000563.

RABE, B., GLEBE, D. & KANN, M. 2006. Lipid-mediated introduction of hepatitis B virus capsids into nonsusceptible cells allows highly efficient replication and facilitates the study of early infection events. *J Virol,* 80**,** 5465-73.

RABE, B., VLACHOU, A., PANTE, N., HELENIUS, A. & KANN, M. 2003. Nuclear import of hepatitis B virus capsids and release of the viral genome. *Proc Natl Acad Sci U S A,* 100**,** 9849-54.

RADZIWILL, G., TUCKER, W. & SCHALLER, H. 1990. Mutational analysis of the hepatitis B virus P gene product: domain structure and RNase H activity. *J Virol,* 64**,** 613-20.

RAMAKRISHNAN, D., XING, W., BERAN, R. K., CHEMURU, S., ROHRS, H., NIEDZIELA-MAJKA, A., MARCHAND, B., MEHRA, U., ZABRANSKY, A., DOLEZAL, M., HUBALEK, M., PICHOVA, I., GROSS, M. L., KWON, H. J. & FLETCHER, S. P. 2019. Hepatitis B Virus X Protein Function Requires Zinc Binding. *J Virol,* 93.

RANEY, A. K., ZHANG, P. & MCLACHLAN, A. 1995. Regulation of transcription from the hepatitis B virus large surface antigen promoter by hepatocyte nuclear factor 3. *J Virol,* 69**,** 3265-72.

RAVID, T. & HOCHSTRASSER, M. 2008. Diversity of degradation signals in the ubiquitin-proteasome system. *Nat Rev Mol Cell Biol,* 9**,** 679-90.

REHERMANN, B., FERRARI, C., PASQUINELLI, C. & CHISARI, F. V. 1996. The hepatitis B virus persists for decades after patients' recovery from acute viral hepatitis despite active maintenance of a cytotoxic T-lymphocyte response. *Nat Med,* 2**,** 1104-8.

RESHETNYAK, V. I., KARLOVICH, T. I. & ILCHENKO, L. U. 2008. Hepatitis G virus. *World J Gastroenterol,* 14**,** 4725-34.

ROEHL, I., SEIFFERT, S., BRIKH, C., QUINET, J., JAMARD, C., DORFLER, N., LOCKRIDGE, J. A., COVA, L. & VAILLANT, A. 2017. Nucleic Acid Polymers with Accelerated Plasma and Tissue Clearance for Chronic Hepatitis B Therapy. *Mol Ther Nucleic Acids,* 8**,** 1-12.

ROST, M., MANN, S., LAMBERT, C., DORING, T., THOME, N. & PRANGE, R. 2006. Gamma-adaptin, a novel ubiquitin-interacting adaptor, and Nedd4 ubiquitin ligase control hepatitis B virus maturation. *J Biol Chem,* 281**,** 29297-308.

RUNKEL, L., FISCHER, M. & SCHALLER, H. 1993. Two-codon insertion mutations of the HBx define two separate regions necessary for its trans-activation function. *Virology,* 197**,** 529-36.

RUSSNAK, R. H. 1991. Regulation of polyadenylation in hepatitis B viruses: stimulation by the upstream activating signal PS1 is orientation-dependent, distance-independent, and additive. *Nucleic Acids Res,* 19**,** 6449-56.

SACO, T. V., STRAUSS, A. T. & LEDFORD, D. K. 2018. Hepatitis B vaccine nonresponders: Possible mechanisms and solutions. *Ann Allergy Asthma Immunol,* 121**,** 320-327.

SAHA, A. & DESHAIES, R. J. 2008. Multimodal activation of the ubiquitin ligase SCF by Nedd8 conjugation. *Mol Cell,* 32**,** 21-31.

SAKURAI, F., MITANI, S., YAMAMOTO, T., TAKAYAMA, K., TACHIBANA, M., WATASHI, K., WAKITA, T., IIJIMA, S., TANAKA, Y. & MIZUGUCHI, H. 2017. Human induced-pluripotent stem cell-derived hepatocyte-like cells as an in vitro model of human hepatitis B virus infection. *Sci Rep,* 7**,** 45698.

SALISSE, J. & SUREAU, C. 2009. A function essential to viral entry underlies the hepatitis B virus "a" determinant. *J Virol,* 83**,** 9321-8.

SCHIECK, A., MULLER, T., SCHULZE, A., HABERKORN, U., URBAN, S. & MIER, W. 2010. Solid-phase synthesis of the lipopeptide Myr-HBVpreS/2-78, a hepatitis B virus entry inhibitor. *Molecules,* 15**,** 4773-83.

SCHLICKSUP, C. J., WANG, J. C., FRANCIS, S., VENKATAKRISHNAN, B., TURNER, W. W., VANNIEUWENHZE, M. & ZLOTNICK, A. 2018. Hepatitis B virus core protein allosteric modulators can distort and disrupt intact capsids. *Elife,* 7.

SCHLUEP, T., LICKLITER, J., HAMILTON, J., LEWIS, D. L., LAI, C. L., LAU, J. Y., LOCARNINI, S. A., GISH, R. G. & GIVEN, B. D. 2017. Safety, Tolerability, and Pharmacokinetics of ARC-520 Injection, an RNA Interference-Based Therapeutic for the Treatment of Chronic Hepatitis B Virus Infection, in Healthy Volunteers. *Clin Pharmacol Drug Dev,* 6**,** 350-362.

SCHMITT, S., GLEBE, D., ALVING, K., TOLLE, T. K., LINDER, M., GEYER, H., LINDER, D., PETER-KATALINIC, J., GERLICH, W. H. & GEYER, R. 1999. Analysis of the pre-S2 N- and O-linked glycans of the M surface protein from human hepatitis B virus. *J Biol Chem,* 274**,** 11945-57.

SCHMITZ, A., SCHWARZ, A., FOSS, M., ZHOU, L., RABE, B., HOELLENRIEGEL, J., STOEBER, M., PANTE, N. & KANN, M. 2010. Nucleoporin 153 arrests the nuclear import of hepatitis B virus capsids in the nuclear basket. *PLoS Pathog,* 6**,** e1000741.

SCHREIBER, A. & PETER, M. 2014. Substrate recognition in selective autophagy and the ubiquitin-proteasome system. *Biochim Biophys Acta,* 1843**,** 163-81.

SCHULZE, A., GRIPON, P. & URBAN, S. 2007. Hepatitis B virus infection initiates with a large surface protein-dependent binding to heparan sulfate proteoglycans. *Hepatology,* 46**,** 1759-68.

SCHULZE, A., MILLS, K., WEISS, T. S. & URBAN, S. 2012. Hepatocyte polarization is essential for the productive entry of the hepatitis B virus. *Hepatology,* 55**,** 373-83.

SCHULZE, A., SCHIECK, A., NI, Y., MIER, W. & URBAN, S. 2010. Fine mapping of pre-S sequence requirements for hepatitis B virus large envelope protein-mediated receptor interaction. *J Virol,* 84**,** 1989-2000.

SEEGER, C., GANEM, D. & VARMUS, H. E. 1986. Biochemical and genetic evidence for the hepatitis B virus replication strategy. *Science,* 232**,** 477-84.

SEEGER, C. & SOHN, J. A. 2014. Targeting Hepatitis B Virus With CRISPR/Cas9. *Mol Ther Nucleic Acids,* 3**,** e216.

SEEGER, C. & SOHN, J. A. 2016. Complete Spectrum of CRISPR/Cas9-induced Mutations on HBV cccDNA. *Mol Ther,* 24**,** 1258-66.

SEITZ, S., IANCU, C., VOLZ, T., MIER, W., DANDRI, M., URBAN, S. & BARTENSCHLAGER, R. 2016. A Slow Maturation Process Renders Hepatitis B Virus Infectious. *Cell Host Microbe,* 20**,** 25-35.

SEKIBA, K., OTSUKA, M., OHNO, M., YAMAGAMI, M., KISHIKAWA, T., SEIMIYA, T., SUZUKI, T., TANAKA, E., ISHIBASHI, R., FUNATO, K. & KOIKE, K. 2019a. Pevonedistat, a Neuronal Precursor Cell-Expressed Developmentally Down-Regulated Protein 8-Activating Enzyme Inhibitor, Is a Potent Inhibitor of Hepatitis B Virus. *Hepatology,* 69**,** 1903-1915.

SEKIBA, K., OTSUKA, M., OHNO, M., YAMAGAMI, M., KISHIKAWA, T., SUZUKI, T., ISHIBASHI, R., SEIMIYA, T., TANAKA, E. & KOIKE, K. 2019b. Inhibition of HBV Transcription From cccDNA With Nitazoxanide by Targeting the HBx-DDB1 Interaction. *Cell Mol Gastroenterol Hepatol,* 7**,** 297-312.

SELLS, M. A., CHEN, M. L. & ACS, G. 1987. Production of hepatitis B virus particles in Hep G2 cells transfected with cloned hepatitis B virus DNA. *Proc Natl Acad Sci U S A,* 84**,** 1005-9.

SELLS, M. A., ZELENT, A. Z., SHVARTSMAN, M. & ACS, G. 1988. Replicative intermediates of hepatitis B virus in HepG2 cells that produce infectious virions. *J Virol,* 62**,** 2836-44.

SHEN, F., LI, Y., WANG, Y., SOZZI, V., REVILL, P. A., LIU, J., GAO, L., YANG, G., LU, M., SUTTER, K., DITTMER, U., CHEN, J. & YUAN, Z. 2018. Hepatitis B virus sensitivity to interferon-alpha in hepatocytes is more associated with cellular interferon response than with viral genotype. *Hepatology,* 67**,** 1237-1252.

SHERAZ, M., CHENG, J., TANG, L., CHANG, J. & GUO, J. T. 2019. Cellular DNA topoisomerases are required for the synthesis of hepatitis B virus covalently closed circular DNA. *J Virol*.

SHIMURA, S., WATASHI, K., FUKANO, K., PEEL, M., SLUDER, A., KAWAI, F., IWAMOTO, M., TSUKUDA, S., TAKEUCHI, J. S., MIYAKE, T., SUGIYAMA, M., OGASAWARA, Y., PARK, S. Y., TANAKA, Y., KUSUHARA, H., MIZOKAMI, M., SUREAU, C. & WAKITA, T. 2017. Cyclosporin derivatives inhibit hepatitis B virus entry without interfering with NTCP transporter activity. *J Hepatol,* 66**,** 685-692.

SHLOMAI, A., SCHWARTZ, R. E., RAMANAN, V., BHATTA, A., DE JONG, Y. P., BHATIA, S. N. & RICE, C. M. 2014. Modeling host interactions with hepatitis B virus using primary and induced pluripotent stem cell-derived hepatocellular systems. *Proc Natl Acad Sci U S A,* 111**,** 12193-8.

SHORT, J. M., CHEN, S., ROSEMAN, A. M., BUTLER, P. J. & CROWTHER, R. A. 2009. Structure of hepatitis B surface antigen from subviral tubes determined by electron cryomicroscopy. *J Mol Biol,* 390**,** 135-41.

SLAGLE, B. L., ANDRISANI, O. M., BOUCHARD, M. J., LEE, C. G., OU, J. H. & SIDDIQUI, A. 2015. Technical standards for hepatitis B virus X protein (HBx) research. *Hepatology,* 61**,** 1416-24.

SLAGLE, B. L. & BOUCHARD, M. J. 2016. Hepatitis B Virus X and Regulation of Viral Gene Expression. *Cold Spring Harb Perspect Med,* 6**,** a021402.

SLAGLE, B. L. & BOUCHARD, M. J. 2018. Role of HBx in hepatitis B virus persistence and its therapeutic implications. *Curr Opin Virol,* 30**,** 32-38.

SONG, M., SUN, Y., TIAN, J., HE, W., XU, G., JING, Z. & LI, W. 2018. Silencing Retinoid X Receptor Alpha Expression Enhances Early-Stage Hepatitis B Virus Infection In Cell Cultures. *J Virol,* 92.

SOUCY, T. A., SMITH, P. G., MILHOLLEN, M. A., BERGER, A. J., GAVIN, J. M., ADHIKARI, S., BROWNELL, J. E., BURKE, K. E., CARDIN, D. P., CRITCHLEY, S., CULLIS, C. A., DOUCETTE, A., GARNSEY, J. J., GAULIN, J. L., GERSHMAN, R. E., LUBLINSKY, A. R., MCDONALD, A., MIZUTANI, H., NARAYANAN, U., OLHAVA, E. J., PELUSO, S., REZAEI, M., SINTCHAK, M. D., TALREJA, T., THOMAS, M. P., TRAORE, T., VYSKOCIL, S., WEATHERHEAD, G. S., YU, J., ZHANG, J., DICK, L. R., CLAIBORNE, C. F., ROLFE, M., BOLEN, J. B. & LANGSTON, S. P. 2009. An inhibitor of NEDD8-activating enzyme as a new approach to treat cancer. *Nature,* 458**,** 732-6.

SPRINZL, M. F., OBERWINKLER, H., SCHALLER, H. & PROTZER, U. 2001. Transfer of hepatitis B virus genome by adenovirus vectors into cultured cells and mice: crossing the species barrier. *J Virol,* 75**,** 5108-18.

STANAWAY, J. D., FLAXMAN, A. D., NAGHAVI, M., FITZMAURICE, C., VOS, T., ABUBAKAR, I., ABU-RADDAD, L. J., ASSADI, R., BHALA, N., COWIE, B., FOROUZANFOUR, M. H., GROEGER, J., HANAFIAH, K. M., JACOBSEN, K. H., JAMES, S. L., MACLACHLAN, J., MALEKZADEH, R., MARTIN, N. K., MOKDAD, A. A., MOKDAD, A. H., MURRAY, C. J. L., PLASS, D., RANA, S., REIN, D. B., RICHARDUS, J. H., SANABRIA, J., SAYLAN, M., SHAHRAZ, S., SO, S., VLASSOV, V. V., WEIDERPASS, E., WIERSMA, S. T., YOUNIS, M., YU, C., EL SAYED ZAKI, M. & COOKE, G. S. 2016. The global burden of viral hepatitis from 1990 to 2013: findings from the Global Burden of Disease Study 2013. *Lancet,* 388**,** 1081-1088.

STANDRING, D. N., OU, J. H., MASIARZ, F. R. & RUTTER, W. J. 1988. A signal peptide encoded within the precore region of hepatitis B virus directs the secretion of a heterogeneous population of e antigens in Xenopus oocytes. *Proc Natl Acad Sci U S A,* 85**,** 8405-9.

STAPRANS, S., LOEB, D. D. & GANEM, D. 1991. Mutations affecting hepadnavirus plus-strand DNA synthesis dissociate primer cleavage from translocation and reveal the origin of linear viral DNA. *J Virol,* 65**,** 1255-62.

STEINAU, M., RAJEEVAN, M. S. & UNGER, E. R. 2006. DNA and RNA references for qRT-PCR assays in exfoliated cervical cells. *J Mol Diagn,* 8**,** 113-8.

STRAY, S. J., BOURNE, C. R., PUNNA, S., LEWIS, W. G., FINN, M. G. & ZLOTNICK, A. 2005. A heteroaryldihydropyrimidine activates and can misdirect hepatitis B virus capsid assembly. *Proc Natl Acad Sci U S A,* 102**,** 8138-43.

STRAY, S. J., JOHNSON, J. M., KOPEK, B. G. & ZLOTNICK, A. 2006. An in vitro fluorescence screen to identify antivirals that disrupt hepatitis B virus capsid assembly. *Nat Biotechnol,* 24**,** 358-62.

STRAY, S. J. & ZLOTNICK, A. 2006. BAY 41-4109 has multiple effects on Hepatitis B virus capsid assembly. *J Mol Recognit,* 19**,** 542-8.

SULLIVAN, G. J., HAY, D. C., PARK, I. H., FLETCHER, J., HANNOUN, Z., PAYNE, C. M., DALGETTY, D., BLACK, J. R., ROSS, J. A., SAMUEL, K., WANG, G., DALEY, G. Q., LEE, J. H., CHURCH, G. M., FORBES, S. J., IREDALE, J. P. & WILMUT, I. 2010. Generation of functional human hepatic endoderm from human induced pluripotent stem cells. *Hepatology,* 51**,** 329-35.

SUMMERS, J. & MASON, W. S. 1982. Replication of the genome of a hepatitis B--like virus by reverse transcription of an RNA intermediate. *Cell,* 29**,** 403-15.

SUMMERS, J., SMITH, P. M. & HORWICH, A. L. 1990. Hepadnavirus envelope proteins regulate covalently closed circular DNA amplification. *J Virol,* 64**,** 2819-24.

SUN, D. & NASSAL, M. 2006. Stable HepG2- and Huh7-based human hepatoma cell lines for efficient regulated expression of infectious hepatitis B virus. *J Hepatol,* 45**,** 636-45.

TAHAEI, S. M., MOHEBBI, S. R. & ZALI, M. R. 2012. Enteric hepatitis viruses. *Gastroenterol Hepatol Bed Bench,* 5**,** 7-15.

TAKAHASHI, K. & YAMANAKA, S. 2006. Induction of pluripotent stem cells from mouse embryonic and adult fibroblast cultures by defined factors. *Cell,* 126**,** 663-76.

TAN, Z., MAGUIRE, M. L., LOEB, D. D. & ZLOTNICK, A. 2013. Genetically altering the thermodynamics and kinetics of hepatitis B virus capsid assembly has profound effects on virus replication in cell culture. *J Virol,* 87**,** 3208-16.

TANG, H., DELGERMAA, L., HUANG, F., OISHI, N., LIU, L., HE, F., ZHAO, L. & MURAKAMI, S. 2005. The transcriptional transactivation function of HBx protein is important for its augmentation role in hepatitis B virus replication. *J Virol,* 79**,** 5548-56.

TANG, H. M., GAO, W. W., CHAN, C. P., CHENG, Y., CHAUDHARY, V., DENG, J. J., YUEN, K. S., WONG, C. M., NG, I. O., KOK, K. H., ZHOU, J. & JIN, D. Y. 2014. Requirement of CRTC1 coactivator for hepatitis B virus transcription. *Nucleic Acids Res,* 42**,** 12455-68.

TANG, L., SHERAZ, M., MCGRANE, M., CHANG, J. & GUO, J. T. 2019. DNA Polymerase alpha is essential for intracellular amplification of hepatitis B virus covalently closed circular DNA. *PLoS Pathog,* 15**,** e1007742.

TATE, V. E. & PHILIPSON, L. 1979. Parental adenovirus DNA accumulates in nucleosome-like structures in infected cells. *Nucleic Acids Res,* 6**,** 2769-85.

TAVIS, J. E., CHENG, X., HU, Y., TOTTEN, M., CAO, F., MICHAILIDIS, E., AURORA, R., MEYERS, M. J., JACOBSEN, E. J., PARNIAK, M. A. & SARAFIANOS, S. G. 2013. The hepatitis B virus ribonuclease H is sensitive to inhibitors of the human immunodeficiency virus ribonuclease H and integrase enzymes. *PLoS Pathog,* 9**,** e1003125.

TAVIS, J. E. & LOMONOSOVA, E. 2015. The hepatitis B virus ribonuclease H as a drug target. *Antiviral Res,* 118**,** 132-8.

TAVIS, J. E., ZOIDIS, G., MEYERS, M. J. & MURELLI, R. P. 2018. Chemical Approaches to Inhibiting the Hepatitis B Virus Ribonuclease H. *ACS Infect Dis*.

TCHESNOKOV, E. P., OBIKHOD, A., SCHINAZI, R. F. & GOTTE, M. 2008. Delayed chain termination protects the anti-hepatitis B virus drug entecavir from excision by HIV-1 reverse transcriptase. *J Biol Chem,* 283**,** 34218-28.

TENNEY, D. J., ROSE, R. E., BALDICK, C. J., POKORNOWSKI, K. A., EGGERS, B. J., FANG, J., WICHROSKI, M. J., XU, D., YANG, J., WILBER, R. B. & COLONNO, R. J. 2009. Long-term monitoring shows hepatitis B virus resistance to entecavir in nucleoside-naive patients is rare through 5 years of therapy. *Hepatology,* 49**,** 1503-14.

THOMAS, E., YONEDA, M. & SCHIFF, E. R. 2015. Viral hepatitis: past and future of HBV and HDV. *Cold Spring Harb Perspect Med,* 5**,** a021345.

TOH, Q. C., TAN, T. L., TEO, W. Q., HO, C. Y., PARIDA, S. & CHEN, W. N. 2005. Identification of cellular membrane proteins interacting with hepatitis B surface antigen using yeast split-ubiquitin system. *Int J Med Sci,* 2**,** 114-7.

TROPBERGER, P., MERCIER, A., ROBINSON, M., ZHONG, W., GANEM, D. E. & HOLDORF, M. 2015. Mapping of histone modifications in episomal HBV cccDNA uncovers an unusual chromatin organization amenable to epigenetic manipulation. *Proc Natl Acad Sci U S A,* 112**,** E5715-24.

TRUJILLO, M. A., LETOVSKY, J., MAGUIRE, H. F., LOPEZ-CABRERA, M. & SIDDIQUI, A. 1991. Functional analysis of a liver-specific enhancer of the hepatitis B virus. *Proc Natl Acad Sci U S A,* 88**,** 3797-801.

TU, T., BUDZINSKA, M. A., SHACKEL, N. A. & URBAN, S. 2017. HBV DNA Integration: Molecular Mechanisms and Clinical Implications. *Viruses,* 9.

TUTTLEMAN, J. S., POURCEL, C. & SUMMERS, J. 1986. Formation of the pool of covalently closed circular viral DNA in hepadnavirus-infected cells. *Cell,* 47**,** 451-60.

UNCHWANIWALA, N., SHERER, N. M. & LOEB, D. D. 2016. Hepatitis B Virus Polymerase Localizes to the Mitochondria, and Its Terminal Protein Domain Contains the Mitochondrial Targeting Signal. *J Virol,* 90**,** 8705-19.

URBAN, S., BARTENSCHLAGER, R., KUBITZ, R. & ZOULIM, F. 2014. Strategies to inhibit entry of HBV and HDV into hepatocytes. *Gastroenterology,* 147**,** 48-64.

URBAN, S., BREINER, K. M., FEHLER, F., KLINGMULLER, U. & SCHALLER, H. 1998. Avian hepatitis B virus infection is initiated by the interaction of a distinct pre-S subdomain with the cellular receptor gp180. *J Virol,* 72**,** 8089-97.

URBAN, S. & GRIPON, P. 2002. Inhibition of duck hepatitis B virus infection by a myristoylated pre-S peptide of the large viral surface protein. *J Virol,* 76**,** 1986-90.

VAN BREUGEL, P. C., ROBERT, E. I., MUELLER, H., DECORSIERE, A., ZOULIM, F., HANTZ, O. & STRUBIN, M. 2012. Hepatitis B virus X protein stimulates gene expression selectively from extrachromosomal DNA templates. *Hepatology,* 56**,** 2116-24.

VAN DE KLUNDERT, M. A., VAN DEN BIGGELAAR, M., KOOTSTRA, N. A. & ZAAIJER, H. L. 2016a. Hepatitis B Virus Protein X Induces Degradation of Talin-1. *Viruses,* 8.

VAN DE KLUNDERT, M. A., ZAAIJER, H. L. & KOOTSTRA, N. A. 2016b. Identification of FDA-approved drugs that target hepatitis B virus transcription. *J Viral Hepat,* 23**,** 191-201.

VOLZ, T., ALLWEISS, L., BEN, M. M., WARLICH, M., LOHSE, A. W., POLLOK, J. M., ALEXANDROV, A., URBAN, S., PETERSEN, J., LUTGEHETMANN, M. & DANDRI, M. 2013. The entry inhibitor Myrcludex-B efficiently blocks intrahepatic virus spreading in humanized mice previously infected with hepatitis B virus. *J Hepatol,* 58**,** 861-7.

VOSOUGH, M., OMIDINIA, E., KADIVAR, M., SHOKRGOZAR, M. A., POURNASR, B., AGHDAMI, N. & BAHARVAND, H. 2013. Generation of functional hepatocyte-like cells from human pluripotent stem cells in a scalable suspension culture. *Stem Cells Dev,* 22**,** 2693-705.

WALDEN, H., PODGORSKI, M. S., HUANG, D. T., MILLER, D. W., HOWARD, R. J., MINOR, D. L., JR., HOLTON, J. M. & SCHULMAN, B. A. 2003. The structure of the APPBP1-UBA3-NEDD8-ATP complex reveals the basis for selective ubiquitin-like protein activation by an E1. *Mol Cell,* 12**,** 1427-37.

WANG, G. H. & SEEGER, C. 1992. The reverse transcriptase of hepatitis B virus acts as a protein primer for viral DNA synthesis. *Cell,* 71**,** 663-70.

WANG, J., CHEN, X., WU, Y., CAO, Z., WANG, L., HUANG, H., CHEN, X. & LU, F. 2018. Serum HBV RNA is a Potential Predictor of Hepatitis B Surface Antigen Reversion. *Hepatol Commun,* 2**,** 1168-1171.

WANG, J., QU, B., ZHANG, F., ZHANG, C., DENG, W., DAO THI, V. L. & XIA, Y. 2019. Stem Cell-Derived Hepatocyte-Like Cells as Model for Viral Hepatitis Research. *Stem Cells Int,* 2019**,** 9605252.

WANG, J., SHEN, T., HUANG, X., KUMAR, G. R., CHEN, X., ZENG, Z., ZHANG, R., CHEN, R., LI, T., ZHANG, T., YUAN, Q., LI, P. C., HUANG, Q., COLONNO, R., JIA, J., HOU, J., MCCRAE, M. A., GAO, Z., REN, H., XIA, N., ZHUANG, H. & LU, F. 2016. Serum hepatitis B virus RNA is encapsidated pregenome RNA that may be associated with persistence of viral infection and rebound. *J Hepatol,* 65**,** 700-710.

WANG, J., SHENG, Q., DING, Y., CHEN, R., SUN, X., CHEN, X., DOU, X. & LU, F. 2017. HBV RNA virion-like particles produced under nucleos(t)ide analogues treatment are mainly replication-deficient. *J Hepatol*.

WANG, X., LI, Y., MAO, A., LI, C., LI, Y. & TIEN, P. 2010. Hepatitis B virus X protein suppresses virus-triggered IRF3 activation and IFN-beta induction by disrupting the VISA-associated complex. *Cell Mol Immunol,* 7**,** 341-8.

WANG, X. Y., WEI, Z. M., WU, G. Y., WANG, J. H., ZHANG, Y. J., LI, J., ZHANG, H. H., XIE, X. W., WANG, X., WANG, Z. H., WEI, L., WANG, Y. & CHEN, H. S. 2012. In vitro inhibition of HBV replication by a novel compound, GLS4, and its efficacy against adefovir-dipivoxil-resistant HBV mutations. *Antivir Ther,* 17**,** 793-803.

WATASHI, K., SLUDER, A., DAITO, T., MATSUNAGA, S., RYO, A., NAGAMORI, S., IWAMOTO, M., NAKAJIMA, S., TSUKUDA, S., BORROTO-ESODA, K., SUGIYAMA, M., TANAKA, Y., KANAI, Y.,

KUSUHARA, H., MIZOKAMI, M. & WAKITA, T. 2014. Cyclosporin A and its analogs inhibit hepatitis B virus entry into cultured hepatocytes through targeting a membrane transporter, sodium taurocholate cotransporting polypeptide (NTCP). *Hepatology,* 59**,** 1726-37.

WEBER, M., BRONSEMA, V., BARTOS, H., BOSSERHOFF, A., BARTENSCHLAGER, R. & SCHALLER, H. 1994. Hepadnavirus P protein utilizes a tyrosine residue in the TP domain to prime reverse transcription. *J Virol,* 68**,** 2994-9.

WEBER, N. D., STONE, D., SEDLAK, R. H., DE SILVA FEELIXGE, H. S., ROYCHOUDHURY, P., SCHIFFER, J. T., AUBERT, M. & JEROME, K. R. 2014. AAV-mediated delivery of zinc finger nucleases targeting hepatitis B virus inhibits active replication. *PLoS One,* 9**,** e97579.

WEBER, O., SCHLEMMER, K. H., HARTMANN, E., HAGELSCHUER, I., PAESSENS, A., GRAEF, E., DERES, K., GOLDMANN, S., NIEWOEHNER, U., STOLTEFUSS, J., HAEBICH, D., RUEBSAMEN-WAIGMANN, H. & WOHLFEIL, S. 2002. Inhibition of human hepatitis B virus (HBV) by a novel non-nucleosidic compound in a transgenic mouse model. *Antiviral Res,* 54**,** 69-78.

WEI, C., NI, C., SONG, T., LIU, Y., YANG, X., ZHENG, Z., JIA, Y., YUAN, Y., GUAN, K., XU, Y., CHENG, X., ZHANG, Y., YANG, X., WANG, Y., WEN, C., WU, Q., SHI, W. & ZHONG, H. 2010. The hepatitis B virus X protein disrupts innate immunity by downregulating mitochondrial antiviral signaling protein. *J Immunol,* 185**,** 1158-68.

WEI, W., GUO, H., LIU, X., ZHANG, H., QIAN, L., LUO, K., MARKHAM, R. B. & YU, X. F. 2014. A first-in-class NAE inhibitor, MLN4924, blocks lentiviral infection in myeloid cells by disrupting neddylation-dependent Vpx-mediated SAMHD1 degradation. *J Virol,* 88**,** 745-51.

WELLS, M. J., HATTON, M. W., HEWLETT, B., PODOR, T. J., SHEFFIELD, W. P. & BLAJCHMAN, M. A. 1997. Cytokeratin 18 is expressed on the hepatocyte plasma membrane surface and interacts with thrombin-antithrombin complexes. *J Biol Chem,* 272**,** 28574-81.

WENTZ, M. J., BECKER, S. A. & SLAGLE, B. L. 2000. Dissociation of DDB1-binding and transactivation properties of the hepatitis B virus X protein. *Virus Res,* 68**,** 87-92.

WHITBY, F. G., XIA, G., PICKART, C. M. & HILL, C. P. 1998. Crystal structure of the human ubiquitin-like protein NEDD8 and interactions with ubiquitin pathway enzymes. *J Biol Chem,* 273**,** 34983-91.

WILL, H., REISER, W., WEIMER, T., PFAFF, E., BUSCHER, M., SPRENGEL, R., CATTANEO, R. & SCHALLER, H. 1987. Replication strategy of human hepatitis B virus. *J Virol,* 61**,** 904-11.

WINER, B. Y., HUANG, T. S., PLUDWINSKI, E., HELLER, B., WOJCIK, F., LIPKOWITZ, G. E., PAREKH, A., CHO, C., SHRIRAO, A., MUIR, T. W., NOVIK, E. & PLOSS, A. 2017. Long-term hepatitis B infection in a scalable hepatic co-culture system. *Nat Commun,* 8**,** 125.

WOODDELL, C. I., ROZEMA, D. B., HOSSBACH, M., JOHN, M., HAMILTON, H. L., CHU, Q., HEGGE, J. O., KLEIN, J. J., WAKEFIELD, D. H., OROPEZA, C. E., DECKERT, J., ROEHL, I., JAHN-HOFMANN, K., HADWIGER, P., VORNLOCHER, H. P., MCLACHLAN, A. & LEWIS, D. L. 2013. Hepatocyte-targeted RNAi therapeutics for the treatment of chronic hepatitis B virus infection. *Mol Ther,* 21**,** 973-85.

WOODDELL, C. I., YUEN, M. F., CHAN, H. L., GISH, R. G., LOCARNINI, S. A., CHAVEZ, D., FERRARI, C., GIVEN, B. D., HAMILTON, J., KANNER, S. B., LAI, C. L., LAU, J. Y. N., SCHLUEP, T., XU, Z.,

LANFORD, R. E. & LEWIS, D. L. 2017. RNAi-based treatment of chronically infected patients and chimpanzees reveals that integrated hepatitis B virus DNA is a source of HBsAg. *Sci Transl Med,* 9.

WU, G., LIU, B., ZHANG, Y., LI, J., ARZUMANYAN, A., CLAYTON, M. M., SCHINAZI, R. F., WANG, Z., GOLDMANN, S., REN, Q., ZHANG, F. & FEITELSON, M. A. 2013. Preclinical characterization of GLS4, an inhibitor of hepatitis B virus core particle assembly. *Antimicrob Agents Chemother,* 57**,** 5344-54.

WU, T. T., COATES, L., ALDRICH, C. E., SUMMERS, J. & MASON, W. S. 1990. In hepatocytes infected with duck hepatitis B virus, the template for viral RNA synthesis is amplified by an intracellular pathway. *Virology,* 175**,** 255-61.

XIA, Y., CARPENTIER, A., CHENG, X., BLOCK, P. D., ZHAO, Y., ZHANG, Z., PROTZER, U. & LIANG, T. J. 2017a. Human stem cell-derived hepatocytes as a model for hepatitis B virus infection, spreading and virus-host interactions. *J Hepatol,* 66**,** 494-503.

XIA, Y., CHENG, X., BLOSSEY, C. K., WISSKIRCHEN, K., ESSER, K. & PROTZER, U. 2017b. Secreted Interferon-Inducible Factors Restrict Hepatitis B and C Virus Entry In Vitro. *J Immunol Res,* 2017**,** 4828936.

XIA, Y. & PROTZER, U. 2017. Control of Hepatitis B Virus by Cytokines. *Viruses,* 9.

XIA, Y., STADLER, D., LUCIFORA, J., REISINGER, F., WEBB, D., HOSEL, M., MICHLER, T., WISSKIRCHEN, K., CHENG, X., ZHANG, K., CHOU, W. M., WETTENGEL, J. M., MALO, A., BOHNE, F., HOFFMANN, D., EYER, F., THIMME, R., FALK, C. S., THASLER, W. E., HEIKENWALDER, M. & PROTZER, U. 2016. Interferon-gamma and Tumor Necrosis Factor-alpha Produced by T Cells Reduce the HBV Persistence Form, cccDNA, Without Cytolysis. *Gastroenterology,* 150**,** 194-205.

XIANG, C., DU, Y., MENG, G., SOON YI, L., SUN, S., SONG, N., ZHANG, X., XIAO, Y., WANG, J., YI, Z., LIU, Y., XIE, B., WU, M., SHU, J., SUN, D., JIA, J., LIANG, Z., SUN, D., HUANG, Y., SHI, Y., XU, J., LU, F., LI, C., XIANG, K., YUAN, Z., LU, S. & DENG, H. 2019. Long-term functional maintenance of primary human hepatocytes in vitro. *Science,* 364**,** 399-402.

YAMOAH, K., OASHI, T., SARIKAS, A., GAZDOIU, S., OSMAN, R. & PAN, Z. Q. 2008. Autoinhibitory regulation of SCF-mediated ubiquitination by human cullin 1's C-terminal tail. *Proc Natl Acad Sci U S A,* 105**,** 12230-5.

YAN, H., PENG, B., LIU, Y., XU, G., HE, W., REN, B., JING, Z., SUI, J. & LI, W. 2014. Viral entry of hepatitis B and D viruses and bile salts transportation share common molecular determinants on sodium taurocholate cotransporting polypeptide. *J Virol,* 88**,** 3273-84.

YAN, H., ZHONG, G., XU, G., HE, W., JING, Z., GAO, Z., HUANG, Y., QI, Y., PENG, B., WANG, H., FU, L., SONG, M., CHEN, P., GAO, W., REN, B., SUN, Y., CAI, T., FENG, X., SUI, J. & LI, W. 2012. Sodium taurocholate cotransporting polypeptide is a functional receptor for human hepatitis B and D virus. *Elife,* 3.

YAN, R., ZHAO, X., CAI, D., LIU, Y., BLOCK, T. M., GUO, J. T. & GUO, H. 2015. The Interferon-Inducible Protein Tetherin Inhibits Hepatitis B Virus Virion Secretion. *J Virol,* 89**,** 9200-12.

YANG, B. & BOUCHARD, M. J. 2012. The hepatitis B virus X protein elevates cytosolic calcium signals by modulating mitochondrial calcium uptake. *J Virol,* 86**,** 313-27.

YANG, W. & SUMMERS, J. 1998. Infection of ducklings with virus particles containing linear double-stranded duck hepatitis B virus DNA: illegitimate replication and reversion. *J Virol,* 72**,** 8710-7.

YAO, F. Y., TERRAULT, N. A., FREISE, C., MASLOW, L. & BASS, N. M. 2001. Lamivudine treatment is beneficial in patients with severely decompensated cirrhosis and actively replicating hepatitis B infection awaiting liver transplantation: a comparative study using a matched, untreated cohort. *Hepatology,* 34**,** 411-6.

YEH, C. T., LIAW, Y. F. & OU, J. H. 1990. The arginine-rich domain of hepatitis B virus precore and core proteins contains a signal for nuclear transport. *J Virol,* 64**,** 6141-7.

YUEN, M. F., GANE, E. J., KIM, D. J., WEILERT, F., YUEN CHAN, H. L., LALEZARI, J., HWANG, S. G., NGUYEN, T., FLORES, O., HARTMAN, G., LIAW, S., LENZ, O., KAKUDA, T. N., TALLOEN, W., SCHWABE, C., KLUMPP, K. & BROWN, N. 2019. Antiviral Activity, Safety, and Pharmacokinetics of Capsid Assembly Modulator NVR 3-778 in Patients with Chronic HBV Infection. *Gastroenterology,* 156**,** 1392-1403 e7.

YUEN, M. F., SETO, W. K., CHOW, D. H., TSUI, K., WONG, D. K., NGAI, V. W., WONG, B. C., FUNG, J., YUEN, J. C. & LAI, C. L. 2007. Long-term lamivudine therapy reduces the risk of long-term complications of chronic hepatitis B infection even in patients without advanced disease. *Antivir Ther,* 12**,** 1295-303.

ZHANG, T. Y., CHEN, H. Y., CAO, J. L., XIONG, H. L., MO, X. B., LI, T. L., KANG, X. Z., ZHAO, J. H., YIN, B., ZHAO, X., HUANG, C. H., YUAN, Q., XUE, D., XIA, N. S. & YUAN, Y. A. 2019. Structural and functional analyses of hepatitis B virus X protein BH3-like domain and Bcl-xL interaction. *Nat Commun,* 10**,** 3192.

ZHANG, Y. Y., ZHANG, B. H., THEELE, D., LITWIN, S., TOLL, E. & SUMMERS, J. 2003. Single-cell analysis of covalently closed circular DNA copy numbers in a hepadnavirus-infected liver. *Proc Natl Acad Sci U S A,* 100**,** 12372-7.

ZHANG, Z. & TAVIS, J. E. 2006. The duck hepatitis B virus reverse transcriptase functions as a full-length monomer. *J Biol Chem,* 281**,** 35794-801.

ZHAO, Y., MORGAN, M. A. & SUN, Y. 2014. Targeting Neddylation pathways to inactivate cullin-RING ligases for anticancer therapy. *Antioxid Redox Signal,* 21**,** 2383-400.

ZHOU, S. L. & STANDRING, D. N. 1991. Production of hepatitis B virus nucleocapsidlike core particles in Xenopus oocytes: assembly occurs mainly in the cytoplasm and does not require the nucleus. *J Virol,* 65**,** 5457-64.

ZHOU, X., SHI, H., YANG, S. & SUN, P. 2017. An efficient rapid system for assaying HBx-mediated transactivation. *Biotechnol Lett,* 39**,** 1091-1099.

ZHU, Y., YAMAMOTO, T., CULLEN, J., SAPUTELLI, J., ALDRICH, C. E., MILLER, D. S., LITWIN, S., FURMAN, P. A., JILBERT, A. R. & MASON, W. S. 2001. Kinetics of hepadnavirus loss from the liver during inhibition of viral DNA synthesis. *J Virol,* 75**,** 311-22.

ZLOTNICK, A., LEE, A., BOURNE, C. R., JOHNSON, J. M., DOMANICO, P. L. & STRAY, S. J. 2007. In vitro screening for molecules that affect virus capsid assembly (and other protein association reactions). *Nat Protoc,* 2**,** 490-8.

ZOULIM, F., SAPUTELLI, J. & SEEGER, C. 1994. Woodchuck hepatitis virus X protein is required for viral infection in vivo. *J Virol,* 68**,** 2026-30.

ZUCKERMAN, A. J. 1996. Hepatitis Viruses. *In:* TH & BARON, S. (eds.) *Medical Microbiology.* Galveston (TX): University of Texas Medical Branch at Galveston
The University of Texas Medical Branch at Galveston.